ANALYSIS OF HIV-1 GAG MATRIX AND CAPSID DOMAIN MUTATIONS AND THEIR EFFECTS ON VIRUS ASSEMBLY AND INFECTIVITY

By

Isabel Gabriele Scholz

A DISSERTATION

Presented to the Department of

Molecular Microbiology & Immunology

at Oregon Health & Science University

in partial fulfillment of

the requirements for the degree of

Doctor of Philosophy

October 2007

School of Medicine
Oregon Health & Science University

CERTIFICATE OF APPROVAL

This is certify that the Ph.D. dissertation of

Isabel Gabriele Scholz

has been approved

TABLE OF CONTENTS

Index of figures and tables

Acknowledgments

There are many people to whom I owe thanks, and it is impossible to put my appreciation into adequate words. First and foremost, my parents have always been incredibly supportive of all my varied interests, be they educational, recreational, or travel-oriented. They have raised me with a great appreciation for the value of education, and they have always been there for me. Annette deserves my thanks for being a wonderful sister to have, and she has become a good friend to me as we've both grown up. Much thanks also goes to my extended family. The Hakenbergs, Gabi, Peter, Jan, Anna, Marie, and Chilly, have been an important part of my life for a long time, and we've been through many adventures. Their support has been invaluable, and they have provided me with great conversation, food, friendship, and much more. Jen, my best friend and adopted sister, has been a constant source of support for many years and in many ways. She made me retain some degree of sanity, fed me great food, traveled with me, read various drafts of this writing, and also helped me subdue computer applications. The Münch family and their dogs have been an important part of my life since my earliest days. Judi has been a supportive friend and helped me in many instances. A number of friends throughout my life have made life much more pleasant, and, more recently, made Portland a great place to live.

None of this work would have been possible without the mentoring of Eric Barklis, who has provided me with mountains of advice, education, and support with

regard to science as well as hiking. He also introduced me to pigmania and competitive croquet. His sense of humor and creativity make the lab a productive and interesting place to work. I am also grateful to the members of my thesis advisory and examination committee, Caroline Enns, Jorge Crosa, Ashlee Moses, and Scott Wong, for all the time and advice they have given me. Throughout the years, I have worked with a number of wonderful people in the Barklis lab, who have taught me and made life in the lab and outside enjoyable. Special thanks to Amelia Still, Ayna Alfadhli, Carrie McQuaw, Tenzin Choesang, Ben Kukull, Binder Colman, Robin Barklis, Brian Arvidson, Keith Mayo, Doug Huseby, and Liam Finlay. Thanks also to the Johnson lab, especially Todd Wisner and Brent Ryckman, the Nelson lab, and the Kabat lab, especially Sue Kozak, for providing reagents and advice on so many occasions. I am also grateful for all the help I received from the MMI office staff, especially Chris Langford and Kathy Shinall.

To Sigrid and Dieter, the best parents anyone could ever wish for.

Abbreviations

AIDS	acquired immunodeficiency syndrome
APOBEC	apolipoprotein B editing catalytic polypeptide 1-like protein
ARV	AIDS-associated retrovirus
β-gal	β-galactosidase
BlaM	β-lactamase
BME	β-mercaptoethanol
BMH	bis-maleimido-hexane
CA	capsid
CTD	C-terminal domain
CypA	cyclophilin A
DAG	diacylglycerol
DC	dendritic cell
DIS	dimerization initiation sequence
DNA	deoxyribonucleic acid
EM	electron microscopy
Env	envelope protein
ER	endoplasmic reticulum
ESCRT	endosomal sorting complex required for transport
GBG	Gag-β-galactosidase
GFP	green fluorescent protein
gp	glycoprotein
gpt	guanosine phosphoribosyl transferase
gRNA	genomic RNA
HAART	highly active antiretroviral therapy
HIV	human immunodeficiency virus
HTLV-III	human T-cell lymphotropic virus type III
IFN	interferon
IL	interleukin
IN	integrase
LAV	lymphadenopathy-associated virus
LTR	long terminal repeat
Luc	luciferase
MA	matrix
MBD	membrane-binding domain
MHC	major histocompatibility
miRNA	microRNA
MLV	murine leukemia virus
mRNA	messenger RNA
MVB	multivesicular body
NC	nucleocapsid
NES	nuclear export signal

NK	natural killer
NLS	nuclear localization signal
NPC	nuclear pore complex
NTD	N-terminal domain
PBS	primer-binding site
PCR	polymerase chain reaction
PDB	phorbol dibutyrate
PH	pleckstrin homology
PIC	preintegration complex
PI	phosphatidylinositol
$PI(3,4)P_2$	phosphatidylinositol-(3,4)-bisphosphate
$PI(3,4,5)P_3$	phosphatidylinositol-(3,4,5)-trisphosphate
$PI(4,5)P_2$	phosphatidylinositol-(4,5)-bisphosphate
PLC	phospholipase C δ 1
PKC	phosphokinase Cγ
PKC-CBD	phosphokinase Cγ cysteine-rich C1a plus C1b binding domain
PM	plasma membrane
PMA	phorbol myristate acetate
PPT	polypurine tract
PR	protease
PrGag	precursor Gag
PrGag-Pol	precursor Gag-Pol
RNA	ribonucleic acid
RRE	Rev response element
RT	reverse transcriptase
SDS-PAGE	sodium dodecyl sulfate polyacrylamide electrophoresis
SL	stem-loop
SP1	spacer peptide 1
SP2	spacer peptide 2
SU	surface
TAR	Tat response element
TIP47	tail-interacting protein 47
TM	transmembrane
TNF	tumor necrosis factor
TRIM5α	tripartite motif 5, splicing isoform α
tRNA	transfer RNA
VLP	virus-like particle
vRNA	viral RNA
VSV	vesicular stomatitis virus
WT	wildtype

Abstract

The work presented herein aims to characterize molecular interactions of importance to the assembly and maturation of human immunodeficiency virus type 1 (HIV-1). Production of infectious virus particles depends on proper protein-protein interactions, protein-membrane interactions, and protein-nucleic acid interactions. PrGag and PrGag-Pol proteins have to be targeted to functional assembly sites within the producer cell, interact in a specific fashion, bud off from the cells, and undergo a concerted mechanism of proteolytic processing in order to become infectious.

Extensive X-ray and NMR studies have elucidated details about the structures of the HIV-1 capsid (CA) protein. The predominantly α-helical N-terminal domains (NTDs) have been modeled to form hexamer rings in the mature cores of virions, whereas the C-terminal domains (CTDs) are thought to engage in dimerization. A role for a histidine switch model involving one or more of the highly conserved histidine residues in the CA NTD had been proposed. We chose to examine substitutions at histidine residue 84 (H84), which has been modeled at the outside of hexamer rings, and H87, which is less well conserved and lies in the cyclophilin A (CypA) binding loop. Mutations at H84 resulted in poorly infectious virus with aberrant cores and low reverse transcriptase activities in cores, whereas mutations at H87 yielded virus with only a slight reduction in infectivity. Our results suggest that HIV-1 CA residue 84 may be involved in stabilizing CA monomer tertiary structure and contributes to an arrangement which helps control

either NTD hexamer assembly or the organization of hexamers into higher-order structures.

Membrane targeting of PrGag and incorporation of HIV-1 Env have been attributed to the matrix (MA) domain of HIV-1 PrGag. To evaluate the specific requirements for the MA membrane-binding domain (MBD) in HIV-1 assembly and replication, we replaced MA with alternative MBDs. We chose the pleckstrin homology (PH) domains from AKT protein kinase and phospholipase C δ1, as well as the cysteine-rich binding domain of phosphokinase C γ. Our results demonstrated that alternative MBDs could promote VLP assembly and release, but the viruses were not infectious. Notably, PrGag processing was reduced, while cleavage of GagPol precursors resulted in the accumulation of Pol-derived intermediates within virions. Our results indicate that the HIV-1 assembly machinery can accommodate considerable variations in MA with regard to its means of membrane association, but that alternative MBDs can interfere with the structural rearrangement of virus cores during maturation.

Chapter 1

INTRODUCTION

1.1 Overview

In the mid-1980s, several laboratories isolated T-cell-tropic virus samples from patients presenting with lymphadenopathy. The isolates were named by different laboratory groups: lymphadenopathy-associated virus (LAV) by Luc Montagnier's group (28, 315), human T-cell lymphotropic virus type III (HTLV-III) by Robert Gallo's group (21, 150, 402), and acquired immunodeficiency syndrome (AIDS)-associated retrovirus (ARV) by Jay Levy's group (261). The International Committee on Taxonomy of Viruses recommended the name by which this virus is currently known: human immunodeficiency virus (HIV) (85, 132, 140).

Two distinct subtypes are known: HIV-1 and HIV-2. HIV-1 predominates and is found throughout the world, whereas HIV-2 mostly occurs in West Africa (85, 132).
HIVs cause AIDS in humans. Epidemiologic studies suggest that HIV-2 is not transmitted as easily as HIV-1 and is subject to a longer incubation period (85, 132, 166, 167, 365).

HIV is transmitted by direct sexual contact, by blood or blood products, or from infected mother to infant during birth or through breast-feeding (85, 103, 116, 132, 396, 397, 429). There is no evidence that HIV can be spread by casual contact or insect bites. In the United States and Western Europe, infection is predominantly spread by needle-sharing and homosexual contact, but worldwide, heterosexual contact is the primary mode of transmission, with a large proportion of commercial sex workers infected (1, 85, 103).

As of December 2006, nearly 40 million people were estimated to be living with HIV-1 around the world, with 4.3 million new infections having occurred in that year. AIDS claimed 2.9 million lives in 2006 alone. Two thirds of people currently infected with HIV live in sub-Saharan Africa, where 34% of all AIDS-related deaths occurred in 2006. The steepest increases in HIV infection were observed in East Asia, Central Asia, and Eastern Europe (1).

HIV belongs to the genus Lentivirus within the *Retroviridae* family. Lentiviruses are characterized by cylindrical or conical nucleoprotein cores within the mature virion, and they carry regulatory genes in addition to the basic genes of simple retroviruses (85, 143, 486). Virus isolates have been assigned to two major groups: group M, containing at least seven subtypes (or clades), and group O (132, 392). More recently, a group N was identified (132). Evidence suggests that the virus was first transmitted to humans from sooty mangabeys or chimpanzees (85, 192).

HIV can infect a variety of cell types in culture, including dendritic cells, B cells, natural killer cells, epithelial cells, and many others. However, in infected hosts, the virus is found consistently and predominantly in CD4+ T cells and cells of the macrophage lineage (85).

1.2 Immune response to HIV-1 infection

The natural killer (NK) cells of the host immune system efficiently recognize and kill virus-infected cells. Thus, viruses have to be adept at evading the immune response of the infected organism in order to establish a successful infection. HIV-1 has adopted a variety of strategies to deal with the immune system. The time from infection to disease

can vary considerably, ranging from the development of AIDS in patients 6 to 12 months after infection to long-term non-progressors remaining asymptomatic 25 years after infection (246).

HIV-1 infects cells of the immune system bearing its receptor, CD4, and a coreceptor, such as CCR5 or CXCR4. Infectious provirus can be recovered from dendritic cells (DCs), NK cells, and B cells (102, 233, 282, 313, 458). After an initial increase in viral load, the amount of virus in the blood decreases significantly, until another rise late in infection, when the CD4+ T-cell count has decreased and disease symptoms appear. During the acute phase of the infection, a stable reservoir of resting memory CD4+ T-cells harboring HIV is established (57, 82, 130, 246, 485). The innate immune system provides the initial response to HIV-1 infection. NK cell numbers are greatly increased and may be involved in decreasing the viral load. DCs also play a role in triggering the immune response. HIV-1 RNA activates DCs, which then induce the immune system via high levels of interferon-α (IFN-α), interleukin-12 (IL-12), tumor necrosis factor-α (TNF-α), and IL-6 (32, 191, 246, 335). Antibodies to HIV-1 are made within the first few weeks of infection, some of which have neutralizing capabilities to the predominant circulating virus. This, in turn, drives evolution of the virus to mutations not recognized by the antibody, different antibodies are made, the virus adapts, and the process keeps repeating itself, resulting in a large number of virus strains circulating in the system (145, 390, 391, 475). As the infection enters the chronic phase, however, the antibody response ceases to contribute to the control of the virus by the immune system, and antibody-generating B cells are depleted (246). After virus infection, CD8+ T cell numbers rapidly expand, and they appear to be involved in control of viral load (53, 239).

In the early phase of infection, CD4+ T cells directed against HIV-1 are induced and assist CD8+ T cells (96). However, this cellular immune response decreases over the first few months of infection (246, 269).

Slow, gradual depletion of CD4+ T cells has been thought to cause the eventual failure of the immune system. Mathematical modeling attempts have disputed that notion (494). Recent studies have suggested that the initial massive viral replication during acute infection depletes CCR5+ CD4+ effector memory cells to the extent that the immune system is damaged considerably. Naïve and most central memory T cells are spared by this initial assault. Frequent activation results in the proliferation of short-lived effector CCR5+ CD4+ effector cells, which can control life-threatening infections, but also provide targets for the virus. Through this process, the regenerative capacity of the immune system is strained, leading to eventual collapse (175, 376, 377).

More recently, the importance of cellular microRNAs (miRNA) in defense against a variety of viral infections has come to light. Evidence has been found that HIV-1 is also subject to cellular RNA interference and employs mechanisms to counteract it (37, 254, 457, 463, 495). The cellular proteins Dicer and Drosha have been reported to inhibit virus replication, and siRNA-mediated knockdown of their expression accelerated HIV-1 replication (457). Clusters of cellular miRNAs were reported to be upregulated in the presence of HIV-1 infection, and further analysis indicated that these miRNAs downregulated the cellular histone acetylase PCAF, a Tat cofactor known to aid HIV-1 replication (457). Other reports found an interaction of Tat with Dicer, and suggested that overexpression of Tat reduces miRNA processing in cells (36). Studies have also argued that HIV-1 encodes a miRNA capable of inhibiting viral and possibly cellular mRNAs

(341). In addition, TAR RNA may be processed into a miRNA by the cellular processing machinery (232). However, other investigators dispute these findings. They argue that exhaustive cDNA cloning of small RNA from infected cells does not yield viral siRNAs or miRNAs (271, 375), and that HIV-1 Tat does not block cellular miRNA function or RNAi against cellular genes (271).

1.3 HIV-1 lifecycle

An overview of the HIV-1 lifecycle is shown in figure 1.1

1.3.1 Binding and entry

Virus particles encountering a susceptible cell first bind to CD4 molecules on the surface of the cell (54). The normal function of CD4 is to stabilize the interaction of the T-cell receptor on the surface of T lymphocytes with major histocompatibility (MHC) class II molecules encountered on antigen-presenting cells. The C3 and C4 domains on HIV Envelope (Env) gp120 are necessary for high-affinity binding between gp120 and CD4, but a more discontinuous domain that is conformation-dependent plays a role (140). However, subsequent interaction of HIV Env with a coreceptor is essential for membrane fusion and virus entry. The coreceptors used by HIV belong to the CC or CXC families of chemokine receptors. The two most important coreceptors for HIV are CXCR4 (on T lymphocytes) and CCR5 (on macrophages) (38, 39). The HIV-1 Env V1 and V2 loops appear to influence coreceptor usage. The V3 loop on gp120 plays an important role for interaction with coreceptor, and thus influences HIV tropism (337). In addition, highly conserved regions on gp120 that are exposed upon CD4 binding are involved in coreceptor interactions (140). First, binding of CD4 to gp120 occurs, resulting in

conformational changes in gp120 that enhance interactions with the coreceptor, followed by conformational changes in HIV Env gp41 that lead to membrane fusion (337). The viral membrane directly fuses with the cellular membrane, allowing entry of the viral core into the cytoplasm (140). Alternatively, virus particles can be transferred to uninfected cells by direct cell-to-cell contact through virological synapses. These virological synapses share characteristics with immunological synapses, and HIV may use components of the immunological synapse machinery for its own spread (155, 219, 424).

1.3.2 Uncoating

The viral core enters the cytoplasm and loses its protective capsid shell, retaining some viral proteins, but this process of uncoating is not well understood. HIV-infected cells produce a high proportion of defective virus particles, and this has made study of uncoating mechanisms difficult. Studies have suggested that uncoating may be influenced by capsid protein phosphorylation (469) and cellular factors (22). The cellular restriction factor TRIM5α has been suggested to exert part of its activity by modulating uncoating of the incoming viral capsid (436, 437). Uncoating unveils the pre-integration complex (PIC) and appears to be important for delivery of the PIC to the nucleus (108). Initiation of reverse transcription can initiate within the core, but disassembly is crucial for it to progress (68, 137, 140).

1.3.3 Reverse transcription

The hallmark of retroviruses is their ability to convert single-stranded RNA genomes into double-stranded DNA, which then can be integrated into the host cell genome (310, 449, 450). The enzyme responsible for this process is reverse transcriptase (RT), which is incorporated into the virion (311, 451) together with two copies of single-stranded positive-sense viral RNAs. These RNAs are held together near their 5' ends, in part by the dimerization initiation sequence (DIS). Reverse transcription produces double-stranded DNA, termed the DNA provirus, which is transported to the nucleus as a component of the PIC containing viral structural proteins (85, 140, 381, 389). This process is discussed in more detail in section 1.6.1.

1.3.4 Integration

The double-stranded viral genomic DNA is integrated into the chromosomal DNA, becoming a part of the host cell genome. This DNA provirus then serves as a template for synthesis of viral RNA. Integration is catalyzed by the viral enzyme integrase (IN) and involves cleavage of host cell genomic DNA, ligation of viral DNA to cellular DNA, and gap repair mediated by the host cell. The integration process is well preserved across retrovirus species, and the viruses depend on the success of this process for their replication (30, 85, 140, 144, 223, 355, 356). Integration is discussed in more detail in section 1.6.2.

1.3.5 Transcription and translation

High levels of viral RNA are synthesized in an RNA polymerase II-dependent fashion, using the integrated proviral DNA as a template. The integrated HIV-1 long

terminal repeat (LTR) serves as a promoter, providing a platform for the assembly of the cellular transcription complex (366). Processivity of transcription is greatly enhanced by the viral protein Tat, which is necessary for efficient virus replication (97, 131). In addition, the viral protein Rev mediates the transport of unspliced or partially spliced HIV transcripts from the nucleus (421).

Viral structural precursor Gag (PrGag) and precursor Gag-Pol (PrGag-Pol) proteins are synthesized on free cytoplasmic ribosomes, whereas the gp160 Env precursor protein is translated in the endoplasmic reticulum. In about 5% of PrGag translation events, a frameshift occurs in the p6 region, resulting in read-through and giving rise to PrGag-Pol proteins. The truncated remainder of p6 is referred to as p6* (85, 140, 210, 358).

1.3.6 Assembly and egress

The retroviral structural polyprotein PrGag is both necessary and sufficient for the assembly of virus-like particles (VLPs) (104, 159, 178, 483). It is translated in the cytoplasm from the unspliced, full-length viral RNA transcript (140). Gag and GagPol proteins interact with cellular proteins, viral RNA, and intracellular membranes, are trafficked to assembly sites, and form progeny virions that contain two copies of the viral RNA as well as viral and cellular proteins (483). During or shortly after budding from the cell, the viral protease (PR) encoded by GagPol liberates itself by autocatalytic processing and then proceeds to cleave the Gag polyprotein into its constituents: matrix (MA, p17), capsid (CA, p24), a spacer peptide (SP1 or p2), nucleocapsid (NC, p7), a second spacer peptide (SP2 or p1), and p6 (225, 256, 307). This maturation process is

essential for viral infectivity, as are the incorporation of viral genomic RNA and the viral Env glycoproteins (85, 140, 141, 170, 202, 225, 234, 364). Maturation also results in rearrangement of the proteins within the virus particle and formation of the typical conical core (85, 140).

A body of evidence suggests that the site of virus assembly is dependent on the cell type. In T cells, assembly is thought to occur at the plasma membrane, whereas in macrophages, evidence suggests that assembly may occur at intracellular membranes in multivesicular bodies (345, 348). More recent reports have disputed this notion (129, 221, 401). The cellular targeting machinery may differ between cell types, resulting in alternate assembly sites.

1.4 Cellular post-entry blocks to HIV-1 infection

After entering target cells, retroviruses encounter blocks to various steps in replication. Two of the best-studied restriction factors facing HIV-1 are TRIM5α and APOBEC3G (140, 422).

HIV-1 does not infect cells of Old World monkey origin very efficiently, and the blocks appear to occur both before and after reverse transcription (489). The restriction factor can be saturated with high titers of affected virus, and the susceptibility determinant in HIV-1 has been mapped to the cyclophilin-binding loop within the capsid (CA) domain (350, 371, 417). Indeed, interaction of CA with CypA affects the sensitivity of HIV-1 host cell restriction (422, 423, 456). The cellular factor responsible for restriction was shown to be the cytoplasmic body protein tripartite motif 5 α (TRIM5α) (436). TRIM5α consists of a RING domain with ubiquitin ligase activity, a B-box 2

domain, a coiled-coil domain, and a SPRY domain. The SPRY domain is only present in the α-isoform of the TRIM5 proteins, and it appears to be responsible for recognizing specific CA proteins (368, 426, 438). A different variant of TRIM5 has been found in owl monkey cells, which exhibit strong anti-HIV restriction. This was shown to be mediated by a TRIM-CypA fusion protein, created by retrotransposition of the complete CypA cDNA into the TRIM5 gene (407). The CypA domain of this fusion protein recognizes HIV-1 capsids in place of the SPRY domain found in TRIM5α proteins, leading to specific and efficient restriction. The SPRY domain of TRIM5α and the CypA domain of TRIMCyp are required for the CA-specificity of restriction (266, 407, 437, 438). Studies have indicated that trimeric TRIM5α recognizes the hexameric CA lattices on the surface of capsids, involving multiple points of contact in recognition (265, 309, 414, 437). It has been suggested that TRIM5α snatches incoming viral capsids, accelerates uncoating, and targets reverse transcriptase complexes for proteasomal degradation (107, 437). Ubiquitin ligase activity of TRIM appears to play a role in restriction. Mutation of the RING finger sequences or blocking the proteasome can rescue reverse transcription, but does not relieve the infection block, suggesting that TRIM5α may inhibit virus replication at multiple steps (17, 369, 437, 489). TRIM5α itself, however, is stabilized by treatment with proteasome inhibitors (107). Interestingly, a recent study (405) indicated that TRIM5α mRNA could be upregulated by interferon α (IFN-α). This correlates with enhancement of restriction activity, suggesting an interplay between classical innate immunity and cellular restriction factors affecting retroviruses (405). TRIM5α may also be involved in degradation of Gag proteins in producer cells, as recent results have indicated (406).

Another post-entry restriction inflicted upon HIV-1 is mediated by cytidine deaminase enzymes. The proteins of the apolipoprotein B editing catalytic polypeptide 1-like protein (ABOBEC) family, in particular APOBEC3G and APOBEC3F, have been shown to cause hypermutation in HIV-1 genomes and inhibit HIV-1 replication (49, 292, 293, 323, 394, 412, 496, 498). In the absence of the viral protein Vif, APOBEC3G is incorporated into virions and may exert mutational activities directly on the packaged viral genome (49, 50, 498). Recent studies have also shown that APOBEC proteins retain antiviral activity even in the absence of cytidine deaminase activity, leading to the suspicion that they may exert additional detrimental effects on virus replication (48, 200, 201).

1.5 HIV-1 RNA

Proviral DNA serves as the template for transcription of the viral RNA. Unspliced, full-length transcripts serve as genomic RNAs as well as mRNAs for Gag and Gag-Pol translation products. Partially spliced mRNAs encode Env, Vif, Vpu, and Vpr, and multiply spliced RNAs yield Rev, Tat, and Nef (85, 140). Rev is necessary for unspliced viral RNAs to be exported from the nucleus, since the cell normally prevents unspliced RNAs from exiting (125, 140, 287).

The first 330 nucleotides of the viral RNA are highly structured (31) and contain the Tat response element (TAR) (31, 286), the primer-binding site (PBS) (31), the major splice donor site (31), the encapsidation (Psi) element (31, 188, 222), and the dimerization initiation sequence (DIS) (83, 92). Further downstream, a frameshifting motif, the central polypurine tract (PPT_C), splice acceptors, the Rev response element

(RRE) (98, 99, 289, 380), the canonical 3’ PPT (206, 340, 388), and the polyadenylation signal can be found (51, 62, 140).

Two copies of full-length retroviral RNA are specifically incorporated into virus particles (33, 42, 295, 500). The two RNA molecules included in the virion are noncovalently linked at the 5’ end of each molecule, using the DIS, a complementary sequence at the crown of stemloop 1 (SL1) (34, 252). During assembly, the viral RNA is packaged into particles, and this process depends on the Psi region of RNA as well as the CCHC motif of NC (40, 41, 188, 222, 279). The RNA has been suggested to function as a scaffold on which Gag proteins multimerize (13, 137, 140, 501).

1.6 HIV-1 nonstructural proteins

1.6.1 Reverse transcriptase (RT) and reverse transcription

During translation of the gag gene, ribosomal frameshifting occurs in 5-10% of cases, resulting in translation of PrGag-Pol (210). The viral enzymes protease (PR), reverse transcriptase (RT), and integrase (IN) are cleaved from the PrGag-Pol precursor protein. The PR domains in the PrGag polyproteins dimerize, and through autocatalytic processing, the PR enzyme liberates itself from the precursor and processes PrGag and PrGag-Pol into their constituents (326, 372, 373). One of these is the viral reverse transcriptase, RT (106). In about 50% of PrGag-Pol processing event, an additional PR cleavage site within RT is cut, yielding a truncated, 51-kDa form of the 66-kDa RT domain, lacking the C-terminal RNaseH domain (123, 270, 324, 455, 474). The p66 and p51 subunits preferentially form functional asymmetric heterodimers (2, 211, 393, 419, 474).

RT contains two enzymatic centers: A DNA polymerase that is responsible for generating the DNA provirus from the viral genomic RNA template, and RNAse H, which degrades the tRNA primer and gRNA in DNA-RNA hybrids during reverse transcription (162, 181, 235, 312, 393, 454, 474, 484).

Reverse transcription is primed by a $tRNA^{Lys}$ associated with the viral RNA (24, 25, 85, 140, 215, 340). Minus-strand synthesis initiates from this tRNA toward the 5' end of the viral genome. Concurrently, the RNA template in the newly formed DNA-RNA hybrid is digested by the RNAse H activity, leaving a short DNA fragment, referred to as 'minus-strand strong-stop DNA' (165, 409). This DNA fragment then hybridizes to the 3' end of the viral RNA genome at the R region, a short, repeated region present at both 5' and 3' ends of the genome in a reaction referred to as 'strand transfer' (363). Minus-strand DNA synthesis proceeds along the RNA template to the primer-binding site (PBS) near the 5' end of the genome. This process is accompanied by removal of RNA from the DNA-RNA hybrid by RNAse H activity, leaving only small pieces of RNA more resistant to digestion (147, 148, 162). These fragments serve as primers for plus-strand synthesis. The central polypurine tract (PPT_C) appears to be particularly important in this process in HIV. RNAse H displaces the tRNA primer after a portion of it is copied, exposing the PBS at the end of the 3' end of minus-strand DNA, and positive-strand DNA hybridizes with the homologous region at the 3' end of minus-strand DNA (140, 147).

1.6.2 Integrase (IN) and integration

A hallmark feature of retroviruses is their ability to insert a reverse-transcribed viral genomic DNA, the DNA provirus, into the host cell genome, thus establishing an infection that persists for the life of the host cell. The integration reaction is catalyzed by the viral integrase protein (IN), a 32-kDa protein generated by PR-mediated cleavage of the C-terminal fragment of the PrGag-Pol precursor protein. IN consists of an N-terminal domain that can bind zinc, a catalytic core domain, and a DNA-binding C-terminal domain, which is not very well conserved (223, 280, 459, 461, 462). IN may be involved in transport of the PIC into the nucleus in nondividing cells, but this has not been clearly demonstrated, and some studies have implicated MA and Vpr in PIC nuclear import (69, 70, 179, 464). Additionally, NC is found in the PIC and is thought to enhance the efficiency of integration (74, 140, 249, 250, 378).

The mechanism of the integration reaction is well preserved across different members of the retrovirus family. IN removes two or three nucleotides from the blunt 3' end of the linear viral DNA, catalyzes a cleavage in the cellular target DNA, followed by joining of the ends of the viral DNA to the cleaved cellular DNA. The cellular gap repair machinery then fills in gaps left by the reaction, perhaps aided by IN (140). Circular viral DNA species are also found in the nucleus of infected cells: 1-LTR circles, formed by homologous DNA recombination, and 2-LTR circles, formed by the non-homologous end-joining pathway (137, 140).

1.6.3 Tat

Tat is an essential viral protein which increases processivity of the RNA polymerase II transcription complex in virus-infected cells. Tat binds to the so-called

TAR element, a sequence downstream of the start site for viral RNA synthesis. The TAR element forms a characteristic three-dimensional RNA structure. Tat increases the steady-state levels of viral RNA in infected cells considerably, and mutagenesis of Tat results in lack of progeny virions (26, 56, 58, 94, 128, 140, 158, 228, 245, 328).

1.6.4 Rev

Viral RNAs in HIV-1-infected cells occur as unspliced genomic RNAs, which also serve as mRNAs for Gag and Gag-Pol, partially spliced RNA, which are translated into Vif, Vpu, Vpr, and Env proteins, and spliced RNAs, which encode Nef, Rev, and Tat proteins. An abundance of viral mRNA species is the result of variable usage of five splice donor sites and more than ten splice acceptor sites within the viral genome. Cellular mechanisms usually prevent the export of unspliced or incompletely spliced RNAs from the nucleus, but the viral protein Rev permits nuclear export of HIV-1 unspliced RNAs. Rev binds to the complex RNA secondary structure named the Rev response element (RRE), which is present in all unspliced and partially spliced viral mRNAs. Rev also binds to the cellular protein Crm1/exportin 1 and mediates export of its cargo via the nuclear pore complex (NPC) (125, 140, 177, 180, 285, 288, 289, 395, 421).

1.6.5 Protease (PR)

The proteolytic cleavage of Pr55Gag shortly after virus budding and the subsequent reorganization of the viral core are critical steps in formation of a mature, infectious virion (170, 234, 364). The viral protease enzyme is related to cellular aspartic protease enzymes, using two apposed Asp residues in the active site. The viral protease

functions as a dimer, with the active site in a cleft formed between the monomers (274, 308, 325, 361).

During or shortly after virion detachment from the cell, PR domains on adjacent PrGag-Pol molecules dimerize, activating the enzyme (325, 326). PR cleaves itself from the Gag-Pol precursor, likely by an intramolecular mechanism (373). PR then proceeds to cleave the remaining proteins from both Gag-Pol and Gag. The fastest cleavage appears to occur between SP1 and NC, followed by scission in the p6* transframe region, and subsequent liberation of the RT and IN enzymes (372, 373). PrGag processing proceeds in a similarly ordered fashion, with the cleavage at the N-terminus of NC being the most rapid, and the CA-SP1 cleavage being the slowest step. This orderly process is necessary for proper rearrangement of the core and infectivity of the virus (85, 170, 202, 225, 234, 364). Both overly active PR and mutations that disturb the order of processing disrupt proper virus assembly (65, 227, 281).

PR inhibitors have been employed as effective antiviral drugs in patients, usually in the combinatorial context of highly active antiretroviral therapy (HAART) (384). These inhibitors have conventionally targeted the PR active site, but newer inhibitor developments have endeavored to block target sites on protease substrates (10, 224, 262, 263, 384, 403, 420, 504-506). However, drug-resistant virus variants tend to appear during treatment, drug-resistant viruses are transmitted, and some individuals harbor viruses with a variety of drug resistances (6, 140, 384, 503).

1.6.6 Vpu

The 81-amino-acid integral membrane phosphoprotein Vpu plays a role in both degradation of the cellular surface protein CD4 and enhancing the release of virus particles (47, 258, 259, 491, 492).

Interestingly, Vpu can enhance virus release of divergent retroviruses that do not encode their own Vpu proteins (168, 359, 413). The virus release-stimulating activity of Vpu has been mapped to its N-terminal domain, and it appears to be cell-type-dependent, occurring in human T-cell lines, primary lymphocytes, monocyte-derived macrophages, and epithelial cell lines (327). Evidence suggests that Vpu may overcome a cellular inhibitor of virus release (460).

One of the pathways employed by HIV-1 for downregulating cell-surface expression of CD4 involves degradation of CD4 by the host ubiquitin/proteasome pathway and is mediated by Vpu. Vpu binds to CD4 in the ER, targeting it for destruction and releasing the viral Env protein from its interaction with CD4 and permitting continued Env transport to the cell surface. As inhibition studies have shown, proteasome activity is necessary for Vpu-mediated CD4 degradation (140, 258, 259, 442, 482, 491).

1.6.7 Vpr

Vpr interacts with a leucine-rich motif near the C-terminus of the Gag component p6 and is incorporated efficiently into virions (78, 251, 360). Vpr, a 96-amino-acid protein, stimulates gene expression from the HIV-1 LTR as well as cellular promoters (203, 321), induces arrest of Vpr-expressing cells in the G_2 phase of the cell cycle (81, 105, 189), facilitates the transport of the PIC into the nucleus of the infected cell (69, 105, 203), and induces apoptosis (212, 432, 433, 493). Vpr may promote nuclear import of the

PIC by interacting directly with nucleoporins (134, 253, 379). Additionally, Vpr also contains a nuclear export signal (NES), permitting it to shuttle between the nucleus and the cytoplasm (415, 416). Interestingly, Vpr mutations have been observed in HIV-1 strains isolated from long-term non-progressors, indicating its importance in *in vivo* HIV-1 replication (140, 404, 425).

1.6.8 Vif

Most lentiviruses express Vif. Mutations in Vif or its absence can cause defects in virus infectivity, resulting in failure to reverse-transcribe the viral genome (161, 427, 465). Vif counteracts the effects of cellular restriction factors, the members of the cytidine deaminase family of the apolipoprotein B mRNA-editing enzyme catalytic polypeptide 1-like protein (ABOBEC) family, especially ABOBEC3G (124, 140, 283, 284, 292, 293, 394, 411), as discussed above.

1.6.9 Nef

The Nef protein is incorporated into the viral core (66, 238, 476, 478). It is a 27kDa membrane-associated phosphoprotein containing a basic domain within its N-terminus and is myristoylated. Nef has been implicated in downregulation of CD4, MHC-I, and MHC-II molecules from the cell surface (11, 18), enhancement of virus infectivity (8, 12, 114, 122, 502), and involvement in cell-to-cell spread via virological synapses in association with the cellular kinase ZAP-70 (140, 424). Nef downregulates CD4 from the cell surface by connecting it with the endocytic machinery and then targeting it to the lysosome (11, 140).

1.7 HIV-1 structural proteins

The HIV-1 Gag protein is initially synthesized as a polyprotein consisting of the MA, CA, SP1, NC, SP2, and p6 domains, and myristoylated at its N-terminus (64, 444, 483). This polyprotein mediates assembly of virus-like particles (159, 178, 226, 418, 483). The viral protease cleaves PrGag into its constituents during or shortly after nascent virions bud off from the producer cell. This processing is referred to as maturation and is a requisite for particle infectivity (85, 170, 202, 225, 234, 364). A schematic of the Gag polyprotein is displayed in figure 1.3.

1.7.1 Matrix

The 132-amino-acid matrix (MA) domain consists of a globular head formed by four α-helices and an α-helix projecting away from the core of the protein (298). Crystal structures have usually yielded MA trimers (195, 299), although newer studies have proposed hexamer arrangements for MA (14). MA monomer and trimer models are shown in figure 1.4.

The MA domains within Pr55Gag function in directing Gag to membranes as well as in facilitating incorporation of Env glycoproteins into particles (85, 132, 140). During translation of PrGag, the N-terminal methionine residue is removed, and a myristic acid is attached to the subsequent glycine residue. A part of the affinity of MA for membranes is due to its myristoylation, and lack of myristoylation has detrimental effects on virus assembly (64, 444, 470). A patch of basic amino acids between residues 15 and 40 within

MA have also been proposed to play a role in Gag-membrane binding by interacting with negatively charged phospholipids on the inner leaflet of the lipid bilayer (138, 344, 348). Phosphatidylinositol-(4,5)-bisphosphate ($PI(4,5)P_2$) has been shown to interact tightly with MA, providing a membrane-targeting signal and anchor, as well as being involved in a myristyl switch mechanism (344, 352, 400, 401, 428, 508). Depletion of $PI(4,5)P_2$ results in disruption of particle assembly (401). MA may not only provide a membrane-targeting signal for virus assembly, but also determine specificity of membrane targeting (140). HIV-1 assembly on the plasma membrane primarily occurs in detergent-resistant, cholesterol-rich lipid raft domains (63, 218, 333, 401).

The MA domain in the context of full-length Gag binds more tightly to membranes than the mature MA protein, due to the exposed myristate (508). Gag multimerization may lead to an increase in the myristate-exposed conformation of the MA domain, resulting in enhancement and/or stabilization of membrane binding during assembly of the virus particle. It has been proposed that a conformational switch (myristyl switch) after maturation leads to sequestration of the myristate moiety, resulting in partial release of MA from the membrane in the mature, extracellular particle (194, 344, 352, 400, 401, 428, 444, 508).

The MA domain associates with the Env glycoprotein and mediates its incorporation into virus particles (95, 139, 142, 319). The cellular adaptor protein TIP47 appears to be involved in this process, interacting with both MA and Env, and these three proteins have been shown to form a ternary complex (275). Interestingly, Gag proteins with large deletions in the MA domain can still yield partially infectious virus, as long as the myristoylation signal is retained and a pseudotyped envelope glycoprotein or an HIV-

1 Env with a gp120 C-terminal deletion is provided (290, 470, 473). These results suggest that in spite of the various functions assigned to MA, an intact MA protein is not absolutely required for virus replication. Myristoylated deletion mutants were able to target the residual Gag protein to membranes and mediate virus assembly. MA is needed for Env incorporation, but heterologous viral glycoproteins or Env proteins with deletions in the long C-terminal tail responsible for virion incorporation are capable of being incorporated into nascent virions (113, 290, 473).

MA has been shown to associate with a variety of other cellular proteins. The N-terminal domain of MA binds to the δ subunit of AP-3, and this interaction may be important for Gag localization to multivesicular bodies (111). Evidence also has shown that residues at the C-terminus of MA mediate PrGag association with the μ subunit of the clathrin-associated adaptor complex AP-2, but that PrGag processing eliminates this interaction (29). Inhibition of the MA-AP-2 interaction increased virus release from producer cells, consistent with the known role of AP-2 in internalization of cargo from the plasma membrane (29). Moreover, MA also binds the cellular motor protein KIF-4, as do matrix proteins from several other retroviruses. This interaction may be involved in subcellular distribution of Gag proteins (448).

The pathways by which Gag proteins are trafficked to productive assembly sites are under scrutiny by various groups. Gag may be directly targeted to plasma membrane sites (129, 221, 401). Alternatively, Gag may associate with intracellular membranes, such as multivesicular bodies (MVBs), and then be delivered to the plasma membrane (PM) by vesicles (121, 268, 344, 345, 348). As evidence exists for both pathways, it is also possible that the itinerary followed by Gag proteins depends on the context and cell

type in which assembly occurs, and components of both transport methods may be involved in productive assembly (172, 221, 345).

A number of studies have also proposed post-entry roles for MA, and it has been reported to be a part of the PIC (71). A putative nuclear localization signal (NLS) was found in the N-terminal domain of MA, which appeared to interact with Importin-α and aided import of the PIC into the nucleus of nondividing cells (70, 149, 179, 464). However, further studies have demonstrated that viruses lacking the MA NLS are capable of infecting nondividing cells (190).

1.7.2 Capsid

The mature capsid protein forms the outer layer of the typical conical core found within HIV-1 particles (85). This protein consists of an N-terminal domain (NTD) comprised of amino acids 1-146 and a smaller C-terminal domain (CTD) (residues 148-231), connected by a short, flexible linker sequence (85, 132, 140). C-terminal to the capsid domain, a short spacer peptide, SP1, also referred to as p2, separates CA from the NC domain (242). The NTD contains seven α-helices and two β-hairpins, whereas the CTD is composed of four α-helices (152, 314, 487). Diagrams of the NTD and CTD are shown in figures 1.5 and 1.6, respectively.The C-terminal domain contains the major homology region (MHR), a region that conserves significant amino acid identity between divergent retroviruses, and plays an important role in CA dimerization (112, 291, 382). Mutations in the MHR have significant effects on particle production and core structure, however, mutant Gag proteins are still capable of associating with wildtype Gag proteins (140, 291).

Capsid proteins can engage in *in vitro* assembly into tubular or spherical forms, depending on solution pH (120, 154, 173, 466). CA-NC proteins are capable of assembly into conical shapes in the presence of RNA or under high-salt conditions (153). PrGag proteins lacking a portion of MA and p6, but retaining CA, SP1, NC, and SP2 were shown to form tubes as well as cones at pH 6.0, but mostly spheres at pH 8.0, with an increasing ratio of spheres to tubes with increasing solution pH between 6.0 and 8.0. However, at pH 9.0, no ordered structures were observed. Further data indicated that no major shift in protein structure was taking place in response to shifting pH (174). Mature CA, on the other hand, tends to form dimers at pH 6.6 and below, at pH 6.8 spheres are found, and at pH 7.0, tubes predominate. At higher pHs, both tubes and spheres exist (120). The morphological switch of CA multimers over a narrow pH range led to the idea of a histidine switch model. In this view, the protonation of one or several histidine residues may promote a conformational switch (120). CA contains five His residues, three of which are highly conserved (244). The His residues are modeled to be surface-localized and not part of α-helices and β-sheets (151, 160, 314). Protonation of H12 or H62 might weaken dimer-dimer interfaces, whereas changes of H84 or H87 may affect proximal α-helices (120).

In the virus assembly context, CA domains within Pr55Gag are thought to dimerize and form hexameric rings of CA dimers (209, 300, 488). Cryotomography studies of immature virions have suggested that ordered Gag lattices do not cover the entire particle, but are interspersed with disordered regions (488). Virus maturation, the rearrangement of the viral core achieved by PR processing, transforms the EM appearance of the virion from having a doughnut-shaped, electron-dense ring underneath

the membrane to having a distinct conical core (300, 488). Upon proteolytic processing, the tight CA packing gives way to a looser structure, in which CA N-terminal domains form hexameric rings that are connected to each other by dimeric interactions mediated by the CA C-terminal domains (300). Mature CA forms a hexagonal lattice forming a conical core closed by 12 ‘pentameric defects’ and involving less-dense CA protein spacing than the immature arrangement (61). The viral core, however, does not simply form by condensation of the immature, radial arrangement of Gag proteins, but rather results from a completely new arrangement of CA proteins separated from their neighboring Gag domains. Studies have suggested that CA hexamers grow from one end of the core, until they encounter the membrane as a barrier and proceed to close off the structure (35, 59). CA hexamer models for immature and mature arrangements are shown in figure 1.6.

Interestingly, it appears that more Gag is packaged into virus particles than is necessary for capsid core formation. About 5000 Gag proteins are thought to be assembled into a virus particle, whereas a core contains only about 1500 capsid proteins. Virions containing more than one core have been observed frequently after maturation, and the virus particle contains a large amount of capsid protein which is not incorporated into the electron-dense core (60, 248).

Optimal core stability is crucial for viral infectivity. The immature particles are relatively resilient, whereas the mature cores are prone to disassembly and difficult to isolate (133, 477). This behavior serves the virus well, allowing the assembly of a sturdy core for exiting the producer cell, then allowing a dissociation of CA from the ribonucleoprotein complex contained within the core after fusion of the virus with the

target cell and continuation of the lifecycle. Mutational analysis has shown that mutations affecting core stability can be detrimental to virus infectivity (133, 410).

The SP1 spacer peptide, modeled as an α-helix, serves to stabilize the immature structure. SP1 appears to be critical for proper assembly and infectivity. It regulates scission efficiency and acts as a 'maturation switch' upon being proteolytically cleaved from the CA CTD, allowing a rearrangement resulting in the formation of a mature core. The CA-SP1 cleavage is the slowest step in Gag processing (3, 174, 332, 374, 488). The other 'maturation switch' results from the cleavage between the MA domain and the CA NTD. This cleavage releases the CA NTD from membrane-bound MA and promotes restructuring and core formation (140, 300, 445).

HIV-1 CA is known to associate with a number of cellular proteins, including the peptidyl-prolyl-*cis*-*trans*-isomerases cyclophilin A (CypA) and cyclophilin B (278, 453). CypA is selectively packaged into virus particles and binds to a region in the N-terminal domain of CA known as the cyclophilin loop. CA residues G89 and P90 fill the active site of CypA, and the peptidyl-prolyl bond between G89 and P90 undergoes isomerization. However, the significance of the isomerization reaction is not known (7, 67, 115, 151, 278, 422, 453).

The cyclophilin loop of CA has been mapped to be the determinant of host cell restriction mediated by the cellular protein TRIM5α (349, 350, 414). But even though CypA from the producer cell is specifically incorporated into the virus particle, more recent results have suggested that only CypA from the target cell is of importance for virus infectivity (186, 480).

1.7.3 Nucleocapsid

The HIV-1 nucleocapsid (NC) protein consists of 55 amino acids. NC contains two zinc-finger motifs of the CCHC type, which are brought together by a basic, flexible linker domain. In PrGag, two small spacer peptides, SP1 and SP2, are located N-terminal and C-terminal to the NC protein domain, respectively (140, 260).

A major function for the highly basic NC protein of HIV-1 Gag consists of binding nucleic acids and incorporating the HIV-1 genomic RNA into virus particles (42, 279), and the CCHC motifs are important for the specificity of this function (40, 41, 163, 222, 294, 500). Retroviral NCs have also been implicated in RNA dimerization (91, 126, 260, 306), reverse transcription (16, 45, 250, 260, 267, 362), and integration (74, 93, 249, 250, 260, 378). Virus replication requires the basic residues as well as the zinc fingers (260). NC can interact with nucleic acids in sequence-specific as well as sequence non-specific manners (42). It appears that specific binding of NC to the HIV-1 RNA depends on the secondary structure adopted by a region of the viral genomic RNA between the 5'LTR and the Gag initiation codon, a sequence known as the packaging signal, the Psi region, or the encapsidation element, consisting of RNA stem-loops SL2 and SL3 (140, 188, 260).

NC has been suggested to play a role in Gag multimerization, possibly due to its RNA binding properties, which then promote assembly of Gag proteins on an RNA scaffold (140). Replacement of the NC domain by cysteine and treatment with crosslinking agents allows assembly of virus-like particles, indicating that dimerization of Gag proteins mediated by NC binding to an RNA scaffold may be an early step in virus assembly (13, 137). Moreover, replacement of NC by dimerization domains has led to

successful assembly of virus-like particles, confirming the notion of NC functioning as an assembly scaffold (4, 216, 501).

The nucleic acid chaperone activity of NC has also been implicated in catalyzing refolding of nucleic acids during reverse transcription and contributing to placement of the $tRNA^{Lys3}$ primer on the RNA primer binding site (PBS), unwinding of the tRNA during initiation of reverse transcription, increased efficiency of minus-strand transfer, removal of annealed RNA fragments, destabilization of nucleic acid secondary structure, stimulation of plus-strand transfer, and promotion of integration of viral DNA (74, 140, 249, 260, 378).

1.7.4 P6

The C-terminus of HIV-1 Gag consists of a proline-rich protein termed p6, which plays a role in a late step in the virus budding process by interacting with cellular factors (297, 435, 439, 468). P6 mutants result in production of particles that fail to detach from the plasma membrane in many cell types (169, 205). This release function maps to a highly conserved Pro-Thr-Ala-Pro (PTAP) motif near the N-terminus of p6. This PTAP motif is an example of a so-called late domain. Retroviral late domains appear to interact with components of the host endosomal sorting machinery as well as cellular ubiquitination factors, promoting virus release from the PM or into the MVB (171, 370, 387, 468). The cellular protein Tsg101, a component of the ESCRT-I complex, interacts with p6, and this interaction is dependent on the PTAP motif (247). Disruption of the endosomal sorting pathway results in defects in particle release (140, 156). Additionally, p6 is responsible for the incorporation of Vpr into virions. Deletions and mutations in p6

can prevent incorporation of Vpr (237, 277, 360). This interaction is dependent on an LXXLF motif within p6 (78, 236). Binding studies have indicated a direct interaction between the p6 domain and Vpr (23, 78, 140, 213). In about 5-10% of cases, a -1 frameshift occurs during translation of the mRNA in the p6 region, giving rise to PrGag-Pol. The p6 region in this protein is referred to as p6* to distinguish it from p6 in the context of Gag (210, 358).

1.7.5 Env

The viral Env glycoprotein precursor is synthesized as a 160kD integral membrane protein, gp160 (43, 240). Glycosylation occurs cotranslationally, and gp160 oligomerizes in the ER (43, 44, 240). Trimerization appears to be predominant, but dimers and tetramers have also been observed (77, 109, 110, 117, 118, 276). In the Golgi complex, proteolytic cleavage of gp160 by cellular enzymes, such as furin or furin-like proteases, results in the production of the mature surface (SU) and transmembrane (TM) glycoproteins, gp120 and gp41 (353, 431). Proper cleavage of Env is required for fusion and virus infectivity (140, 176). A noncovalent association of gp120 and gp41 is critical for the transport of the Env complex to the cell surface (193). The gp120-gp41 complex is rapidly internalized after its arrival on the cell surface, which may help infected cells evade the host immune response (140).

Env glycoproteins are incorporated into virus particles, likely by direct interactions with MA (95, 113, 139, 142, 319). The cellular protein TIP47 appears to be included in a ternary complex with MA and Env and may be required for the interaction of MA and Env (275). The cytoplasmic tail of gp41 is necessary for association of Env

with Gag in the immature virus (113, 139, 142). This C-terminal region has also been implicated in inhibition of fusion of immature virions with target cells. The ability of virions to fuse with target cells had been shown to depend on maturation of the virus, but C-terminal truncations of Env relieved this block (95, 214).

1.8 Virus structures and HIV-1 cores

Viruses form specific structures to protect their genomes during transmission from one cell to another. These structures have to be able to encase the nucleic acids, but must also consist of subunits simple enough not to require significant coding capacity. Crick and Watson initially proposed that the basic structural requirement for a virus shell would be to provide a protective container for its nucleic acid. They thought that virus shells would be highly symmetric objects (90). Based on studies done on plant viruses and small animal viruses, they proposed the hypothesis that "a small virus contains identical subunits, packed together in a regular manner" (90). The packing arrangements of the individual subunits would be repetitive, leading to the building of an object with considerable symmetry (90). Caspar and Klug stated that there were a limited number of efficient designs virus shells could adopt if constructed from many small subunits (75). They also proposed that self-assembly of viral structural proteins resembled crystallization, in that protein subunits came together to form a virus particle, this being their lowest energy state (75). Their predictions for self-assembly of viral structural proteins were confirmed, as later studies of *in vitro* assembly of viral structural proteins have shown (14, 73, 120, 127, 173, 174, 209, 301, 302, 305, 477, 510).

The major structure types formed by virus particles are helical and icosahedral arrangements. Helical structures are organized around a single central axis, and protein subunits coil around the axis and the encased genome, most commonly negative-stranded RNA, and terminate in a capping structure at both ends (75, 132). Icosahedral arrangements of virus cores are more common. An icosahedron consists of twenty triangular faces, and icosahedral bodies contain twofold, threefold, and fivefold symmetry axes. Using icosahedral symmetry, sixty identical subunits can build a virus particle, and this occurs in several small viruses. However, many viruses require larger containers, and those are constructed by a number of viruses by using more subunits. These subunits cannot be all identically situated, but by slight deformations of the bonds, they can be arranged in a nearly equivalent way. The concept of 'quasiequivalence' was put forth by Caspar and Klug (75). A number of viruses employ quasiequivalent designs in their shells. The possible ways of subdividing an icosahedral shell for quasiequivalent subunit arrangements are given by the triangulation number, T, where $T=Pf^2$, and $P=h^2+hk+k^2$, f is any integer, and h and k are zero or positive integers having no common factor. The number of structural subunits is given by S=60T (75, 132, 183). Caspar and Klug were inspired by the work of Buckminster Fuller, whose geodesic domes had attained some fame. The resemblance of these efficiently designed structures to icosahedral viruses led them to their models for virus structures (75).

Closely packing morphological units on the surface of a shell is accomplished efficiently by using hexamers and pentamers. Twelve pentamers are needed for a three-dimensional structure to be closed off, since using only hexamers would deform the structure toward a plane. A shell to accommodate the needs of the virus could be

assembled from hexamers and pentamers (75). In the case of HIV-1, virions initially are assembled as immature particles, formed by radially arranged PrGag proteins. MA domains are found close the membrane, and the C-terminal regions of PrGag are located towards the center of the virion (146, 481). A recent study has modeled myristoylated, membrane-bound MA and MACA proteins as hexamers (14). The central CA domain appears in hexamer arrangements (300, 488). Some of the surface area, however, appears disordered. It is not clear whether the original Gag lattice incorporates pentamers. These may be included in ordered sections (488). The structure of the SP2 region is not quite clear at this point, but it may be included in an α-helical arrangement involving the C-terminal residues of CA and stabilizing CA hexamers in the immature lattice (488). During or shortly after virus budding, proteolytic processing of Gag results into rearrangement of the viral core into a mature virion (140, 307).

A number of studies had suggested icosahedral symmetry for the mature capsid structure of HIV-1 (196, 329). However, several studies reported particles seen by electron microscopy were ‘teardrop-shaped’ (164, 316). Further studies established the model of a conical HIV-1 core. Its outer shell is composed of a hexameric lattice of CA proteins, capped by subsurfaces of buckminsterfullerenes, as observed for elemental carbon structures (243), and containing pentameric ‘defects’ to close the structure. A total of 12 pentamers are needed to close off the structure. From Euler’s theorem, the cone angles of a conical hexagonal lattice are quantized into allowed angles. These are defined by $\sin(\theta/2)=1-(P/6)$, where θ is a cone angle, and P corresponds to the number of pentamers required to close off the narrow end of the cone. Ganser et al. proposed that seven pentamers are incorporated into the wide end, and five pentamers into the narrow

end of the conical core, giving a cone angle θ=19.2˚ (35, 61, 153, 183). A model for such an HIV-1 core is shown in figure 1.8.

1.9 Antiviral agents and assembly inhibitors

Antiviral agents have become an important part in combating the AIDS epidemic. Most commonly, inhibitors of the viral enzymes protease and reverse transcriptase are in use, sometimes combined with entry inhibitors. Clinical trials are under way for integrase inhibitors (230, 384). Another step of the virus life cycle, virus assembly, presents itself as an interesting target for antiviral compounds. Phage display screening studies have led to the characterization of a peptide capable of binding to the C-terminal domain of CA and inhibiting assembly of immature HIV-1, as well as of mature particles, in vitro (434, 452). Gag-derived peptides have also been used to target Gag interfaces and inhibit virus assembly (157, 198, 334). Compounds capable of binding to the NTD of HIV-1 CA have been shown to inhibit maturation and thus interfere with infectivity (230, 443). Maturation can also be impaired by derivatives of betulinic acid, such as PA-457, which bind to the C-terminal domain of CA and prevent scission at the CA-SP1 site (204, 224, 262, 263, 403, 504-506). Interestingly, the mechanism of action of these compounds was discovered by revertant analysis (6, 263). Certainly, much work remains to be done in finding virus assembly inhibitors or compounds that may interfere with virus structure.

1.10 Overview and aims

Our laboratory has been studying the assembly properties of retroviruses for many years. The following chapters present studies seeking to shed light on capsid-capsid

interactions and the role of a highly conserved residue in virus structure, and investigations into intracellular Gag trafficking and Gag-membrane interactions in particle production. In addition, the appendix presents work on finding and characterizing potential small-molecule assembly inhibitors.

As a portion of the HIV PrGag protein, the CA NTDs and CTDs collaborate with each other and with other Gag domains to facilitate virus assembly and budding. Interactions between CA domains are necessary not only for assembly and release, but also for proper maturation and post-maturation replication steps. In vitro experiments suggested an unusual pH-dependent behavior in terms of the structures assembled by HIV-1 Gag proteins. At pH 6.0, PrGag-like proteins were shown to assemble long tubes, whereas at pH 8.0, spheres were formed (174). With mature CA, dimers predominate at pHs below 6.6, spheres predominate at pH 6.8, and tubes are the major form at pH 7.0, while tubes and spheres may coexist at higher pHs (120). The assembly activities of CA in the pH 6.5 to 7.0 range have led to the speculation that capsid assembly or disassembly may involve a histidine switch, perhaps involving one of the three conserved of the five total capsid histidines (120). For this reason, we examined substitutions at H84, and found that replacements of histidine with other amino acids resulted in a loss of infectivity, but CypA incorporation as well as viral RNA and RT levels were not affected. Mutant virus particles contained aberrant cores. The exception was the H84Y mutant, which retained a reduced level of infectivity. This suggested that H84 may be involved in stabilizing aromatic interactions with nearby tryptophan residues W80 and W133 in α-helices 4 and 7 to promote proper structure.

One function of the MA domain of HIV-1 PrGag consists of targeting PrGag proteins to membrane assembly sites. MA also facilitates incorporation of HIV Env proteins into virus particles. To examine the specific requirements for the MA membrane-binding domain (MBD) in HIV-1 assembly and replication, we chose to investigate viruses in which MA was replaced by alternative MBDs. We found that the pleckstrin homology domains of AKT protein kinase (AKT-PH) and phospholipase C δ1 (PLC-PH) efficiently directed the assembly and release of virus-like particles (VLPs) from cells expressing chimeric proteins. To a lesser extent, VLP assembly and release was mediated in a phorbol ester-dependent fashion by the cysteine-rich binding domain of phosphokinase C γ. Although alternative MBDs permitted assembly and release of VLPs, the resultant viruses were not infectious. Interestingly, PrGag processing was reduced, while cleavage of GagPol precursors resulted in the accumulation of Pol-derived intermediates within virions. Our results indicate that the HIV-1 assembly machinery is flexible with regard to its means of membrane association, but that alternative MBDs can interfere with the production of infectious virus cores.

Analogous to our studies involving residue H84 of HIV-1 CA and its importance in virus assembly and maturation, we have begun to examine the function of another highly conserved histidine residue within the N-terminal CA domain, H62. Constructs encoding alternate amino acids were made, and initial results indicate that the replacement mutants are not infectious. The notable exception is H62Y, which retains some infectivity. Preliminary results are presented in Appendix 1.

Our laboratory also has been engaged in the study of potential HIV-1 virus assembly inhibitors. We have screened about 3000 candidate compounds, and proceeded

to analyze further several promising candidates. One substance, termed NCI#75541, may affect virus particles after they have been assembled. Further experiments are under way to examine the mechanism of its action, and preliminary results are presented in Appendix 2 of this thesis.

1.11 Figures

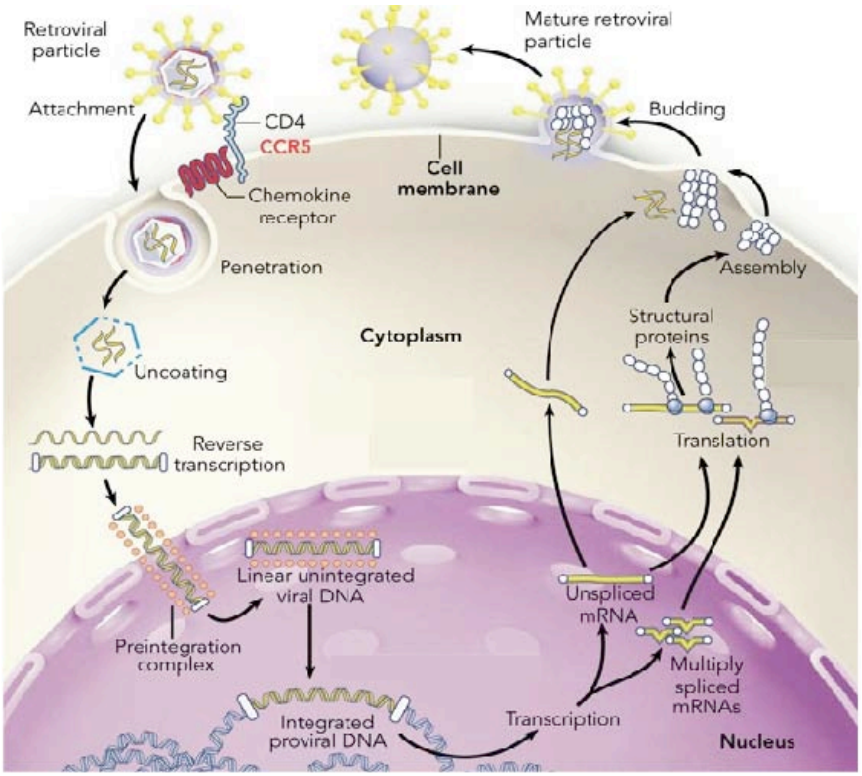

Figure 1.1
Overview of the retrovirus lifecycle
Virions attach to CD4 and a coreceptor and are internalized. Uncoating, reverse transcription, and integration follow. Virus genes are transcribed and translated by the host cell. PrGag proteins associate with membranes and RNA to assemble virus particles, which mature shortly after budding.
Adapted from Furtado et al., N Engl J Med 1999;340(21):1614-22

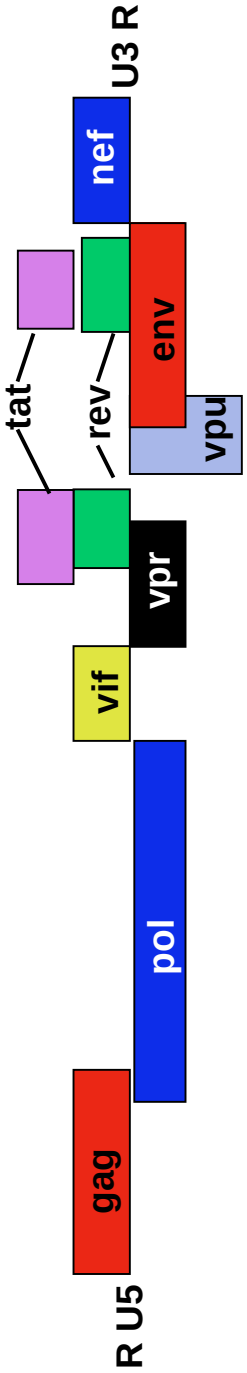

Figure 1.2
Overview of the HIV-1 RNA genome

Figure 1.3
Diagram of Pr55Gag
PrGag contains the matrix (MA), capsid (CA), spacer 1 (SP1), nucleocapsid (NC), spacer 2 (SP2), and p6 domains.
Proteolytic cleavage sites are indicated by vertical lines.

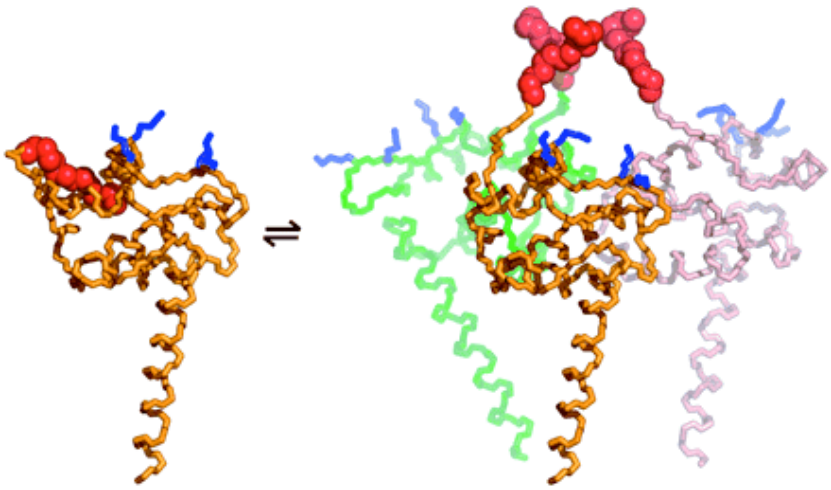

Figure 1.4
Models of MA monomer and MA trimer
On the left, a MA monomer with a sequestered myristate (in red) is shown. On the right, a proposed MA trimer with exposed myristates is displayed.
Taken from Tang et al., PNAS 2004; 101(2): 517-522

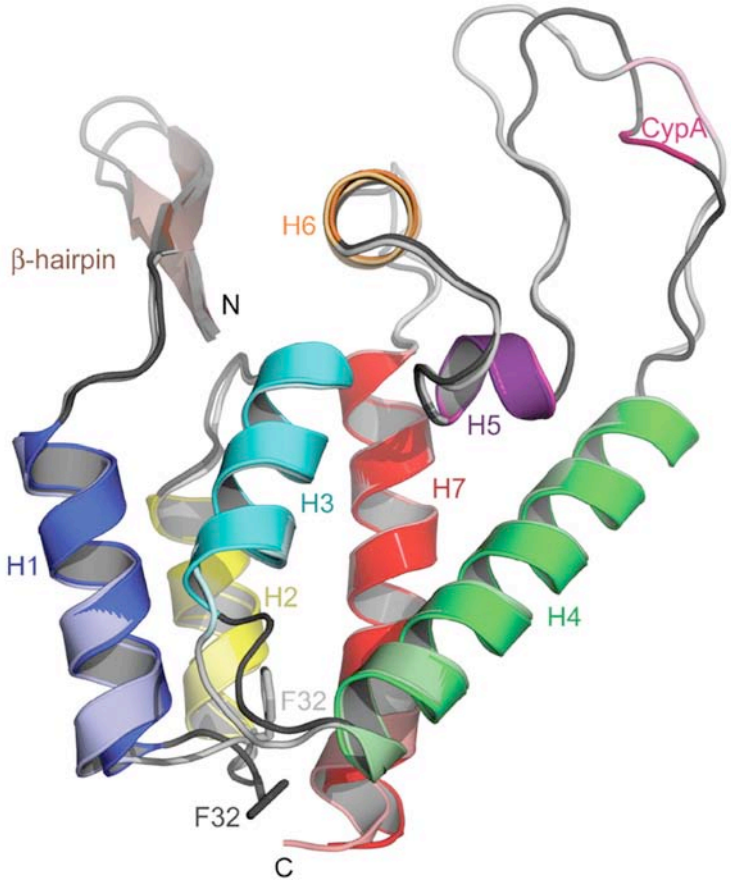

Figure 1.5
Model of HIV-1 CA N-terminal domain
The N-terminal b-hairpin is depicted on the upper left, the C-terminal linker to the C-terminal domain of CA is shown at the bottom.
Taken from Kelly et al, J Mol Biol 2007; 373(2):355-366

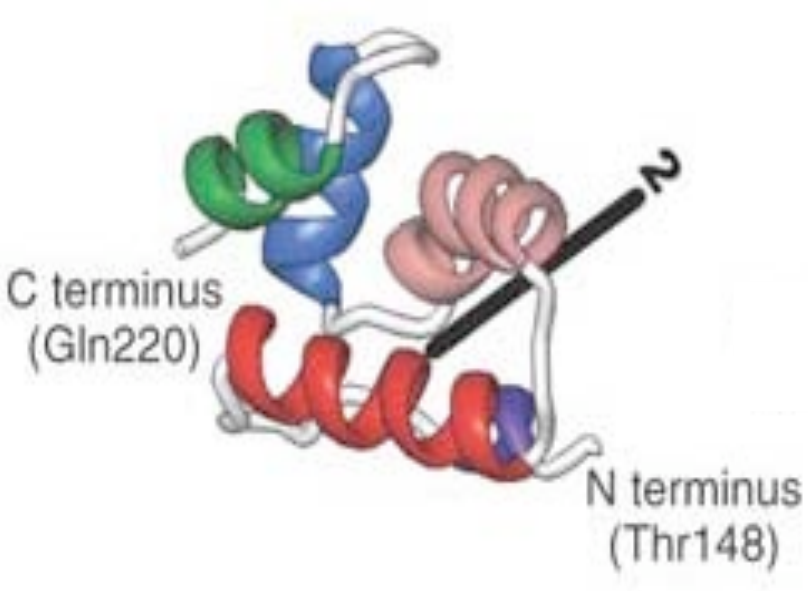

Fig. 1.6
C-terminal domain of HIV-1 CA
The N-terminus connecting to the N-terminal domain of CA and the C-terminus are indicated. The two-fold rotation axis is marked by the black bar.
Taken from Ternois et al., Nat Struct Mol Biol 2005 12, 678-682

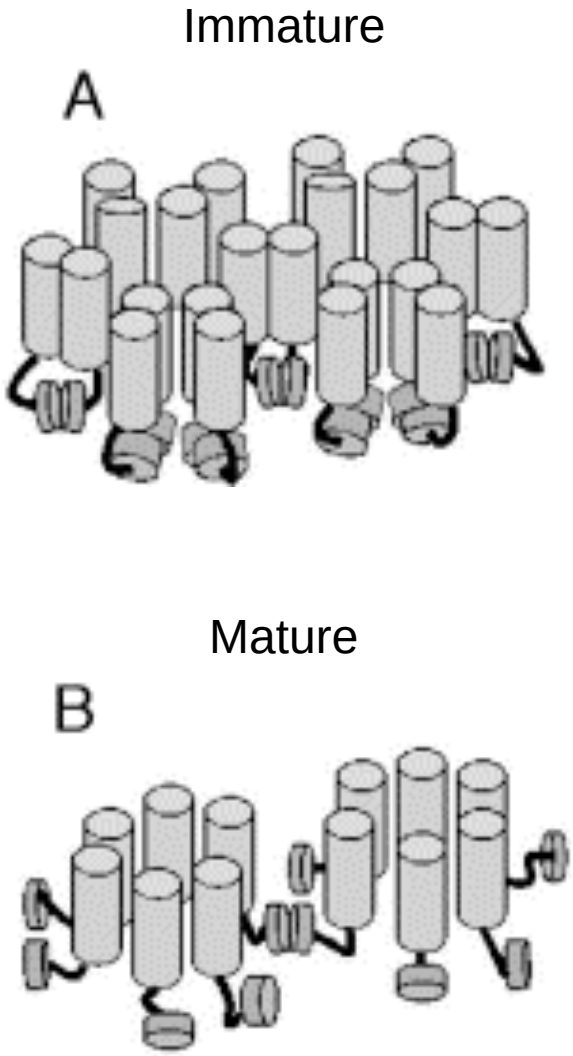

Figure 1.7
Proposed retrovirus capsid arrangements
In this model, the immature arrangement of CA subunits (top) gives way to a more loosely packed arrangement of CA in the mature particle (bottom). The mature arrangement consists of N-terminal hexamer rings linked by C-terminal dimeric contacts.
Taken from Mayo et al., J Mol Biol 2003; 325(1):225-237

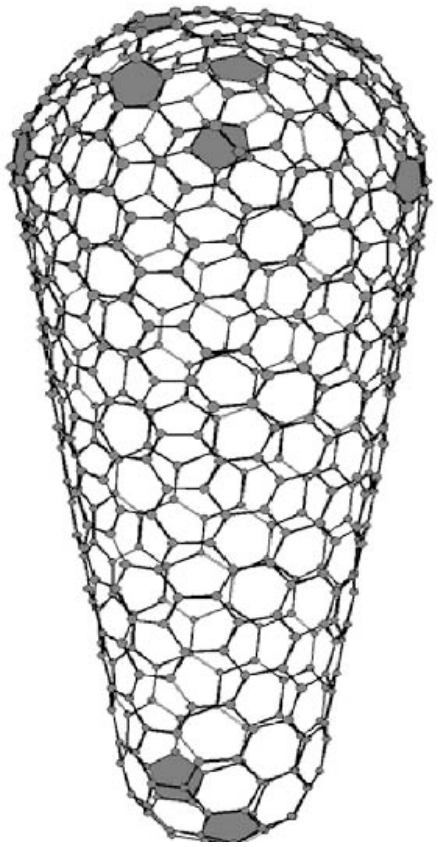

Figure 1.8

Model of a conical HIV-1 core

Stereoview of a capped fullerene core, containing 252 hexagons and 12 pentagons (shaded). The wide end of the core includes 7 pentagons, the narrow end 5.

Taken from Ganser et al., Science 1999; 280: 80-83

Chapter 2

Virus Particle Core Defects Caused by Mutations in the Human Immunodeficiency Virus Capsid N-Terminal Domain

Isabel Scholz, Brian Arvidson, Doug Huseby, and Eric Barklis

Chapter 2 has been published.

J Virol; Feb. 2005; 79:1470-9

Statement of contribution

For chapter 2, I acquired the data shown in figures 1, 3, 5, 6, 7, 10, and table 1. I contributed to the data shown in figures 4 and 9.

2.1 Abstract

The N-terminal domains (NTDs) of the human immunodeficiency virus type 1 (HIV-1) capsid (CA) protein have been modeled to form hexamer rings in the mature cores of virions. In vitro, hexamer ring units organize into either tubes or spheres, in a pH-dependent fashion. To probe factors which might govern hexamer assembly preferences in vivo, we examined the effects of mutations at CA histidine residue 84 (H84), modeled at the outer edges of NTD hexamers, as well as a nearby histidine (H87) in the cyclophilin A (CypA) binding loop. Although mutations at H87 yielded infectious virions, mutations at H84 produced assembly-competent but poorly infectious virions. The H84 mutant viruses incorporated wild-type levels of CypA and viral RNAs and showed nearly normal signals in virus entry assays. However, mutant CA proteins assembled aberrant virus cores, and mutant core fractions retained abnormally high levels of CA but reduced reverse transcriptase activities. Our results suggest that HIV-1 CA residue 84 contributes to a structure which helps control either NTD hexamer assembly or the organization of hexamers into higher-order structures.

2.2 Introduction

A number of functions have been attributed to the human immunodeficiency virus type 1 (HIV-1) capsid (CA) protein. As a portion of the HIV Gag precursor (PrGag) protein, the CA N-terminal domains (NTDs) and C-terminal domains (CTDs) collaborate with each other and with other Gag domains to facilitate virus assembly and budding (20, 80, 85, 112, 133, 151-154, 160, 174, 291, 303, 314, 385, 445-447, 466, 467, 470, 477).

Appropriate CA-CA contacts are necessary not only for assembly and release, but also for proper maturation and postmaturation replication steps (80, 85, 112, 133, 154, 174, 291, 303, 446, 447, 467, 470). Indeed, a variety of HIV-1 capsid mutations have manifested defects in early replication events, such as uncoating and reverse transcription (85, 133, 154, 291, 446, 447, 470). Some of these defects may be attributable to altered interactions with cellular factors, such as cyclophilin A (CypA) (5, 9, 55, 80, 447), and host susceptibility factors, such as Ref1, Trim5, and Lv1 (46, 88, 135, 151, 184, 318, 436).

In terms of a structural role within virions, CA NTDs appear to assemble hexamer rings that are linked via CTD connections (27, 153, 154, 264, 300, 330, 331, 466); evidence suggests that the NTD rings are more tightly packed in immature than in mature virions (300), implying that more CA is assembled into particles than is necessary to build a mature virus core. In vitro experiments have demonstrated unusual pH-dependent characteristics in terms of the structures assembled by HIV-1 Gag proteins. At pH 6.0, PrGag-like proteins have been shown to assemble long tubes, whereas at pH 8.0, spheres are formed (174). The behavior of mature CA is even more complex in that CA dimers predominate at pHs below 6.6, spheres predominate at pH 6.8, and tubes are the major form at pH 7.0, while tubes and spheres may coexist at higher pHs (120). The assembly activities of CA in the pH 6.5 to 7.0 range have led to the speculation that capsid assembly or disassembly may involve a histidine switch, perhaps involving one of the three conserved (H12, H62, and H84) of the five total (H12, H62, H84, H87, and H226) capsid histidines (120).

In light of the histidine switch model, we chose to examine the effects of five substitutions at the HIV-1 CA H84. This residue was of interest because it has been modeled at the outsides of NTD hexamer rings (153, 154, 264) in a position which could modulate hexamer packing differences in immature and mature virions (300). As a control, we also tested substitution effects at the nearby CA histidine 87, a less-well-conserved residue in the CypA binding loop. As expected, a cysteine substitution at H87 had only minimal effects on viral infectivity. In contrast, four of the five H84 mutations were noninfectious, and one of these (H84A) demonstrated dominant negative effects on wild-type (wt) virus infectivity. The exceptional mutation, H84Y, produced virions that were still 30-fold less infectious than wt virions. Detailed comparison of 84A, 84Y, and wt virions showed that the mutant virions were released efficiently from cells, had normal levels of viral genomic RNA and total reverse transcriptase (RT) activity and, in contrast with other reported NTD mutants (440, 447), carried wt levels of CypA. Although H84Y virions had wt levels in entry assays (76, 318), the H84A mutant showed slightly reduced entry signals and morphologically aberrant virus cores. Moreover, both mutants exhibited low RT-to-CA ratios in virus cores and appeared sensitive to proteolytic cleavage near NTD loop regions. Our results suggest that H84 mutations perturb aromatic interactions between HIV-1 CA NTD helices 4 and 7 that are essential to proper core morphogenesis.

2.3 Materials and Methods

Recombinant DNA constructs. A vesicular stomatitis virus (VSV) glycoprotein (G) expression construct, pVSV-G, was the generous gift of Randy Taplitz. The β-

lactamase–vpr fusion protein expression construct BlaM-vpr (318) and the parental HIVLuc construct (pNL-LucE-R) (87) were kindly provided by Nathaniel Landau. To make mutations at capsid residue 84 in the context of HIVLuc, the HIVLuc gag BglII (nucleotide [nt] 680)-to-HindIII (nt 1715) fragment was inserted into the homologous SP72 (Promega) sites, mutagenic double-stranded oligonucleotides were used to replace the wt sequence between the PstI (nt 1415) and SphI (nt 1443) sites, and mutations were cassetted back into HIVLuc, using the BssHII (nt 715) and SpeI (nt 1508) sites. The mutation at residue 87 was created by PCR, in a pGEM-T (Promega) vector, and BssHII-SpeI cassetted into HIVLuc. In all cases, conservative mutations also were introduced to facilitate restriction analysis. The wt and mutant sequences covering CA residues 77 to 91 are as follows, where mutated residues are underlined: wt, GCT GCA GAA TGG GAT AGA GTG CAT CCA GTG CAT GCA GGG CCT ATT; H84A, GCT GCA GAA TGG GAT AGA GTG GCG CCA GTT CAT GCA GGG CCT ATT; H84C, GCT GCA GAA TGG GAT AGA GTC TGC CCA GTT CAT GCA GGG CCT ATT; H84E, GCT GCA GAA TGG GAT AGA GTG GAA CCA GTT CAT GCA GGG CCT ATT; H84K, GCT GCA GAA TGG GAT AGA GTG AAA CCG GTT CAT GCA GGG CCT ATT; H84Y, GCT GCA GAA TGG GAT AGA GTA TAC CCA GTT CAT GCA GGG CCT ATT; H87C, GCT GCA GAA TGG GAT AGA GTG CAT CCA GTG TGC GCA GGG CCC ATT.

Cell culture and transfections. 293T and HiL cell lines were passaged at 37°C in 5% CO_2 in culture medium containing Dulbecco's modified Eagle's medium supplemented with 10 mM HEPES (pH 7.4), penicillin, and streptomycin plus 10% fetal calf serum. For transfections, 10-cm plates of 293T cells were transfected by the calcium

phosphate method (20, 182, 303, 304, 470, 473) with either 24 μg of HIVLuc DNA, 16 μg of HIVLuc plus 8 μg of pVSV-G DNA, or 12 μg of HIVLuc plus 6 μg of pVSV-G plus 6 μg of BlaM-vpr DNA. Briefly, confluent 10-cm dishes of 293T cells were split 1:4 the day prior to transfection. Plasmid DNAs were mixed with 1 ml of HEPES-buffered saline (pH 7.05 to 7.15; 21 mM HEPES, 137 mM NaCl, 5 mM KCl, 0.7 mM sodium phosphate, 5 mM dextrose), after which 40 μl of 2 M $CaCl_2$ was added while vortexing. DNA solutions were incubated at room temperature for 40 min. Following this, culture medium was removed from the cells, DNA solutions were added dropwise to the cell monolayers, and then the cells were incubated at room temperature for 20 min, with gentle rocking once at 10 min. After incubations, 10 ml of culture medium containing 50 μg of gentamicin/ml was added to the cells, and plates were incubated at 37°C and 5% CO_2 for 4 to 5 h. Following incubations, transfection media were removed and cells were washed with 5 ml of serum-free Dulbecco's modified Eagle's medium, incubated in 2.5 ml of 15% glycerol in HEPES-buffered saline for 3 min at 37°C, washed twice, and fed with 10 ml of culture medium plus 50 μg of gentamicin/ml. For sample collection, virus-containing media and cell pellets washed in phosphate-buffered saline (PBS; 9.5 mM sodium potassium phosphate [pH 7.4], 137 mM NaCl, 2.7 mM KCl) were collected 3 days posttransfection and stored at -80°C prior to further processing. Virus particles in filtered (Gelman; 0.45 μm) cell-free medium were concentrated by centrifugation at 4°C through 20% sucrose cushions in PBS (2 h at 82,500 x g [25,000 rpm in an SW28 rotor, 4-ml cushions], or 45 min at 197,000 x g [40,000 rpm, SW41 rotor, 2-ml cushions]). Virus pellets were resuspended in 0.1 ml of PBS per transfected cell plate and stored in aliquots at -80°C.

Protein analysis. For routine analysis of virus protein release, cell samples (20% of cell pellets from each plate) were suspended in IPB (20 mM Tris-hydrochloride [pH 7.5], 150 mM NaCl, 1 mM EDTA, 0.1% sodium dodecyl sulfate [SDS], 0.5% sodium deoxycholate, 1.0% Triton X-100, 0.02% sodium azide), incubated on ice for 5 min, vortexed, and cleared by centrifugation at 13,700 x g for 15 min at 4°C. Soluble material was mixed with 1 volume of 2x sample buffer (12.5 mM Tris-hydrochloride [pH 6.8], 2% SDS, 20% glycerol, 0.25% bromophenol blue) plus 0.1 volume of β-mercaptoethanol (BME), prior to heating (3 to 5 min, 95°C) and SDS-polyacrylamide gel electrophoresis (SDS-PAGE). For virus samples, 50 μl of resuspended virus pellets was mixed with one volume of 2x sample buffer plus 0.1 volume of BME and processed as above. In some cases, virus samples were cross-linked with 1 mM bis-maleimido hexane (BMH; Pierce; diluted from a freshly made 100 mM stock in dimethyl sulfoxide) prior to processing, as described previously (182, 303, 304). Cell and virus protein samples were fractionated by conventional 10% acrylamide Laemmli SDS-PAGE (20, 182, 303, 304, 470, 473) or 16% acrylamide Schagger and von Jagow SDS-PAGE (15, 408), electroblotted, and immunoblotted following previously described methods. Primary antibodies were as follows: Hy183 (from Bruce Chesebro) used at 1:15 from hybridoma culture medium for detection of the HIV-1 CA CTD; NEA 9306001EA (New England Nuclear) used at 1:15,000 for detection of the HIV-1 CA NTD; and SA-296 (BioMol) used at 1:15,000 for detection of CypA. Secondary reagents were alkaline phosphatase-conjugated anti-mouse antibodies (Promega S3721) used at 1:15,000 for detection of anti-HIV-CA primary antibodies and anti-rabbit immunoglobulin G (Sigma-Aldrich A3687) used at 1:2,000 for the anti-CypA polyclonal antibody. Color reactions for visualization of antibody-bound

bands employed nitroblue tetrazolium plus 5-bromo-4-chloro-3-indolyl phosphate in 100 mM Tris-hydrochloride (pH 9.5), 100 mM NaCl, and 5 mM $MgCl_2$ (20, 182, 303, 304, 470, 473). Size estimates for immunoreactive bands on immunoblots were obtained by comparison of mobilities versus those of Bio-Rad and Invitrogen size standards, assuming a linear mobility-to-log molecular weight relationship. Quantitation of band intensities was performed by densitometric scanning on an Epson model G810A scanner, followed by intensity measurement using NIH Image 1.61 software.

Sucrose gradients and core fractionations. For sucrose density gradient fractionation, virus samples in PBS (0.1 ml) were layered on top of 5-ml 20-to-60% sucrose gradients in TSE (50 mM Tris [pH 7.4], 100 mM NaCl, 0.1 mM EDTA) and centrifuged at 4°C, 170,000 x g (average) for 18 h such that particles of ≥12S should have sedimented to equilibrium. After centrifugation, 0.4-ml fractions were collected from the gradient tops to bottoms, and Gag levels in each fraction were determined by immunoblotting as described above. Sucrose densities for fractions were determined by weighing a constant volume of each fraction from a gradient run in parallel. For virus core fractionation, we followed a modification of the protocol of Tang et al. (447). Briefly, 0.1-ml virus samples were mixed gently with an equal volume of 0.6% NP-40 and incubated at room temperature for 10 min. Samples were layered onto 0.2-ml 20% sucrose–PBS cushions and centrifuged at 120,000 x g for 60 min at 4°C. Two 0.2-ml fractions then were collected from the top, and the pellets were resuspended in 0.2 ml of PBS to yield a third fraction. Samples were subjected to RT assays and immunoblot analysis of Gag protein content.

RT assays and RNase protections. Exogenous RT assays were performed with poly(A) and oligo(dT) templates and primers and detergent-disrupted virions (303, 470). Gag-normalized viral samples in PBS were incubated in RT assay cocktail {50 mM Tris (pH 8.3), 20 mM dithiothreitol (DTT), 0.6 mM $MnCl_2$, 60 mM NaCl, 0.05% NP-40, 2.5 μg of oligo(dT) (Pharmacia)/ml, 10 μg of poly(A) (Pharmacia)/ml, 10 μM dTTP (1-Ci/mM [α-^{32}P]dTTP)} at 37°C for 2 h. As controls, dilutions of avian myeloblastosis virus RT (Roche) were run in parallel. After incubations, samples were precipitated by addition of 0.1 volume of 100% trichloroacetic acid (TCA) and incubated overnight at 4°C. TCA precipitates were pelleted by centrifugation for 10 min at 4°C, 13,600 x g, and were washed five times with 10% TCA prior to radioactivity quantitation in a scintillation counter. RNase protections essentially followed the procedure of Wang et al. (473). Probes for RNase protection assays were made by incubation of 1 μg of EcoRI-linearized template plasmid (BlueHX 680–831) with transcription buffer (40 mM Tris [pH 7.4], 10 mM DTT, 6 mM $MgCl_2$, 0.8 mM spermidine), 100 μCi of [α-^{32}P]rGTP, 0.5 mM each of rATP, rCTP, and rUTP, 1 μl of RNasin (Promega), 1 mM DTT, and 20 U of T3 polymerase (Promega) at 37°C for 1 h. Probes then were ethanol precipitated, dried, resuspended, separated on 5% sequencing gels, eluted, and reprecipitated prior to use (473). For protections, Gag-normalized viral samples were precipitated with 10 μg of tRNA. Pellets were resuspended in 80% formamide, 400 mM NaCl, 40 mM piperazine-N,N-bis(2-ethanesulfonic acid) (pH 6.4), and probe, incubated at 75 to 85°C for 5 min, and then incubated at 30°C overnight. Samples then were incubated with RNase treatment buffer (300 mM NaCl, 10 mM Tris [pH 7.5], 5 mM EDTA, 40 μg of RNase A [Roche]/ml, 2 μg of RNase T1 [Roche]/ml) and incubated at 30°C for 30 min, followed

by the addition of 2.5 µl of 20-mg/ml proteinase K (Boehringer) plus 20 µl of 10% SDS and further incubation at 37°C for 15 min. Samples were phenol-chloroform extracted, ethanol precipitated, dried, fractionated on 6% acrylamide sequencing gels, and autoradiographed. Viral genomic RNA bands on autoradiographs were scanned on an Epson G810 scanner and quantitated using NIH Image 1.61 software.

Infections and entry assays. Confluent 10-cm dishes of HiL cells (303, 470, 473) were split 1:5 the day before infections. Growth media were removed from each cell plate, and 2-ml aliquots of filtered transfection supernatants containing 8 µg of Polybrene/ml were added to the cells. Plates were incubated for 3 h at 37°C, after which 8 ml of culture medium per plate was added and plates were incubated an additional 3 days at 37°C. After infections, cells were collected in 1 ml of luciferase lysis buffer (100 mM sodium phosphate [pH 8.0], 4 mM ATP, 1 mM sodium pyrophosphate, 6 mM magnesium chloride, 0.2% Triton X-100) and either processed immediately for luciferase assays or frozen at -80°C until use. For luciferase assays, cells in luciferase lysis buffer were vortexed at room temperature and 30-µl aliquots were mixed with 0.3 ml of luciferase assay buffer (luciferase lysis buffer minus Triton X-100). Luciferase levels were measured on an EG&G Berthold Autolumat LB953 luminometer using a 0.1-ml luciferin pulse of 1 mM D-luciferin (BD Pharmingen). Raw luminometer counts were normalized versus luminometer counts obtained from the transfected cells which produced the virus samples, and mutant virus infectivities were expressed as percentages of wt HIVLuc infectivities from assays performed in parallel. Infections for entry assays (76, 318) used 10-cm confluent plates of HiL cells which were split 1:10 onto 6-cm dishes the day before infections. Cells were infected 5 h at 37°C with 250 µl of virus in

PBS plus 750 μl of serum-containing medium and 8 μg of Polybrene/ml. After incubations, viral samples were removed, cells were washed once with Hank's balanced salt solution (HBSS; without calcium or magnesium), and cells were incubated in 1.5 ml of CCF2/AM loading solution (2 μM CCF2/AM [Invitrogen], 0.8 mg of Pluronic-F127 [Invitrogen]/ml in HBSS) at 26°C, 5% CO_2 overnight. Loading solution then was removed, cells were washed once in HBSS, trypsinized, pelleted, fixed (20 min, 1% formaldehyde in PBS), pelleted, washed in HBSS, pelleted, and resuspended in 1 ml of HBSS. Cells were analyzed as described previously (76, 318, 509) on a Becton-Dickinson Turbo Vantage flow cytometer to detect cleaved product as blue fluorescence and uncleaved substrate as green fluorescence. The percentages of product-positive live cells derived from flow cytometer analysis were normalized for Gag protein levels in virus samples and expressed as percentages of wt HIVLuc levels.

EM. Concentrated virus particle samples were lifted for 2 min onto carbon-coated, UV-treated (shortwave UV, 30 to 120 min) electron microscopy (EM) grids, rinsed for 15 s in water, wicked, stained for 1 min in filtered 1.3% uranyl acetate, wicked, and dried. EM images were collected on a Philips CM120/Biotwin TEM equipped with a Gatan 794 multiscan charge-coupled device camera, searching at 2,300 to 4,000x, and collecting images at 2,300 to 34,000x. Virus particle diameters were determined with the aid of Gatan digital micrograph software, and virus particle images were ported from Gatan DM3 to TIFF or jpeg image format for presentation.

2.4 Results

Release and infectivity of viral mutants. The in vitro assembly properties of HIV-1 CA and PrGag proteins have been shown to be pH dependent. Gross et al. showed that PrGag-like proteins assembled tubes at pH 6.0 but spheres at pH 8.0 (174). Ehrlich et al. (120) observed that CA assembly properties shifted in the range of 6.0 to 7.0, near the pK_a of histidines. Since HIV-1 histidine 84 is well conserved (244), modeled to be at the outer edges of NTD hexamer rings (153, 154, 264), and might influence HIV assembly or morphogenesis, we examined the effects of mutations at this residue. To do so, we initially substituted alanine, lysine, cysteine, and glutamate for histidine 84, creating the H84A, H84K, H84C, and H84E mutations. As a control, we also tested the effects of a cysteine mutation at the nearby poorly conserved histidine 87 residue in the CypA loop.

For monitoring the effects of mutations on virus assembly and release, wt and mutant HIV constructs were transfected into 293T cells and virus and cell samples were collected 3 days posttransfection. Samples were separated by SDS-PAGE and immunoblotted with an anti-HIV capsid antibody. As shown in Fig. 1, wt Gag proteins were released efficiently from cells, yielding the expected PrGag, p41, and CA bands, along with a less-pronounced processed band at 46 to 47 kDa. Relative to wt, H84K, H84E, H84C, H84A, and H87C all released Gag proteins at approximately comparable levels. These results suggest that the H84 and H87 mutations did not compromise the abilities of Gag proteins to assemble and release virus-like particles. Indeed, the only readily apparent differences from wt pertained to protein processing. In particular, for the H84C mutant, slightly higher levels of PrGag and p41 were observed in virus particle samples. Also observed were additional minor processing bands at about 46 kDa and near

the CA band for the four H84 mutants; the nature of these bands is examined further below.

Since the H84 and H87 mutant constructs efficiently released virus from transfected cells, it was of interest to test whether they were also infectious. Thus, 293T cells were co-transfected with wt or mutant HIVLuc constructs plus a plasmid encoding VSV-G. Media from transfected cells were collected and used to infect HiL cells, after which luciferase assays were performed on the infected cells to score for virus-mediated transduction of the luciferase gene. Not surprisingly, VSV-G-pseudotyped wt viruses were infectious, as were viruses produced by the H87C mutant (see below). In contrast, the infectivities of the four H84 mutants all were less than 0.2% that of wt.

Because alanine, cysteine, lysine, and glutamate substitutions for HIV-1 CA H84 essentially abolished virus infectivities, we considered alternate substitutions that might maintain some degree of infectiousness. Inspection of the HIV-1 CA NTD structure (Fig. 2) suggested that in addition to providing a highly conserved basic residue, H84 contributes to an aromatic interaction with tryptophan residues 80 (W80) and 133 (W133) to align the base of the CypA loop and helices IV and VII in a stable tertiary structure. To examine the importance of this arrangement, we created an H84Y mutation on the hypothesis that tyrosine might preserve the residue 84-80-133 aromatic interaction.

Testing of the H84Y mutant assembly and release properties followed the methodology described above, and results are shown in Fig. 3. As observed in Fig. 1, the wt construct directed the efficient assembly and release of virus particles (lanes A and D). Also as observed in Fig. 1, H84A proteins were released efficiently from cells, but additional high-mobility processing bands were especially apparent (B and F). Gag

assembly and release levels for H84Y (C and G) were similar to those of the wt and H84A constructs, implying no impairment of these processes. However, interestingly, the levels of high-mobility processing bands were reduced for H84Y relative to that for H84A (compare F and G).

Since the H84Y mutant gave fewer anomalous CA processing bands than H84A, it seemed possible that it might prove less impaired in terms of infectivity than its counterpart. Thus, infectivity assays were performed for H84Y, along with H84A, H87C, and wt controls. As noted above and illustrated in Fig. 4, the H87C mutant had reduced but still considerable (20% of wt) infectivity, whereas H84A (as well as H84K, H84E, and H84C) showed 0.2% of wt infectivity. The H84Y mutant infectivity was reduced 30-fold compared to wt but, remarkably, it was still greater than 10 times that of the other H84 mutants. To ascertain whether mutant Gag proteins were able to impair the functions of wt Gag proteins, wt and H84A constructs were transfected into 293T cells at different ratios (3:1, 1:1, and 1:3 wt/H84A ratios) along with the VSV-G protein expression construct, and media were collected for infections. As Fig. 4 illustrates, while the 3:1 wt-H84A sample showed slightly reduced infectivity, virus particles produced from the 1:1 and 1:3 wt-H84A mixtures were as noninfectious as H84A itself. These results indicate that the H84A mutant acts as a dominant negative, diminishing the ability of wt Gag proteins to assemble infectious particles. The mechanism by which mutations at HIV-1 CA H84 inhibit infectivity is examined below.

CypA incorporation into viral mutants. One possible cause for the noninfectivity of viral mutants might be differences in their abilities to interact with CypA. Although CypA appears to exert its major effects on HIV-1 within newly infected

cells (5, 9), studies have shown that the noninfectivity of some HIV-1 NTD mutants correlates with an impaired ability to incorporate CypA into virions (55, 80, 447). Because our mutations mapped within or adjacent to the CypA loop, examination of CypA levels in virions appeared warranted. For this analysis, we chose to examine our partially infectious H84 mutant, H84Y, and one noninfectious mutant, H84A, along with negative and positive controls. Virus samples were immunoblotted for the parallel detection of CA (Fig. 5A) and CypA (Fig. 5B) proteins. As illustrated, while CypA was not released from cells in the absence of HIV-1 expression (Fig. 5B, - lane), its release from cells appeared roughly equivalent for wt, H84A, and H84Y viruses (compare Fig. 5A, CA signal, versus B, CypA signal); these results suggest that mutations at H84 did not affect CypA binding to CA.

We also monitored CypA incorporation into H87C virions and found that CypA assembly into virions was not affected by this CypA loop mutation (Fig. 5E, - lane). Interestingly, treatment of H87C virus with the cysteine-specific cross-linker BMH yielded a novel anti-CypA-reactive 45-kDa band (Fig. 5E, + lane) which corresponded to an anti-CA-reactive cross-link band in H87C (Fig. 5D) but not wt (Fig. 5C) samples. These results indicate that the introduced cysteine at residue 87 readily crosslinked to a free CypA cysteine. An additional cross-link band, observed only with the anti-CA antibody (Fig. 5D), migrated slightly slower than the PrGag band. We interpret this product to represent either a CA-CA dimer or a heterodimer of CA with an undetermined cellular protein. In either case, our results with H84 and H87 did not demonstrate the correlation between loss of infectivity and loss of CypA interaction that has been observed for some other NTD mutations (447).

RNA and RT analysis. Since CypA levels in wt and noninfectious mutant virions were equivalent, we probed for RNA and RT defects that might yield replication-defective, assembly-competent phenotypes. For RNA analysis, RNAs were isolated from equivalent amounts of virus, and samples were analyzed by RNase protection, as described in Materials and Methods. Results (Table 1) demonstrated that virion-associated HIV genomic RNA levels were roughly equivalent for wt, H84Y, and H84A viruses. Similar studies also were performed on viruses to measure RT levels via exogenous template RT assays (see Materials and Methods). As shown in Table 1, RT levels were comparable in samples from WT, partially infectious H84Y, and noninfectious H84A virions. Thus, RNA encapsidation and/or RT incorporation defects do not explain the low infectivities of the H84 mutants.

Cleavage site analysis of mutant proteins. Although H84 mutant viruses gave wt levels of RNA and RT, we noted that the H84 mutants displayed a number of high-mobility CA processing bands (Fig. 1 and 3). On most gels, the number of processing bands appeared greater for the H84A mutant than for the H84Y mutant, suggesting a correlation between aberrant processing and loss of infectivity. To examine this finding in more detail, wt, H84A, and H84Y viral proteins were analyzed on 10 and 16% gels and fragment sizes were calculated from log molecular weight-versus-migration distance plots. As illustrated in Fig. 6, anti–HIV-1–CA–reactive bands were observed at calculated sizes of 21.7, 19.2, 17.1, 15.2, 14.3, and 10.5 kDa. The epitope for the antibody employed binds to the CTD, C-terminal to the CA major homology region (85, 291). Thus, if the CA-sp1 junction for these NTD mutants were cleaved appropriately, the novel processing sites within the NTD could be estimated from fragment size data. Based on this

assumption, the approximate aberrant CA cleavage sites for H84A and H84Y were mapped (Fig. 2) as black dots, where the size of the dot represents the frequency of cleavage site usage. Although these cleavage site estimates are likely to be accurate only to the nearest few residues, it is interesting that one of the predicted cleavage sites maps close to residue 84 and the others tend to occur at or near loop regions in the NTD or between the NTD and CTD. These results suggest that H84A mutations perturbed tertiary or quaternary interactions such that the capsid proteins became more sensitive to proteolytic action.

Morphologies of mutant virions. Since H84 mutant proteins were processed anomalously in virions, we found it important to characterize the virus particles further. Particles collected by ultracentrifugation were subjected to equilibrium centrifugation on 20-to-60% sucrose gradients to analyze virion densities. As shown in Fig. 7, the peak density for wt virions (top panel) was 1.15 g/ml, within the 1.15- to 1.19-g/ml range observed for HIV-1 virions (20, 470). We also observed a smaller peak in fraction B (1.10 g/ml) and a shoulder of denser virus particles. The partially infectious H84Y mutant displayed a similar density pattern as wt, with a peak in fraction G, a smaller peak in fraction B, and a shoulder containing virions of higher density. In contrast, noninfectious H84A mutant viruses showed a slightly shifted peak fraction (fraction F) and a considerably broader range of densities with a higher proportion of lower density virions. Although our density gradient fractionation protocol is subject to some variability, the results with H84A suggested that these mutant virus particles might be morphologically anomalous.

Based on sucrose density gradient results, we decided to compare virion morphologies of wt and H84A particles by EM. To do so, purified virus samples were lifted onto EM grids, washed, negatively stained, and analyzed by transmission EM. A simple examination of virus particle diameters (Fig. 8A) showed similar results for the two samples: most virus particles were in the 110- to 120-nm range, with an average wt particle diameter of 118 ± 20 nm (mean ± standard deviation) and a slightly smaller H84A average at 112 ± 20 nm. Notwithstanding the similarities in particle diameters, a significant difference was observed in particle core morphologies. Figure 8B shows a gallery of wt (panels A to H) and H84A (panels I to P) particles, stained so that lipid envelope drying and breakage revealed the internal core structure, or completely liberated cores from envelopes (Fig. 8B, panel H). It is noteworthy that all (n = 29) of the wt particles displayed visible conical or cylindrical cores (panels A to H), as is typical for HIV (85, 153, 477). In contrast, H84A cores either were round, barrel shaped, or anomalously shaped (panels I to P). No particles with clearly conical or cylindrical cores were observed for the H84A mutant (n = 39).

Analysis of postassembly defects. Although H84A virions had aberrant mature cores, the exact relationship between this morphological defect and the lack of infectivity was unclear. To examine postassembly defects of H84 mutants further, entry assays (76, 318) were performed to monitor the capability of virus cores to enter target cells. To generate viruses for these assays, 293T cells were cotransfected with the wt or mutant HIVLuc constructs, the VSV-G protein expression construct, and a construct encoding a vpr-β-lactamase fusion protein (318). Under our transfection and infection conditions (see Materials and Methods), we expected a multiplicity of infection in the range of

0.01%, about 10- to 20-fold higher than we have observed with HIV vectors pseudotyped with retroviral envelope proteins (303). Successful virus entry was probed as described previously (76, 318, 509) by measuring cleavage of the fluorescent β-lactamase substrate CCF2 in target cells: CCF2 cleavage is accompanied by a fluorescent shift from green to blue, and percentages of entry-positive versus -negative cells were quantitated by flow cytometry (76, 318, 509). Employing these assays with wt, H84Y, and H84A viruses gave the results shown in Fig. 9. As illustrated, while 0.01% of the mock- infected cells scored as entry positive based on blue fluorescence emission, 0.86% of the wt-infected cells gave a positive signal. Relative to wt levels, H84Y (1.04%) and H84A (0.38%) yielded higher and lower entry signals, respectively. Nevertheless, when entry results were normalized for virus particle-associated Gag protein levels in two independent experiments, entry assay results showed no impairment for H84Y (134% ± 60% wt levels) and only a slight impairment for H84A (61% ± 3% wt levels). Thus, reduced entry into target cells did not readily account for the >500-fold reduction in infectivity for H84A virions.

As an alternative approach to the analysis of particle defects, we decided to subject virions to a detergent treatment-fractionation protocol, since recent studies have revealed unusual fractionation profiles for certain HIV-1 CA NTD mutants (447). Consequently, wt, H84Y, and H84A viruses were detergent treated and fractionated on sucrose step gradients to obtain mature virus core-enriched pellets, as described by Tang et al. (447). Fractionation results for wt, H84Y, and H84A are shown in Fig. 10. In the case of the wt sample, the pellet fraction (lane C) preferentially contained immature and incompletely processed virions, which were not enriched in the top (lane A) or middle

(lane B) fractions. As expected from prior analysis (133, 447, 477), only a small proportion of mature CA pelleted. The H84Y fractionation pattern was similar to the one observed with wt, although there was a slight increase of capsid in the pellet fraction (lane C). This trend was magnified with the H84A sample, which showed a large capsid signal in the pellet fraction. Although similar fractionation results have been observed with other HIV-1 CA NTD mutants (447), we repeated the experiment and obtained similar fractionation profiles, indicating that these were not atypical results. We also performed RT assays on each of the detergent treatment fractions. Interestingly, RT levels in all mutant fractions were lower than in their wt counterparts, suggesting a difference in wt versus mutant virus RT stabilities during the core fractionation protocol. Comparison of CA and RT levels demonstrated that although pellet-associated CA levels were increased with the H84 mutants, RT levels in the pellet (C) fractions were reduced twofold relative to wt. These observations suggest that high CA-to-RT ratios in core pellet fractions correlate with H84 mutant replication defects and are consistent with the notion that mutant virus replication is blocked after target cell entry, at a reverse transcription step.

2.5 Discussion

Although the structure and some of the functions of the HIV-1 CA NTD have been clarified (80, 85, 112, 133, 151, 154, 160, 174, 303, 385, 445-447, 466, 467, 470), many structure-function relationships remain to be explained. Within mature HIV-1 cores, NTDs appear to assemble hexamer rings (27, 264, 300), and although hexamer contacts have not been determined, they have been modeled to employ NTD helices I and

II (153, 154, 264). In this arrangement, histidine residues H84 and 87 would occupy positions at the outer edges of hexamer rings and might be well suited to mediate putative interhexamer associations and/or histidine switch activities (120). Consequently, we probed these residues by using a mutational analysis approach.

Because HIV-1 CA H87 is not well conserved (244), it was not surprising that our cysteine substitution mutant (H87C) was infectious (Fig. 4). Our cross-linking experiments also demonstrated that H87C readily cross-linked to a free CypA cysteine, whereas the natural CA CTD cysteines did not (Fig. 5). In contrast to H87C, mutations at the highly conserved H84 substantially reduced virus infectivity (Fig. 4). Surprisingly, unlike recently described (447) mutations at CA NTD W23A and F40A at helices I and II, respectively, mutations at H84, adjacent to the CypA loop, did not reduce CypA assembly into virions (Fig. 5). However, both H84A and H84Y mutants were similar to the W23A and F40A mutants (447) in that detergent treatment experiments yielded significantly increased capsid/RT ratios in mature core fractions. These results are consistent with the interpretation that mutations at H84 reduce virus infectivity via an impairment of reverse transcription steps.

Given that H84A cores exhibited a clearly aberrant morphology (Fig. 8), a putative block at reverse transcription does not seem an unexpected phenotype. However, it is not immediately obvious why mutations at H84, which is not modeled to participate in NTD hexamer formation (153, 154, 264), should give a phenotype similar to mutations W23A and F40A in helices I and II, which have been modeled at hexamer interfaces. One possible explanation is that changes at H84 telegraph to helices I and II to alter hexamer interfaces. Alternatively, the CA NTD helix I-II and IV-VII faces may play

complementary roles in assembly, perhaps in forming hexamers and in bundling hexamers into higher-order structures. Finally, mutations at CA residues 23, 40, and 84 all may have a significant impact on the folding of capsid monomers, and this common folding defect may result in related assembly anomalies. Regardless of the role of H84 in CA oligomerization, the fact that substitution with tyrosine yielded viruses that were over 10 times more infectious than alanine, cysteine, lysine, and glutamate variants implies that the natural histidine residue is most important for its ability to participate in aromatic interactions. While this does not preclude a histidine switch (120) activity for H84, the infectivity of the H84Y mutant, albeit 30-fold less than that of wt, argues against an absolutely required H84 histidine switch. Assuming that the effect of mutations at H84 is to destabilize NTD helix IV and VII associations by weakening H84-W80-W133 aromatic interactions, the observation of aberrant CA processing products (Fig. 6) may not be surprising. However, for H84A, the combination of an increased susceptibility to processing and an increased resistance to detergent-mediated disassembly (Fig. 10) may seem contradictory. We suggest that the conformation stabilized by H84 helps control promiscuous protein oligomerization or aggregation. Our results support the concept that CA must satisfy a precarious balance between assembly and disassembly (133) and that H84 exerts a critical influence on this balance.

Acknowledgments

The HIVLuc and BlaM-vpr constructs were kindly provided by Nathaniel Landau, and the VSV-G protein expression construct was a generous gift from Randy

Taplitz. We are thankful for the help and advice we've received from Ayna Alfadhli, Tenzin Choesang, and Amelia Still.

This work was supported by Public Health Service grant R01 GM060170-06 from the National Institute of General Medical Sciences.

2.6 Figures and tables

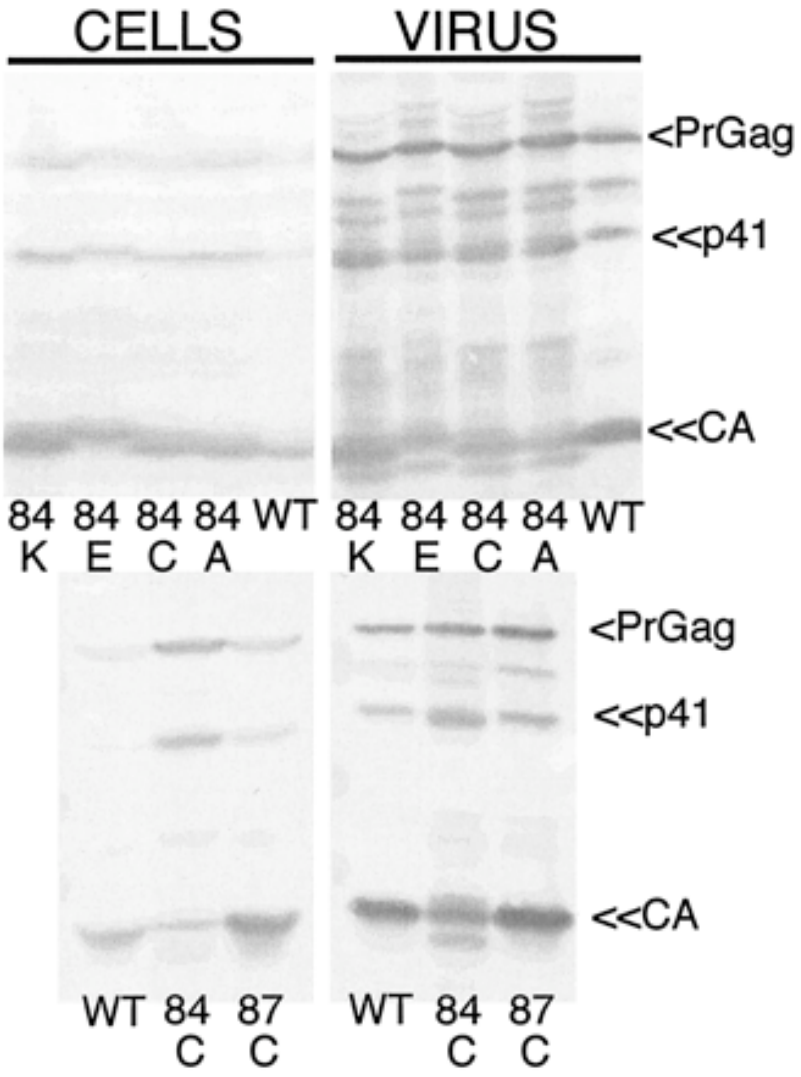

Figure 2.1
Virus particle release. 293T cells were transfected with wt and mutant HIV constructs. Cell lysates and pelleted virus samples were collected at 72 h posttransfection and subjected to SDS-PAGE followed by immunodetection for Gag proteins with an anti-HIV-1 CA antibody. Sample identities and bands for PrGag, CA, and the p41 processing intermediate are indicated.

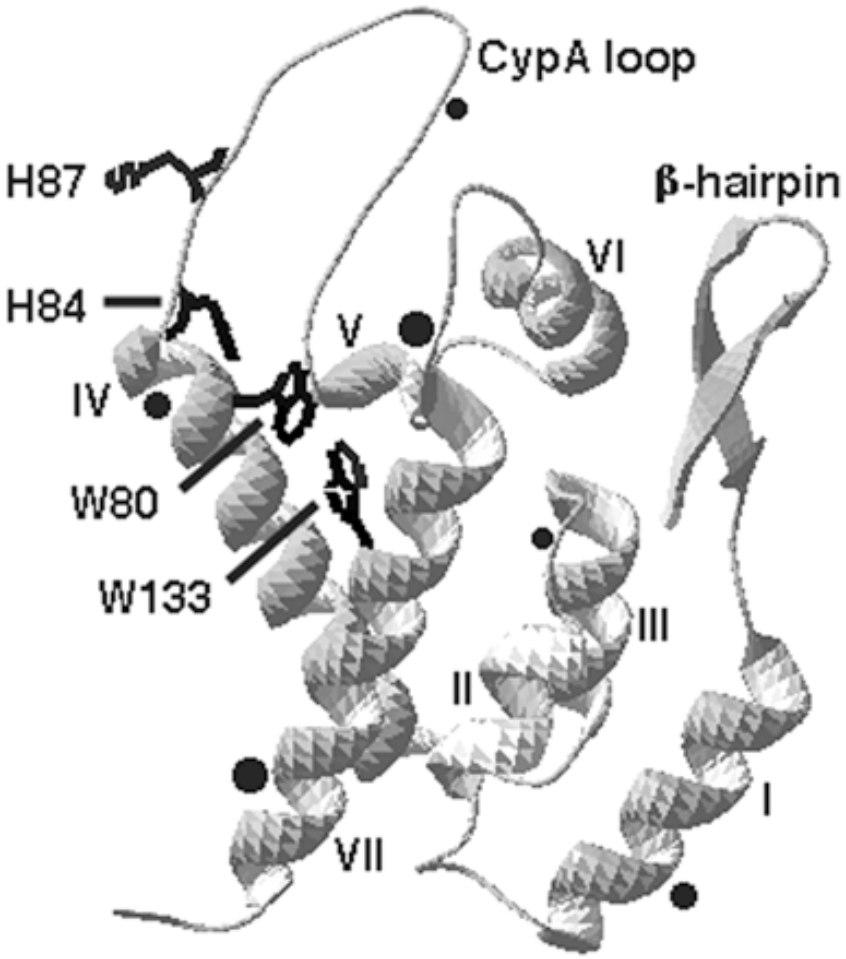

Figure 2.2
Structural features of the HIV-1 CA NTD. Shown is the structural model (pdb 1GWP) for the HIV-1 CA NTD, from the N-terminal proline at the end of the β-hairpin to the C-terminal connection to the CTD (bottom left). The seven NTD helices are indicated, as are the locations of mutated residues H84 and H87 and the tryptophan residues (W80 and W133) which participate in aromatic interactions with H84. Approximate locations of anomalous processing sites (determined below in Fig. 6) are indicated with black dots, where dot sizes represent the frequencies of cleavage site usage, based on immunoblotting band intensities. Note that residue numbers reflect those of the mature capsid protein, in which the first capsid residue corresponds to codon 133 from HIV-1 gag.

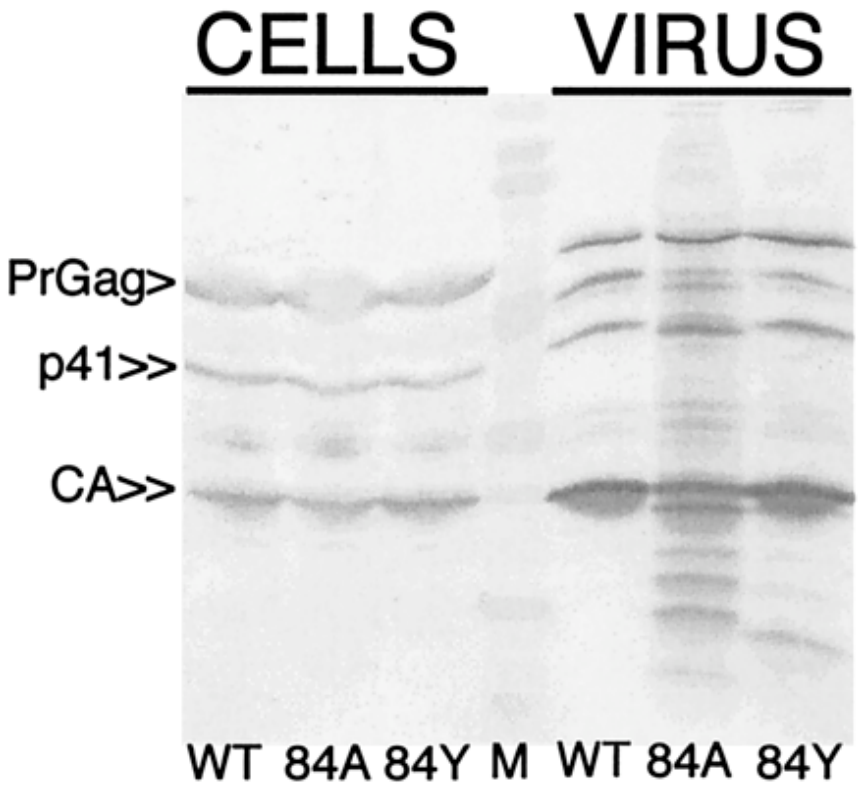

Figure 2.3
Release of wt, H84A, and H84Y particles. 293T cells were transfected with wt and mutant HIV constructs. Cell lysates and pelleted virus samples were subjected to SDS-PAGE, followed by immunodetection for Gag proteins using an anti–HIV-1–CA antibody. Sample identities were as indicated, where M denotes the molecular weight size marker. Bands for PrGag, CA, and the p41 processing intermediate are indicated.

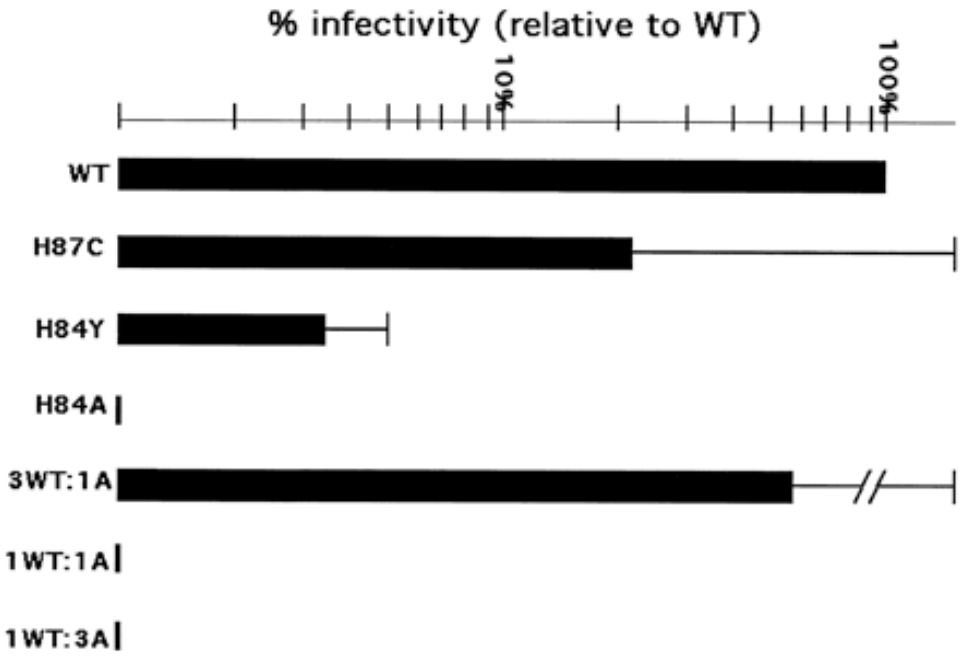

Figure 2.4
Relative virus infectivities. HiL cells were infected with viruses derived from cotransfecting the indicated HIV-luciferase (HIVLuc) construct with the VSV-G expression construct pVSV-G. Infectivities were monitored by luciferase assay of infected cell lysates, and results were normalized to luciferase activities of the corresponding transfected cells. Infectivities were plotted relative to wt HIVLuc levels on a log scale graph and were based on two or more (H87C = 4; H84Y = 3; H84A = 7) independent sets of infections. Note that the 3WT:1A, 1WT:1A, and 1WT:3A bars correspond to cotransfections using different ratios of wt and H84A constructs and that values for the H84E, H84K, and H84C viruses were 0.2% that of wt.

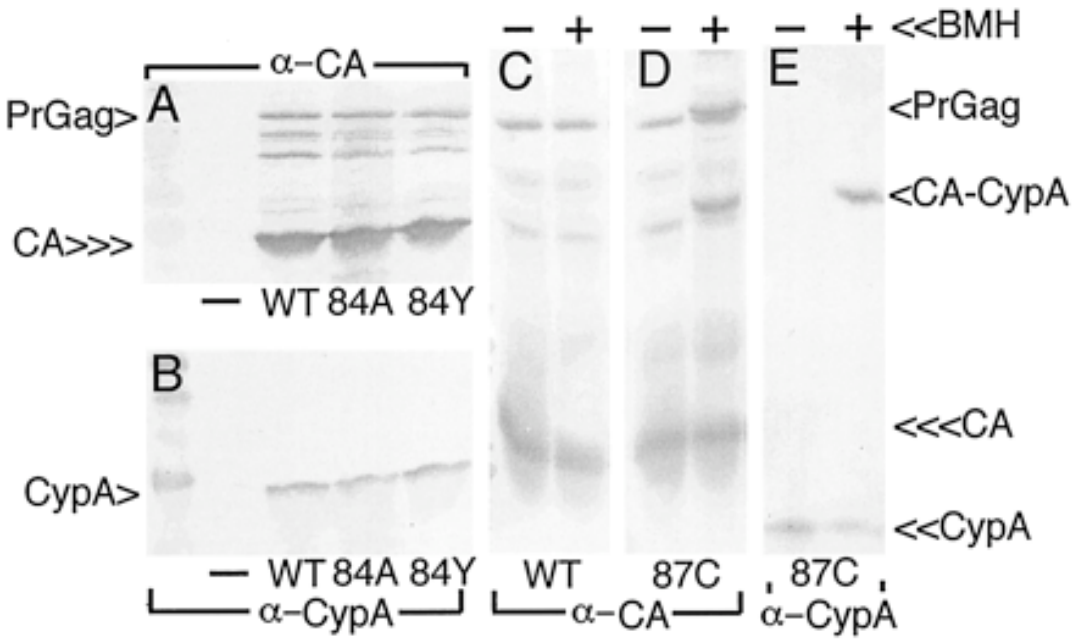

Figure 2.5
CypA assembly into virus particles. (A and B) 293T cells were mock transfected (-) or transfected with the indicated constructs, and medium supernatants were collected 72 h posttransfection and then subjected to ultracentrifugation. Pelleted virus samples were resuspended in buffer and subjected to SDS-PAGE and parallel immunodetection with the indicated antibodies. (C to E) Samples were mock treated (-) or treated (+) with the cysteine-specific cross-linker BMH prior to SDS-PAGE and immunodetection. CypA, CA, PrGag, and CA-CypA cross-link products (D and E, crosslink lanes) are indicated. Note a putative CA-CA dimer crosslink product in the panel D crosslink lane, just above the PrGag band.

Construct	RNA level	RT level
wt	100	100
H84Y	94	113 ± 12
H84A	109 ± 9	106 ± 51

Table 2.1
Viral genomic RNA (RNA) and RT levels in wt, H84Y, and H84A viruses are expressed as percentages of the values obtained for wt viruses. RNA levels were determined by RNAse protection using RNA isolated from equivalent amounts of virus. Relative levels were quantitated densitometrically from one (H84Y) or two (wt, H84A) independent experiments. RT values are derived from three independent measurements for each construct and were determined using exogenous RT assays, normalized for capsid protein levels by densitometric quantitation from immunoblots.

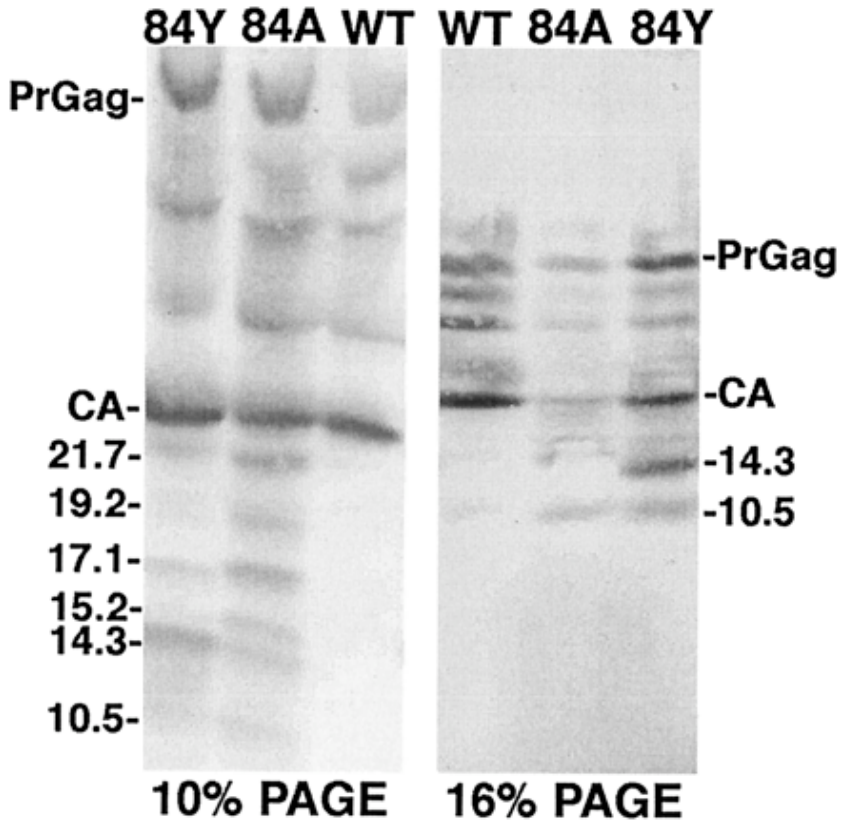

Figure 2.6
Capsid protein processing products. The indicated virus samples were electrophoresed in parallel on conventional SDS–10% PAGE and SDS–16% PAGE Schagger gels. After electrophoresis, CA fragments were detected by immunoblotting with an anti–HIV-1–CA antibody which recognizes the HIV-1 CTD. Approximate fragment sizes in kilodaltons are indicated and were estimated by comparison with migration distances of known standards, assuming a linear relationship between migration and log molecular mass.

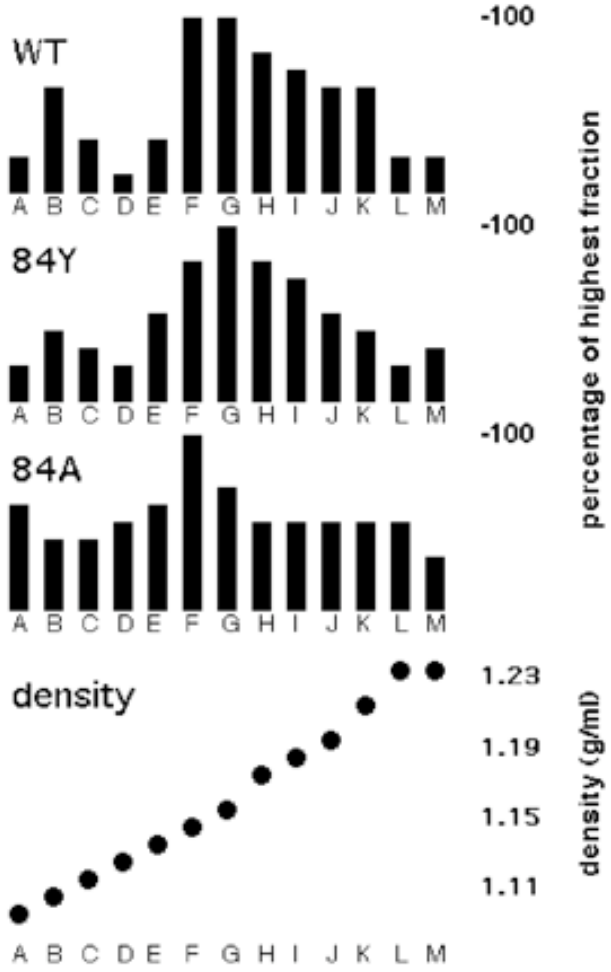

Figure 2.7
Virus density gradient fractionation. Samples of the indicated viruses were loaded onto 20-to-60% sucrose density gradients and centrifuged at 170,000 x g (average) for 18 h in an SW 50.1 rotor such that particles of 12S should have sedimented to equilibrium. After centrifugation, 0.4-ml fractions were collected from the gradient tops (A) to bottoms (M) and Gag levels in each fraction were measured by densitometry of immunoblot bands. Gag levels for each fraction are plotted relative to the gradient fraction with the highest Gag signal (100%). Sucrose densities were determined by weighing a constant volume of each fraction from a gradient run in parallel, although these values should be considered approximate, as our observed gradient-to-gradient variation was about 0.005 g/ml in any given fraction.

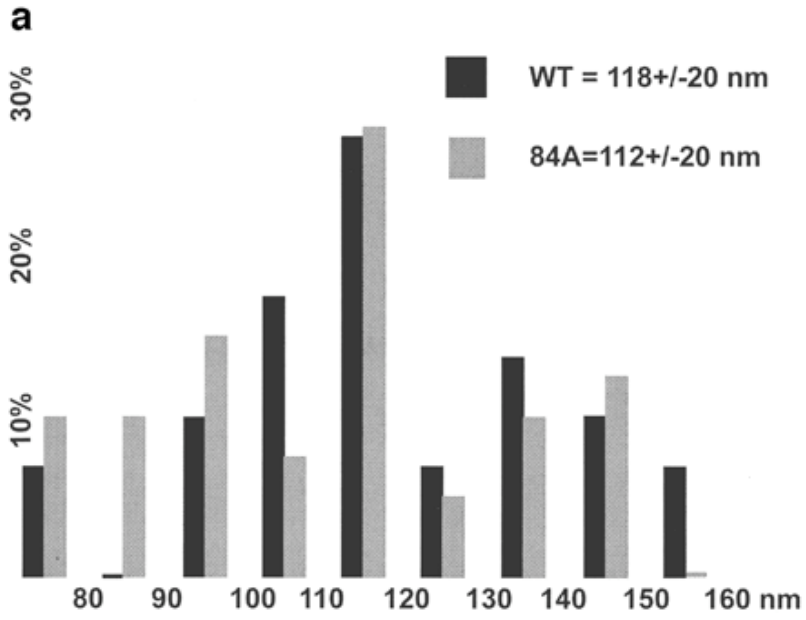

Figure 2.8.A
Analysis of virus morphologies. Virus particles from wt HIVLuc- and H84A HIVLuc-transfected cells were isolated, lifted onto carbon-coated grids, stained with uranyl acetate, and imaged by transmission EM. (a) Histogram of particle diameters. Diameters of wt (n = 29) and H84A (n = 39) virus particles were plotted in 10-nm size bins relative to the frequencies (percentage of total sample) observed for each size bin.

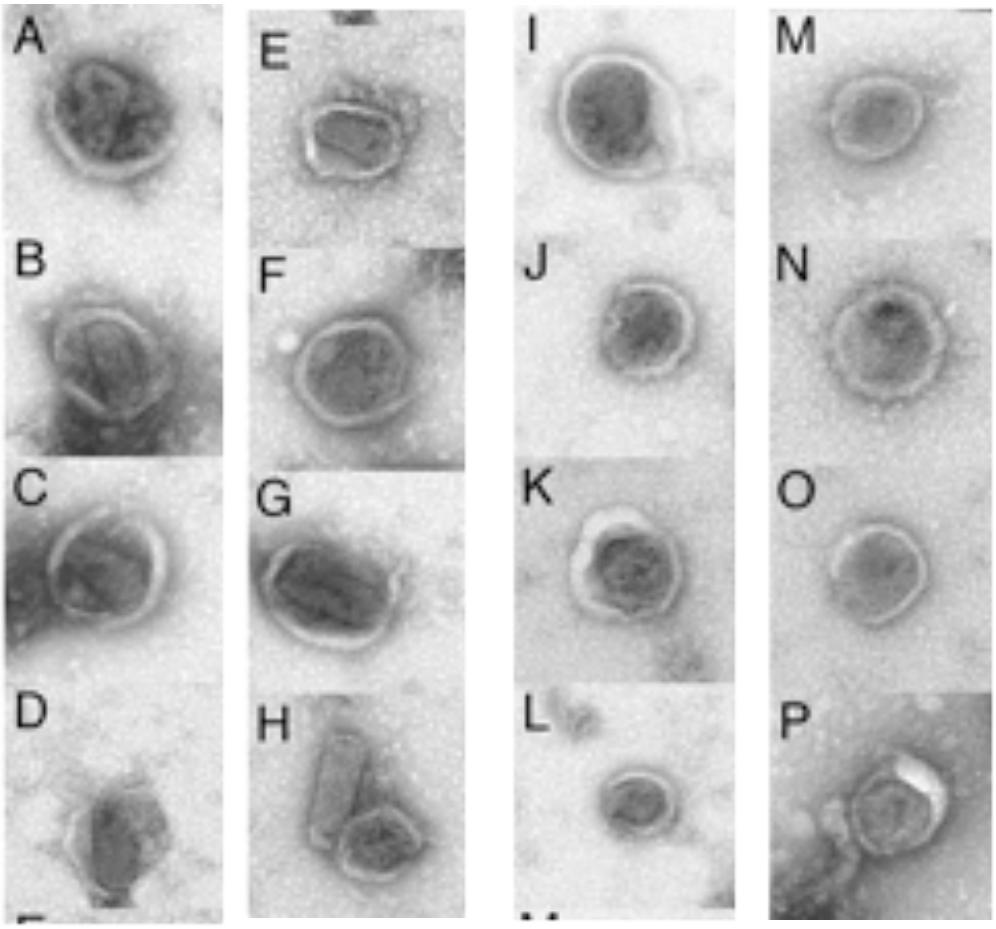

Figure 2.8.B
Analysis of virus morphologies. Virus particles from wt HIVLuc- and H84A HIVLuc transfected cells were isolated, lifted onto carbon-coated grids, stained with uranyl acetate, and imaged by transmission EM. (b) Galleries of virus particle images. Images of eight wt (A to H) and H84A (I to P) virus particles are shown within 262- by 262-nm windows. Note that panel H shows a wt core, apparently released from a broken virus during preparation. Note also that all wt virions (n = 29) showed discernible cylindrical or conical cores, whereas only panel I showed a possible cylindrical core for H84A (n = 39).

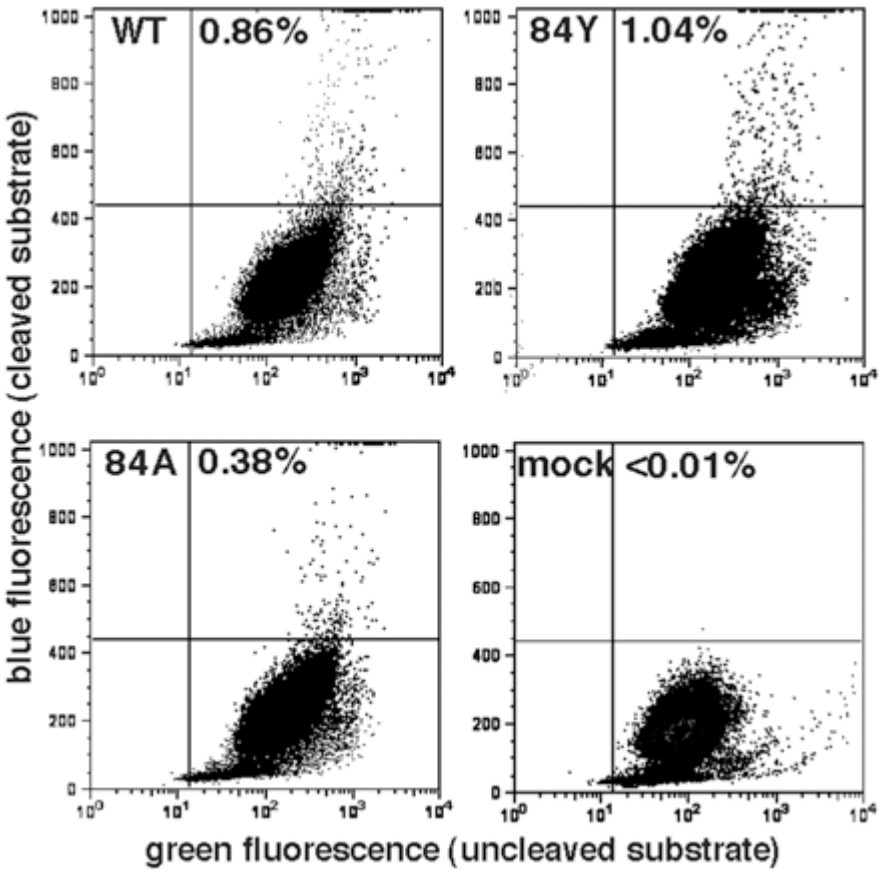

Figure 2.9
Virus entry assays. Virus core entry into target cells was assessed using viruses produced by cotransfection of wt, H84Y, or H84A or mock expression constructs along with expression constructs of the VSV-G (pVSV-G) and a β -lactamase–vpr (BlaM-vpr) fusion protein. Viruses were used to infect HiL cells in serum-containing medium plus 8 μg of Polybrene/ml for 5 h at 37°C. After incubations, viral samples were removed and cells were incubated an additional 18 h at 26°C in fluorescent β-lactamase substrate (CCF2/AM) loading solution. Virus entry was measured by flow cytometry detection of live cells manifesting uncleaved substrate (green fluorescence) versus cleaved product (blue fluorescence). The percentages of product-positive live cells are shown. When normalized for Gag protein levels, the average (n = 2) entry assay signals for H84A and H84Y relative to that of wt were 61% ± 3% (H84A) and 134% ± 60% (H84Y).

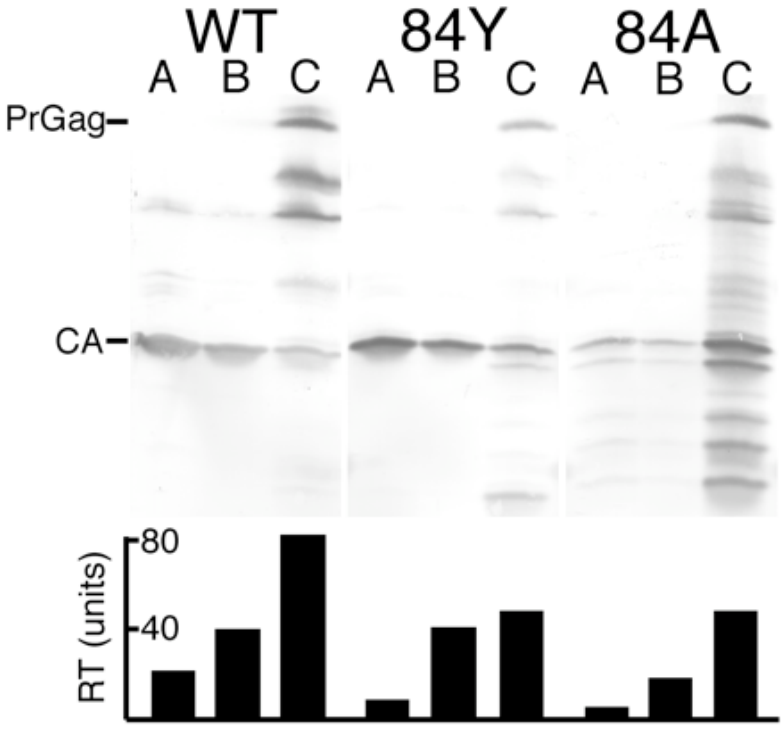

Figure 2.10
Analysis of virus cores. Viruses collected from transfected cells were treated with 0.3% NP-40 for 10 min, layered onto an equal volume of 20% sucrose, and centrifuged at 120,000 x g for 60 min at 4°C. Top fractions (A), bottom fractions (B), and virus core-containing pellet fractions (C) were collected and subjected in parallel to RT assays (bottom panel) as well as SDS-PAGE and immunoblotting with anti–HIV-1–CA antibody. PrGag and mature CA bands are indicated on the immunoblots. RT units were determined by comparison with activities of known amounts of avian myeloblastosis virus RT.

Chapter 3

Analysis of Human Immunodeficiency Virus Matrix Domain Replacements

Isabel Scholz, Amelia Still, Tenzin Choesang Dhenub, Kelsey Coday, Mike Webb, and Eric Barklis

Chapter 3 has been accepted for publication.

Virology, in press.

Statement of contribution

For chapter 2, I acquired the data shown in figures 3, 5, and 8. I contributed to the data shown in figures 2, 4, 6, and 7.

3.1 Abstract

The matrix (MA) domain of the HIV-1 structural precursor Gag (PrGag) protein targets PrGag proteins to membrane assembly sites, and facilitates incorporation of envelope proteins into virions. To evaluate the specific requirements for the MA membrane-binding domain (MBD) in HIV-1 assembly and replication, we examined viruses in which MA was replaced by alternative MBDs. Results demonstrated that the pleckstrin homology domains of AKT protein kinase and phospholipase C δ1 efficiently directed the assembly and release of virus-like particles (VLPs) from cells expressing chimeric proteins. VLP assembly and release also was mediated in a phorbol ester-dependent fashion by the cysteine-rich binding domain of phosphokinase C γ. Although alternative MBDs promoted VLP assembly and release, the viruses were not infectious. Notably, PrGag processing was reduced, while cleavage of GagPol precursors resulted in the accumulation of Pol-derived intermediates within virions. Our results indicate that the HIV-1 assembly machinery is flexible with regard to its means of membrane association, but that alternative MBDs can interfere with the elaboration of infectious virus cores.

3.2 Introduction

The matrix (MA) domain of the HIV-1 precursor Gag (PrGag) protein serves at least two assembly functions: it targets PrGag proteins to membrane assembly sites, and it facilitates the incorporation of the SU/TM envelope (Env) glycoprotein complex into virions (290, 343-345, 347, 348, 354, 470, 473, 490, 497, 507). In terms of membrane targeting, there is some debate as to the pathways by which PrGag proteins travel to

arrive at productive assembly sites. One possible itinerary involves PrGag association with intracellular membranes such as multivesicular bodies (MVBs), followed by vesicular delivery to the plasma membrane (PM) (64, 95, 113, 139, 142). This model is compatible with the transport of preassembled virions to the PM as vesicle cargoes, or with the delivery of PrGag proteins on vesicle cytoplasmic faces to final PM assembly sites (220). An alternative travel plan for PrGag proteins is a direct route to the PM (221, 345, 401). In this case, the accumulation of PrGag proteins on intracellular membranes could be viewed as representing dead end assembly products, or internalized PM components, enroute to lysosomal degradation. An intermediate hypothesis is that direct PM targeting and vesicle-mediated transport both can yield infectious virions, depending on the cell type or context (345).

A number of biochemical and genetic studies have identified different features of HIV-1 MA that influence PrGag localization, membrane binding, and assembly (64, 121, 273, 320, 343-345, 354, 401, 444, 470, 473, 499). With regard to localization, the amino-terminal α-helical segment of HIV-1 MA recently was shown to associate with the δ subunit of the AP-3, and this interaction appears important for PrGag MVB localization (111). Evidence also has shown that residues at the C-terminus of MA mediate PrGag association with the μ subunit of the clathrin-associated adapter complex AP-2, but that PrGag processing eliminates this interaction (29). Consistent with the role of AP-2 in PM cargo internalization, inhibition of MA-AP-2 binding increased virus particle release from cells (29). In addition to adapter protein binding, HIV-1 MA also contributes to the binding of the cellular motor protein KIF-4, an association that plausibly regulates the distribution of PrGag (448). Recent investigations also demonstrated that MA residues 5-

16 are necessary for PrGag binding to the tail interacting protein TIP47, which mediates a functional association of MA with Env (275).

While the above protein-protein interactions affect virus infectivity and PrGag localization, membrane binding is impacted greatly through MA-lipid interactions. The MA N-terminus is critical in this process. Like other mammalian retrovirus matrix proteins, HIV-1 MA is myristoylated at its N-terminus, and myristoylation is essential for efficient membrane binding, virus assembly, and infectivity (64, 354, 401, 444, 470). Studies support a myristoyl switch model for MA membrane association, in which the myristate group of PrGag inserts into membranes to promote binding, but that this fatty acid is retracted on proteolytic processing of PrGag, conferring a reduced membrane affinity for mature MA proteins (194, 352, 428, 444). Although the MA myristate is necessary for tight PrGag-membrane binding, it is not the only contributor. Analysis indicates that basic amino acids between residues 15 and 40 facilitate electrostatic interactions with negatively charged phospholipid headgroups on the cytoplasmic faces of membranes (320, 344, 507). However, HIV-1 MA also specifically associates with phosphatidylinositol (4,5) bisphosphate [$PI(4,5)P_2$] (342, 401). In particular, the $PI(4,5)P_2$ headgroup and 2'-acyl chain are accommodated by a cleft in the protein, and binding results both in the membrane-anchoring by the $PI(4,5)P_2$ 2'-acyl chain, and in triggering the exposure of the MA myristate (401). Given the affinity of MA for $PI(4,5)P_2$, it is plausible that $PI(4,5)P_2$ helps direct PrGag to cholesterol- and dihydrosphingomyelin-rich membrane domains, where HIV-1 assembly appears to occur (52, 63, 199, 333, 346).

Despite the many documented roles for HIV-1 MA, it is not absolutely required for virus infectivity. We originally demonstrated the infectivity of a 106 residue MA

deletion mutant that retained only the myristoylation signal and matrix-capsid (CA) cleavage site (473), an observation that subsequently was confirmed by others (386). In such cases, infection required either an Env protein pseudotype, or truncation of the HIV-1 Env cytoplasmic tail (386, 473). These deletion mutant results imply that wild type (wt) HIV-1 Env function requires MA, but that intact MA is not strictly required for viral replication.

The studies above suggest that any membrane targeting and anchor protein might suffice for directing the assembly of infectious HIV-1 particles. However, a caveat to this interpretation is that the aforementioned MA deletion proteins retained myristoylation signals (386, 473). Thus, a narrower hypothesis is that membrane interactions mediated by myristate are compatible with HIV-1 assembly and infectivity, while other membrane interaction motifs may or may not serve this role. To analyze this hypothesis further, we have examined HIV-1 MA protein substitution variants for their abilities to replace MA. For our investigations, we chose three alternative membrane binding domains (MBDs). One of these was the AKT protein kinase pleckstrin homology (PH) domain, which preferentially binds to 3' phosphatidyl inositol (PI) lipids such as phosphatidyl inositol (3,4) bisphosphate [$PI(3,4)P_2$], and the PM-enriched phosphatidyl inositol (3,4,5) trisphosphate [$PI(3,4,5)P_3$] (187, 208, 257, 296). The second MBD was the PH of phospholipase C δ1 (PLC), which has affinity for PM-localized $PI(4,5)P_2$ (208, 257, 430). Finally, we examined the phosphokinase Cγ cysteine-rich C1a plus C1b binding domain (CBD), which binds PM diacylglycerol (DAG), and can be activated by phorbol esters to move from intracellular stores to the PM (86, 119, 208, 338, 339). When the AKTPH, PLCPH, and PKCCBD were employed as substitutes for MA, we found that the

two PH domains readily directed PrGag proteins to assemble and release virus-like particles (VLPs) from cells, while PKCCBD-Gag proteins could be induced to release VLPs with phorbol esters. However, the VLPs that used alternative MBDs were noninfectious, either with HIV-1 Env, or with other Env pseudotypes. Assembly-competent but non-infectious AKTPH- and PLCPH-derived VLPs showed nearly normal viral RNA (vRNA), Env protein pseudotype, and entry levels, but had reduced reverse transcriptase (RT) activities, and were defective for DNA synthesis in target cells. Moreover, all MA substitution viruses showed moderate protease (PR) processing defects of the PrGag proteins. Additionally, precursor GagPol (PrGagPol) processing resulted in the accumulation of Pol-derived intermediates in virions, suggesting unexpected MBD effects on the regulation of later Pol protein cleavage steps. Our results indicate that while the membrane-targeting and assembly functions of HIV-1 MA can be replaced, alternative MBDs compromise virus infectivity by perturbation of virus core structure and function.

3.3 Materials and Methods

Recombinant DNA constructs. Wild type (wt) versions of the HIV-1 *gag* gene, expressed in the presence of *pol* gene products were produced from the previously described HIVgpt construct (351, 470, 473). The myristoylation-minus (Myr- HIV) and protease-minus (PR-; HIVgpt2498T) variants of HIVgpt also have been described before (303, 470, 472, 499). HIVgpt-MAGFP, encodes a Gag-GFP fusion protein similar to that reported by Muller *et al.* (317), in which the green fluorescent protein (GFP) open reading frame (orf) has been inserted near the C-terminus of the *gag* matrix domain. In

HIVgpt-MAGFP, the backbone construct is HIVgpt (351, 470, 473), and the source of the GFP orf was pEGFP-c1 (Clontech). The 5' juncture sequence is GCT GCG CTA GCG CTA CCG GTC GCC ACC ATG, the first codon corresponds to HIV HXB2 *gag* codon 120, while the last codon is the first GFP codon. The 3' juncture sequence is AAG TCC GGA CTC AGA TCC GCT GAC, where the first codon corresponds to the final coding codon of wt GFP, and the last codon is *gag* codon 121.

Alternative membrane-binding domain (MBD) constructs derived from pEGFPc1-AKTPH, pEGFPc1-PLCδPH, and GFP-pcDNA3-PKCγCys1ACys1B, which all were kindly provided by Tobias Meyer (187, 208, 296, 338, 339, 430). For GFP-AKTPH-Gag and GFP-PLCPH-Gag, the MA-truncated HXB2 *gag* orf was inserted C-terminal to the different pleckstrin homology (PH) domains, yielding constructs in which the pEGFPc1 cytomegalovirus (CMV) promoter drives expression of GFP-PH-Gag fusion proteins. The PH-*gag* juncture sequences for GFP-AKTPH-Gag and GFP-PLCPH-Gag are respectively CTG GGC CCA ACG AAT TCA TCT AGA GCT, and AAG GAG CTC GGG ATA TCT AGA GCT, where the final codon in each sequence corresponds to *gag* codon 120. For PKCCBD-GFP-Gag, the pcDNA3 (Invitrogen) CMV promoter drives expression of a fusion composed of PKC cysteine-rich membrane-binding domain (CBD), GFP, and the MA-truncated HIV *gag* orf: the GFP-*gag* juncture sequence is CTG TAC ACC GCG GGA TCC TCT AGA GCT, where the final codon is *gag* codon 120. Note that the HIV sequences in these constructs extend to the BclI site at HXBC2 nt 2432, but that PR activity is killed via fusion to a translation termination codon in an XbaI site, with juncture sequences of TAT GAT CTC TAG A.

To create the MA replacement constructs HIVgpt-AKTPH, HIVgpt-PLCPH, and HIVgpt-PKCCBD in the HIVgpt (351, 470, 473) backbone, the myristoylation-minus, *gag* second codon glycine-to-alanine HIVgpt mutant plasmid (470, 474) was used as a parent. These constructs harbor alternative MBDs between *gag* codons 15 and 120. The N-terminal and C-terminal juncture sequences, with codons 15 and 120 italicized are as follows: AKTPH and PLCPH N-junctures, *CGA* TGG GGA TCC; AKTPH and PLCPH C-junctures, TCT AGA *GCT*; PKCCBD N-juncture, *CGA* TAC ATG GGG GCC CGG TAC CTT; PKCCBD C-juncture, CGG TAC CAT GCC GCG GCC GGA TCC TCT AGA *GCT*. Other constructs used in these studies have been reported previously. They include the following: Blam-vpr (318, 410); the MuLV gag expression construct, pXMGPE (182, 304); the HIV Gag-β-galactosidase expression construct, HIVGBG (472); pBluescribeHIV831-680 (473, 499), for RNAse protection probe production; and the glycoprotein expression constructs pVSV-G (410), SV-A-MLVenv (470, 473), and HIV-env (470, 473).

Cells and viruses. Human embryonic kidney (HEK) 293T (410) and HiJ (410, 470, 473) HeLa cells expressing human CD4 were grown at 37˚C in 5% CO_2 in culture medium composed of Dulbecco's modified Eagle medium (DMEM) supplemented with 10% fetal calf serum, penicillin, streptomycin, and 10 mM HEPES (pH 7.4). For transfections, 10 cm dishes of 293T cells were transfected by the calcium phosphate method (410, 470, 473). For Gag analysis, 24 μg of plasmid DNAs (Figure 1) were used; for infection assays, 16 μg HIV-derived DNAs were cotransfected with 8 μg envelope protein expression plasmids; for entry assays, transfections employed 12 μg of HIV-derived DNAs, plus 6 μg of pVSV-G expression plasmid (410), plus 6 μg of BlaM-Vpr

DNA (318, 410); while for Gag-β-galactosidase (Gag-β-gal) experiments, 16 μg of Gag expression plasmids were cotransfected with 8 μg of HIVGBG (472). Routinely, cell and virus samples were collected 3 d post-transfection. In some cases, the effects of phorbol esters were tested by treatment with a 1:1000 dilution of 1 mM phorbol myristate acetate (PMA; Sigma) or phorbol dibutyrate (PDB) at 24 h and again at 6 h prior to sample collection. Cell pellets were collected and washed in phosphate-buffered saline (PBS; 9.5 mM sodium potassium phosphate [pH 7.4], 137 mM NaCl, 2.7 mM KCl). Virus-containing media were filtered through 0.45 μm-pore filters (Gelman) and concentrated by centrifugation through 20% sucrose in PBS cushions (2 h at 82,500 x *g* [25,000 rpm in a Beckman SW28 rotor, 4 ml cushions] or 45 min at 197,000 x *g* [40,000 rpm, SW41 rotor, 2 ml cushions]). Virus pellets were resuspended in 0.1 ml PBS per cell plate and stored in aliquots at -80˚C.

To test virus infectivities, confluent 10 cm dishes of HiJ cells were split 1:40 onto 35 mm dishes the day before infections. For infections, cells were incubated at 37°C for 72 h in the presence of filtered virus in a total volume of 2 ml culture media. Subsequently, cells were transferred to 10 cm dishes and fed with selection media containing 9.35 ml of culture media, 0.65 ml of *gpt* supplement solution (3.85 mg/ml xanthine, 0.046 mg/ml hypoxanthine, 0.062 mg/ml thymidine, 0.154 mg/ml glycine, 2.308 mg/ml glutamine), and 15 μl of mycophenolic acid (Gibco) per plate. Cells were selected for 10-14 d, with selection media changed at 3-4 d intervals. After selection, *gpt*-positive colonies were stained with 0.5 % methylene blue in 50 % methanol, gently rinsed in water and dried prior to colony counting. Infectivity was calculated as follows:

Virus titer = (colonies)(virus dilution factor)(cell split ratio)/(cell proliferation between infection and selection). Results were normalized to input virus Gag protein levels.

Protein analysis. For protein analysis, cell samples (20% of pellets from each 10 cm plate) were suspended in IPB (20 mM Tris-HCl [pH 7.5], 150 mM NaCl, 1 mM ethylenediamine tetraacetic acid [EDTA], 0.1% sodium dodecyl sulfate [SDS], 0.5% sodium deoxylate, 1.0% Triton X-100, 0.02% sodium azide), incubated on ice for 5 min, vortexed, and subjected to centrifugation 13,000 x *g* for 15 min at 4˚C. Soluble material was collected, mixed with 1 volume of 2 x sample buffer (12.5 mM Tris-HCl [pH 6.8], 2% SDS, 20% glycerol, 0.25% bromophenol blue) and 0.1 volume of β-mercaptoethanol (β-Me). For virus samples, 40 μl aliquots of resuspended virus pellets were mixed with one volume of 2 x sample buffer and 0.1 volume of β-Me. Cell and virus samples were heated to 95˚C for 3 to 5 min, and subjected to SDS-polyacrylamide electrophoresis (SDS-PAGE). After SDS-PAGE fractionation, proteins were electroblotted, and immunoblotted following previously described methods (182, 220, 303, 304, 410, 470, 472, 473, 499). The antibody used for detection of HIV-1 CA was Hy183 (kindly provided by Bruce Chesebro), used at 1:15 dilution from the hybridoma culture medium. Antibodies obtained through the NIH AIDS Research and Reference Reagent Program, Division of AIDS, NIAID, NIH were the HIV-1 RT monoclonal antibody (MAb21) from Dr. Stephen Hughes, used at 1:300; and HIV-1 protease antisera from HIVSF2 from BioMolecular Technology, used at 1:1000. Other primary antibodies were anti-VSV-G (Roche), used at 1:400; and anti-GFP (Invitrogen #A11121), used at 1:1000. In all cases, the secondary antibody was an anti-mouse IgG alkaline phosphatase-conjugated secondary antibody (Promega) was used at 1:15,000. Color reactions for visualization of

antibody-bound bands employed nitroblue tetrazolium plus 5-bromo-4-chloro-3-indolyl phosphate in AP buffer (100 mM Tris-hydrochloride [pH 9.5], 100 mM NaCl, 5 mM $MgCl_2$). For quantitation, immunoblots were air-dried and scanned using an Epson G810A scanner. Band intensities of scanned TIFF images were quantitated using NIH Image 1.61 software.

Nucleic acid analysis. For RNA analysis, viral RNA samples were obtained from virus pellets that were resuspended in 200 μl PBS, and supplemented with 2 μl of 10% SDS plus1 μl of 10 mg/ml carrier *E. coli* tRNA (Roche). Samples were extracted twice with 200 μl of 1:1 phenol:chloroform, extracted twice with 200 μl chloroform, ethanol-precipitated, dried, and resuspended in 50 μl of TE buffer (10 mM Tris [pH 7.8], 0.1 mM EDTA). To isolate cellular RNA samples, 10 cm dishes of cell monolayers were washed, suspended in 1 ml of GTC mix (4 M guanidium thiocyanate, 25 mM sodium citrate [pH 7.0], 0.5% sarkosyl, 0.1 M β-Me), layered onto CsCl/EDTA (6.2 M CsCl, 0.1 M EDTA [pH 7.0]) cushions, and centrifuged at 115,000 x *g* (35,000 rpm in a Beckman SW50.1 rotor) for 18 h at 15˚C. After centrifugation, supernatants were removed, and pellets were resuspended in 400 μl TE, phenol-choloroform-extracted twice, chloroform-extracted once, ethanol-precipitated, dried, and resuspended in 100 μl TE. Samples were quantitated by measuring UV absorbance at 260 nm in a Beckman DU-64 spectrophotometer, assuming an extinction coefficient of 1 optical density (O.D.) unit per 40 ug/ml RNA at a pathlength of 1 cm.

Probes for RNase detection were made by incubation of 1 μg of EcoRI-linearized template plasmid (pBluescribeHIV831-680; (470, 499)) with transcription buffer (40 mM Tris [pH 7.4], 10 mM DTT, 6 mM $MgCl_2$, 0.8 mM spermidine), 100 μCi of [α-^{32}P]rGTP,

0.5 mM each of rATP, rCTP, and rUTP, 1 μl of RNasin (Promega), 1 mM dithiothreotol [DTT], and 20 U of T3 polymerase (Promega) at 37°C for 1 h. Probes then were ethanol precipitated, dried, resuspended, separated on 5% sequencing gels (470, 499), eluted, and reprecipitated prior to use (470, 499). For RNAse protections, RNA-normalized cell samples or Gag-normalized viral samples were precipitated with 10 μg of tRNA. Pellets were resuspended in 30 μl of 80% formamide, 400 mM NaCl, 40 mM piperazine-N,N-bis(2-ethanesulfonic acid) (PIPES, pH 6.4), mixed with probe, incubated at 75-85°C for 5 min, and then incubated at 30°C overnight. Overnight incubation samples were supplemented with 350 μl RNase treatment buffer (300 mM NaCl, 10 mM Tris [pH 7.5], 5 mM EDTA, 40 μg/ml RNAse A [Rochel, 2 μg/ml RNAse T1 [Roche]) and incubated at 30°C for 30 min, followed by the addition of 2.5 μl of 20 mg/ml proteinase K (Boehringer) plus 20 μl of 10% SDS and further incubation at 37°C for 15 min. Samples subsequently were phenol-chloroform extracted, chloroform extracted, ethanol precipitated, dried, fractionated on 6% acrylamide sequencing gels, and autoradiographed. Viral genomic RNA bands on autoradiographs were scanned using an Epson G810A scanner, and quantitated using NIH Image 1.61 software.

For detection of one long terminal repeat (1-LTR) circles in infected cells, HiJ cells were split 1:40 onto 35-mm plates one day prior to infection. Cells on plates were infected 72 h in a total volume of 2 ml virus plus media, and then washed, collected in 500 μl PBS, pelleted, suspended in 200 μl PCR lysis buffer (10 mM Tris [pH 8.3], 50 mM KCl, 1.5 mM $MgCl_2$, 0.01% gelatin, 0.45% NP-40, 0.45% Tween-20, 100 μg/ml proteinase K [Sigma]), incubated at 55˚C 2-20 h, heated to 100˚C for 10 min, and then stored at -80˚C. One and two LTR circles in 0-4 μl lysate samples were amplified by

polymerase chain reaction (PCR). Reactions employed Taq DNA polymerase (New England Biolabs; NEB) plus primers corresponding to HIV-1 HXB2 nucleotides 9038-9058 and 1221-1202, and were performed for 35-45 cycles with cycle times of 95°C 1 min, 55 °C 1 min, 72 °C 2.5 min. Aliquots of PCR reactions were fractionated electrophoretically on horizontal 0.9% agarose-TBE (89 mM Tris, 89 mM boric acid, 2 mM EDTA, pH 8.2) gels in parallel with Lambda HindIII and PhiX HaeIII DNA size standards, and stained with ethidium bromide. Stained DNA bands were imaged under UV light using a Kodak EDAS 290 Gel Photo system, and 1-LTR circle products were quantitated as a marker for reverse transcription in infected cells (72) using NIH Image 1.61 software.

Enzyme assays. Exogenous reverse transcriptase (RT) assays were performed with poly(A) and oligo(dT) templates and primers and detergent-disrupted virions (410, 470). Gag-normalized virus samples in PBS were incubated at 37°C for 2 h in RT assay cocktail (50 mM Tris [pH 8.3], 20 mM dithiothreitol [DTT], 0.6 mM $MnCl_2$, 60 mM NaCl, 0.05% NP-40, 2.5 μg/ml of oligo[dT] [Pharmacia], 10 μg/ml of poly[A][Pharmacia], 10 μM dTTP [1 Ci/mM {α-^{32}P}dTTP]). Dilutions of avian myeloblastosis virus (AMV) RT (Roche) were run in parallel as controls. Following incubations, samples were precipitated by addition of 0.1 volume of 100% trichloroacetic acid (TCA) and incubated overnight at 4˚C. TCA precipitates were pelleted by centrifugation for 10 min at 13,600 x *g* at 4˚C, washed five times with 10% TCA, and quantitated in a scintillation counter (Beckman).

For β-galactosidase (β-gal) assays, cells and viruses were collected from 10 cm plates and processed as described above. Sample aliquots (half of each virus sample, or

10% of each cell sample) in 150 μl PBS were mixed with 1.5 μl of 10% SDS and 600 μl of PM2 buffer (33 mM NaH_2PO_4, 66 mM Na_2HPO_4, 0.1 mM $MnCl_2$, 2 mM $MgSO_4$, 40 mM β-Me), and vortexed. Reactions were initiated by the addition of 150 μl of 4 mg/ml o-nitrophenyl β-D-galactopyranoside (ONPG; Sigma) in PM2; incubations proceeded at 37˚C until color changes were observed; reactions were quenched with 375 μl of 1 M Na_2CO_3; and β-gal activities were calculated from 420 nm absorbance readings as described previously (220, 472).

Enzymatic entry assays followed previously reported protocols and scored for β-lactamase activity delivered to target cells by BlaM-Vpr fusion proteins (318, 410). Confluent 10 cm dishes of HiJ cells were split 1:40 onto 35-mm dishes the day before infections. Cells were infected overnight at 37˚C in a total volume of 2 ml cell culture media. After infections, supernatants were removed, cells were washed with Hank's balanced salt solution (HBSS) without calcium or magnesium, and then incubated in 1 ml CCF2/AM loading solution (2 μM CCF2/AM; Invitrogen) at 26˚C and in 5% CO_2 for 4 h. Loading solution then was removed, cells were washed in HBSS, trypsinized, pelleted, fixed in 1% paraformaldehyde in PBS for 20 min, pelleted, washed in HBSS, pelleted, and resuspended in 500 μl HBSS. For analysis, fluorescence profiles of infected cells were monitored on a Becton-Dickinson Turbo Vantage flow cytometer to quantitate cleaved product as blue fluorescence and uncleaved substrate as green fluorescence signals. Cells were gated on the infected, unstained control samples, and the percentages of cells positive for product were normalized to Gag protein levels in input virus samples.

Microscopy. To examine GFP-positive virus particles, 20 μl aliquots of suspended virus particle preparations were deposited on microscope slides, covered with

22 mm x 22 mm coverslips (Fisher), viewed on a Zeiss Axioplan fluorescence microscope, and imaged using Improvision OpenLab software. For fluorescence microscopy of transfected cells, 22 mm x 22 mm coverslips in 6 well dishes were pretreated with 0.7% porcine gelatin (Sigma) at 4˚C for 30 minutes, after which gelatin was replaced with media. Transfected cells were split 1:40 or 1:80 from 10 cm plates onto coverslips one day post-transfection, incubated for another two days, and then either mounted for GFP fluorescence or processed for immunofluorescence and then mounted. For GFP fluorescence, cells were washed once in PBS, fixed in 4% paraformaldehyde (Sigma) in PBS at room temperature for 1 h, washed in PBS, and mounted on slides (Fisher) in Fluoro-G mounting medium (Southern Biotech). For immunofluorescence, cells were fixed and washed as above, and then permeabilized in 0.2% Triton X-100 in PBS at room temperature for 10 min, washed once, and incubated in culture medium for 10 min. Subsequently, anti-HIV-1 CA primary antibody (Hy183, from Bruce Chesebro) in culture medium or medium alone for negative controls was added, and cells were incubated at 37˚C for 1 h, rocking every 15 min. After primary antibody incubations, coverslips were washed three times in culture medium, then secondary antibody (anti-mouse AlexaFluor 594; Invitrogen) diluted 1:500 in media was added, and the samples were incubated at 37˚C for 30 min, rocking once at 15 min. Following incubations, the cells were washed twice in culture medium and three times in PBS, followed by mounting onto microscope slides in Fluoro-G mounting medium. Samples were viewed on a Zeiss Axioplan fluorescence microscope, and photographed using Improvision OpenLab software. For quantitation of cell surface staining, rectangular sections from cell centers to cell edges taken from 10 cells per sample were cut and analyzed. To do so,

brightness intensity signals ([number of pixels] x [pixel brightness – backround brightness]) from the outermost 20% of sampled areas were divided by brightness intensity signals from the entire sample areas. These ratios, multiplied by 100 were designated as percentages of cell surface staining.

Electron microscopy (EM) of negatively stained virus particles was performed as described by Scholz *et al.* (410). Concentrated virus particle samples were lifted for 2 min onto carbon-coated UV-treated EM grids, rinsed for 15 s in water, stained for 1 min in filtered 1.3% uranyl acetate, wicked, and dried. EM images were collected on a Philips CM120/Biotwin TEM equipped with a Gatan 794 multiscan charge-coupled device (CCD) camera. Virus particle diameters were determined with the aid of Gatan digital micrograph software, and particles were scored as having conical or cylindrical cores if projection images showed negatively stained triangular, rectangular, or trapezoidal structures. For EM of cells, transfected cells were fixed, postfixed, prestained, dehydrated, infiltrated, embedded, sectioned and stained as described by Arvidson *et al.* (20). EM was performed on a Philips CM120/Biotwin, and 1024 pixel x 1024 pixel images were collected electronically on a Gatan 794 multiscan CCD camera.

3.4 Results

Particle release directed by alternative membrane binding domains

To analyze whether the AKTPH, PLCPH, or PKCCBD membrane-binding domains could replace HIV-1 MA in directing the assembly and budding of HIV virus-like particles, we initially examined VLPs released from cells transfected with the matrix substitution constructs GFP-AKTPH-Gag, GFP-PLCPH-Gag, and PKCCBD-GFP-Gag.

As illustrated in Figure 1, these plasmids express PrGag proteins from PR- constructs in which the HIV-1 wild type (wt) Gag domains from CA through p6 were linked to N-terminal modules composed of green fluorescence protein (GFP) and MBD units. For controls in these studies, we employed a wt HIV-1 Gag expression construct, HIVgpt (304, 351, 470, 472, 473, 499), as well as HIVgpt-MAGFP (Figure 1), in which the GFP coding region has been inserted near the C-terminus of MA, in a fashion similar to the GFP-Gag construct described by Muller *et al.* (317).

Consistent with previous results (303, 470, 473, 499), in transfected cells, the wt HIVgpt construct expressed Gag proteins and efficiently assembled and released virus particles. When cells transfected with the wt construct were treated with the phorbol esters PMA or PDB, we did not observe any noticeable changes on wt virus release levels (Figure 2). Relative to the wt construct, our HIVgpt-MAGFP construct appeared to release slightly reduced Gag protein levels, while results with our matrix replacement constructs were varied (Figure 2). With the PH substitutions GFP-AKTPH-Gag and GFP-PLCPH-Gag VLPs were assembled and released efficiently (Figure 2). In contrast, PKCCBD-GFP-Gag proteins failed to release VLPs to media samples. However, because PKCCBD binds DAG and is activated by phorbol esters (86, 119, 208, 338, 339), we also tested whether phorbol myristate acetate (PMA) or phorbol dibutyrate (PDB) could mobilize the release of PKCCBD-GFP-Gag VLPs. Interestingly, while the phorbol esters had no apparent effect on the release of wt HIV particles, they clearly increased particle release directed by the PKCCBD (Figure 2).

To verify that GFP modules were retained on the full-length PrGag proteins expressed by the matrix replacement constructs, VLP samples were electrophoresced in

parallel and then immunoblotted for detection of either HIV-1 CA or GFP. Not surprisingly, none of the wt HIV-1 bands detected with our CA antibody were observed when the anti-GFP antibody was employed whereas with matrix replacement VLPs, each of the lowest mobility PrGag proteins visualized with anti-CA, also were seen with anti-GFP, supporting the conclusion that these represent the full-length PrGag proteins (data not shown). The incorporation of GFP into the VLPs of GFP-AKTPH-Gag, GFP-PLCPH-Gag, and PKCCBD-GFP-Gag permitted us monitor VLP formation via fluorescence microscopy, and as a control, we took advantage of the availability of HIVgpt-MAGFP particles. When subjected to fluorescence microscopy, HIVgpt-MAGFP VLPs were observed as bright green spots (data not shown), similar to the appearance of vpr-GFP-labeled HIV-1 particles (322). Particles assembled and released by the PH replacement Gag proteins also were imaged as green spots, while for PKCCBD-GFP-Gag, fluorescent VLP release required phorbol ester induction. These results lend qualitative support to the results presented in Figure 2.

Cellular localization of alternative Gag proteins

Where do matrix replacement Gag proteins accumulate within cells? We addressed this question via microscopic tracking of fluorescent proteins in transfected cells. With HIVgpt-MAGFP, the fluorescent proteins were observed at cell surfaces and perinuclear regions, as well as in a heterogeneously staining pattern throughout cells (Figure 3A). This staining profile was similar to that observed previously for wt HIVgpt CA (303, 470, 473, 499), and for the MAGFP Gag protein of Muller *et al.* (317), and was not altered appreciably by the addition of phorbol esters (Figure 3B). Interestingly, AKT

PH, which binds to 3' PIs, and PLC PH, which binds $PI(4,5)P_2$ both targeted their respective Gag proteins to the PM, as indicated by the strong cell surface staining of the GFP-AKTPH-Gag (Figure 3C) and GFP-PLCPH-Gag proteins (Figure 3D). For PKCCBD-GFP-Gag, proteins accumulated in large aggregates, often adjacent to cell nuclei (Figure 3E), but this pattern was shifted somewhat to smaller aggregates and more surface staining on PMA treatment (Figure 3F).

In an effort to quantitate our fluorescence staining observations, we calculated cell surface staining levels. To do so, fluorescence levels corresponding to the outermost 20% of cell radii were expressed as percentages of total cell fluorescence signals (see Materials and Methods) to give percentages of cell surface staining. For HIVgpt-MAGFP, we calculated the cell surface staining percentage to be 29 $\pm$ 4 %, presumably reflecting the fact that wt PrGag proteins localize both to the PM and to intracellular membrane and vesicle compartments (111, 221, 272, 336, 345). PMA treatment did not alter this surface staining percentage (28 $\pm$ 5 %). Relative to these levels, the PH replacement proteins demonstrated higher surface staining, with percentages of 36 $\pm$ 7 % for GFP-AKTPH-Gag and 39 $\pm$ 6 % for GFP-PLCPH-Gag. Not surprisingly, surface staining levels were low (15 $\pm$ 5 %) for PKCCBD-GFP-Gag, but increased slightly to 23 $\pm$ 4 % on PMA treatment.

As another approach to the localization of Gag proteins within cells, we resorted to electron microscopy (EM), relying on the tendency of Gag protein aggregates to stain darkly in negatively stained thin sections (20, 121, 197). For a control in these studies, we used a PR- but otherwise wt HIV-1 Gag expression construct (HIVgpt PR-) (303, 470, 472, 499). In agreement with previous work (20), wt PR- HIV-1 particles were observed

budding and at cell surfaces (Figure 4A-C). In contrast, the GFP-AKTPH-Gag proteins showed a variety of structures (Figure 4D-F). Occasionally, large vesicles containing black rimmed smaller vesicles and darkly staining virus-sized spherical structures were observed (Figure 4D). However, virus-like budding structures, or VLPs within budding structures (Figures 4E, F) also were seen. Relative to the structures assembled in GFP-AKTPH-Gag-transfected cells, those formed by GFP-PLCPH-Gag (Figure 4G-I) and PKCCBD-GFP-Gag (Figure 4J-L) were more consistent. In particular, for GFP-PLCPH-Gag, particle assembly occurred at the PM. This was indicated by the appearance of electron dense nascent buds at the PM (Figure 4G), as well as small (Figure 4H) and large (Figure 4I) budding structures. For PKCCBD-GFP-Gag, the picture was quite different. Rather than assembly at the PM, these proteins associated in large (Figures 4J,K) or small clusters or aggresomes (217). We did not observe any obvious reduction in the numbers of aggresomes in PMA treated PKCCBD-GFP-Gag-transfected cells (data not shown), suggesting that the quantitative effects of phorbol esters on the release (Figure 2) and localization (Figure 3) were not dramatic enough to be scored by EM.

Despite the localization differences between the wt and matrix replacement Gag proteins, it was of interest to assess whether the proteins might cross paths within cells. We examined this by coexpression of wt HIV-1 Gag-β-galactosidase (Gag-β-gal) fusion proteins along with wt or MA substitution Gag proteins in cotransfected HEK 293 cells. As previously observed (472), expression of HIV-1 Gag-β-gal in the absence of any helper proteins resulted in very low levels of Gag-β-gal release from cells, and treatment with PMA or coexpression with murine leukemia virus (MuLV) Gag proteins failed to increase levels of release. However, cellular coexpression of HIV-1 Gag-β-gal and wt

HIV-1 Gag proteins caused the efficient assembly and release of β-gal-positive (β-gal$^+$) VLPs (data not shown), as described previously (472). The Gag proteins with PH domains also efficiently facilitated the efficient release of β-gal$^+$ VLPs, while PKCCBD-GFP-Gag proteins induced β-gal release to a lower extent, and in a phorbol ester-dependent fashion (data not shown). Altogether, these results demonstrate that despite their different membrane-targeting signals, wt and MA substitution proteins are able to associate with each other within cells.

Replication defects of chimeric Gag proteins

Since alternative MBDs were able to direct the release of VLPs, albeit to different degrees, and with potentially different morphologies, we next tested whether they were compatible with virus replication. For these studies, we replaced the MA domain in HIVgpt (351, 470) with MBDs, excluding GFP domains. The resulting constructs, HIVgpt-AKTPH, HIVgpt-PLCPH, and HIVgpt-PKCCBD, retained the wt HIV-1 MA-CA cleavage region and the MA N-terminus, but bore the glycine-to-alanine mutation at *gag* codon 2, to prevent Gag protein myristoylation (64, 470, 472). We scored for replication in single cycle infections via cotransfection of HIVgpt-derived constructs with a Vesicular Stomatitis virus glycoprotein (VSV-G) expression construct (pVSV-G) into HEK 293 cells, collection of released virions for infection of CD4$^+$ HeLa (HiJ) (410, 470, 473) cells, and selection for *gpt* gene expression. As illustrated in Figure 5, while mock-infected HiJ cells were killed in *gpt* selective media, numerous darkly staining colonies derived from wt HIVgpt infected cells survived selection. In our hands, with Gag-normalized input virus, our GFP insertion construct HIVgpt-MAGFP (Figure 1) proved

to be about 10% as infectious as wt (Figure 5). This level of infection was about 10-fold higher than that observed by Muller *et al.* (317), but those investigators used a slightly different MAGFP construct, employed the wt HIV-1 Env protein, and scored infection in an alternative fashion. In contrast to HIVgpt and HIVgpt-MAGFP, our matrix replacement HIVgpt constructs failed to demonstrate any infectivity (Figure 5), and identical results were observed when we pseudotyped the viruses with either HIV-1 Env, or an amphotropic MuLV Env (data not shown). We then verified that vRNAs transcribed by MA substitution constructs could be encapsidated, reverse transcribed, integrated and expressed in target cells. To do so, constructs were cotransfected with pVSV-G plus a wt *gpt*-minus HIV-1 Gag expression construct (HIV-Luc) (410), and infectivities of released viruses were scored by selection for *gpt*. In these studies, wt Gag proteins efficiently fostered the transduction of HIVgpt-AKTPH, HIVgpt-PLCPH, and HIVGPT-PKCCBD genomes to target cells (data not shown), implying that the matrix replacement vRNAs did not carry a *cis*-active defect for replication.

The lack of infectivity for HIVgpt-AKTPH, HIVgpt-PLCPH, and HIVgpt-PKCCBD viruses did not appear to be a consequence of impaired particle assembly and release, since the constructs yielded detectable levels of PrGag and CA proteins in pelleted media samples (Figure 6, top panel; lanes E-H). Compared with cellular Gag protein levels (Figure 6, top panel, lanes A-D), HIVgpt wt and HIVgpt-PLCPH showed similar VLP release levels (Figure 6, middle panel), HIVgpt-AKTPH showed about a two-fold reduction in VLP release (Figure 6, middle panel), and HIVgpt-PKCCBD showed at least a ten-fold release reduction (Figure 6, middle panel) even in the presence

of PMA. However, these release reductions were comparatively small, relative to the observed infectivity block of over a thousand-fold (Figure 5).

Despite the appearance of PrGag and CA bands for the matrix substitution HIVgpt variants, several anomalies were evident. In particular, HIVgpt-AKTPH and HIVgpt-PLCPH VLP preparations both showed immunoreactive bands of slightly slower mobility than their respective predicted 57-58 kDa PrGag proteins (Figure 6, top panel, lanes F, G). Because the intensities of these low mobility species varied from preparation to preparation, we hypothesized that they might represent variable post-translational modification forms; but they were resistant to endoglycosidase F, and were unreactive to anti-phosphotyrosine, anti-phosphothreonine, and anti-phosphoserine antibodies, suggesting that they did not result from N-glycosidation or phosphorylation (data not shown). In addition to these low mobility species, some Gag processing differences were noted. Although all of the MA replacement particle preparations looked similar to wt with regard to their levels of partial processing intermediates, PrGag percentages were increased, at the expense of mature CA (Figure 6, bottom panel). These processing differences appeared relatively minor for HIVgpt-AKTPH, but were clearly skewed for HIVgpt-PLCPH, where only a third of the particle-associated Gag protein was in the mature form (Figure 6, bottom panel).

Because MA substitution viruses were functionally impaired, we decided to examine VLP morphologies of HIVgpt wt, and the two well-released MBD variants (AKTPH and PLCPH) by EM. To do so, pelleted particles from transfected cell media samples were applied to EM grids, dried, stained and imaged, as we have done previously (410). Examination of 100 particles of each virus type showed that they had comparable

diameters (Figure 7, lower right). We also scored for the percentages of particles with roughly conical or cylindrical cores, and found that wt and HIVgpt-AKTPH results were similar (65%), while the percentage for HIVgpt-PLCPH was slightly reduced (50%; Figure 7, upper right). However, we noted some differences that were difficult to quantitate. In particular, HIVgpt-AKTPH cores occasionally appeared to have abnormalities (Figure 7, AKTPH, leftmost image), and frequently stained poorly at the narrow cone ends (right two images). HIVgpt-PLCPH cores seemed even more aberrant, and were often short (PLCPH, leftmost two images) or poorly staining (rightmost image) at narrow ends.

The above observations suggest that alternative MBDs interfere with the formation of mature infectious virus cores. To examine the replication defects of HIVgpt-AKTPH and HIVgpt-PLCPH particles in more detail, viruses produced by these constructs were subjected to additional assays: we excluded HIVgpt-PKCCBD from these analyses, due to difficulties in obtaining sufficient material. For quantitation of vRNA encapsidation, virus particle vRNA levels were determined by RNAse protection, as we have done previously (410, 473, 499). However, since we have demonstrated that HIV-1 MA is not needed for efficient vRNA encapsidation (473), it was not surprising that our PH HIVgpt variants incorporated 83% (AKTPH) to 104% (PLCPH) wt amounts of vRNA into viruses. Another parameter that conceivably could have affected infectivity was the efficiency of VSV-G pseudotyping. We assayed this via parallel immunoblotting of virus samples for detection of Gag and VSV-G, but found that VSV-G-to-Gag ratios either were not reduced (AKTPH) or only slightly reduced (PLCPH) relative to wt ratios. These observations were consistent with our entry assay results. Here, we followed

previously reported methodology (318, 410) (see Materials and Methods) to score for virus-mediated β-lactamase Vpr (BlaM-Vpr) fusion protein delivery to HiJ target cells. Although entry levels ranged between two-thirds (PLCPH) and 170% (AKTPH) that of wt levels, these differences were small compared to the infectivity block (Figure 5). Thus, the dominant defect of our MA substitution variants does not appear to be virus core delivery to new cells.

While delivery of HIVgpt-AKTPH and HIVgpt-PLCPH VLP cores to HiJ cells was not impaired appreciably, the replicative capacities of the cores were compromised. One indication of this defect was a reduction in the RT levels associated with matrix replacement VLPs. Indeed, Gag-normalized RT levels for HIVgpt-AKTPH particles were reduced two-fold from wt, while activities for HIVgpt-PLCPH were only 15% of wt levels. These RT defects were more evident when reverse transcription products were monitored in infected cells. For these assays, one long terminal repeat (1-LTR) RT byproducts (72) in infected cells were measured after PCR amplification as described in the Materials and Methods. Importantly, 1-LTR products were detected readily for HIVgpt wt, but were undetectable with the MBD variants, indicating that their virus cores failed to complete RT steps in target cells. We further examined this RT defect by immunoblot analysis of RT proteins in HIVgpt wt, HIVgpt-AKTPH, HIVgpt-PLCPH, and HIVgpt-PKCCBD VLPs. Surprisingly, whereas wt VLPs showed the expected 66 kDa RT-RNAse H (RT-RH) and 51 kDa RT species, our three MBD variant VLPs each revealed a single immunoreactive band at a mobility of about 75 kDa (Figure 8). Because species with this mobility also were detected with an anti-PR antibody (data not shown), our data indicate that these bands represent PR-RT-RH processing intermediates (372,

373). These results suggest that MA replacements exert an influence on PrGagPol cleavages that occur after Gag and Pol are separated, and are consistent with reduced RT and PrGag processing levels in our chimeric viruses.

3.5 Discussion

The HIV-1 matrix domain targets PrGag proteins to assembly sites on cellular membranes, and is required for incorporation of full-length HIV-1 Env proteins into virus particles (64, 95, 113, 139, 142, 290, 343-345, 347, 348, 354, 470, 473, 490, 497, 507). However, PrGag proteins with MA deletions that retain myristoylation signals and MA/CA cleavage sites are able to direct the assembly of infectious virions, provided that the particles are pseudotyped with heterologous Env proteins or C-terminally truncated HIV-1 Env proteins (386, 473). These results may suggest that both full-length and MA-deleted, myristoylated HIV-1 PrGag proteins are targeted to membrane sites that are permissive for the assembly of infectious virions. Alternatively, virus assembly simply may require the delivery of the C-terminal Gag domains to a membrane surface, with few additional requirements.

Our results suggest that the HIV-1 assembly machinery is relatively tolerant of the MBD used to foster membrane association. Specifically, the AKT PH, which binds 3' PI lipids (187, 208, 257, 296), and the PLC PH, which binds $PI(4,5)P_2$ (208, 257, 430), both mediated the assembly and release of VLPs (Figures 2, 6). Efficient VLP release occurred in the absence of PI 3-kinase and PI(4)P 5-kinase activation, implying that basal levels of PM $PI(3,4,5)P_3$ and $PI(4,5)P_2$ were sufficient for cell surface localization. In contrast to the two PH domains, the cysteine-rich membrane-binding domain of PKC

(PKCCBD) (86, 119, 208, 338, 339) directed Gag protein accumulation into large aggresomes (217) (Figures 3, 4). However, consistent with the ability of the PKCCPD to bind DAG and phorbol esters (86, 119, 208, 338, 339), cell treatment with PMA or PDB boosted VLP release from cells (Figures 2, 6). Despite their different cellular itineraries and membrane-binding mechanisms, all of our MA substitution Gag proteins were able to facilitate the release of wt HIV-1 Gag-β-gal proteins from cotransfected cells, which demonstrates that there is some overlap in the pathway taken by Gag-β-gal proteins with wt MA domains, and the assembly and release routes taken by the matrix replacement proteins.

Although our alternative MBDs sufficed for VLP assembly and release, they failed to support virus replication (Figure 5). For the PH variants, vRNA encapsidation, VSV-G pseudotyping, and entry all occurred at wt or slightly diminished levels. However, reverse transcription in infected cells was greatly impaired, and viruses showed reduced RT activities, moderate to severe PrGag processing defects (Figure 6), and the appearance of altered mature cores (Figure 7). Notably, VLPs assembled by all three MA replacements carried PR-RT-RH proteins, and did not show the normal 66 kDa RT-RH and 51 kDa RT products (Figure 8). This finding is consistent with the observed RT and PrGag processing detects of MBD variant viruses. However, our results imply that MBDs influence PrGagPol processing steps that occur after Pol domains are freed from their co-translated partners. Formally, MBDs could interfere with later PrGagPol cleavages via a direct interaction with PR domains. Alternatively, they may exert their effects as a consequence of their specific membrane assembly sites, or through flexibility constraints imposed on the viral proteins.

Previous reports have demonstrated that while the globular head of HIV-1 MA can exert a negative effect on virus assembly in some cellular contexts (185, 207, 367), large sequence insertions into MA can be accommodated for the purposes of VLP assembly and release (268, 317, 471). Moreover, matrix domain swapping studies have revealed that some chimeric retrovirus PrGag proteins efficiently assemble virions that can be infectious (79, 383). We have extended these studies by showing that the HIV-1 assembly machinery is flexible with regard to its means of membrane association, but that alternative MBDs directly or indirectly may interfere with the elaboration of infectious virus cores.

Acknowledgements

We are grateful to Tobias Meyer (Stanford) for the AKTPH, PLCPH and PKCCBD plasmids, and advice concerning their use. We also appreciate the assistance and advice from lab members Ayna Alfadhli, Ben Kukull, and Carolyn McQuaw. We thank Mandy Boyd for acquisition of flow cytometry data. This work was supported by National Institutes of Health Grants GM060170 and AI071798 to EB.

3.6 Figures

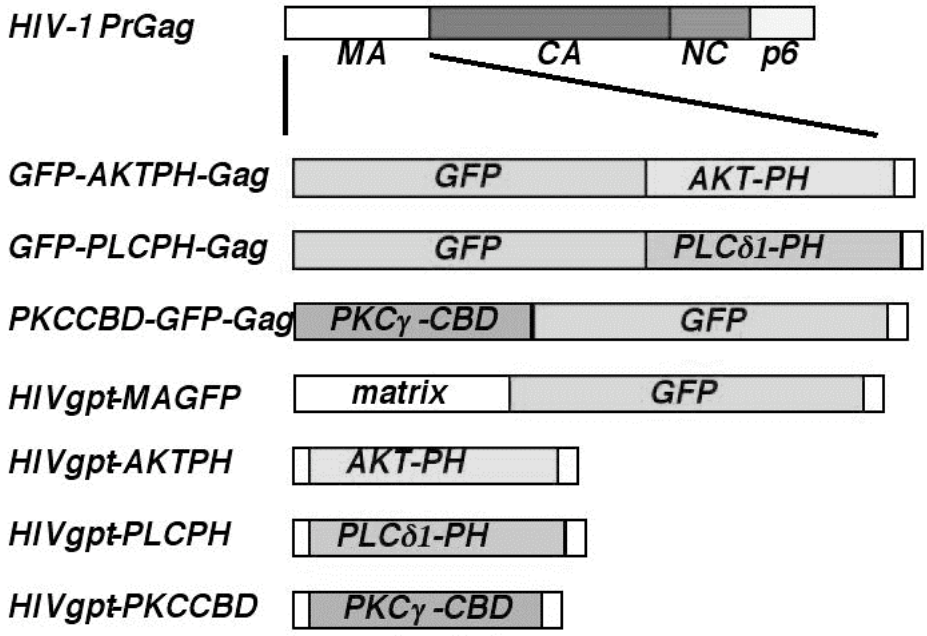

Figure 3.1
Recombinant DNA constructs. All recombinant constructs express variants of the HIV-1 HXB2 gag gene that ordinarily is translated into the precursor Gag (PrGag) protein. Wild type (wt) versions of the HIV-1gag gene, expressed in the presence of pol gene products, were produced from the previously described HIVgpt construct. In control experiments, HIV-1 protease-minus (PR-) proteins were expressed from the previously described HIVgpt2498T plasmid. GFP-AKTPH-Gag, GFP-PLCPH-Gag, and PKCCBD-GFP-Gag generate PR- Gag fusion proteins in which the HIV MA domain has been replaced with the green fluorescence protein (GFP) plus the AKT protein kinase pleckstrin homology (PH), the phospholipase Cd1 (PLC) PH domain, or the cysteine-rich membrane-binding domain (CBD) from phosphokinase Cg (PKC). The depicted HIVgpt constructs are variants of the wt HIVgpt plasmid and express proteins in the presence of HIV-1 pol gene products. HIVgpt-MAGFP carries the GFP coding region in-frame as an insert near the C-terminal end of MA. HIVgpt-AKTPH, HIVgpt-PLCPH, and HIVgpt-PKCCBD derive from a myristoylation-minus HIVgpt construct, and replace matrix residues downstream from codon 16 and upstream from the MA/CA juncture region (codon 120) with the AKTPH, PLCPH, or PKCCBD membrane-binding domains. Juncture sequences and construct details are provided in the Materials and Methods.

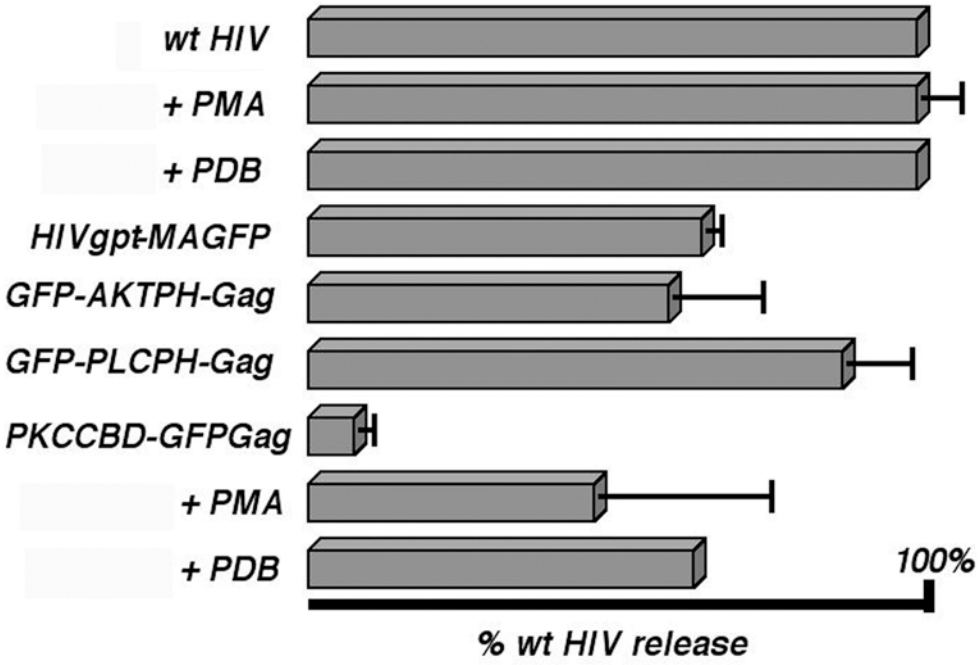

Figure 3.2
Release of virus-like particles. Cells were transfected with wt HIVgpt (wt HIV) or the indicated constructs and either untreated or treated with 1 mM PMA or PDB. At 72 h post-transfection, cell and VLP samples were collected, subjected to SDS-PAGE and anti-HIVCA immunoblotting. Cellular PrGag and VLP PrGag plus CA levels were quantitated densitometrically, raw release levels ([VLP PrGag + CA]/[Cell PrGag]) were calculated and are shown, normalized to untreated wt HIVgpt release levels. Results derive from one (wt HIV + PDB; PKCCBD-GFP-Gag + PDB), two (wt HIV + PMA; HIVgpt-MAGFP), three (PCKCBD-GFP-Gag + PMA), or four (GFP-AKTPH-Gag; GFP-PLCPH-Gag; PKCCBD-GFPGag) separate experiments. Standard deviations are as shown.

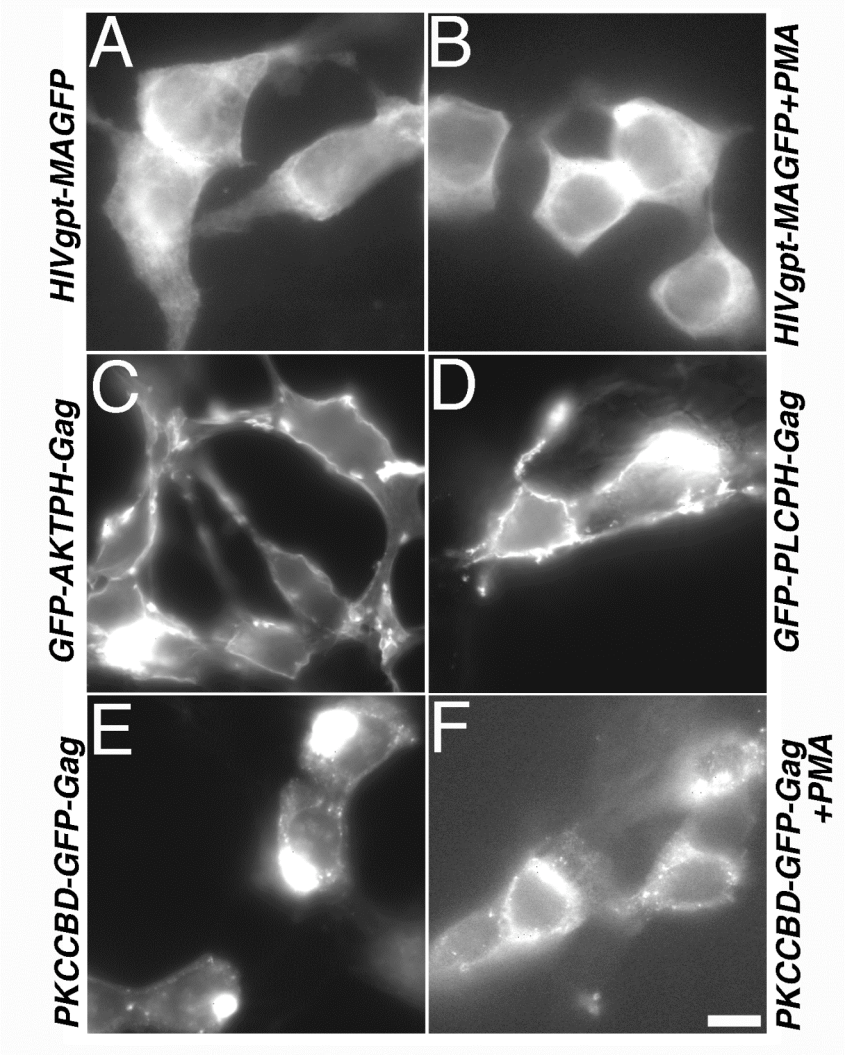

Figure 3.3
Fluorescence localization of proteins in transfected cells.
Cells on coverslips that were transfected with the indicated constructs were either untreated (Panels A, C, D, E) or treated with 1 uM PMA (Panels B, F). Subsequently, cells were processed for microscopic analysis of GFP proteins as described in the Materials and Methods section, imaged on a Zeiss Axioplan fluorescence microscope, and photographed using Improvision OpenLab software. A 20 micron size bar for all panels is provided at the bottom of the panel.

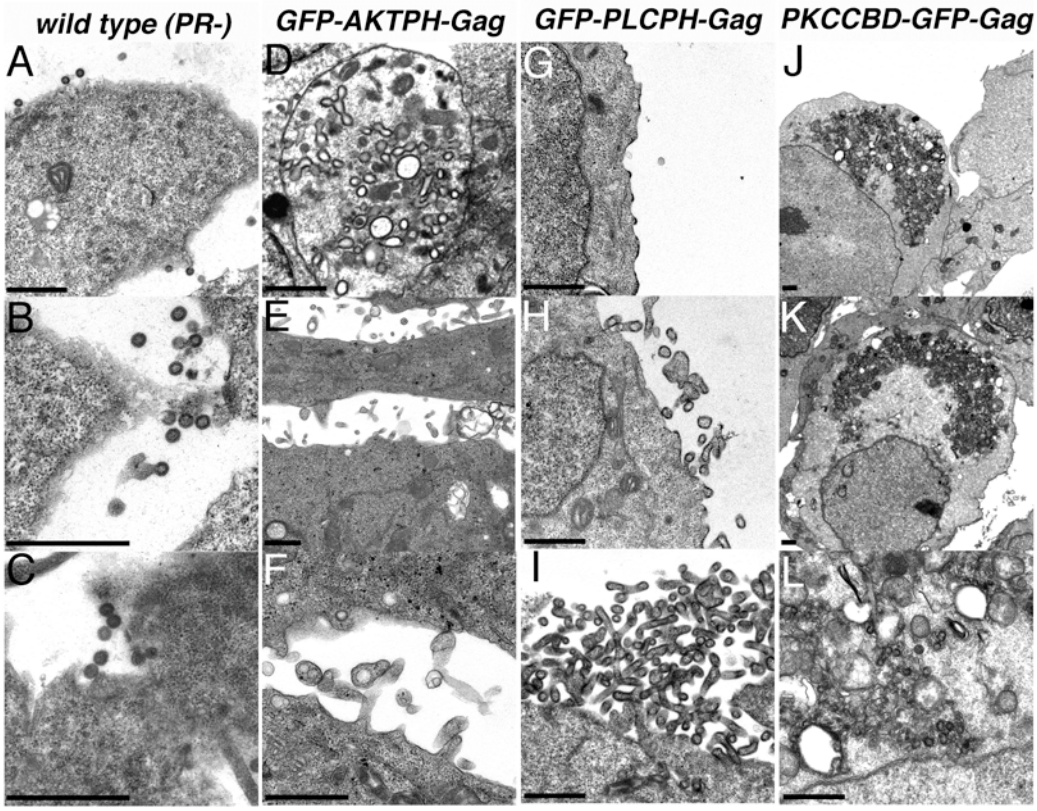

Figure 3.4
Electron microscopy of transfected cells. Cells were transfected with constructs expressing protease-minus but otherwise wild type HIV Gag (wild type Pr-; panels A-C), GFP-AKTPH-Gag (panels D-F), GFP-PLCPH-Gag (panels G-I), or PKCCBD-GFP-Gag (panels J-L). At 3 days post-transfection, cells were fixed, post-fixed, dehydrated, embedded, sectioned, and stained for electron microscopy as described in the Materials and Methods. As illustrated, relatively homogeneous wild type PR- particles were observed at the surfaces of cells (A-C), while structures assembled by GFP-AKTPH-Gag proteins were pleiomorphic and appeared as VLPs or darkly rimmed vesicles within intracellular vacuoles (D), particles released at the cell surface (E), or preformed VLPs near the cell surface or within attached or sheared filopodia (F). In contrast, assembly of spherical or tubular GFP-PLCPH-Gag VLPs occurred specifically at cell surfaces (G-I), and PKCCBD-GFP-Gag proteins assembled into large intracellular aggresomes (J-L).

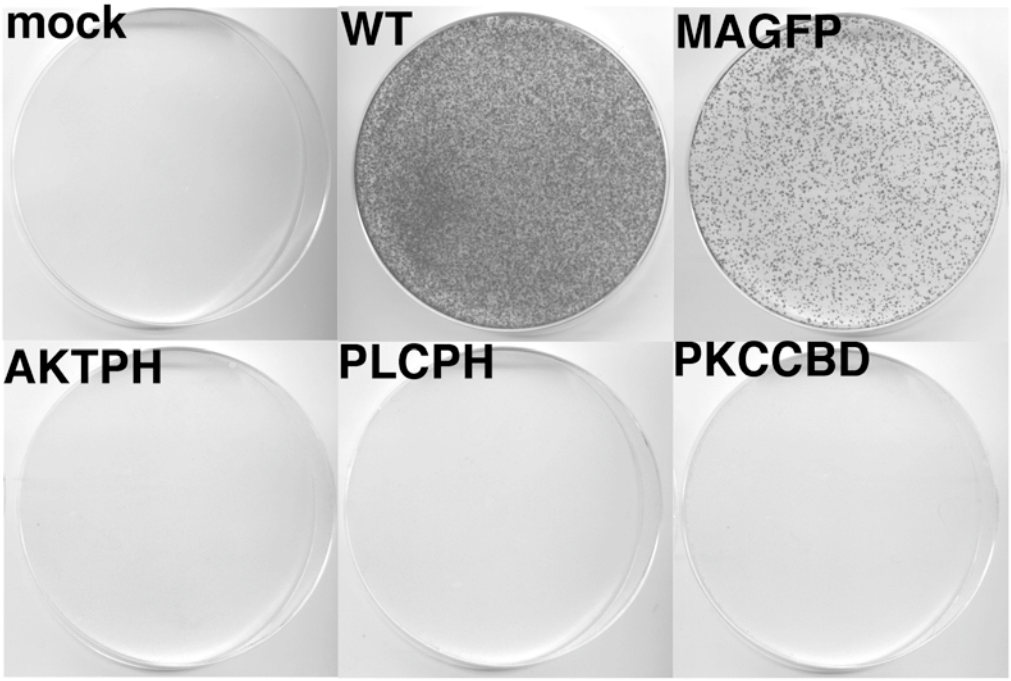

Figure 3.5
Virus infectivity. Viruses were produced by mock transfection (mock) or co-transfection of 293T cells with a VSV G expression vector plus HIVgpt (WT), HIVgpt-MAGFP (MAGFP), HIVgpt-AKTPH (AKTPH), HIVgpt-PLCPH (PLCPH) or HIVgpt-PKCCBD (PKCCBD). For production of PKCCBD viruses, transfected cells were treated with 1 mM PMA as described in the Materials and Methods to improve particle release. At 3 days post-transfection, virus-containing media supernatants were collected, filtered through 0.45 micron sterile filters and used to infect HiJ cells. Three days post-infection, HiJ cells were split 1:10 into gpt selective media, and colonies expressing proviral gpt genes were grown for 7-10 d prior to staining.

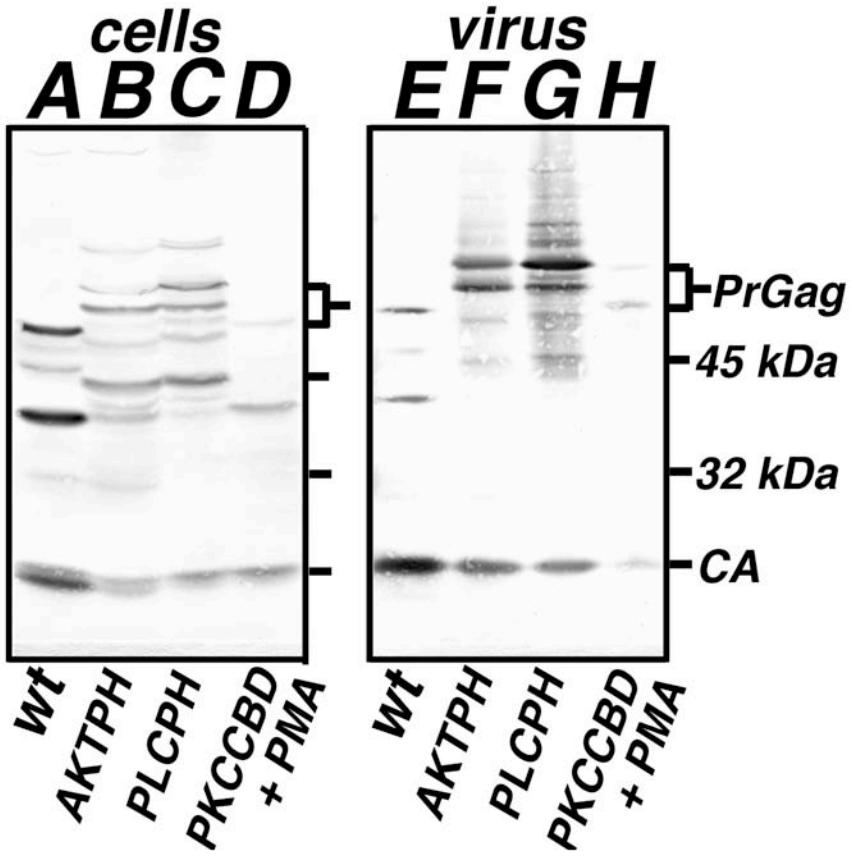

Figure 3.6.A
Virus-like particle release and processing. Top panel. Cell lysate (A-D) and VLP (E-H) samples were collected from cells transfected with wt HIVgpt (wt), HIVgpt-AKTPH (AKTPH), HIVgpt-PLCPH (PLCPH) or HIVgpt-PKCCBD (PKCCBD), and either untreated or treated with 1 mM PMA (+PMA). Gag proteins in samples were fractionated by SDS-PAGE, and detected by immunoblotting using an anti-HIVCA primary antibody. Size marker mobilities, as well as PrGag and CA bands, are indicated.

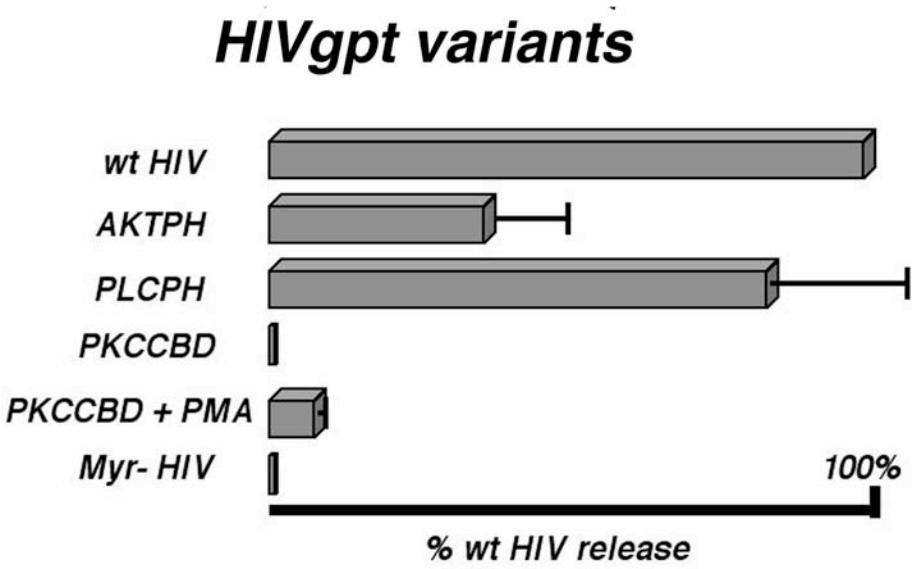

Figure 3.6.B
Virus-like particle release and processing.
Middle panel. Virus-like particle assembly and release levels, normalized to that of wt HIVgpt, were determined as described in Figure 2, including a myristoylation-minus HIVgpt construct (Myr- HIV) as a negative control. Values derive from two (PKCCBD, Myr- HIV), three (PKCCBD), or four (AKTPH, PKCCBD + PMA) independent experiments, with standard deviations as shown.

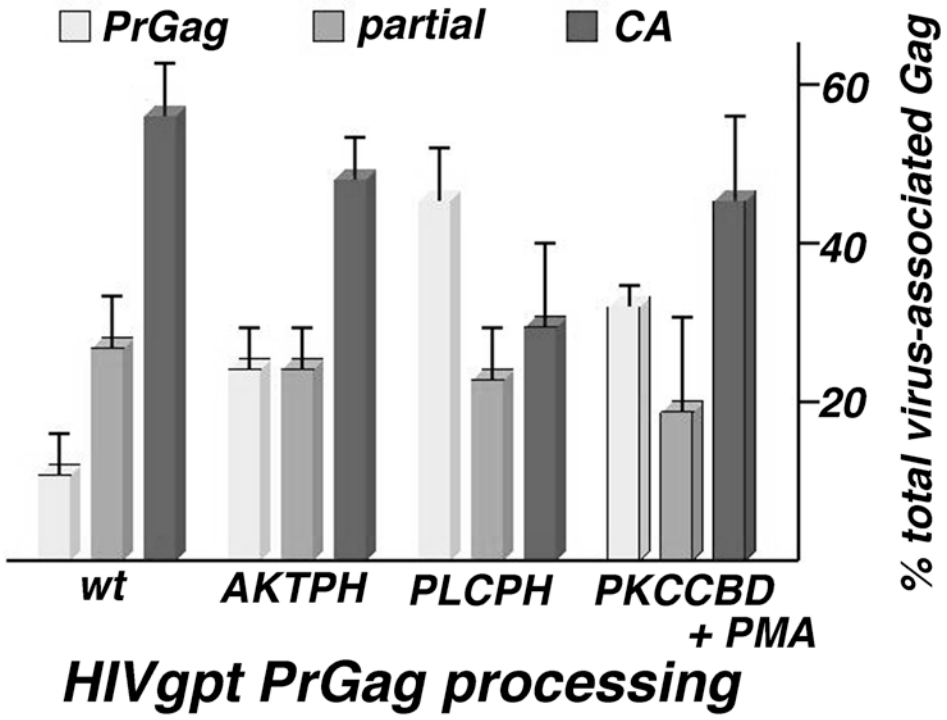

Figure 3.6.C
Virus-like particle release and processing. Bottom panel. PrGag processing levels for VLPs produced from cells expressing wt HIVgpt (wt), AKTPH, PLCPH, and PKCCBD (in the presence of PMA) were determined by densitometric quantitation of PrGag (light gray), processing intermediates (medium gray), and CA bands (dark gray) from immunoblots. Values represent percentages of the total virus-associated Gag levels (plus standard deviations) and derive from three (PKCCBD +PMA), four (AKTPH, PLCPH), or seven (wt) independent VLP preparations.g.

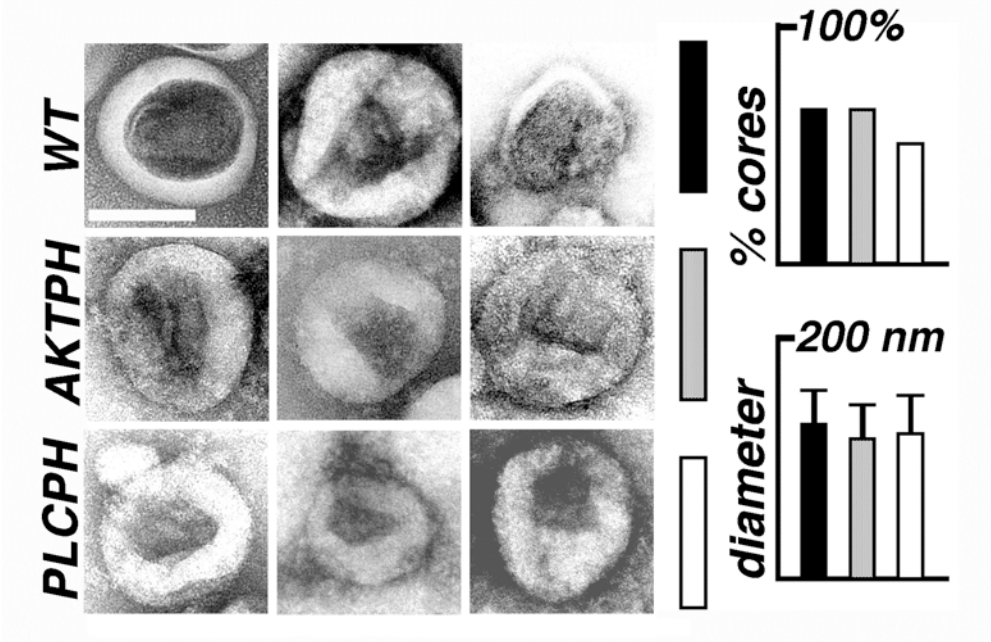

Figure 3.7
Electron microscopy of virus-like particles. Wild type (wt; black bars) HIVgpt, HIVgpt-AKTPH (AKTPH; gray bars), and HIVgpt-PLCPH (PLCPH; white bars) virus-like particles (VLPs) were lifted onto EM grids, stained, dried, and imaged by electron microscopy (EM). Micrographs show VLPs with central, roughly conical cores, and the white size bar in the upper right panel corresponds to 100 nm for all pictures. The graphs on the right shows the average VLP diameters, and the percentages of VLPs with discernable, roughly conical or cylindrical cores: each value was derived from 100 separate VLP images.

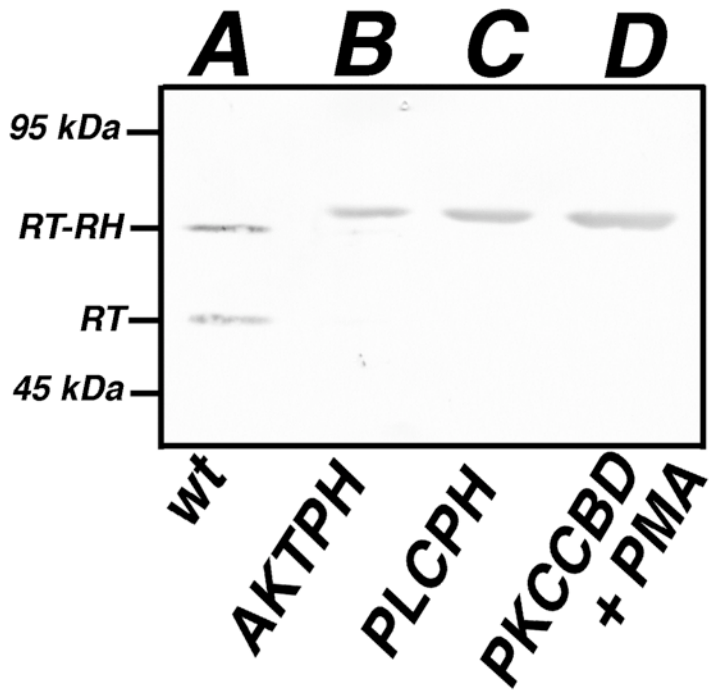

Figure 3.8
Analysis of viral reverse transcriptase proteins. VLP samples were collected from cells transfected with wt HIVgpt (A), HIVgpt-AKTPH (B), HIVgpt-PLCPH (C), or HIVgpt-PKCCBD (D), and either untreated or treated with 1 mM PMA (+PMA). Proteins in Gag-normalized samples were fractionated by SDS-PAGE, and detected by immunoblotting using an anti-HIVRT primary antibody. Size marker mobilities, as well as 66 kDa RT-RH and 51 kDa RT bands, are indicated. Note that no other bands were detected with the anti-RT antibody, but that similarly sized bands for the MBD variants (B-D) were detected in parallel immunoblots with an anti-HIVPR antibody.

Chapter 4

Conclusions

4.1 Conclusions

HIV-1 assembly is a carefully choreographed pathway. PrGag proteins have to interact with viral genomic RNA and cellular membranes at locations suitable to assembly, and to form particles stable enough to bud off from cells (159, 178, 226, 418, 483). Subsequently, PrGag has to undergo proper proteolytic processing in order for a mature, infectious particle to form (202, 225, 326). The studies presented herein have sought to shed light on the delicate roles of protein interactions in HIV-1 core assembly, and the pathways by which PrGag proteins are targeted to assembly sites.

Mutations at HIV-1 capsid residue 84

We have shown that mutating the highly conserved histidine residue 84 (H84) in the HIV-1 capsid N-terminal domain can have detrimental effects on viral core assembly. CA exhibits an unusual pattern of assembly behavior in the pH range between 6.5 and 7.0, near the pK_a of histidines. This led to the suggestion of a histidine switch model (120). PrGag proteins have been observed to assemble long tubes at pH 6.0, and spheres at pH 8.0 (174). Mature CA primarily appears dimeric at pHs below 6.6, spheres are found at pH 6.8, and tubes are observed at pH 7.0 (120). HIV-1 CA contains five histidines, three of which are highly conserved, suggesting that they may play a crucial role in virus assembly. According to the model, protonation of a histidine due to a change in pH might mediate structural changes in the CA protein, resulting in the different arrangements observed (120).

In our studies, viruses with H84 replaced by cysteine, alanine, lysine, or glutamate displayed aberrant cores and were noninfectious, even though mutant viruses were shown

to be capable of entering target cells. Interestingly, we found by mixing varying ratios of wildtype and H84A constructs that the mutant exerted a dominant-negative effect on infectivity. However, replacing H84 with a tyrosine residue rescued some degree of infectivity, indicating that H84 is very important for proper core structure, but not strictly required. Mutation of H84 does not abolish incorporation of RT, viral RNA, or CypA, as other NTD mutation studies had previously found (133, 154, 446, 447). The mutant Gag proteins displayed anomalous proteolytic processing, resulting in additional smaller cleaved fragments of capsid, suggesting that the mutation disturbed capsid protein structure sufficiently to allow for increased protease sensitivity. Interestingly, these extra processing bands were far less numerous in the H84Y virions. Core fractionation studies revealed much lower RT-to-capsid ratios in the mutant cores, corresponding to the inability of the mutants to initiate an infectious cycle in target cells. These results further indicate H84 mutation effects on stability and proper protein arrangement.

The NTD of HIV-1 capsid consists of a β-hairpin and seven α-helices (160). The tertiary structure of the protein can be disturbed by well-placed mutations. H84 is one of the residues highly conserved across HIV strains, suggesting it may play a crucial role in stabilizing mature capsid structure. One model suggests that H84 is important in stabilizing the proper alignment of α-helices within capsid monomers, possibly by aromatic interactions with nearby tryptophan residues W80 and W133 in α-helices 4 and 7. In this case, replacement of H84 with a tyrosine residue would maintain aromatic interactions to some degree, stabilizing monomer tertiary structures. The aromatic stabilization within the CA NTD monomer structure may be the major contribution of H84. Disruption of the monomeric capsid structure could cause defects throughout the

core, resulting in aberrant core assembly by not permitting proper refolding of the capsid proteins upon virus maturation.

Another possible explanation for the observed infectivity defects may be abnormalities in quaternary interactions of capsid proteins. H84 has been modeled to be on the outsides of capsid protein hexameric rings (153, 154, 264), and may affect the way rings are rearranged during maturation. It has been thought that formation of the mature capsid proceeds by "growth" of the capsid hexamer and pentamer rings within the virion after proteolytic processing (153). H84 is not modeled to participate in NTD hexamer formation (153, 154). However, an amino acid substitution at H84 might alter interfaces between hexamers. According to this model, as the core grows, the structure is not built up correctly, and the conical core typical of HIV-1 does not develop.

These results highlight the finely tuned assembly reactions resulting in functional cores. After the initial assembly of the immature, rather stable virus, sequential proteolytic processing liberates the constituents of Gag, and refolding of the individual proteins and the assembly of new structures ensues. These steps have to be thoroughly organized to yield a functional, infectious virion which is capable of entering a target cell, uncoating, and initiating reverse transcription. Our mutant viruses were competent for assembly, egress, and entry of target cells, but appear to be subject to a post-entry block. Previous studies have demonstrated the importance of optimal core stability (133). The virion must meet the requirements for stable egress from the producer cell and uncoating at just the right time after entering the target cell. Any structural modifications that upset this balance are likely to have a detrimental effect on infectivity. Since maturation is essential for infectivity, small molecules that prevent maturation can be employed to

combat HIV-1 propagation. Indeed, previous studies have shown an inhibitory effect of CAP-1 and CAP-2, compounds capable of binding to the NTD of HIV-1 CA (230, 443). Resultant particles were aberrant, suggesting that maturation was impaired (230, 443). Several studies have been performed using derivatives of betulinic acid. These compounds bind to the C-terminal domain and prevent maturation at the late CA-SP1 cleavage step (204, 224, 262, 263, 403, 504-506). We have identified another site critical to proper virion maturation. This may provide a new target for small compounds that may perturb tertiary structure sufficiently to interfere with maturation, and thus infectivity. Using available structural information, compounds could be designed rationally to bind specifically to this local environment and possibly perturb aromatic interactions between helices 4 and 7.

Substitutions of the HIV-1 MA domain

The pathways taken by PrGag proteins through producer cells to sites of virus assembly are currently under intense scrutiny. Depending on the cell type, virus assembly may occur at the plasma membrane or into multivesicular bodies. More recent studies maintain that virus particles found in multivesicular bodies and endosomal compartments are the result of endocytosis of virions from the plasma membrane, the primary site of Gag targeting (129, 221). The matrix domain of Gag plays a role in targeting PrGag proteins to membranes and maintaining membrane association. A number of studies have analyzed the roles of sequences within matrix and have shown that minimal matrix domains still can target Gag to membranes for assembly.

Previous studies have demonstrated that MA is necessary for wildtype Env incorporation into virions, but not strictly necessary for virus replication (386, 473). These experiments retained myristoylation signals on their PrGag proteins (386, 473). We chose to substitute MA domains of PrGag proteins with heterologous membrane-binding domains to investigate whether these could replace the membrane-targeting properties of MA and result in production of functional progeny virions. Two of the chosen domains, the pleckstrin homology (PH) domains of AKT (AKT-PH), which binds 3'PIs, and the PH domain of phospholipase C (PLC-PH), which associates with $PI(4,5)P_2$, permitted efficient membrane targeting and virus assembly of Gag proteins. A third membrane-binding domain mutant, incorporating the Cys1A and Cys1B domains of protein kinase C (PKCCBD) into Gag, only yielded a small number of virus-like particles. Stimulation by phorbol esters increased PKCCBD particle production to some extent, but nowhere near to the levels seen with wildtype or the other two mutants. However, none of the MA substitution mutant viruses were infectious when pseudotyped with VSV-G or A-MLV Env proteins. Our experiments indicated that the viral RNA was functional in transducing the resistance marker used to quantitate infectivity when a wildtype HIV-1 Gag protein lacking the marker was co-expressed in virus-producing cells. Mutant Gag proteins also were capable of interacting with a Gag-β-gal fusion protein and incorporating it into particles. Virus entry into cells and incorporation of VSV-G appeared comparable to wildtype. However, further studies showed a marked reduction in RT activity and the lack of reverse-transcribed products in the infected cells, as well as differences in PrGag processing. All of the mutants displayed lower ratios of fully-processed CA to full-length PrGag in virus particles. This difference was especially

pronounced for the PLC-PH mutant, where only about a third of the capsid protein was found in the mature form. Mature cores showed abnormalities and slightly lowered percentages of conical cores, especially in the case of the PLC-PH viruses, which displayed a greater extent of PrGag processing defects. These results together indicate that replacement of HIV-1 MA with heterologous membrane-binding domains can lead to the assembly of virus particles that are capable of delivering a core to target cells, but this core is not completely functional, as the differences in PrGag processing and the failure to initiate reverse transcription indicate. This may be due to a number of causes. Defects in PrGag processing may also affect processing of Gag-Pol and the abundance and/or functionality of the resulting RT enzyme. Our analyses have indicated aberrant processing of RT from the GagPol precursor in the mutant viruses. Instead of the expected p66 and p51 bands that occurred in the wildtype lanes on Western blots, a major band of slower mobility was observed. This band also reacted with an anti-HIV-PR antibody, and it appears to be a fusion of the PR and RT domains excised from PrGag-Pol, suggesting impaired processing of Gag-Pol. The effect on processing could be mediated by altered flexibility of the polyproteins, resulting in modified access to cleavage sites, as illustrated in Figure 4.1. Interactions between the membrane-binding domains and PR are another possibility. Moreover, the exact site of virus assembly may play a role. It may influence the cooperativity of PrGag and PrGag-Pol molecules, as well as cellular factors involved in budding.

HIV-1 core structure must maintain a precarious balance between stability and capability for disassembly, and small defects can upset this balance. PR cleavage of PrGag and PrGag-Pol is a highly ordered process, and dimerization of the PR domains in

PrGag-Pol is necessary for enzyme activation (372, 373). Some investigators have argued that myristoylation of PrGag and the membrane-targeting region within MA may influence proteolytic processing (64, 255). As demonstrated by Pettit et al., the structure of PrGag-Pol, the location of PR, and structural determinants outside the active site all appear to be important for PR activation and ordered processing of cleavage sites (372, 373). Alterations of PrGag-Pol structure introduced by MA replacements may affect PR activation and the following cleavage events, leading to the observed core structural aberrations. Additionally, substitutions of the MA domain alter the PrGag-membrane interactions, and this may influence overall PrGag and PrGag-Pol structure.

Interestingly, other investigators have constructed Gag proteins containing heterologous membrane-binding domains in order to specifically target Gag to membranes (221). A replacement of the MA globular head domain by the C2 domain of the cellular protein WWP1 led to targeting of C2-Gag-CFP proteins to the plasma membrane. These particles were processed correctly and, when pseudotyped with VSV-G, could be infectious. These results suggest that the processing defects occurring in our constructs may be a major contributor to the loss of infectivity observed. This may be due to the particular structures of the chosen membrane-binding domains, or their precise location within the Gag protein or to localization to intracellular sites. Our constructs retain the matrix amino acids 120-132, whereas the construct used by Jouvenet *et al.* contains matrix amino acids 116 and following. This difference in constructs may contribute to the processing differences observed. However, our HIV-MA-GFP construct, which inserted GFP between MA amino acids 120 and 121, was released well from producer cells and retained substantial infectivity. The specific membrane-binding

domains chosen for our studies may be responsible for perturbing processing. Alternatively, the site of assembly might have an effect on processing.

A variety of studies have examined functions other than Gag targeting and Env incorporation for MA in the virus life cycle. MA is part of the preintegration complex (PIC), and it has been suggested that MA may be involved in or even be required for translocating the PIC to the nucleus in nondividing cells (69, 179, 231, 464). This function, however, has been disputed, and other work has shown that viruses with almost all of MA deleted can still be infectious (386, 473). Our studies further support the idea that MA is of importance in virus assembly as well as other steps of the virus life cycle. We have shown that replacement of MA by heterologous membrane domains can result in the assembly of notable amounts of virus-like particles, which, however, are not infectious.

Together, the studies presented herein highlight the sensitivity of the HIV-1 core structure to perturbations at critical Gag protein sites. Even though virus particles can be formed in spite of considerable changes in Gag, infectivity frequently is lost. The viral core must satisfy demands both for efficient assembly and egress of particles and for precise disassembly after infection. Through virus evolution, the HIV-1 core has maintained a number of critical residues, and we have shown that HIV-1 CA is one of these. In addition, replacements of MA with alternative membrane-binding domains resulted in production of particles with morphological abnormalities, processing defects, and a lack of functional reverse transcriptase. Even though MA is not strictly required for membrane targeting and assembly, alterations can project significant defects and affect the viral enzymes.

Future directions

Although there are numerous studies examining HIV-1 assembly, many unanswered questions remain. The role of highly conserved residues within capsid warrant further investigation, in order to elucidate their roles in assembling immature and mature virus cores. HIV-1 CA contains five histidines, three of which (H12, H62, and H84) are highly conserved, leading to the suspicion that they may exert important functions in viral core assembly or maturation. The histidine switch hypothesis put forth by the Carter group provides a possible explanation for the importance of CA histidines (120). HIV-1 CA proteins exhibit variations in assembly behavior within a narrow pH range, near the pK_a of histidines. Protonation of one or several of the conserved histidines may lead to necessary local changes in structure during maturation (120). Our laboratory is currently investigating the role of the conserved residue H62 by replacing it with alanine, cysteine, lysine, and tyrosine. Preliminary results suggest that mutant capsid proteins are competent for assembly, but that the mutants are not infectious, with the exception of the H62Y mutant. These data further suggest the importance of conserved histidines in maintaining aromatic interactions, and possibly in stabilizing capsid protein structures. Future studies in the lab are focused on characterization of H62 mutant virus defects.

With regard to MA, it has been shown that this domain is critically responsible for delivering PrGag proteins to preferred assembly sites. The types of phospholipids favored for binding by the matrix protein are likely to have a strong effect on the membrane

targeting of Gag. MA displays a strong preference for $PI(4,5)P_2$, as was shown recently (136, 401). Moreover, PrGag membrane association appears to be concentrated in specific cholesterol-rich membrane domains. Teasing out more detail about MA-membrane association specificity may help elucidate assembly pathways and the requirements for particle assembly. As we have shown, particle assembly can occur even in instances of increased membrane-association promiscuity of Gag proteins, but the resultant virions may be noninfectious. Loss of infectivity may be due to defects in core assembly, as indicated by core abnormalities, PrGag and PrGag-Pol processing defects, and failure to initiate reverse transcription.

In the future, it might prove worthwhile to perform membrane-binding studies in various cell types. Currently, there still exists the contention that assembly pathways vary depending on cell type, perhaps due to different membrane lipid distributions and the presence or absence and the locations of cellular cofactors required for or refractive to assembly. Some studies argue that the major trafficking target for Gag is the plasma membrane in all cell types, but that variations in PrGag expression, endocytosis, and steady-state Gag levels at the plasma membrane account for the observed differences of Gag present at the plasma membrane, as compared to multivesicular bodies and endocytic compartments (221). Additional studies into which types of cellular proteins, membranes, and lipids support productive virus assembly may yield interesting results.

Ultimately, understanding how Gag mutations impair HIV-1 infection may help in the design of antiviral compounds that can inhibit HIV in similar ways. Virus assembly has recently become a focus for development of antiviral compounds, and knowledge of the precise roles MA plays in the virus lifecycle can permit design and discovery of

inhibitors. Retargeting of the assembly machinery to alternate assembly sites might lead to production of defective viruses, by virtue of altered interactions with membranes or cellular factors. Interference with MA-Env interactions would result in assembly of particles incapable of entering target cells. The HIV-1 assembly machinery is providing new targets for combating the propagation of this deadly virus, and continued investigations into the molecular interactions that build the virus particles are furnishing the necessary information.

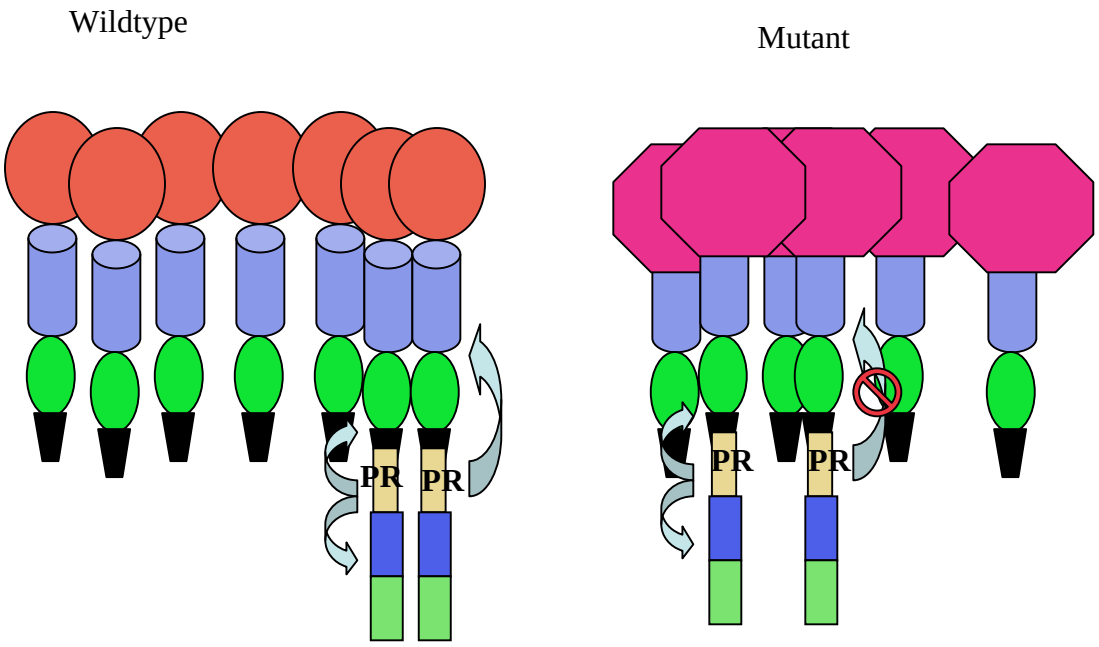

Figure 4.1
Model for processing defects of MA-replacement Gag proteins
PR domains in Gag-Pol have to dimerize to mediate proteolytic cleavagess.
Mutant Gag proteins may be subject to flexibility constraints, resulting in impaired access to cleavage sites.

Appendix 1

Analysis of mutations at HIV-1 CA histidine 62

A.1.1 Introduction

The human immunodeficiency virus (HIV-1) capsid (CA) protein plays a central role in virus assembly and maturation. The HIV Gag precursor (PrGag) protein directs virus assembly, and it consists of the matrix (MA), CA, nucleocapsid (NC), and p6 domains (104, 159, 226, 398, 399). The C-terminal domain (CTD) of CA has been implicated in initial assembly of immature, unprocessed virions, whereas the N-terminal domain (NTD) appears to play a role in maturation and rearrangement of the viral core (20, 80, 85, 112, 133, 152-154, 160, 174, 291, 303, 314, 445, 447, 466, 467, 477). Appropriate interactions between CA proteins are important for virus assembly and release, but also play a role for maturation, uncoating, and initiation of reverse transcription (80, 112, 133, 154, 174, 291, 303, 467). Several studies have analyzed the effects on mutations within the HIV CA domain, and found defects in early replication steps (133, 154, 291, 446, 447, 470).

CA NTDs have been modeled to assemble hexamer rings, which are linked via CTD connections (27, 153, 154, 300, 466). The immature hexamer rings appear to be more tightly packed than those in mature virions (300). Apparently, more CA is incorporated into virions than is necessary for formation of a mature core. The assembly behavior of PrGag and mature CA proteins has been subject to *in vitro* studies, and has shown pH-dependent characteristics. PrGag was found to assemble long tubes at pH 6.0, but spheres occur at pH 8.0 (174). Interestingly, mature CA appears dimeric at pHs below 6.6, spheres are found at pH 6.8, tubes occur at pH 7.0, and at higher pHs, tubes and

spheres may coexist (120). These results have led to the idea that a histidine switch might be involved in capsid assembly or disassembly (120). CA contains a total of five histidines (H12, H62, H84, H87, and H226), of which three are conserved (H12, H62, H84). In a previous study, we examined substitutions of H84 (410). This residue has been modeled at the outsides of capsid hexamer rings (153, 154). In our hands, the H84 substitution mutants produced noninfectious viruses, exhibited dominant-negative effects on wildtype infectivity, and contained aberrant cores. One exceptional substitution, H84Y, retained some level of infectivity, but considerably less than wildtype infectivity. Our mutant viruses contained normal levels of viral genomic RNA, total reverse transcriptase, and CypA, but low RT-to-CA ratios in virus cores. They also were shown to be more sensitive to proteolytic cleavage near loop regions in the NTD. We argued that H84 mutations may adversely affect aromatic interactions between NTD helices 4 and 7 that play a role in core morphogenesis (410).

In this study, we probed another conserved histidine residue in the HIV CA NTD, H62. Alanine, cysteine, lysine, and tyrosine residues were introduced at this position. The mutant Gag proteins assembled virus-like particles, with the exception of H62A, which appears to be due to a problem with the plasmid construct. The viruses produced generally were noninfectious. The notable exception was H62Y, which retained some infectivity, but was significantly less infectious than the wildtype.

A.1.2 Materials and methods

Recombinant DNA constructs. A vesicular stomatitis virus (VSV) glycoprotein (G) expression construct, pVSV-G, was the generous gift of Randy Taplitz. The parental HIVLuc construct (pNL-LucE-R) (87) was kindly provided by Nathaniel Landau.

To make mutations at capsid residue 62 in the context of HIVLuc, NL4-3 fragments from nucleotides (nt) 671 to 1363 and from 1364 to 1726 were inserted into pGEM-T Easy separately. The HIVLuc gag fragment from nt 671 to nt 1361 was amplified by PCR, and additional nucleotides CCA were attached to create an MscI site. A SmaI site at the 5' end of nt 1364 was created by PCR. Mutagenic PCR at nt 1368-1374 was used to create the codons replacing H62 as follows, with H62 codon underlined: WT, GGA CAT CAA; H62A, A GCT CAA; H62C, A TGC CAA; H62K, A AAG CAA; H62Y, A TAT CAA. Inserts from both pGEM-T Easy plasmids were combined by blunt-end ligation, and inserted into HIVLuc WT by using BssHII ad SpeI.

Cell culture and transfections. 293T, HeLa, and HiJ cell lines were passaged at 37°C in 5% CO_2 in culture medium containing Dulbecco's modified Eagle's medium supplemented with 10 mM HEPES (pH 7.4), penicillin, and streptomycin plus 10% fetal calf serum. For transfections, 10-cm plates of 293T cells were transfected by the calcium phosphate method (20, 182, 303, 304, 470, 473) with either 24 μg of HIVLuc DNA or 16 μg of HIVLuc plus 8 μg of pVSV-G DNA. Briefly, confluent 10-cm dishes of 293T cells were split 1:4 the day prior to transfection. Plasmid DNAs were mixed with 1 ml of HEPES-buffered saline (pH 7.05 to 7.15; 21 mM HEPES, 137 mM NaCl, 5 mM KCl, 0.7 mM sodium phosphate, 5 mM dextrose), after which 40 μl of 2 M $CaCl_2$ was added while vortexing. DNA solutions were incubated at room temperature for 40 min. Following

this, culture medium was removed from the cells, DNA solutions were added dropwise to the cell monolayers, and then the cells were incubated at room temperature for 20 min, with gentle rocking once at 10 min. After incubations, 10 ml of culture medium containing 50 μg of gentamicin/ml was added to the cells, and plates were incubated at 37°C and 5% CO_2 for 4 to 5 h. Following incubations, transfection media were removed and cells were washed with 5 ml of serum-free Dulbecco's modified Eagle's medium, incubated in 2.5 ml of 15% glycerol in HEPES-buffered saline for 3 min at 37°C, washed twice, and fed with 10 ml of culture medium plus 50 μg of gentamicin/ml. For sample collection, virus-containing media and cell pellets washed in phosphate-buffered saline (PBS; 9.5 mM sodium potassium phosphate [pH 7.4], 137 mM NaCl, 2.7 mM KCl) were collected 3 days posttransfection and stored at -80°C prior to further processing. Virus particles in filtered (Gelman; 0.45 μm) cell-free medium were concentrated by centrifugation at 4°C through 20% sucrose cushions in PBS (2 h at 82,500g [25,000 rpm in an SW28 rotor, 4-ml cushions], or 45 min at 197,000g [40,000 rpm, SW41 rotor, 2-ml cushions]). Virus pellets were resuspended in 0.1 ml of PBS per transfected cell plate and stored in aliquots at -80°C.

Protein analysis. For routine analysis of virus protein release, cell samples (20% of cell pellets from each plate) were suspended in IPB (20 mM Tris-hydrochloride [pH 7.5], 150 mM NaCl, 1 mM EDTA, 0.1% sodium dodecyl sulfate [SDS], 0.5% sodium deoxycholate, 1.0% Triton X-100, 0.02% sodium azide), incubated on ice for 5 min, vortexed, and cleared by centrifugation at 13,700g for 15 min at 4°C. Soluble material was mixed with 1 volume of 2x sample buffer (12.5 mM Tris-hydrochloride [pH 6.8], 2% SDS, 20% glycerol, 0.25% bromophenol blue) plus 0.1 volume of β-mercaptoethanol,

prior to heating (3 to 5 min, 95°C) and SDS-polyacrylamide gel electrophoresis (SDS-PAGE). For virus samples, 50 μl of resuspended virus pellets was mixed with one volume of 2x sample buffer plus 0.1 volume of β-mercaptoethanol and processed as above. Cell and virus protein samples were fractionated by conventional 10% acryl-amide Laemmli SDS-PAGE (20, 182, 303, 304, 470, 473), electroblotted, and immunoblotted following previously described methods. Primary antibodies were as follows: Hy183 (from Bruce Chesebro) used at 1:60 from hybridoma culture medium for detection of the HIV-1 CA CTD; mAb21 for detection of reverse transcriptase (from NIH AIDS Research and Reference Reagent program, catalog #3483) used at 1:500. Secondary reagents were alkaline phosphatase-conjugated anti-mouse antibodies (Promega S3721) used at 1:15,000 for detection of anti-HIV-CA primary antibodies and anti-RT antibodies. Color reactions for visualization of antibody-bound bands employed nitroblue tetrazolium plus 5-bromo-4-chloro-3-indolyl phosphate in 100 mM Tris-hydrochloride (pH 9.5), 100 mM NaCl, and 5 mM $MgCl_2$ (20, 182, 303, 304, 470, 473).

Infections. Confluent 10-cm dishes of HiJ cells were split 1:80 onto 35mm plates the day before infections. Confluent 10-cm dishes of HeLa cells were split 1:40 onto 35mm plates the day before infections. Growth media were removed from each cell plate, and 1.5 ml of fresh growth medium and 0.5ml of filtered transfection supernatants were added to the cells. Plates were incubated for 3 days at 37°C. After infections, cells were collected in 1 ml of luciferase lysis buffer (100 mM sodium phosphate [pH 8.0], 4 mM ATP, 1 mM sodium pyrophosphate, 6 mM magnesium chloride, 0.2% Triton X-100) and either processed immediately for luciferase assays or frozen at -80°C until use. For luciferase assays, cells in luciferase lysis buffer were vortexed at room temperature and

30µl aliquots were mixed with 0.3 ml of luciferase assay buffer (luciferase lysis buffer minus Triton X-100). Luciferase levels were measured on an EG&G Berthold Autolumat LB953 luminometer using a 0.1-ml luciferin pulse of 1 mM D-luciferin (BD Pharmingen). Raw luminometer counts were normalized versus luminometer counts obtained from the transfected cells, which produced the virus samples, and mutant virus infectivities were expressed as percentages of wt HIVLuc infectivities from assays performed in parallel

A.1.3 Results and discussion

HIV-1 CA contains five histidine residue (H12, H62, H84, H87, and H226). Three of these, H12, H62, and H84, are conserved (244). Previously, we have examined substitutions of H84 and found that replacing this residue with glutamate, lysine, cysteine, or alanine abolished infectivity of the virus (410). Resultant cores displayed abnormal morphology, and combining wildtype with mutant capsid proteins revealed a dominant-negative effect of the mutant proteins on infectivity. Interestingly, introducing a tyrosine residue at H84 led to the retention of some infectivity, arguing against an absolutely required histidine switch for capsid maturation. We suggested that a tyrosine at position 84 may be able to maintain aromatic interactions with tryptophan residues (W80 and W133) in helices IV and VII. These aromatic interactions may serve to stabilize the capsid monomer structure.

We chose to examine substitutions at another conserved histidine residue, H62. These studies further probe the histidine switch model for HIV-1 maturation (120). H62 is located just N-terminal to helix IV in the CA NTD, and it may also be involved in

aromatic interactions, stabilizing the monomer structure of the mature CA protein. The NTD of HIV-1 CA is shown in figure A.1.1, and the location of H62 is indicated.

Wildtype and mutant HIV constructs were transfected into 293T cells. Three days posttransfection, cells and viruses were collected and processed for SDS-PAGE and detection by anti-HIV CA antibody. As shown in Figure A.1.2, constructs were expressed well, and virus-like particles were released efficiently, with the exception of H62A. This may be due with problems within the plasmid, and the construction is currently under reexamination. We proceeded to test whether the viruses were infectious. 293T cells were transfected with HIV constructs and a plasmid encoding VSV-G. Cell-free, filtered supernatants were collected and used to infect HiJ and HeLa cells, which were then processed for luciferase assays to test for virus-mediated transduction of the luciferase gene. Pseudotyped wildtype viruses were infectious, but mutant viruses were not. The exception to this was the H62Y mutant, which retained some infectivity. The infectivity was reduced as compared to wildtype, but notably higher than in any of the other mutants, as illustrated in Figure 2. Due to the findings of our previous study involving replacements of HIV-1 CA residue H84 (410), we suspected that morphological abnormalities might be a cause for infectivity loss. H62 is positioned immediately N-terminal to α-helix 4. As we suggested before, α-helices 4 and 7 may be stabilized by aromatic interactions, mediated by histidine residue 84 at the top of helix 4 and tryptophan residues 80 in helix 4 and W133 in helix 7 (410). Considering the position of H62, this residue may also be involved in putative aromatic interactions within this region. Previous studies by Tang et al. demonstrated a loss of infectivity and appearance of aberrant cores with their HIV-1 CA W23A and F40A mutations (446, 447). These

mutations resulted in aberrant virus cores, decreased RT in cores, and, interestingly, lack of CypA incorporation, suggesting that mutations at these residues caused structural changes throughout the NTD (446, 447). W23 is located in helix 1 within the CA NTD, and F40 is found in helix 2, and both aromatic residues are conserved. Another aromatic residue, F32, is also located nearby. Structural models of the HIV-1 CA NTD place H62 spatially close to F32 and F40, leading to the suspicion that aromatic interactions may be at play in stabilizing tertiary structure. The residual infectivity retained with the H62Y mutant argue against an absolutely required histidine switch. Together with the demonstrated importance of F40, these results support the notion that aromatic interactions may play a role in stabilizing the monomer structure of the N-terminal domain of HIV-1 CA.

In order to further characterize the infectivity defect of these mutants, virus particle preparations will be analyzed by electron microscopy. Examination of viral entry into target cells, RNA incorporation, and appearance of reverse transcription products may also be of interest. It appears that reverse transcriptase is incorporated into virions and processed (data not shown). Use of the functional H62A mutant will be included in analysis of the success of the mutants in various stages of the virus lifecycle. If morphological abnormalities are indeed found, uncoating and initiation of reverse transcription may also be defective in the mutant viruses. Additional examinations will determine whether aberrant CA-to-RT ratios are found in the viral cores. Work in the near future will elucidate the effects of substitutions at H62, and provide further information on the intricacies of HIV-1 CA structure.

A.1.4

Figures

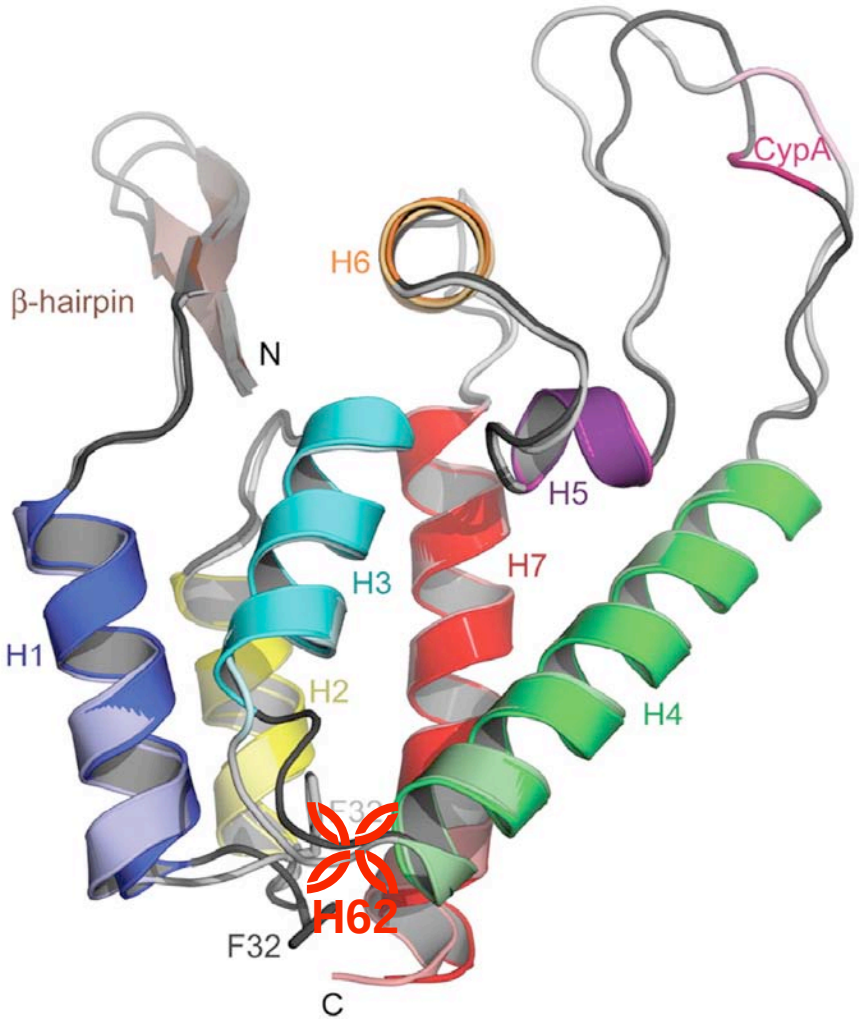

Figure A.1.1
Model of HIV-1 CA N-terminal domain
The N-terminal β-hairpin is depicted on the upper left, the C-terminal linker to the C-terminal domain of CA is shown at the bottom.The location of H62 is indicated in red.
Adapted from Kelly et al, J Mol Biol 2007; 373(2):355-366

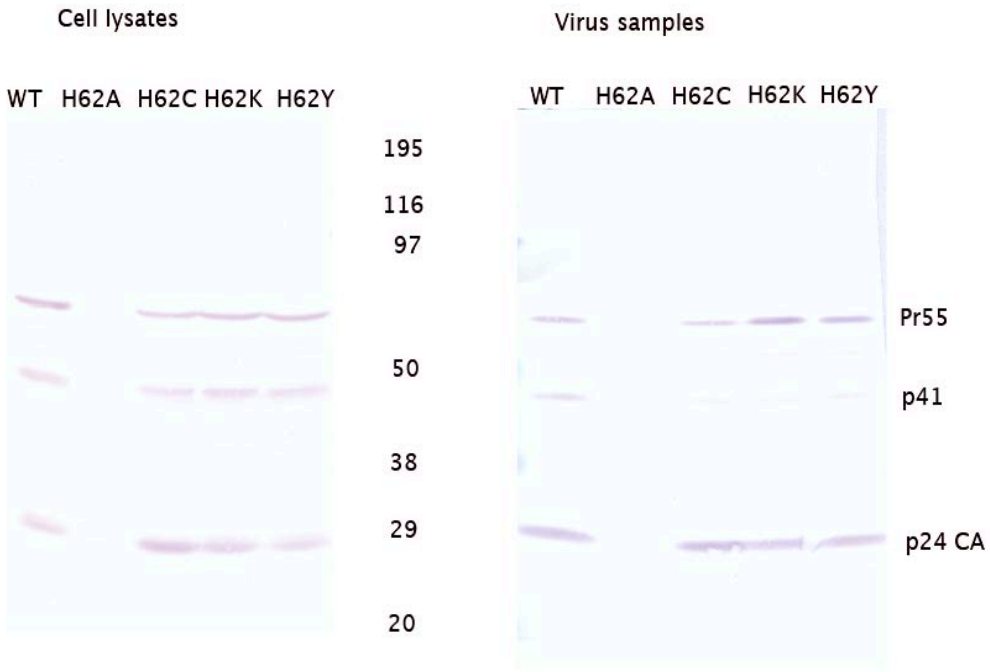

Figure A.1.2
Expression and release of HIV-1 CA H62 mutants
293T cells were transfected with the indicated constructs, and virus and cell samples were collected 3 days posttransfection and processed for SDS-PAGE. A HIV-1 CA antibody (Hy183) was used for immunodetection. The major Pr55Gag, p41 (processing intermediate), and processed CA (p24) bands are indicated. Numbers in the center refer to protein size standards in kDa.

Figure A.1.3
HIV-1 Capsid H62 Mutant Infectivity

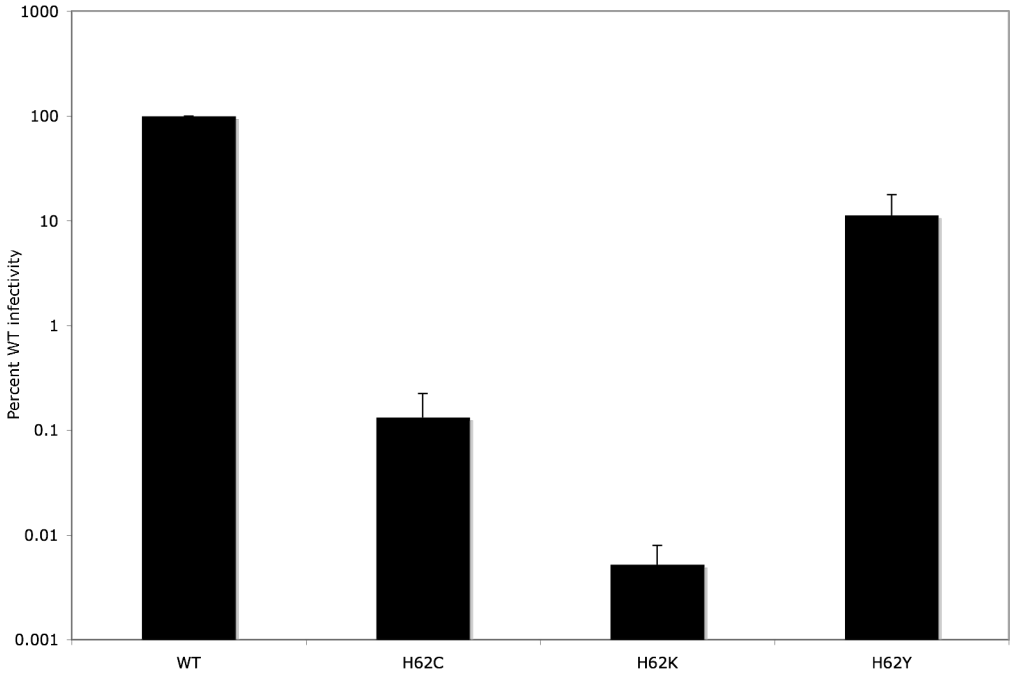

Figure A.1.3
Infectivity of HIVLuc H62 mutants
Viruses were produced by transfecting 293T cells with the indicated HIVLuc constructs and VSV-G. Cell-free, filtered supernatants were collected 3 days posttransfection used to infect HiJ and HeLa cells for 3 days. Infected cells were processed for luciferase assays, and infectivity results were normalized to parallel luciferase assays performed on transfected cells producing the virus. Error bars are standard deviations calculated from four sets of infections for each sample. Wildtype infectivitiy was set to 100% for comparison.

Appendix 2

Characterization of HIV-1 assembly inhibitors

A.2.1 Introduction

In the developed world, mortality due to AIDS has decreased significantly due to combination antiretroviral therapy. Antiretroviral therapy to date mostly targets the viral enzymes reverse transcriptase and protease (101, 384). Reverse transcriptase inhibitors are further subdivided into nucleoside reverse transcriptase inhibitors (NRTIs), non-nucleoside reverse transcriptase inhibitors (NNRTIs), and nucleotide reverse transcriptase inhibitors (NtRIs) (101). Combinations of available drugs are in use to decrease viral load in patients and delay the progression of the disease (100, 101). Emergence of viruses resistant to available drugs complicates treatment considerably, and there is a need for constant exploration of other drug targets and development of new drugs to interfere with HIV-1 replication (100, 101, 384). Other targets for HIV-1 drugs include integration, fusion and virus entry into cells, and virus assembly (100, 101). Enzymes are popular targets for drug action, since they usually exist in low concentrations within cells and work via specific mechanisms (84, 246, 384).

The viral structural proteins are initially expressed as a long precursor protein, PrGag, consisting of the matrix (MA), capsid (CA), nucleocapsid (NC), and p6 domains, as well as two small spacer peptides, SP1 and SP2. PrGag is responsible for forming immature particles, then is cleaved by the viral protease into its constituents during or shortly after budding, resulting in a rearrangement of the particle into its mature, infectious form (89, 229, 479, 481). Virus assembly presents itself as an interesting target for antiviral compounds. Apart from leading to the development of HIV therapeutics

further down the line, efficient assembly inhibitors could be used as valuable tools in laboratory studies.

Much work has been done to elucidate the roles of specific residues within the HIV-1 capsid protein necessary for proper assembly. Phage display screening studies have led to the characterization of a peptide capable of binding to the C-terminal domain of CA and inhibiting assembly of immature HIV-1, as well as of mature particles, in vitro (434, 452). Gag-derived peptides have also been used to target Gag interfaces and inhibit virus assembly (157, 198, 334). CAP-1 and CAP-2 are compounds capable of binding to the NTD of HIV-1 CA that have been shown to inhibit maturation and thus interfere with infectivity (230, 443). Maturation can also be impaired by derivatives of betulinic acid, which bind to the C-terminal domain of CA and prevent scission at the CA-SP1 site, and PA-457, one of the derivatives, shows promise as an antiviral (204, 224, 262, 263, 403, 504-506).

Our laboratory has employed a screening assay to assess the effects of synthetic small-molecule potential inhibitors on virus assembly. Our assay is based on the incorporation of Gag-β-galactosidase fusion proteins into virus particles when coexpressed with an assembly-competent Gag protein. The interaction of the Gag protein and the fusion protein depends on the CA domain (472). Compounds found to inhibit virus production that displayed low cytotoxicity were then further characterized with regard to their inhibitory activity as well as mechanisms of action.

A.2.2 Materials and methods

Plasmids. Wildtype versions of the HIV-1 Gag gene were expressed from the HIVGPT construct, which has been described previously (351, 470, 473), and from the HIVLuc construct (87, 410). The HIV Gag-β-galactosidase expression construct, HIVGBG, has also been reported previously (472). The plasmids pNL4-3 (Cat # 114), expressing the genes for the HIV-1 NL4-3 strain, and pNL4-U35 (Cat # 968), expressing NL4-3 without the Vpu gene, were obtained from the NIH AIDS Research and Reference Reagent Program. The stable cell line HeLa::HXBdPdE+T1RevEnv+HIVGBGRev- (HX#6) was used for initial beta-galactosidase rapid screen assays. HXBdPdE codes for HIV gag, pol, tat, and vif. It includes mutations, deletions, or disruptions of the packaging signal, vpr, vpu, rev, env, nef, and the 3'LTR. T1RevEnv includes the rev and env genes on a tet-suppressor. We added the plasmid HIVGBGRev- to create HX#6 cells and obtain a cell line with HIVGBG and HIV Gag in a tet-inducible system.

Cell culture, cell lines, transfections, and infections. 293T, Vero, HeLa, HiJ, HX, and HX#6 cell lines were passaged at 37°C in 5% CO_2 in Dulbecco's modified Eagle's medium (DMEM) (Gibco) supplemented with 10 mM HEPES (pH 7.4), penicillin, and streptomycin plus 10% fetal calf serum. HX#6 cells were grown in selection medium containing 9.35 ml of culture medium, 0.65 ml of *gpt* supplement solution (3.85 mg/ml xanthine, 0.046 mg/ml hypoxanthine, 0.062 mg/ml thymidine, 0.154 mg/ml glycine, 2.308 mg/ml glutamine), and 10 µl of 10 mg/ml mycophenolic acid (Gibco) per plate. CEM-SS cells were passaged at 37°C in 5% CO_2 in RPMI medium (Gibco) supplemented with 10 mM HEPES (pH 7.4), penicillin, and streptomycin plus 10% fetal calf serum.

For transfections, 10-cm plates of 293T cells were transfected by the calcium phosphate method (20, 182, 303, 304, 470, 473) with a total of 24 μg of plasmid DNA, as indicated. Briefly, confluent 10-cm dishes of 293T cells were split 1:4 the day prior to transfection. Plasmid DNAs were mixed with 1 ml of HEPES-buffered saline (pH 7.05 to 7.15; 21 mM HEPES, 137 mM NaCl, 5 mM KCl, 0.7 mM sodium phosphate, 5 mM dextrose), after which 40 μl of 2 M $CaCl_2$ was added while vortexing. DNA solutions were incubated at room temperature for 40 min. Following this, culture medium was removed from the cells, DNA solutions were added dropwise to the cell monolayers, and then the cells were incubated at room temperature for 20 min, with gentle rocking once at 10 min. After incubations, 10 ml of culture medium containing 50 μg of gentamicin/ml was added to the cells, and plates were incubated at 37°C and 5% CO_2 for 4 to 5 h. Following incubations, transfection media were removed and cells were washed with 5 ml of serum-free Dulbecco's modified Eagle's medium, incubated in 2.5 ml of 15% glycerol in HEPES-buffered saline for 3 min at 37°C, washed twice, and fed with 10 ml of culture medium plus 50 μg of gentamicin/ml. Cells and viruses were collected 3 days posttransfection.

Infections of CEM-SS cells were performed with filtered, cell-free supernatants obtained from transfection of 293T cells with pNL4-3 or pNL4-U35. 500μl virus was added to 4.5 ml of CEM-SS cells in suspension. Infections were monitored by removing aliquots of the culture and analyzing cell lysates for HIV-1 CA expression by immunoblotting.

Treatments of cells. For initial screening β-galactosidase (β-gal) assays, HX#6 cells were split 1:8 without tetracycline 8 days before treatments. Three days before

treatments, cells were treated with 5μM sodium butyrate (Sigma) for 24h and refed with fresh growth medium lacking tetracycline the following day. Two days later, cells were split onto 96-well plates, treated with compounds, and incubated for 3 days.

For treatments of transfected cells, dishes were washed once with serum-free medium 24h after transfection, refed with regular culture medium, and drugs or equivalent amounts of DMSO as indicated. For midiplate treatments, transfected cells were split onto 60-mm tissue culture dishes 24h after transfection in 4ml culture medium, and treated with the indicated concentrations of drugs or controls. Cells and viruses were collected two days after treatments, unless otherwise indicated. Treatments of infected CEM-SS cells were performed by adding drugs to cells washed and resuspended in fresh culture medium.

Sample collection and analysis. For sample collection, virus-containing media and cell pellets washed in phosphate-buffered saline (PBS; 9.5 mM sodium potassium phosphate [pH 7.4], 137 mM NaCl, 2.7 mM KCl) were collected 3 days posttransfection and stored at -80°C prior to further processing. Virus particles in filtered (Gelman; 0.45 μm) cell-free medium were concentrated by centrifugation at 4°C through 20% sucrose cushions in PBS (2 h at 82,500g [25,000 rpm in an SW28 rotor, 4-ml cushions], or 45 min at 197,000g [40,000 rpm, SW41 rotor, 2-ml cushions]). Virus pellets were resuspended in 0.1 ml of PBS per transfected cell plate and stored in aliquots at -80°C. For routine analysis of virus protein release, cell samples (20% of cell pellets from each plate) were suspended in IPB (20 mM Tris- hydrochloride [pH 7.5], 150 mM NaCl, 1 mM EDTA, 0.1% sodium dodecyl sulfate [SDS], 0.5% sodium deoxycholate, 1.0% Triton X-100, 0.02% sodium azide), incubated on ice for 5 min, vortexed, and cleared by

centrifugation at 13,700g for 15 min at 4°C. Soluble material was mixed with 1 volume of 2x sample buffer (12.5 mM Tris-hydrochloride [pH 6.8], 2% SDS, 20% glycerol, 0.25% bromophenol blue) plus 0.1 volume of β-mercaptoethanol, prior to heating (3 to 5 min, 95°C) and SDS-polyacrylamide gel electrophoresis (SDS-PAGE). For virus samples, 50 µl of resuspended virus pellets was mixed with one volume of 2x sample buffer plus 0.1 volume of β-mercaptoethanol and processed as above.

Cell viability assays. Toxicity of potential inhibitory drugs was measured by employing the Cell Titer 96 Aqueous One Solution Cell Proliferation assay (Promega). Confluent Vero cells were split 1:400 into wells of a 96-well plate and treated with drugs. After incubation for 3 days, proliferation assays were performed as instructed by the manufactured. Briefly, 20µl of the reagent was added to each well, and cells were incubated at 37˚C for 1-2 hours. Following incubations, the absorbance at 490nm was read in a Biorad Benchmark Plus Plate Reader.

Beta-galactosidase assays. For virus β-gal assays, 100µl of media from each well were removed to a new 96-well plate. Parallel assays were performed on the cells remaining in the wells. For virus assays, 100µl of 2x PM-2 (33 mM NaH_2PO_4, 66 mM Na_2HPO_4, 0.1 mM $MnCl_2$, 2 mM $MgSO_4$, 40 mM β-mercaptoethanol [BME]) and 5µl of 1% SDS were added to each well, followed by incubation at room temperature for 5 minutes. 40µl of 4 mg/ml o-nitrophenyl β-D-galactopyranoside (ONPG; Sigma) in PM-2 buffer were added, and samples were incubated at 37˚C until color change was observed. Absorbance was read at 420nm in a Biorad Benchmark Plus Plate Reader. Cell assays were performed by adding 40µl of PBS and 0.1% SDS to wells, incubating for 5 minutes at room temperature, adding 160µl of PM-2, then adding 40µl of 4 mg/ml ONPG in PM-

2. Plates were incubated at 37˚C until color change was observed. Absorbance was read at 420nm in a Biorad Benchmark Plus Plate Reader. Both virus and cell plates were stored frozen at -80˚C.

S35 labeling. Transfected, treated cells were washed with serum-free medium once, then refed with labeling medium (DMEM lacking cysteine and methionine and supplemented with 1% dialyzed fetal calf serum, 10mM HEPES [pH 7.4], and penicillin and streptomycin). After 60 min, medium was replaced with fresh labeling medium and appropriate inhibitor drugs, and 300μCi of EasyTag Express Protein Labeling Mix (PerkinElmer) was added. Samples were incubated for 3h, 6h, or 8h, as indicated, in a tissue culture incubator at 37˚C. After incubation, filtered (Gelman; 0.45μm) cell-free supernatants were collected and mixed with 0.25 volumes of 5X IP lysis buffer (250 mM Tris pH 7.4, 500 mM NaCl, 5% NP-40, 2.5% deoxycholate). Cells were gently washed once with PBS, then collected in 500 μl 1X IP lysis buffer. Samples were stored at -80˚C prior to processing.

Immunoprecipitation. Samples were thawed and vortexed. Cell lysates were cleared by centrifugation at 13,700g for 30 min at 4°C. Samples were then mixed with 5μg of anti-HIV IgG (NIH AIDS Research and Reference Reagent Program) and incubated rotating at 4˚C for 1h. Subsequently, 50μl of Pansorbin (Calbiochem) beads were added, and samples were incubated for 1h at 4˚C. After incubations, beads were pelleted by centrifugation at 13,700g for 1 min, supernatants were removed, and beads were washed 3 times with 1x IP lysis buffer. Then, beads were resuspended in 1X IP lysis buffer, mixed with one volume of 2x sample buffer plus 0.1 volume of β-mercaptoethanol and frozen.

SDS-PAGE and immunoblotting. Cell and virus protein samples were fractionated by conventional 10% acrylamide Laemmli SDS-PAGE (20, 182, 303, 304, 470, 473), electroblotted, and immunoblotted following previously described methods. Primary antibodies were as follows: Hy183 (from Bruce Chesebro) used at 1:15 from hybridoma culture medium for detection of the HIV-1 CA CTD. Secondary reagents were alkaline phosphatase-conjugated anti-mouse antibodies (Promega S3721) used at 1:15,000 for detection of anti-HIV-CA primary antibodies. Color reactions for visualization of antibody-bound bands employed nitroblue tetrazolium plus 5-bromo-4-chloro-3-indolyl phosphate in 100 mM Tris-hydrochloride (pH 9.5), 100 mM NaCl, and 5 mM $MgCl_2$ (20, 182, 303, 304, 470, 473). For metabolically labeled samples, 50% of the sample were loaded onto a 10% acrylamide gel and fractionated. Gels were fixed in Gel Fix (30% methanol, 10% acetic acid) for 30 to 60 min, dried onto Whatman paper, and set up for exposure on a phosphorimager storage screen (Molecular Dynamics) overnight. Cassettes were read by a Molecular Dynamics SI phosphorimager.

A.2.3 Results and discussion

Various steps of the HIV-1 lifecycle have been subjected to inhibition by pharmacological means, most notably by ways of blocking the enzymes protease, integrase, and reverse transcriptase (84, 246, 384). Only a handful of inhibitors of virus assembly have been characterized, some of them peptides capable of binding to the capsid domain and interfering with Gag multimerization (157, 198, 334, 434, 452). Our approach employed small-molecule libraries to be analyzed in a screen, followed by closer inspection of the inhibitory properties of promising compounds. For our purposes,

we obtained a compound library of about 1100 members from the Boston University Center for Chemical Methodology and Library Development (BU-CMLD), and the National Cancer Institute (NCI) diversity set of compounds, composed of about 2000 members.

Several compounds that showed promise in the initial screens were analyzed further by transfection of 293T cells with HIV constructs and treatments to examine protein expression and virus release by Western blot. We attempted to characterize the effects of these compounds on transfected cells and virus release. 293T cells were transfected with various plasmids encoding HIV-1 Gag, including HIVGPT, which encodes Gag derived from the HXB2 strain, and HIVLuc, which contains the genes for the NL4-3 strain. Both vectors carry deletions of their Env genes, replaced with the *gpt* selection marker in the HIVGPT vector, and the luciferase reporter gene in the HIVLuc plasmid. Treatment of transfected 293T or HeLa cells, however, did not reproduce the magnitude of virus release reduction observed in the initial screens. To examine potential virus release inhibition by more sensitive means, we employed metabolic labeling of treated cells with ^{35}S-methionine and ^{35}S-cysteine, followed by SDS-PAGE and imaging by phosphorimager. Some of our results indicated that NCI#75541, a steroid (shown in Figure 4.2.1), may increase processing of Gag by the viral protease enzyme. Premature processing of Gag tends to affect virus assembly and structure negatively (19, 65, 227, 241, 281, 357, 441). It may also be possible that NCI#75541 acts directly on virus particles after they have been released. To date, we have not observed changes in virus release comparable to the initial screens in protein-based assays. However, recent results indicate that NCI#75541 does not adversely affect β-gal activity per se, but may have an

effect on β-gal-containing virus particles. Further studies will examine how NCI#75541 may affect virus particles after assembly and activity of the viral protease. To this end, β-gal-containing viruses with a defective protease will be examined for susceptibility to NCI#75541. Other options include production of metabolically labeled virus particles resulting from transfection or stable infection, followed by incubation with different concentrations of NCI#75541 for different amounts of time. Moreover, *in vitro* protease assays could be used to examine effects of NCI#75541 on PR activity, using different substrates and incubation conditions. Electron microscopy of virions treated with NCI#75541 may be of interest as well, to examine whether any effect on morphology is apparent. At this point, the actions of NCI#75541 on virus particles are not known. Possibilities include minor structural distortions in PrGag-Pol or PrGag in viruses assembled from treated cells, resulting in increased access to cleavage sites by PR. Structural changes may allow earlier activation of PR enzymatic activity. Alternatively, NCI#75541 might subtly alter the balance between Gag and Gag-Pol incorporation into virus particles in favor of Gag-Pol, thus resulting in a higher proportion of PR being present in virion particles. Actions of NCI#75541 on already assembled virus particles may consist of an overly active protease, possibly resulting in inappropriate cleavage events. Results indicating that NCI#75541 may act on virus particles were obtained by examining β-galactosidase activity of HIVGag-β-gal fusion proteins in virions. Overly active PR may exert a negative effect on the β-gal enzyme packaged into virions.

Hopefully, additional studies will be able to dissect mechanisms of action for a potential antiviral compound, which may have uses both for laboratory analyses and possible future therapeutics. Virus assembly and maturation appears to be a good target

for antiviral action, since small perturbations in the structure can have detrimental effects on the further propagation of the virus.

A.2.4

Figures

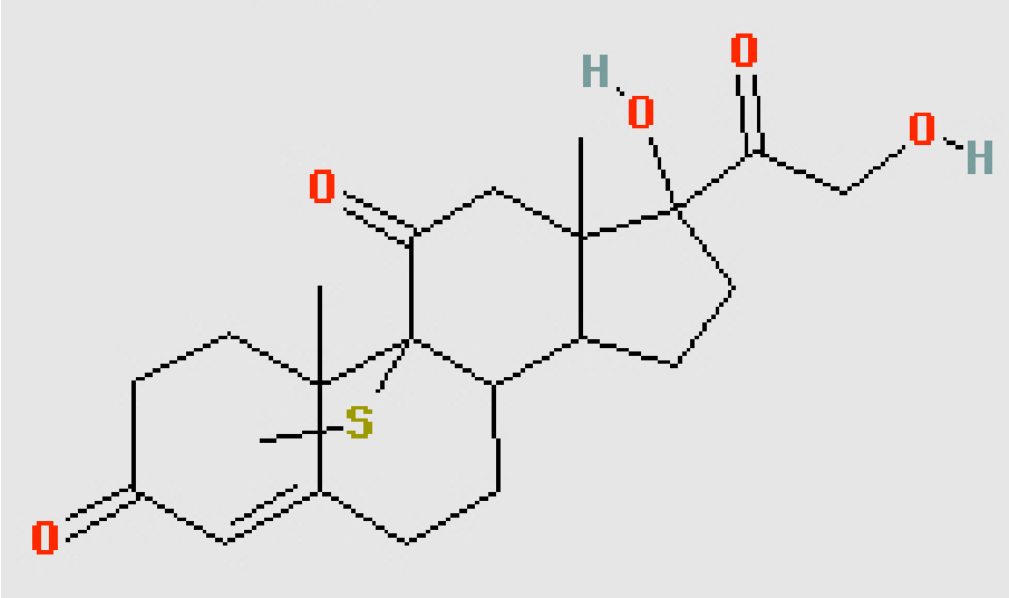

Figure A.2.1
Molecular structure of NCI#75541, a potential antiviral compound currently under investigation

References

1. 2006. AIDS Epidemic Update. *In* U. a. W. H. Organization (ed.). UNAIDS and World Health Organization.
2. **Abram, M. E., and M. A. Parniak.** 2005. Virion instability of human immunodeficiency virus type 1 reverse transcriptase (RT) mutated in the protease cleavage site between RT p51 and the RT RNase H domain. J Virol **79:**11952-61.
3. **Accola, M. A., S. Hoglund, and H. G. Gottlinger.** 1998. A putative alpha-helical structure which overlaps the capsid-p2 boundary in the human immunodeficiency virus type 1 Gag precursor is crucial for viral particle assembly. J Virol **72:**2072-8.
4. **Accola, M. A., B. Strack, and H. G. Gottlinger.** 2000. Efficient particle production by minimal Gag constructs which retain the carboxy-terminal domain of human immunodeficiency virus type 1 capsid-p2 and a late assembly domain. J Virol **74:**5395-402.
5. **Ackerson, B., O. Rey, J. Canon, and P. Krogstad.** 1998. Cells with high cyclophilin A content support replication of human immunodeficiency virus type 1 Gag mutants with decreased ability to incorporate cyclophilin A. J Virol **72:**303-8.
6. **Adamson, C. S., S. D. Ablan, I. Boeras, R. Goila-Gaur, F. Soheilian, K. Nagashima, F. Li, K. Salzwedel, M. Sakalian, C. T. Wild, and E. O. Freed.** 2006. In vitro resistance to the human immunodeficiency virus type 1 maturation inhibitor PA-457 (Bevirimat). J Virol **80:**10957-71.
7. **Agresta, B. E., and C. A. Carter.** 1997. Cyclophilin A-induced alterations of human immunodeficiency virus type 1 CA protein in vitro. J Virol **71:**6921-7.
8. **Aiken, C.** 1998. Mechanistic independence of Nef and cyclophilin A enhancement of human immunodeficiency virus type 1 infectivity. Virology **248:**139-47.
9. **Aiken, C.** 1997. Pseudotyping human immunodeficiency virus type 1 (HIV-1) by the glycoprotein of vesicular stomatitis virus targets HIV-1 entry to an endocytic pathway and suppresses both the requirement for Nef and the sensitivity to cyclosporin A. J Virol **71:**5871-7.
10. **Aiken, C., and C. H. Chen.** 2005. Betulinic acid derivatives as HIV-1 antivirals. Trends Mol Med **11:**31-6.
11. **Aiken, C., J. Konner, N. R. Landau, M. E. Lenburg, and D. Trono.** 1994. Nef induces CD4 endocytosis: requirement for a critical dileucine motif in the membrane-proximal CD4 cytoplasmic domain. Cell **76:**853-64.
12. **Aiken, C., and D. Trono.** 1995. Nef stimulates human immunodeficiency virus type 1 proviral DNA synthesis. J Virol **69:**5048-56.
13. **Alfadhli, A., T. C. Dhenub, A. Still, and E. Barklis.** 2005. Analysis of human immunodeficiency virus type 1 Gag dimerization-induced assembly. J Virol **79:**14498-506.
14. **Alfadhli, A., D. Huseby, E. Kapit, D. Colman, and E. Barklis.** 2007. Human immunodeficiency virus type 1 matrix protein assembles on membranes as a hexamer. J Virol **81:**1472-8.
15. **Alfadhli, A., E. Steel, L. Finlay, H. P. Bachinger, and E. Barklis.** 2002. Hantavirus nucleocapsid protein coiled-coil domains. J Biol Chem **277:**27103-8.
16. **Allain, B., M. Lapadat-Tapolsky, C. Berlioz, and J. L. Darlix.** 1994. Transactivation of the minus-strand DNA transfer by nucleocapsid protein during reverse transcription of the retroviral genome. Embo J **13:**973-81.
17. **Anderson, J. L., E. M. Campbell, X. Wu, N. Vandegraaff, A. Engelman, and T. J. Hope.** 2006. Proteasome inhibition reveals that a functional preintegration complex intermediate can be generated during restriction by diverse TRIM5 proteins. J Virol **80:**9754-60.
18. **Anderson, S. J., M. Lenburg, N. R. Landau, and J. V. Garcia.** 1994. The cytoplasmic domain of CD4 is sufficient for its down-regulation from the cell surface by human immunodeficiency virus type 1 Nef. J Virol **68:**3092-101.
19. **Arrigo, S. J., and K. Huffman.** 1995. Potent inhibition of human immunodeficiency virus type 1 (HIV-1) replication by inducible expression of HIV-1 PR multimers. J Virol **69:**5988-94.
20. **Arvidson, B., J. Seeds, M. Webb, L. Finlay, and E. Barklis.** 2003. Analysis of the retrovirus capsid interdomain linker region. Virology **308:**166-77.
21. **Arya, S. K., R. C. Gallo, B. H. Hahn, G. M. Shaw, M. Popovic, S. Z. Salahuddin, and F. Wong-Staal.** 1984. Homology of genome of AIDS-associated virus with genomes of human T-cell leukemia viruses. Science **225:**927-30.

22. **Auewarakul, P., P. Wacharapornin, S. Srichatrapimuk, S. Chutipongtanate, and P. Puthavathana.** 2005. Uncoating of HIV-1 requires cellular activation. Virology **337:**93-101.
23. **Bachand, F., X. J. Yao, M. Hrimech, N. Rougeau, and E. A. Cohen.** 1999. Incorporation of Vpr into human immunodeficiency virus type 1 requires a direct interaction with the p6 domain of the p55 gag precursor. J Biol Chem **274:**9083-91.
24. **Barat, C., S. F. Le Grice, and J. L. Darlix.** 1991. Interaction of HIV-1 reverse transcriptase with a synthetic form of its replication primer, tRNA(Lys,3). Nucleic Acids Res **19:**751-7.
25. **Barat, C., V. Lullien, O. Schatz, G. Keith, M. T. Nugeyre, F. Gruninger-Leitch, F. Barre-Sinoussi, S. F. LeGrice, and J. L. Darlix.** 1989. HIV-1 reverse transcriptase specifically interacts with the anticodon domain of its cognate primer tRNA. Embo J **8:**3279-85.
26. **Barboric, M., and B. M. Peterlin.** 2005. A new paradigm in eukaryotic biology: HIV Tat and the control of transcriptional elongation. PLoS Biol **3:**e76.
27. **Barklis, E., J. McDermott, S. Wilkens, S. Fuller, and D. Thompson.** 1998. Organization of HIV-1 capsid proteins on a lipid monolayer. J Biol Chem **273:**7177-80.
28. **Barre-Sinoussi, F., U. Mathur-Wagh, F. Rey, F. Brun-Vezinet, S. R. Yancovitz, C. Rouzioux, L. Montagnier, D. Mildvan, and J. C. Chermann.** 1985. Isolation of lymphadenopathy-associated virus (LAV) and detection of LAV antibodies from US patients with AIDS. Jama **253:**1737-9.
29. **Batonick, M., M. Favre, M. Boge, P. Spearman, S. Honing, and M. Thali.** 2005. Interaction of HIV-1 Gag with the clathrin-associated adaptor AP-2. Virology **342:**190-200.
30. **Battula, N., and H. M. Temin.** 1977. Infectious DNA of spleen necrosis virus is integrated at a single site in the DNA of chronically infected chicken fibroblasts. Proc Natl Acad Sci U S A **74:**281-5.
31. **Baudin, F., R. Marquet, C. Isel, J. L. Darlix, B. Ehresmann, and C. Ehresmann.** 1993. Functional sites in the 5' region of human immunodeficiency virus type 1 RNA form defined structural domains. J Mol Biol **229:**382-97.
32. **Beignon, A. S., K. McKenna, M. Skoberne, O. Manches, I. DaSilva, D. G. Kavanagh, M. Larsson, R. J. Gorelick, J. D. Lifson, and N. Bhardwaj.** 2005. Endocytosis of HIV-1 activates plasmacytoid dendritic cells via Toll-like receptor-viral RNA interactions. J Clin Invest **115:**3265-75.
33. **Bender, W., Y. H. Chien, S. Chattopadhyay, P. K. Vogt, M. B. Gardner, and N. Davidson.** 1978. High-molecular-weight RNAs of AKR, NZB, and wild mouse viruses and avian reticuloendotheliosis virus all have similar dimer structures. J Virol **25:**888-96.
34. **Bender, W., and N. Davidson.** 1976. Mapping of poly(A) sequences in the electron microscope reveals unusual structure of type C oncornavirus RNA molecules. Cell **7:**595-607.
35. **Benjamin, J., B. K. Ganser-Pornillos, W. F. Tivol, W. I. Sundquist, and G. J. Jensen.** 2005. Three-dimensional Structure of HIV-1 Virus-like Particles by Electron Cryotomography. Journal of Molecular Biology **346:**577-588.
36. **Bennasser, Y., and K. T. Jeang.** 2006. HIV-1 Tat interaction with Dicer: requirement for RNA. Retrovirology **3:**95.
37. **Bennasser, Y., S. Y. Le, M. Benkirane, and K. T. Jeang.** 2005. Evidence that HIV-1 encodes an siRNA and a suppressor of RNA silencing. Immunity **22:**607-19.
38. **Berger, E. A., R. W. Doms, E. M. Fenyo, B. T. M. Korber, D. R. Littman, J. P. Moore, Q. J. Sattentau, H. Schuitemaker, J. Sodroski, and R. A. Weiss.** 1998. A new classification for HIV-1. Nature **391:**240-240.
39. **Berger, E. A., P. M. Murphy, and J. M. Farber.** 1999. CHEMOKINE RECEPTORS AS HIV-1 CORECEPTORS: Roles in Viral Entry, Tropism, and Disease. Annual Review of Immunology **17:**657.
40. **Berkowitz, R. D., and S. P. Goff.** 1994. Analysis of binding elements in the human immunodeficiency virus type 1 genomic RNA and nucleocapsid protein. Virology **202:**233-46.
41. **Berkowitz, R. D., J. Luban, and S. P. Goff.** 1993. Specific binding of human immunodeficiency virus type 1 gag polyprotein and nucleocapsid protein to viral RNAs detected by RNA mobility shift assays. J Virol **67:**7190-200.
42. **Berkowitz, R. D., A. Ohagen, S. Hoglund, and S. P. Goff.** 1995. Retroviral nucleocapsid domains mediate the specific recognition of genomic viral RNAs by chimeric Gag polyproteins during RNA packaging in vivo. J Virol **69:**6445-56.

43. **Berman, P. W., W. M. Nunes, and O. K. Haffar.** 1988. Expression of membrane-associated and secreted variants of gp160 of human immunodeficiency virus type 1 in vitro and in continuous cell lines. J Virol **62:**3135-42.
44. **Berman, P. W., L. Riddle, G. Nakamura, O. K. Haffar, W. M. Nunes, P. Skehel, R. Byrn, J. Groopman, T. Matthews, and T. Gregory.** 1989. Expression and immunogenicity of the extracellular domain of the human immunodeficiency virus type 1 envelope glycoprotein, gp160. J Virol **63:**3489-98.
45. **Berthoux, L., C. Pechoux, M. Ottmann, G. Morel, and J. L. Darlix.** 1997. Mutations in the N-terminal domain of human immunodeficiency virus type 1 nucleocapsid protein affect virion core structure and proviral DNA synthesis. J Virol **71:**6973-81.
46. **Besnier, C., Y. Takeuchi, and G. Towers.** 2002. Restriction of lentivirus in monkeys. Proc Natl Acad Sci U S A **99:**11920-5.
47. **Binette, J., and E. A. Cohen.** 2004. Recent advances in the understanding of HIV-1 Vpu accessory protein functions. Curr Drug Targets Immune Endocr Metabol Disord **4:**297-307.
48. **Bishop, K. N., R. K. Holmes, and M. H. Malim.** 2006. Antiviral potency of APOBEC proteins does not correlate with cytidine deamination. J Virol **80:**8450-8.
49. **Bishop, K. N., R. K. Holmes, A. M. Sheehy, N. O. Davidson, S. J. Cho, and M. H. Malim.** 2004. Cytidine deamination of retroviral DNA by diverse APOBEC proteins. Curr Biol **14:**1392-6.
50. **Bishop, K. N., R. K. Holmes, A. M. Sheehy, and M. H. Malim.** 2004. APOBEC-mediated editing of viral RNA. Science **305:**645.
51. **Bohnlein, S., J. Hauber, and B. R. Cullen.** 1989. Identification of a U5-specific sequence required for efficient polyadenylation within the human immunodeficiency virus long terminal repeat. J Virol **63:**421-4.
52. **Booth, A. M., Y. Fang, J. K. Fallon, J. M. Yang, J. E. Hildreth, and S. J. Gould.** 2006. Exosomes and HIV Gag bud from endosome-like domains of the T cell plasma membrane. J Cell Biol **172:**923-35.
53. **Borrow, P., H. Lewicki, B. H. Hahn, G. M. Shaw, and M. B. Oldstone.** 1994. Virus-specific CD8+ cytotoxic T-lymphocyte activity associated with control of viremia in primary human immunodeficiency virus type 1 infection. J Virol **68:**6103-10.
54. **Bour, S., R. Geleziunas, and M. A. Wainberg.** 1995. The human immunodeficiency virus type 1 (HIV-1) CD4 receptor and its central role in promotion of HIV-1 infection. Microbiol. Rev. **59:**63-93.
55. **Braaten, D., E. K. Franke, and J. Luban.** 1996. Cyclophilin A is required for an early step in the life cycle of human immunodeficiency virus type 1 before the initiation of reverse transcription. J Virol **70:**3551-60.
56. **Brady, J., and F. Kashanchi.** 2005. Tat gets the "green" light on transcription initiation. Retrovirology **2:**69.
57. **Brenchley, J. M., B. J. Hill, D. R. Ambrozak, D. A. Price, F. J. Guenaga, J. P. Casazza, J. Kuruppu, J. Yazdani, S. A. Migueles, M. Connors, M. Roederer, D. C. Douek, and R. A. Koup.** 2004. T-cell subsets that harbor human immunodeficiency virus (HIV) in vivo: implications for HIV pathogenesis. J Virol **78:**1160-8.
58. **Brigati, C., M. Giacca, D. M. Noonan, and A. Albini.** 2003. HIV Tat, its TARgets and the control of viral gene expression. FEMS Microbiol Lett **220:**57-65.
59. **Briggs, J. A., K. Grunewald, B. Glass, F. Forster, H. G. Krausslich, and S. D. Fuller.** 2006. The mechanism of HIV-1 core assembly: insights from three-dimensional reconstructions of authentic virions. Structure **14:**15-20.
60. **Briggs, J. A., M. N. Simon, I. Gross, H. G. Krausslich, S. D. Fuller, V. M. Vogt, and M. C. Johnson.** 2004. The stoichiometry of Gag protein in HIV-1. Nat Struct Mol Biol **11:**672-5.
61. **Briggs, J. A., T. Wilk, R. Welker, H. G. Krausslich, and S. D. Fuller.** 2003. Structural organization of authentic, mature HIV-1 virions and cores. Embo J **22:**1707-15.
62. **Brown, P. H., L. S. Tiley, and B. R. Cullen.** 1991. Efficient polyadenylation within the human immunodeficiency virus type 1 long terminal repeat requires flanking U3-specific sequences. J Virol **65:**3340-3.
63. **Brugger, B., B. Glass, P. Haberkant, I. Leibrecht, F. T. Wieland, and H. G. Krausslich.** 2006. The HIV lipidome: a raft with an unusual composition. Proc Natl Acad Sci U S A **103:**2641-6.

64. **Bryant, M., and L. Ratner.** 1990. Myristoylation-dependent replication and assembly of human immunodeficiency virus 1. Proc Natl Acad Sci U S A **87:**523-7.
65. **Bukovsky, A., and H. Gottlinger.** 1996. Lack of integrase can markedly affect human immunodeficiency virus type 1 particle production in the presence of an active viral protease. J Virol **70:**6820-5.
66. **Bukovsky, A. A., T. Dorfman, A. Weimann, and H. G. Gottlinger.** 1997. Nef association with human immunodeficiency virus type 1 virions and cleavage by the viral protease. J Virol **71:**1013-8.
67. **Bukovsky, A. A., A. Weimann, M. A. Accola, and H. G. Gottlinger.** 1997. Transfer of the HIV-1 cyclophilin-binding site to simian immunodeficiency virus from Macaca mulatta can confer both cyclosporin sensitivity and cyclosporin dependence. Proc Natl Acad Sci U S A **94:**10943-8.
68. **Bukrinsky, M.** 2004. A hard way to the nucleus. Mol Med **10:**1-5.
69. **Bukrinsky, M. I., and O. K. Haffar.** 1998. HIV-1 nuclear import: matrix protein is back on center stage, this time together with Vpr. Mol Med **4:**138-43.
70. **Bukrinsky, M. I., S. Haggerty, M. P. Dempsey, N. Sharova, A. Adzhubel, L. Spitz, P. Lewis, D. Goldfarb, M. Emerman, and M. Stevenson.** 1993. A nuclear localization signal within HIV-1 matrix protein that governs infection of non-dividing cells. Nature **365:**666-9.
71. **Bukrinsky, M. I., N. Sharova, T. L. McDonald, T. Pushkarskaya, W. G. Tarpley, and M. Stevenson.** 1993. Association of integrase, matrix, and reverse transcriptase antigens of human immunodeficiency virus type 1 with viral nucleic acids following acute infection. Proc Natl Acad Sci U S A **90:**6125-9.
72. **Butler, S. L., M. S. Hansen, and F. D. Bushman.** 2001. A quantitative assay for HIV DNA integration in vivo. Nat Med **7:**631-4.
73. **Campbell, S., and A. Rein.** 1999. In vitro assembly properties of human immunodeficiency virus type 1 Gag protein lacking the p6 domain. J Virol **73:**2270-9.
74. **Carteau, S., S. C. Batson, L. Poljak, J. F. Mouscadet, H. de Rocquigny, J. L. Darlix, B. P. Roques, E. Kas, and C. Auclair.** 1997. Human immunodeficiency virus type 1 nucleocapsid protein specifically stimulates Mg2+-dependent DNA integration in vitro. J Virol **71:**6225-9.
75. **Caspar, D. L., and A. Klug.** 1962. Physical principles in the construction of regular viruses. Cold Spring Harb Symp Quant Biol **27:**1-24.
76. **Cavrois, M., C. De Noronha, and W. C. Greene.** 2002. A sensitive and specific enzyme-based assay detecting HIV-1 virion fusion in primary T lymphocytes. Nat Biotechnol **20:**1151-4.
77. **Chan, D. C., D. Fass, J. M. Berger, and P. S. Kim.** 1997. Core structure of gp41 from the HIV envelope glycoprotein. Cell **89:**263-73.
78. **Checroune, F., X. J. Yao, H. G. Gottlinger, D. Bergeron, and E. A. Cohen.** 1995. Incorporation of Vpr into human immunodeficiency virus type 1: role of conserved regions within the P6 domain of Pr55gag. J Acquir Immune Defic Syndr Hum Retrovirol **10:**1-7.
79. **Chen, B. K., I. Rousso, S. Shim, and P. S. Kim.** 2001. Efficient assembly of an HIV-1/MLV Gag-chimeric virus in murine cells. Proc Natl Acad Sci U S A **98:**15239-44.
80. **Chiu, H. C., F. D. Wang, S. Y. Yao, and C. T. Wang.** 2002. Effects of gag mutations on human immunodeficiency virus type 1 particle assembly, processing, and cyclophilin A incorporation. J Med Virol **68:**156-63.
81. **Chowdhury, I. H., X. F. Wang, N. R. Landau, M. L. Robb, V. R. Polonis, D. L. Birx, and J. H. Kim.** 2003. HIV-1 Vpr activates cell cycle inhibitor p21/Waf1/Cip1: a potential mechanism of G2/M cell cycle arrest. Virology **305:**371-7.
82. **Chun, T. W., L. Stuyver, S. B. Mizell, L. A. Ehler, J. A. Mican, M. Baseler, A. L. Lloyd, M. A. Nowak, and A. S. Fauci.** 1997. Presence of an inducible HIV-1 latent reservoir during highly active antiretroviral therapy. Proc Natl Acad Sci U S A **94:**13193-7.
83. **Clever, J. L., M. L. Wong, and T. G. Parslow.** 1996. Requirements for kissing-loop-mediated dimerization of human immunodeficiency virus RNA. J Virol **70:**5902-8.
84. **Coen, D. M., and D. D. Richman.** 2006. Antiviral Agents, p. 447 to 485, Fields Virology, 5th ed, vol. 1. Lippincott Williams & Wilkins.
85. **Coffin, J. M., Hughes S.H., Varmus, H.E.** 1997. Retroviruses. Cold Spring Harbor Laboratory Press.
86. **Colon-Gonzalez, F., and M. G. Kazanietz.** 2006. C1 domains exposed: from diacylglycerol binding to protein-protein interactions. Biochim Biophys Acta **1761:**827-37.

87. **Connor, R. I., B. K. Chen, S. Choe, and N. R. Landau.** 1995. Vpr is required for efficient replication of human immunodeficiency virus type-1 in mononuclear phagocytes. Virology **206:**935-44.
88. **Cowan, S., T. Hatziioannou, T. Cunningham, M. A. Muesing, H. G. Gottlinger, and P. D. Bieniasz.** 2002. Cellular inhibitors with Fv1-like activity restrict human and simian immunodeficiency virus tropism. Proc Natl Acad Sci U S A **99:**11914-9.
89. **Crawford, S., and S. P. Goff.** 1985. A deletion mutation in the 5' part of the pol gene of Moloney murine leukemia virus blocks proteolytic processing of the gag and pol polyproteins. J Virol **53:**899-907.
90. **Crick, F. H., and J. D. Watson.** 1956. Structure of small viruses. Nature **177:**473-5.
91. **Cruceanu, M., M. A. Urbaneja, C. V. Hixson, D. G. Johnson, S. A. Datta, M. J. Fivash, A. G. Stephen, R. J. Fisher, R. J. Gorelick, J. R. Casas-Finet, A. Rein, I. Rouzina, and M. C. Williams.** 2006. Nucleic acid binding and chaperone properties of HIV-1 Gag and nucleocapsid proteins. Nucleic Acids Res **34:**593-605.
92. **Darlix, J. L., C. Gabus, M. T. Nugeyre, F. Clavel, and F. Barre-Sinoussi.** 1990. Cis elements and trans-acting factors involved in the RNA dimerization of the human immunodeficiency virus HIV-1. J Mol Biol **216:**689-99.
93. **Darlix, J. L., M. Lapadat-Tapolsky, H. de Rocquigny, and B. P. Roques.** 1995. First glimpses at structure-function relationships of the nucleocapsid protein of retroviruses. J Mol Biol **254:**523-37.
94. **Das, A. T., A. Harwig, M. M. Vrolijk, and B. Berkhout.** 2007. The TAR Hairpin of Human Immunodeficiency Virus Type 1 Can Be Deleted When Not Required for Tat-Mediated Activation of Transcription. J. Virol. **81:**7742-7748.
95. **Davis, M. R., J. Jiang, J. Zhou, E. O. Freed, and C. Aiken.** 2006. A mutation in the human immunodeficiency virus type 1 Gag protein destabilizes the interaction of the envelope protein subunits gp120 and gp41. J Virol **80:**2405-17.
96. **Day, C. L., and B. D. Walker.** 2003. Progress in defining CD4 helper cell responses in chronic viral infections. J Exp Med **198:**1773-7.
97. **Dayton, A. I., J. G. Sodroski, C. A. Rosen, W. C. Goh, and W. A. Haseltine.** 1986. The trans-activator gene of the human T cell lymphotropic virus type III is required for replication. Cell **44:**941-7.
98. **Dayton, E. T., D. A. Konings, D. M. Powell, B. A. Shapiro, L. Butini, J. V. Maizel, and A. I. Dayton.** 1992. Extensive sequence-specific information throughout the CAR/RRE, the target sequence of the human immunodeficiency virus type 1 Rev protein. J Virol **66:**1139-51.
99. **Dayton, E. T., D. M. Powell, and A. I. Dayton.** 1989. Functional analysis of CAR, the target sequence for the Rev protein of HIV-1. Science **246:**1625-9.
100. **De Clercq, E.** 2005. New approaches toward anti-HIV chemotherapy. J Med Chem **48:**1297-313.
101. **De Clercq, E.** 2002. New developments in anti-HIV chemotherapy. Biochim Biophys Acta **1587:**258-75.
102. **De Silva, F. S., D. S. Venturini, E. Wagner, P. R. Shank, and S. Sharma.** 2001. CD4-independent infection of human B cells with HIV type 1: detection of unintegrated viral DNA. AIDS Res Hum Retroviruses **17:**1585-98.
103. **de Vincenzi, I.** 1994. A longitudinal study of human immunodeficiency virus transmission by heterosexual partners. European Study Group on Heterosexual Transmission of HIV. N Engl J Med **331:**341-6.
104. **Delchambre, M., D. Gheysen, D. Thines, C. Thiriart, E. Jacobs, E. Verdin, M. Horth, A. Burny, and F. Bex.** 1989. The GAG precursor of simian immunodeficiency virus assembles into virus-like particles. Embo J **8:**2653-60.
105. **Di Marzio, P., S. Choe, M. Ebright, R. Knoblauch, and N. R. Landau.** 1995. Mutational analysis of cell cycle arrest, nuclear localization and virion packaging of human immunodeficiency virus type 1 Vpr. J Virol **69:**7909-16.
106. **di Marzo Veronese, F., T. D. Copeland, A. L. DeVico, R. Rahman, S. Oroszlan, R. C. Gallo, and M. G. Sarngadharan.** 1986. Characterization of highly immunogenic p66/p51 as the reverse transcriptase of HTLV-III/LAV. Science **231:**1289-91.

107. **Diaz-Griffero, F., X. Li, H. Javanbakht, B. Song, S. Welikala, M. Stremlau, and J. Sodroski.** 2006. Rapid turnover and polyubiquitylation of the retroviral restriction factor TRIM5. Virology **349:**300-15.
108. **Dismuke, D. J., and C. Aiken.** 2006. Evidence for a functional link between uncoating of the human immunodeficiency virus type 1 core and nuclear import of the viral preintegration complex. J Virol **80:**3712-20.
109. **Doms, R. W., P. L. Earl, S. Chakrabarti, and B. Moss.** 1990. Human immunodeficiency virus types 1 and 2 and simian immunodeficiency virus env proteins possess a functionally conserved assembly domain. J Virol **64:**3537-40.
110. **Doms, R. W., P. L. Earl, and B. Moss.** 1991. The assembly of the HIV-1 env glycoprotein into dimers and tetramers. Adv Exp Med Biol **300:**203-19; discussion 220-1.
111. **Dong, X., H. Li, A. Derdowski, L. Ding, A. Burnett, X. Chen, T. R. Peters, T. S. Dermody, E. Woodruff, J. J. Wang, and P. Spearman.** 2005. AP-3 directs the intracellular trafficking of HIV-1 Gag and plays a key role in particle assembly. Cell **120:**663-74.
112. **Dorfman, T., A. Bukovsky, A. Ohagen, S. Hoglund, and H. G. Gottlinger.** 1994. Functional domains of the capsid protein of human immunodeficiency virus type 1. J Virol **68:**8180-7.
113. **Dorfman, T., F. Mammano, W. A. Haseltine, and H. G. Gottlinger.** 1994. Role of the matrix protein in the virion association of the human immunodeficiency virus type 1 envelope glycoprotein. J Virol **68:**1689-96.
114. **Dorfman, T., E. Popova, M. Pizzato, and H. G. Gottlinger.** 2002. Nef enhances human immunodeficiency virus type 1 infectivity in the absence of matrix. J Virol **76:**6857-62.
115. **Dorfman, T., A. Weimann, A. Borsetti, C. T. Walsh, and H. G. Gottlinger.** 1997. Active-site residues of cyclophilin A are crucial for its incorporation into human immunodeficiency virus type 1 virions. J Virol **71:**7110-3.
116. **Dunn, D. T., M. L. Newell, A. E. Ades, and C. S. Peckham.** 1992. Risk of human immunodeficiency virus type 1 transmission through breastfeeding. Lancet **340:**585-8.
117. **Earl, P. L., R. W. Doms, and B. Moss.** 1992. Multimeric CD4 binding exhibited by human and simian immunodeficiency virus envelope protein dimers. J Virol **66:**5610-4.
118. **Earl, P. L., R. W. Doms, and B. Moss.** 1990. Oligomeric structure of the human immunodeficiency virus type 1 envelope glycoprotein. Proc Natl Acad Sci U S A **87:**648-52.
119. **Edwards, A. S., and A. C. Newton.** 1997. Regulation of protein kinase C betaII by its C2 domain. Biochemistry **36:**15615-23.
120. **Ehrlich, L. S., T. Liu, S. Scarlata, B. Chu, and C. A. Carter.** 2001. HIV-1 capsid protein forms spherical (immature-like) and tubular (mature-like) particles in vitro: structure switching by pH-induced conformational changes. Biophys J **81:**586-94.
121. **Facke, M., A. Janetzko, R. L. Shoeman, and H. G. Krausslich.** 1993. A large deletion in the matrix domain of the human immunodeficiency virus gag gene redirects virus particle assembly from the plasma membrane to the endoplasmic reticulum. J Virol **67:**4972-80.
122. **Fackler, O. T., A. Moris, N. Tibroni, S. I. Giese, B. Glass, O. Schwartz, and H. G. Krausslich.** 2006. Functional characterization of HIV-1 Nef mutants in the context of viral infection. Virology **351:**322-39.
123. **Fan, N., K. B. Rank, J. W. Leone, R. L. Heinrikson, C. A. Bannow, C. W. Smith, D. B. Evans, S. M. Poppe, W. G. Tarpley, D. J. Rothrock, and et al.** 1995. The differential processing of homodimers of reverse transcriptases from human immunodeficiency viruses type 1 and 2 is a consequence of the distinct specificities of the viral proteases. J Biol Chem **270:**13573-9.
124. **Fang, L., and N. R. Landau.** 2007. Analysis of Vif-induced APOBEC3G degradation using an alpha-complementation assay. Virology **359:**162-9.
125. **Felber, B. K., M. Hadzopoulou-Cladaras, C. Cladaras, T. Copeland, and G. N. Pavlakis.** 1989. rev protein of human immunodeficiency virus type 1 affects the stability and transport of the viral mRNA. Proc Natl Acad Sci U S A **86:**1495-9.
126. **Feng, Y. X., T. D. Copeland, L. E. Henderson, R. J. Gorelick, W. J. Bosche, J. G. Levin, and A. Rein.** 1996. HIV-1 nucleocapsid protein induces "maturation" of dimeric retroviral RNA in vitro. Proc Natl Acad Sci U S A **93:**7577-81.

127. **Feng, Y. X., T. Li, S. Campbell, and A. Rein.** 2002. Reversible binding of recombinant human immunodeficiency virus type 1 gag protein to nucleic acids in virus-like particle assembly in vitro. J Virol **76:**11757-62.
128. **Fenrick, R., M. H. Malim, J. Hauber, S. Y. Le, J. Maizel, and B. R. Cullen.** 1989. Functional analysis of the Tat trans activator of human immunodeficiency virus type 2. J Virol **63:**5006-12.
129. **Finzi, A., A. Orthwein, J. Mercier, and E. A. Cohen.** 2007. Productive Human Immunodeficiency Virus Type 1 Assembly Takes Place at the Plasma Membrane. J. Virol. **81:**7476-7490.
130. **Finzi, D., M. Hermankova, T. Pierson, L. M. Carruth, C. Buck, R. E. Chaisson, T. C. Quinn, K. Chadwick, J. Margolick, R. Brookmeyer, J. Gallant, M. Markowitz, D. D. Ho, D. D. Richman, and R. F. Siliciano.** 1997. Identification of a reservoir for HIV-1 in patients on highly active antiretroviral therapy. Science **278:**1295-300.
131. **Fisher, A. G., M. B. Feinberg, S. F. Josephs, M. E. Harper, L. M. Marselle, G. Reyes, M. A. Gonda, A. Aldovini, C. Debouk, R. C. Gallo, and et al.** 1986. The trans-activator gene of HTLV-III is essential for virus replication. Nature **320:**367-71.
132. **Flint, S. J., L. W. Enquist, R. M. Krug, V. R. Racaniello, and A. M. Skalka.** 2000. Principles of virology: molecular biology, pathogenesis, and control. ASM Press, Washington, D.C.
133. **Forshey, B. M., U. von Schwedler, W. I. Sundquist, and C. Aiken.** 2002. Formation of a human immunodeficiency virus type 1 core of optimal stability is crucial for viral replication. J Virol **76:**5667-77.
134. **Fouchier, R. A., B. E. Meyer, J. H. Simon, U. Fischer, A. V. Albright, F. Gonzalez-Scarano, and M. H. Malim.** 1998. Interaction of the human immunodeficiency virus type 1 Vpr protein with the nuclear pore complex. J Virol **72:**6004-13.
135. **Franke, E. K., H. E. Yuan, and J. Luban.** 1994. Specific incorporation of cyclophilin A into HIV-1 virions. Nature **372:**359-62.
136. **Freed, E. O.** 2006. HIV-1 Gag: Flipped out for PI(4,5)P2. PNAS **103:**11101-11102.
137. **Freed, E. O.** 2001. HIV-1 replication. Somat Cell Mol Genet **26:**13-33.
138. **Freed, E. O., G. Englund, and M. A. Martin.** 1995. Role of the basic domain of human immunodeficiency virus type 1 matrix in macrophage infection. J Virol **69:**3949-54.
139. **Freed, E. O., and M. A. Martin.** 1996. Domains of the human immunodeficiency virus type 1 matrix and gp41 cytoplasmic tail required for envelope incorporation into virions. J Virol **70:**341-51.
140. **Freed, E. O., and M. A. Martin.** 2006. HIVs and their replication, p. 2107 to 2185, Fields Virology, 5th ed, vol. 2. Lippincott Williams & Wilkins.
141. **Freed, E. O., and M. A. Martin.** 1995. The role of human immunodeficiency virus type 1 envelope glycoproteins in virus infection. J Biol Chem **270:**23883-6.
142. **Freed, E. O., and M. A. Martin.** 1995. Virion incorporation of envelope glycoproteins with long but not short cytoplasmic tails is blocked by specific, single amino acid substitutions in the human immunodeficiency virus type 1 matrix. J Virol **69:**1984-9.
143. **Freed, E. O., and A. J. Mouland.** 2006. The cell biology of HIV-1 and other retroviruses. Retrovirology **3:**77.
144. **Fritsch, E., and H. M. Temin.** 1977. Formation and structure of infectious DNA of spleen necrosis virus. J Virol **21:**119-30.
145. **Frost, S. D., T. Wrin, D. M. Smith, S. L. Kosakovsky Pond, Y. Liu, E. Paxinos, C. Chappey, J. Galovich, J. Beauchaine, C. J. Petropoulos, S. J. Little, and D. D. Richman.** 2005. Neutralizing antibody responses drive the evolution of human immunodeficiency virus type 1 envelope during recent HIV infection. Proc Natl Acad Sci U S A **102:**18514-9.
146. **Fuller, S. D., T. Wilk, B. E. Gowen, H. G. Krausslich, and V. M. Vogt.** 1997. Cryo-electron microscopy reveals ordered domains in the immature HIV-1 particle. Curr Biol **7:**729-38.
147. **Furfine, E. S., and J. E. Reardon.** 1991. Human immunodeficiency virus reverse transcriptase ribonuclease H: specificity of tRNA(Lys3)-primer excision. Biochemistry **30:**7041-6.
148. **Furfine, E. S., and J. E. Reardon.** 1991. Reverse transcriptase.RNase H from the human immunodeficiency virus. Relationship of the DNA polymerase and RNA hydrolysis activities. J Biol Chem **266:**406-12.
149. **Gallay, P., S. Swingler, C. Aiken, and D. Trono.** 1995. HIV-1 infection of nondividing cells: C-terminal tyrosine phosphorylation of the viral matrix protein is a key regulator. Cell **80:**379-88.

150. **Gallo, R. C., S. Z. Salahuddin, M. Popovic, G. M. Shearer, M. Kaplan, B. F. Haynes, T. J. Palker, R. Redfield, J. Oleske, B. Safai, and et al.** 1984. Frequent detection and isolation of cytopathic retroviruses (HTLV-III) from patients with AIDS and at risk for AIDS. Science **224:**500-3.
151. **Gamble, T. R., F. F. Vajdos, S. Yoo, D. K. Worthylake, M. Houseweart, W. I. Sundquist, and C. P. Hill.** 1996. Crystal structure of human cyclophilin A bound to the amino-terminal domain of HIV-1 capsid. Cell **87:**1285-94.
152. **Gamble, T. R., S. Yoo, F. F. Vajdos, U. K. von Schwedler, D. K. Worthylake, H. Wang, J. P. McCutcheon, W. I. Sundquist, and C. P. Hill.** 1997. Structure of the carboxyl-terminal dimerization domain of the HIV-1 capsid protein. Science **278:**849-53.
153. **Ganser, B. K., S. Li, V. Y. Klishko, J. T. Finch, and W. I. Sundquist.** 1999. Assembly and analysis of conical models for the HIV-1 core. Science **283:**80-3.
154. **Ganser-Pornillos, B. K., U. K. von Schwedler, K. M. Stray, C. Aiken, and W. I. Sundquist.** 2004. Assembly properties of the human immunodeficiency virus type 1 CA protein. J Virol **78:**2545-52.
155. **Garcia, E., M. Pion, A. Pelchen-Matthews, L. Collinson, J. F. Arrighi, G. Blot, F. Leuba, J. M. Escola, N. Demaurex, M. Marsh, and V. Piguet.** 2005. HIV-1 trafficking to the dendritic cell-T-cell infectious synapse uses a pathway of tetraspanin sorting to the immunological synapse. Traffic **6:**488-501.
156. **Garrus, J. E., U. K. von Schwedler, O. W. Pornillos, S. G. Morham, K. H. Zavitz, H. E. Wang, D. A. Wettstein, K. M. Stray, M. Cote, R. L. Rich, D. G. Myszka, and W. I. Sundquist.** 2001. Tsg101 and the vacuolar protein sorting pathway are essential for HIV-1 budding. Cell **107:**55-65.
157. **Garzon, M. T., M. C. Lidon-Moya, F. N. Barrera, A. Prieto, J. Gomez, M. G. Mateu, and J. L. Neira.** 2004. The dimerization domain of the HIV-1 capsid protein binds a capsid protein-derived peptide: a biophysical characterization. Protein Sci **13:**1512-23.
158. **Gatignol, A., and K. T. Jeang.** 2000. Tat as a transcriptional activator and a potential therapeutic target for HIV-1. Adv Pharmacol **48:**209-27.
159. **Gheysen, D., E. Jacobs, F. de Foresta, C. Thiriart, M. Francotte, D. Thines, and M. De Wilde.** 1989. Assembly and release of HIV-1 precursor Pr55gag virus-like particles from recombinant baculovirus-infected insect cells. Cell **59:**103-12.
160. **Gitti, R. K., B. M. Lee, J. Walker, M. F. Summers, S. Yoo, and W. I. Sundquist.** 1996. Structure of the amino-terminal core domain of the HIV-1 capsid protein. Science **273:**231-5.
161. **Goncalves, J., Y. Korin, J. Zack, and D. Gabuzda.** 1996. Role of Vif in human immunodeficiency virus type 1 reverse transcription. J Virol **70:**8701-9.
162. **Gopalakrishnan, V., J. A. Peliska, and S. J. Benkovic.** 1992. Human immunodeficiency virus type 1 reverse transcriptase: spatial and temporal relationship between the polymerase and RNase H activities. Proc Natl Acad Sci U S A **89:**10763-7.
163. **Gorelick, R. J., S. M. Nigida, Jr., J. W. Bess, Jr., L. O. Arthur, L. E. Henderson, and A. Rein.** 1990. Noninfectious human immunodeficiency virus type 1 mutants deficient in genomic RNA. J Virol **64:**3207-11.
164. **Goto, T., K. Ikuta, J. J. Zhang, C. Morita, K. Sano, M. Komatsu, H. Fujita, S. Kato, and M. Nakai.** 1990. The budding of defective human immunodeficiency virus type 1 (HIV-1) particles from cell clones persistently infected with HIV-1. Arch Virol **111:**87-101.
165. **Gotte, M., S. Fackler, T. Hermann, E. Perola, L. Cellai, H. J. Gross, S. F. Le Grice, and H. Heumann.** 1995. HIV-1 reverse transcriptase-associated RNase H cleaves RNA/RNA in arrested complexes: implications for the mechanism by which RNase H discriminates between RNA/RNA and RNA/DNA. Embo J **14:**833-41.
166. **Gottlieb, G. S., S. E. Hawes, H. D. Agne, J. E. Stern, C. W. Critchlow, N. B. Kiviat, and P. S. Sow.** 2006. Lower levels of HIV RNA in semen in HIV-2 compared with HIV-1 infection: implications for differences in transmission. Aids **20:**895-900.
167. **Gottlieb, G. S., P. S. Sow, S. E. Hawes, I. Ndoye, M. Redman, A. M. Coll-Seck, M. A. Faye-Niang, A. Diop, J. M. Kuypers, C. W. Critchlow, R. Respess, J. I. Mullins, and N. B. Kiviat.** 2002. Equal plasma viral loads predict a similar rate of CD4+ T cell decline in human immunodeficiency virus (HIV) type 1- and HIV-2-infected individuals from Senegal, West Africa. J Infect Dis **185:**905-14.

168. **Gottlinger, H. G., T. Dorfman, E. A. Cohen, and W. A. Haseltine.** 1993. Vpu protein of human immunodeficiency virus type 1 enhances the release of capsids produced by gag gene constructs of widely divergent retroviruses. Proc Natl Acad Sci U S A **90:**7381-5.
169. **Gottlinger, H. G., T. Dorfman, J. G. Sodroski, and W. A. Haseltine.** 1991. Effect of mutations affecting the p6 gag protein on human immunodeficiency virus particle release. Proc Natl Acad Sci U S A **88:**3195-9.
170. **Gottlinger, H. G., J. G. Sodroski, and W. A. Haseltine.** 1989. Role of capsid precursor processing and myristoylation in morphogenesis and infectivity of human immunodeficiency virus type 1. Proc Natl Acad Sci U S A **86:**5781-5.
171. **Gottwein, E., S. Jager, A. Habermann, and H. G. Krausslich.** 2006. Cumulative mutations of ubiquitin acceptor sites in human immunodeficiency virus type 1 gag cause a late budding defect. J Virol **80:**6267-75.
172. **Grigorov, B., F. Arcanger, P. Roingeard, J. L. Darlix, and D. Muriaux.** 2006. Assembly of infectious HIV-1 in human epithelial and T-lymphoblastic cell lines. J Mol Biol **359:**848-62.
173. **Gross, I., H. Hohenberg, and H. G. Krausslich.** 1997. In vitro assembly properties of purified bacterially expressed capsid proteins of human immunodeficiency virus. Eur J Biochem **249:**592-600.
174. **Gross, I., H. Hohenberg, T. Wilk, K. Wiegers, M. Grattinger, B. Muller, S. Fuller, and H. G. Krausslich.** 2000. A conformational switch controlling HIV-1 morphogenesis. Embo J **19:**103-13.
175. **Grossman, Z., M. Meier-Schellersheim, W. E. Paul, and L. J. Picker.** 2006. Pathogenesis of HIV infection: what the virus spares is as important as what it destroys. Nat Med **12:**289-95.
176. **Guo, H. G., F. M. Veronese, E. Tschachler, R. Pal, V. S. Kalyanaraman, R. C. Gallo, and M. S. Reitz, Jr.** 1990. Characterization of an HIV-1 point mutant blocked in envelope glycoprotein cleavage. Virology **174:**217-24.
177. **Hadzopoulou-Cladaras, M., B. K. Felber, C. Cladaras, A. Athanassopoulos, A. Tse, and G. N. Pavlakis.** 1989. The rev (trs/art) protein of human immunodeficiency virus type 1 affects viral mRNA and protein expression via a cis-acting sequence in the env region. J Virol **63:**1265-74.
178. **Haffar, O., J. Garrigues, B. Travis, P. Moran, J. Zarling, and S. L. Hu.** 1990. Human immunodeficiency virus-like, nonreplicating, gag-env particles assemble in a recombinant vaccinia virus expression system. J Virol **64:**2653-9.
179. **Haffar, O. K., S. Popov, L. Dubrovsky, I. Agostini, H. Tang, T. Pushkarsky, S. G. Nadler, and M. Bukrinsky.** 2000. Two nuclear localization signals in the HIV-1 matrix protein regulate nuclear import of the HIV-1 pre-integration complex. J Mol Biol **299:**359-68.
180. **Hammarskjold, M. L., J. Heimer, B. Hammarskjold, I. Sangwan, L. Albert, and D. Rekosh.** 1989. Regulation of human immunodeficiency virus env expression by the rev gene product. J Virol **63:**1959-66.
181. **Hansen, J., T. Schulze, W. Mellert, and K. Moelling.** 1988. Identification and characterization of HIV-specific RNase H by monoclonal antibody. Embo J **7:**239-43.
182. **Hansen, M. S., and E. Barklis.** 1995. Structural interactions between retroviral Gag proteins examined by cysteine cross-linking. J Virol **69:**1150-9.
183. **Harrison, S. C.** 2006. Principles of virus structure, p. 59 to 98, Fields Virology, 5th ed, vol. 1. Lippincott Williams & Wilkins.
184. **Hatziioannou, T., S. Cowan, S. P. Goff, P. D. Bieniasz, and G. J. Towers.** 2003. Restriction of multiple divergent retroviruses by Lv1 and Ref1. Embo J **22:**385-94.
185. **Hatziioannou, T., J. Martin-Serrano, T. Zang, and P. D. Bieniasz.** 2005. Matrix-induced inhibition of membrane binding contributes to human immunodeficiency virus type 1 particle assembly defects in murine cells. J Virol **79:**15586-9.
186. **Hatziioannou, T., D. Perez-Caballero, S. Cowan, and P. D. Bieniasz.** 2005. Cyclophilin interactions with incoming human immunodeficiency virus type 1 capsids with opposing effects on infectivity in human cells. J Virol **79:**176-83.
187. **Haugh, J. M., F. Codazzi, M. Teruel, and T. Meyer.** 2000. Spatial sensing in fibroblasts mediated by 3' phosphoinositides. J Cell Biol **151:**1269-80.
188. **Hayashi, T., T. Shioda, Y. Iwakura, and H. Shibuta.** 1992. RNA packaging signal of human immunodeficiency virus type 1. Virology **188:**590-9.

189. **He, J., S. Choe, R. Walker, P. Di Marzio, D. O. Morgan, and N. R. Landau.** 1995. Human immunodeficiency virus type 1 viral protein R (Vpr) arrests cells in the G2 phase of the cell cycle by inhibiting p34cdc2 activity. J Virol **69:**6705-11.
190. **Hearps, A. C., and D. A. Jans.** 2007. Regulating the functions of the HIV-1 matrix protein. AIDS Res Hum Retroviruses **23:**341-6.
191. **Hecht, F. M., M. P. Busch, B. Rawal, M. Webb, E. Rosenberg, M. Swanson, M. Chesney, J. Anderson, J. Levy, and J. O. Kahn.** 2002. Use of laboratory tests and clinical symptoms for identification of primary HIV infection. Aids **16:**1119-29.
192. **Heeney, J. L., A. G. Dalgleish, and R. A. Weiss.** 2006. Origins of HIV and the Evolution of Resistance to AIDS. Science **313:**462-466.
193. **Helseth, E., U. Olshevsky, C. Furman, and J. Sodroski.** 1991. Human immunodeficiency virus type 1 gp120 envelope glycoprotein regions important for association with the gp41 transmembrane glycoprotein. J Virol **65:**2119-23.
194. **Hermida-Matsumoto, L., and M. D. Resh.** 1999. Human immunodeficiency virus type 1 protease triggers a myristoyl switch that modulates membrane binding of Pr55(gag) and p17MA. J Virol **73:**1902-8.
195. **Hill, C. P., D. Worthylake, D. P. Bancroft, A. M. Christensen, and W. I. Sundquist.** 1996. Crystal structures of the trimeric human immunodeficiency virus type 1 matrix protein: implications for membrane association and assembly. Proc Natl Acad Sci U S A **93:**3099-104.
196. **Hockley, D. J., M. V. Nermut, C. Grief, J. B. Jowett, and I. M. Jones.** 1994. Comparative morphology of Gag protein structures produced by mutants of the gag gene of human immunodeficiency virus type 1. J Gen Virol **75 (Pt 11):**2985-97.
197. **Hockley, D. J., R. D. Wood, J. P. Jacobs, and A. J. Garrett.** 1988. Electron microscopy of human immunodeficiency virus. J Gen Virol **69 (Pt 10):**2455-69.
198. **Hoglund, S., J. Su, S. S. Reneby, A. Vegvari, S. Hjerten, I. M. Sintorn, H. Foster, Y. P. Wu, I. Nystrom, and A. Vahlne.** 2002. Tripeptide interference with human immunodeficiency virus type 1 morphogenesis. Antimicrob Agents Chemother **46:**3597-605.
199. **Holm, K., K. Weclewicz, R. Hewson, and M. Suomalainen.** 2003. Human immunodeficiency virus type 1 assembly and lipid rafts: Pr55(gag) associates with membrane domains that are largely resistant to Brij98 but sensitive to Triton X-100. J Virol **77:**4805-17.
200. **Holmes, R. K., F. A. Koning, K. N. Bishop, and M. H. Malim.** 2007. APOBEC3F can inhibit the accumulation of HIV-1 reverse transcription products in the absence of hypermutation. Comparisons with APOBEC3G. J Biol Chem **282:**2587-95.
201. **Holmes, R. K., M. H. Malim, and K. N. Bishop.** 2007. APOBEC-mediated viral restriction: not simply editing? Trends Biochem Sci **32:**118-28.
202. **Hoshikawa, N., A. Kojima, A. Yasuda, E. Takayashiki, S. Masuko, J. Chiba, T. Sata, and T. Kurata.** 1991. Role of the gag and pol genes of human immunodeficiency virus in the morphogenesis and maturation of retrovirus-like particles expressed by recombinant vaccinia virus: an ultrastructural study. J Gen Virol **72 (Pt 10):**2509-17.
203. **Hrimech, M., X. J. Yao, F. Bachand, N. Rougeau, and E. A. Cohen.** 1999. Human immunodeficiency virus type 1 (HIV-1) Vpr functions as an immediate-early protein during HIV-1 infection. J Virol **73:**4101-9.
204. **Huang, L., X. Yuan, C. Aiken, and C. H. Chen.** 2004. Bifunctional anti-human immunodeficiency virus type 1 small molecules with two novel mechanisms of action. Antimicrob Agents Chemother **48:**663-5.
205. **Huang, M., J. M. Orenstein, M. A. Martin, and E. O. Freed.** 1995. p6Gag is required for particle production from full-length human immunodeficiency virus type 1 molecular clones expressing protease. J Virol **69:**6810-8.
206. **Huber, H. E., and C. C. Richardson.** 1990. Processing of the primer for plus strand DNA synthesis by human immunodeficiency virus 1 reverse transcriptase. J Biol Chem **265:**10565-73.
207. **Hubner, W., and B. K. Chen.** 2006. Inhibition of viral assembly in murine cells by HIV-1 matrix. Virology **352:**27-38.
208. **Hurley, J. H., and T. Meyer.** 2001. Subcellular targeting by membrane lipids. Curr Opin Cell Biol **13:**146-52.
209. **Huseby, D., R. L. Barklis, A. Alfadhli, and E. Barklis.** 2005. Assembly of human immunodeficiency virus precursor gag proteins. J Biol Chem **280:**17664-70.

210. **Jacks, T., M. D. Power, F. R. Masiarz, P. A. Luciw, P. J. Barr, and H. E. Varmus.** 1988. Characterization of ribosomal frameshifting in HIV-1 gag-pol expression. Nature **331:**280-3.
211. **Jacobo-Molina, A., J. Ding, R. G. Nanni, A. D. Clark, Jr., X. Lu, C. Tantillo, R. L. Williams, G. Kamer, A. L. Ferris, P. Clark, and et al.** 1993. Crystal structure of human immunodeficiency virus type 1 reverse transcriptase complexed with double-stranded DNA at 3.0 A resolution shows bent DNA. Proc Natl Acad Sci U S A **90:**6320-4.
212. **Jacotot, E., L. Ravagnan, M. Loeffler, K. F. Ferri, H. L. Vieira, N. Zamzami, P. Costantini, S. Druillennec, J. Hoebeke, J. P. Briand, T. Irinopoulou, E. Daugas, S. A. Susin, D. Cointe, Z. H. Xie, J. C. Reed, B. P. Roques, and G. Kroemer.** 2000. The HIV-1 viral protein R induces apoptosis via a direct effect on the mitochondrial permeability transition pore. J Exp Med **191:**33-46.
213. **Jenkins, Y., O. Pornillos, R. L. Rich, D. G. Myszka, W. I. Sundquist, and M. H. Malim.** 2001. Biochemical analyses of the interactions between human immunodeficiency virus type 1 Vpr and p6(Gag). J Virol **75:**10537-42.
214. **Jiang, J., and C. Aiken.** 2007. Maturation-Dependent Human Immunodeficiency Virus Type 1 Particle Fusion Requires a Carboxyl-Terminal Region of the gp41 Cytoplasmic Tail. J Virol **81:**9999-10008.
215. **Jiang, M., J. Mak, A. Ladha, E. Cohen, M. Klein, B. Rovinski, and L. Kleiman.** 1993. Identification of tRNAs incorporated into wild-type and mutant human immunodeficiency virus type 1. J Virol **67:**3246-53.
216. **Johnson, M. C., H. M. Scobie, Y. M. Ma, and V. M. Vogt.** 2002. Nucleic acid-independent retrovirus assembly can be driven by dimerization. J Virol **76:**11177-85.
217. **Johnston, J. A., C. L. Ward, and R. R. Kopito.** 1998. Aggresomes: a cellular response to misfolded proteins. J Cell Biol **143:**1883-98.
218. **Jolly, C., I. Mitar, and Q. J. Sattentau.** 2007. Requirement for an intact T-cell actin and tubulin cytoskeleton for efficient assembly and spread of human immunodeficiency virus type 1. J Virol **81:**5547-60.
219. **Jolly, C., and Q. J. Sattentau.** 2005. Human immunodeficiency virus type 1 virological synapse formation in T cells requires lipid raft integrity. J Virol **79:**12088-94.
220. **Jones, T. A., G. Blaug, M. Hansen, and E. Barklis.** 1990. Assembly of gag-beta-galactosidase proteins into retrovirus particles. J Virol **64:**2265-79.
221. **Jouvenet, N., S. J. Neil, C. Bess, M. C. Johnson, C. A. Virgen, S. M. Simon, and P. D. Bieniasz.** 2006. Plasma membrane is the site of productive HIV-1 particle assembly. PLoS Biol **4:**e435.
222. **Jowett, J. B., D. J. Hockley, M. V. Nermut, and I. M. Jones.** 1992. Distinct signals in human immunodeficiency virus type 1 Pr55 necessary for RNA binding and particle formation. J Gen Virol **73 (Pt 12):**3079-86.
223. **Kalpana, G. V., and S. P. Goff.** 1993. Genetic analysis of homomeric interactions of human immunodeficiency virus type 1 integrase using the yeast two-hybrid system. Proc Natl Acad Sci U S A **90:**10593-7.
224. **Kanamoto, T., Y. Kashiwada, K. Kanbara, K. Gotoh, M. Yoshimori, T. Goto, K. Sano, and H. Nakashima.** 2001. Anti-human immunodeficiency virus activity of YK-FH312 (a betulinic acid derivative), a novel compound blocking viral maturation. Antimicrob Agents Chemother **45:**1225-30.
225. **Kaplan, A. H., J. A. Zack, M. Knigge, D. A. Paul, D. J. Kempf, D. W. Norbeck, and R. Swanstrom.** 1993. Partial inhibition of the human immunodeficiency virus type 1 protease results in aberrant virus assembly and the formation of noninfectious particles. J Virol **67:**4050-5.
226. **Karacostas, V., K. Nagashima, M. A. Gonda, and B. Moss.** 1989. Human immunodeficiency virus-like particles produced by a vaccinia virus expression vector. Proc Natl Acad Sci U S A **86:**8964-7.
227. **Karacostas, V., E. J. Wolffe, K. Nagashima, M. A. Gonda, and B. Moss.** 1993. Overexpression of the HIV-1 gag-pol polyprotein results in intracellular activation of HIV-1 protease and inhibition of assembly and budding of virus-like particles. Virology **193:**661-71.
228. **Kashanchi, F., S. N. Khleif, J. F. Duvall, M. R. Sadaie, M. F. Radonovich, M. Cho, M. A. Martin, S. Y. Chen, R. Weinmann, and J. N. Brady.** 1996. Interaction of human

immunodeficiency virus type 1 Tat with a unique site of TFIID inhibits negative cofactor Dr1 and stabilizes the TFIID-TFIIA complex. J Virol **70:**5503-10.

229. **Katoh, I., Y. Yoshinaka, A. Rein, M. Shibuya, T. Odaka, and S. Oroszlan.** 1985. Murine leukemia virus maturation: protease region required for conversion from "immature" to "mature" core form and for virus infectivity. Virology **145:**280-92.
230. **Kelly, B. N., S. Kyere, I. Kinde, C. Tang, B. R. Howard, H. Robinson, W. I. Sundquist, M. F. Summers, and C. P. Hill.** 2007. Structure of the Antiviral Assembly Inhibitor CAP-1 Complex with the HIV-1 CA Protein. J Mol Biol **373:**355-66.
231. **Kiernan, R. E., A. Ono, G. Englund, and E. O. Freed.** 1998. Role of matrix in an early postentry step in the human immunodeficiency virus type 1 life cycle. J Virol **72:**4116-26.
232. **Klase, Z., P. Kale, R. Winograd, M. V. Gupta, M. Heydarian, R. Berro, T. McCaffrey, and F. Kashanchi.** 2007. HIV-1 TAR element is processed by Dicer to yield a viral micro-RNA involved in chromatin remodeling of the viral LTR. BMC Mol Biol **8:**63.
233. **Knight, S. C., S. E. Macatonia, and S. Patterson.** 1990. HIV I infection of dendritic cells. Int Rev Immunol **6:**163-75.
234. **Kohl, N. E., E. A. Emini, W. A. Schleif, L. J. Davis, J. C. Heimbach, R. A. Dixon, E. M. Scolnick, and I. S. Sigal.** 1988. Active human immunodeficiency virus protease is required for viral infectivity. Proc Natl Acad Sci U S A **85:**4686-90.
235. **Kohlstaedt, L. A., J. Wang, J. M. Friedman, P. A. Rice, and T. A. Steitz.** 1992. Crystal structure at 3.5 A resolution of HIV-1 reverse transcriptase complexed with an inhibitor. Science **256:**1783-90.
236. **Kondo, E., and H. G. Gottlinger.** 1996. A conserved LXXLF sequence is the major determinant in p6gag required for the incorporation of human immunodeficiency virus type 1 Vpr. J Virol **70:**159-64.
237. **Kondo, E., F. Mammano, E. A. Cohen, and H. G. Gottlinger.** 1995. The p6gag domain of human immunodeficiency virus type 1 is sufficient for the incorporation of Vpr into heterologous viral particles. J Virol **69:**2759-64.
238. **Kotov, A., J. Zhou, P. Flicker, and C. Aiken.** 1999. Association of Nef with the human immunodeficiency virus type 1 core. J Virol **73:**8824-30.
239. **Koup, R. A., J. T. Safrit, Y. Cao, C. A. Andrews, G. McLeod, W. Borkowsky, C. Farthing, and D. D. Ho.** 1994. Temporal association of cellular immune responses with the initial control of viremia in primary human immunodeficiency virus type 1 syndrome. J Virol **68:**4650-5.
240. **Kozarsky, K., M. Penman, L. Basiripour, W. Haseltine, J. Sodroski, and M. Krieger.** 1989. Glycosylation and processing of the human immunodeficiency virus type 1 envelope protein. J Acquir Immune Defic Syndr **2:**163-9.
241. **Krausslich, H. G.** 1991. Human immunodeficiency virus proteinase dimer as component of the viral polyprotein prevents particle assembly and viral infectivity. Proc Natl Acad Sci U S A **88:**3213-7.
242. **Krausslich, H. G., M. Facke, A. M. Heuser, J. Konvalinka, and H. Zentgraf.** 1995. The spacer peptide between human immunodeficiency virus capsid and nucleocapsid proteins is essential for ordered assembly and viral infectivity. J Virol **69:**3407-19.
243. **Krishnan, A., E. Dujardin, M. M. J. Treacy, J. Hugdahl, S. Lynum, and T. W. Ebbesen.** 1997. Graphitic cones and the nucleation of curved carbon surfaces. Nature **388:**451-454.
244. **Kuiken, C., B. Foley, E. O. Freed, B. Hahn, P. A. Marx, F. McCutchan, J. Mellors, S. Wolinsky, and B. Korber.** 2002. HIV sequence compendium 2002. Theoretical Biology and Biophysics Group, Los Alamos National Laboratory, Los Alamos, NM, USA.
245. **Kuppuswamy, M., T. Subramanian, A. Srinivasan, and G. Chinnadurai.** 1989. Multiple functional domains of Tat, the trans-activator of HIV-1, defined by mutational analysis. Nucleic Acids Res **17:**3551-61.
246. **Kuritzkes, D. R., and B. D. Walker.** 2006. HIV-1: Pathogenesis, Clinical Manifestations, and Treatment, p. 2187 to 2214, Fields Virology, vol. 2. Lippincott Williams & Wilkins.
247. **Langelier, C., U. K. von Schwedler, R. D. Fisher, I. De Domenico, P. L. White, C. P. Hill, J. Kaplan, D. Ward, and W. I. Sundquist.** 2006. Human ESCRT-II complex and its role in human immunodeficiency virus type 1 release. J Virol **80:**9465-80.

248. **Lanman, J., T. T. Lam, M. R. Emmett, A. G. Marshall, M. Sakalian, and P. E. Prevelige, Jr.** 2004. Key interactions in HIV-1 maturation identified by hydrogen-deuterium exchange. Nat Struct Mol Biol **11:**676-7.
249. **Lapadat-Tapolsky, M., H. De Rocquigny, D. Van Gent, B. Roques, R. Plasterk, and J. L. Darlix.** 1993. Interactions between HIV-1 nucleocapsid protein and viral DNA may have important functions in the viral life cycle. Nucleic Acids Res **21:**831-9.
250. **Lapadat-Tapolsky, M., C. Gabus, M. Rau, and J. L. Darlix.** 1997. Possible roles of HIV-1 nucleocapsid protein in the specificity of proviral DNA synthesis and in its variability. J Mol Biol **268:**250-60.
251. **Lavallee, C., X. J. Yao, A. Ladha, H. Gottlinger, W. A. Haseltine, and E. A. Cohen.** 1994. Requirement of the Pr55gag precursor for incorporation of the Vpr product into human immunodeficiency virus type 1 viral particles. J Virol **68:**1926-34.
252. **Lawrence, D. C., C. C. Stover, J. Noznitsky, Z. Wu, and M. F. Summers.** 2003. Structure of the intact stem and bulge of HIV-1 Psi-RNA stem-loop SL1. J Mol Biol **326:**529-42.
253. **Le Rouzic, E., A. Mousnier, C. Rustum, F. Stutz, E. Hallberg, C. Dargemont, and S. Benichou.** 2002. Docking of HIV-1 Vpr to the nuclear envelope is mediated by the interaction with the nucleoporin hCG1. J Biol Chem **277:**45091-8.
254. **Lecellier, C. H., P. Dunoyer, K. Arar, J. Lehmann-Che, S. Eyquem, C. Himber, A. Saib, and O. Voinnet.** 2005. A cellular microRNA mediates antiviral defense in human cells. Science **308:**557-60.
255. **Lee, Y.-M., C.-J. Tian, and X.-F. Yu.** 1998. A Bipartite Membrane-Binding Signal in the Human Immunodeficiency Virus Type 1†Matrix Protein Is Required for the Proteolytic Processing of Gag Precursors in a Cell Type-Dependent Manner. J. Virol. **72:**9061-9068.
256. **Leis, J., D. Baltimore, J. M. Bishop, J. Coffin, E. Fleissner, S. P. Goff, S. Oroszlan, H. Robinson, A. M. Skalka, H. M. Temin, and et al.** 1988. Standardized and simplified nomenclature for proteins common to all retroviruses. J Virol **62:**1808-9.
257. **Lemmon, M. A.** 2003. Phosphoinositide recognition domains. Traffic **4:**201-13.
258. **Lenburg, M. E., and N. R. Landau.** 1993. Vpu-induced degradation of CD4: requirement for specific amino acid residues in the cytoplasmic domain of CD4. J Virol **67:**7238-45.
259. **Levesque, K., Y. S. Zhao, and E. A. Cohen.** 2003. Vpu exerts a positive effect on HIV-1 infectivity by down-modulating CD4 receptor molecules at the surface of HIV-1-producing cells. J Biol Chem **278:**28346-53.
260. **Levin, J. G., J. Guo, I. Rouzina, and K. Musier-Forsyth.** 2005. Nucleic acid chaperone activity of HIV-1 nucleocapsid protein: critical role in reverse transcription and molecular mechanism. Prog Nucleic Acid Res Mol Biol **80:**217-86.
261. **Levy, J. A., A. D. Hoffman, S. M. Kramer, J. A. Landis, J. M. Shimabukuro, and L. S. Oshiro.** 1984. Isolation of lymphocytopathic retroviruses from San Francisco patients with AIDS. Science **225:**840-2.
262. **Li, F., R. Goila-Gaur, K. Salzwedel, N. R. Kilgore, M. Reddick, C. Matallana, A. Castillo, D. Zoumplis, D. E. Martin, J. M. Orenstein, G. P. Allaway, E. O. Freed, and C. T. Wild.** 2003. PA-457: a potent HIV inhibitor that disrupts core condensation by targeting a late step in Gag processing. Proc Natl Acad Sci U S A **100:**13555-60.
263. **Li, F., D. Zoumplis, C. Matallana, N. R. Kilgore, M. Reddick, A. S. Yunus, C. S. Adamson, K. Salzwedel, D. E. Martin, G. P. Allaway, E. O. Freed, and C. T. Wild.** 2006. Determinants of activity of the HIV-1 maturation inhibitor PA-457. Virology **356:**217-24.
264. **Li, S., C. P. Hill, W. I. Sundquist, and J. T. Finch.** 2000. Image reconstructions of helical assemblies of the HIV-1 CA protein. Nature **407:**409-413.
265. **Li, X., B. Gold, C. O'HUigin, F. Diaz-Griffero, B. Song, Z. Si, Y. Li, W. Yuan, M. Stremlau, C. Mische, H. Javanbakht, M. Scally, C. Winkler, M. Dean, and J. Sodroski.** 2007. Unique features of TRIM5alpha among closely related human TRIM family members. Virology **360:**419-33.
266. **Li, X., Y. Li, M. Stremlau, W. Yuan, B. Song, M. Perron, and J. Sodroski.** 2006. Functional replacement of the RING, B-box 2, and coiled-coil domains of tripartite motif 5alpha (TRIM5alpha) by heterologous TRIM domains. J Virol **80:**6198-206.
267. **Li, X., Y. Quan, E. J. Arts, Z. Li, B. D. Preston, H. de Rocquigny, B. P. Roques, J. L. Darlix, L. Kleiman, M. A. Parniak, and M. A. Wainberg.** 1996. Human immunodeficiency virus Type

1 nucleocapsid protein (NCp7) directs specific initiation of minus-strand DNA synthesis primed by human tRNA(Lys3) in vitro: studies of viral RNA molecules mutated in regions that flank the primer binding site. J Virol **70:**4996-5004.

268. **Liao, W. H., H. C. Chiu, and C. T. Wang.** 2004. Effects of mutations in an HIV-1 gag gene containing a 107-codon tandem repeat in the matrix region on assembly and processing of the protein product. J Med Virol **74:**528-35.
269. **Lichterfeld, M., D. E. Kaufmann, X. G. Yu, S. K. Mui, M. M. Addo, M. N. Johnston, D. Cohen, G. K. Robbins, E. Pae, G. Alter, A. Wurcel, D. Stone, E. S. Rosenberg, B. D. Walker, and M. Altfeld.** 2004. Loss of HIV-1-specific CD8+ T cell proliferation after acute HIV-1 infection and restoration by vaccine-induced HIV-1-specific CD4+ T cells. J Exp Med **200:**701-12.
270. **Lightfoote, M. M., J. E. Coligan, T. M. Folks, A. S. Fauci, M. A. Martin, and S. Venkatesan.** 1986. Structural characterization of reverse transcriptase and endonuclease polypeptides of the acquired immunodeficiency syndrome retrovirus. J Virol **60:**771-5.
271. **Lin, J., and B. R. Cullen.** 2007. Analysis of the interaction of primate retroviruses with the human RNA interference machinery. J Virol **81:**12218-26.
272. **Lindwasser, O. W., and M. D. Resh.** 2004. Human immunodeficiency virus type 1 Gag contains a dileucine-like motif that regulates association with multivesicular bodies. J Virol **78:**6013-23.
273. **Lindwasser, O. W., and M. D. Resh.** 2002. Myristoylation as a target for inhibiting HIV assembly: unsaturated fatty acids block viral budding. Proc Natl Acad Sci U S A **99:**13037-42.
274. **Loeb, D. D., C. A. Hutchison, 3rd, M. H. Edgell, W. G. Farmerie, and R. Swanstrom.** 1989. Mutational analysis of human immunodeficiency virus type 1 protease suggests functional homology with aspartic proteinases. J Virol **63:**111-21.
275. **Lopez-Verges, S., G. Camus, G. Blot, R. Beauvoir, R. Benarous, and C. Berlioz-Torrent.** 2006. Tail-interacting protein TIP47 is a connector between Gag and Env and is required for Env incorporation into HIV-1 virions. PNAS **103:**14947-14952.
276. **Lu, M., S. C. Blacklow, and P. S. Kim.** 1995. A trimeric structural domain of the HIV-1 transmembrane glycoprotein. Nat Struct Biol **2:**1075-82.
277. **Lu, Y. L., P. Spearman, and L. Ratner.** 1993. Human immunodeficiency virus type 1 viral protein R localization in infected cells and virions. J Virol **67:**6542-50.
278. **Luban, J., K. L. Bossolt, E. K. Franke, G. V. Kalpana, and S. P. Goff.** 1993. Human immunodeficiency virus type 1 Gag protein binds to cyclophilins A and B. Cell **73:**1067-78.
279. **Luban, J., and S. P. Goff.** 1991. Binding of human immunodeficiency virus type 1 (HIV-1) RNA to recombinant HIV-1 gag polyprotein. J Virol **65:**3203-12.
280. **Lutzke, R. A., C. Vink, and R. H. Plasterk.** 1994. Characterization of the minimal DNA-binding domain of the HIV integrase protein. Nucleic Acids Res **22:**4125-31.
281. **Luukkonen, B. G., E. M. Fenyo, and S. Schwartz.** 1995. Overexpression of human immunodeficiency virus type 1 protease increases intracellular cleavage of Gag and reduces virus infectivity. Virology **206:**854-65.
282. **Macatonia, S. E., R. Lau, S. Patterson, A. J. Pinching, and S. C. Knight.** 1990. Dendritic cell infection, depletion and dysfunction in HIV-infected individuals. Immunology **71:**38-45.
283. **Madani, N., and D. Kabat.** 2000. Cellular and viral specificities of human immunodeficiency virus type 1 vif protein. J Virol **74:**5982-7.
284. **Malim, M. H.** 2006. Natural resistance to HIV infection: The Vif-APOBEC interaction. C R Biol **329:**871-5.
285. **Malim, M. H., S. Bohnlein, J. Hauber, and B. R. Cullen.** 1989. Functional dissection of the HIV-1 Rev trans-activator--derivation of a trans-dominant repressor of Rev function. Cell **58:**205-14.
286. **Malim, M. H., R. Fenrick, D. W. Ballard, J. Hauber, E. Bohnlein, and B. R. Cullen.** 1989. Functional characterization of a complex protein-DNA-binding domain located within the human immunodeficiency virus type 1 long terminal repeat leader region. J Virol **63:**3213-9.
287. **Malim, M. H., J. Hauber, S. Y. Le, J. V. Maizel, and B. R. Cullen.** 1989. The HIV-1 rev trans-activator acts through a structured target sequence to activate nuclear export of unspliced viral mRNA. Nature **338:**254-7.
288. **Malim, M. H., D. F. McCarn, L. S. Tiley, and B. R. Cullen.** 1991. Mutational definition of the human immunodeficiency virus type 1 Rev activation domain. J Virol **65:**4248-54.

289. **Malim, M. H., L. S. Tiley, D. F. McCarn, J. R. Rusche, J. Hauber, and B. R. Cullen.** 1990. HIV-1 structural gene expression requires binding of the Rev trans-activator to its RNA target sequence. Cell **60:**675-83.
290. **Mammano, F., E. Kondo, J. Sodroski, A. Bukovsky, and H. G. Gottlinger.** 1995. Rescue of human immunodeficiency virus type 1 matrix protein mutants by envelope glycoproteins with short cytoplasmic domains. J Virol **69:**3824-30.
291. **Mammano, F., A. Ohagen, S. Hoglund, and H. G. Gottlinger.** 1994. Role of the major homology region of human immunodeficiency virus type 1 in virion morphogenesis. J Virol **68:**4927-36.
292. **Mariani, R., D. Chen, B. Schrofelbauer, F. Navarro, R. Konig, B. Bollman, C. Munk, H. Nymark-McMahon, and N. R. Landau.** 2003. Species-specific exclusion of APOBEC3G from HIV-1 virions by Vif. Cell **114:**21-31.
293. **Marin, M., K. M. Rose, S. L. Kozak, and D. Kabat.** 2003. HIV-1 Vif protein binds the editing enzyme APOBEC3G and induces its degradation. Nat Med **9:**1398-403.
294. **Mark-Danieli, M., N. Laham, M. Kenan-Eichler, A. Castiel, D. Melamed, M. Landau, N. M. Bouvier, M. J. Evans, and E. Bacharach.** 2005. Single point mutations in the zinc finger motifs of the human immunodeficiency virus type 1 nucleocapsid alter RNA binding specificities of the gag protein and enhance packaging and infectivity. J Virol **79:**7756-67.
295. **Marquet, R., F. Baudin, C. Gabus, J. L. Darlix, M. Mougel, C. Ehresmann, and B. Ehresmann.** 1991. Dimerization of human immunodeficiency virus (type 1) RNA: stimulation by cations and possible mechanism. Nucleic Acids Res **19:**2349-57.
296. **Marshall, J. G., J. W. Booth, V. Stambolic, T. Mak, T. Balla, A. D. Schreiber, T. Meyer, and S. Grinstein.** 2001. Restricted accumulation of phosphatidylinositol 3-kinase products in a plasmalemmal subdomain during Fc gamma receptor-mediated phagocytosis. J Cell Biol **153:**1369-80.
297. **Martin-Serrano, J., and P. D. Bieniasz.** 2003. A bipartite late-budding domain in human immunodeficiency virus type 1. J Virol **77:**12373-7.
298. **Massiah, M. A., M. R. Starich, C. Paschall, M. F. Summers, A. M. Christensen, and W. I. Sundquist.** 1994. Three-dimensional structure of the human immunodeficiency virus type 1 matrix protein. J Mol Biol **244:**198-223.
299. **Massiah, M. A., D. Worthylake, A. M. Christensen, W. I. Sundquist, C. P. Hill, and M. F. Summers.** 1996. Comparison of the NMR and X-ray structures of the HIV-1 matrix protein: evidence for conformational changes during viral assembly. Protein Sci **5:**2391-8.
300. **Mayo, K., D. Huseby, J. McDermott, B. Arvidson, L. Finlay, and E. Barklis.** 2003. Retrovirus capsid protein assembly arrangements. J Mol Biol **325:**225-37.
301. **Mayo, K., J. McDermott, and E. Barklis.** 2002. Hexagonal organization of Moloney murine leukemia virus capsid proteins. Virology **298:**30-8.
302. **Mayo, K., M. L. Vana, J. McDermott, D. Huseby, J. Leis, and E. Barklis.** 2002. Analysis of Rous sarcoma virus capsid protein variants assembled on lipid monolayers. J Mol Biol **316:**667-78.
303. **McDermott, J., L. Farrell, R. Ross, and E. Barklis.** 1996. Structural analysis of human immunodeficiency virus type 1 Gag protein interactions, using cysteine-specific reagents. J Virol **70:**5106-14.
304. **McDermott, J., S. Karanjia, Z. Love, and E. Barklis.** 2000. Crosslink analysis of N-terminal, C-terminal, and N/B determining regions of the Moloney murine leukemia virus capsid protein. Virology **269:**190-200.
305. **McDermott, J., K. Mayo, and E. Barklis.** 2000. Three-dimensional organization of retroviral capsid proteins on a lipid monolayer. J Mol Biol **302:**121-33.
306. **Meric, C., and P. F. Spahr.** 1986. Rous sarcoma virus nucleic acid-binding protein p12 is necessary for viral 70S RNA dimer formation and packaging. J Virol **60:**450-9.
307. **Mervis, R. J., N. Ahmad, E. P. Lillehoj, M. G. Raum, F. H. Salazar, H. W. Chan, and S. Venkatesan.** 1988. The gag gene products of human immunodeficiency virus type 1: alignment within the gag open reading frame, identification of posttranslational modifications, and evidence for alternative gag precursors. J Virol **62:**3993-4002.
308. **Miller, M., M. Jaskolski, J. K. Rao, J. Leis, and A. Wlodawer.** 1989. Crystal structure of a retroviral protease proves relationship to aspartic protease family. Nature **337:**576-9.

309. **Mische, C. C., H. Javanbakht, B. Song, F. Diaz-Griffero, M. Stremlau, B. Strack, Z. Si, and J. Sodroski.** 2005. Retroviral restriction factor TRIM5alpha is a trimer. J Virol **79:**14446-50.
310. **Mizutani, S., D. Boettiger, and H. M. Temin.** 1970. A DNA-depenent DNA polymerase and a DNA endonuclease in virions of Rous sarcoma virus. Nature **228:**424-7.
311. **Mizutani, S., and H. M. Temin.** 1971. Enzymes and nucleotides in virions of Rous sarcoma virus. J Virol **8:**409-16.
312. **Moelling, K., D. P. Bolognesi, and H. Bauer.** 1971. Polypeptides of avian RNA tumor viruses. 3. Purification and identification of a DNA synthesizing enzyme. Virology **45:**298-302.
313. **Moir, S., A. Malaspina, Y. Li, T. W. Chun, T. Lowe, J. Adelsberger, M. Baseler, L. A. Ehler, S. Liu, R. T. Davey, Jr., J. A. Mican, and A. S. Fauci.** 2000. B cells of HIV-1-infected patients bind virions through CD21-complement interactions and transmit infectious virus to activated T cells. J Exp Med **192:**637-46.
314. **Momany, C., L. C. Kovari, A. J. Prongay, W. Keller, R. K. Gitti, B. M. Lee, A. E. Gorbalenya, L. Tong, J. McClure, L. S. Ehrlich, M. F. Summers, C. Carter, and M. G. Rossmann.** 1996. Crystal structure of dimeric HIV-1 capsid protein. Nat Struct Biol **3:**763-70.
315. **Montagnier, L., J. C. Chermann, F. Barre-Sinoussi, D. Klatzmann, S. Wain-Hobson, M. Alizon, F. Clavel, F. Brun-Vezinet, E. Vilmer, C. Rouzioux, and et al.** 1984. Lymphadenopathy associated virus and its etiological role in AIDS. Princess Takamatsu Symp **15:**319-31.
316. **Morita, C., K. Ikuta, T. Goto, K. Sano, M. Nakai, K. Hirai, and S. Kato.** 1990. Isolation and characterization of cell clones persistently producing teardrop-shaped particles of human immunodeficiency virus type 1. J Acquir Immune Defic Syndr **3:**231-7.
317. **Muller, B., J. Daecke, O. T. Fackler, M. T. Dittmar, H. Zentgraf, and H. G. Krausslich.** 2004. Construction and characterization of a fluorescently labeled infectious human immunodeficiency virus type 1 derivative. J Virol **78:**10803-13.
318. **Munk, C., S. M. Brandt, G. Lucero, and N. R. Landau.** 2002. A dominant block to HIV-1 replication at reverse transcription in simian cells. Proc Natl Acad Sci U S A **99:**13843-8.
319. **Murakami, T., and E. O. Freed.** 2000. Genetic evidence for an interaction between human immunodeficiency virus type 1 matrix and alpha-helix 2 of the gp41 cytoplasmic tail. J Virol **74:**3548-54.
320. **Murray, P. S., Z. Li, J. Wang, C. L. Tang, B. Honig, and D. Murray.** 2005. Retroviral matrix domains share electrostatic homology: models for membrane binding function throughout the viral life cycle. Structure **13:**1521-31.
321. **Muthumani, K., S. Kudchodkar, E. Papasavvas, L. J. Montaner, D. B. Weiner, and V. Ayyavoo.** 2000. HIV-1 Vpr regulates expression of beta chemokines in human primary lymphocytes and macrophages. J Leukoc Biol **68:**366-72.
322. **Muthumani, K., L. J. Montaner, V. Ayyavoo, and D. B. Weiner.** 2000. Vpr-GFP virion particle identifies HIV-infected targets and preserves HIV-1Vpr function in macrophages and T-cells. DNA Cell Biol **19:**179-88.
323. **Navarro, F., and N. R. Landau.** 2004. Recent insights into HIV-1 Vif. Curr Opin Immunol **16:**477-82.
324. **Navarro, J. M., L. Damier, J. Boretto, S. Priet, B. Canard, G. Querat, and J. Sire.** 2001. Glutamic residue 438 within the protease-sensitive subdomain of HIV-1 reverse transcriptase is critical for heterodimer processing in viral particles. Virology **290:**300-8.
325. **Navia, M. A., P. M. Fitzgerald, B. M. McKeever, C. T. Leu, J. C. Heimbach, W. K. Herber, I. S. Sigal, P. L. Darke, and J. P. Springer.** 1989. Three-dimensional structure of aspartyl protease from human immunodeficiency virus HIV-1. Nature **337:**615-20.
326. **Navia, M. A., and B. M. McKeever.** 1990. A role for the aspartyl protease from the human immunodeficiency virus type 1 (HIV-1) in the orchestration of virus assembly. Ann N Y Acad Sci **616:**73-85.
327. **Neil, S. J., S. W. Eastman, N. Jouvenet, and P. D. Bieniasz.** 2006. HIV-1 Vpu promotes release and prevents endocytosis of nascent retrovirus particles from the plasma membrane. PLoS Pathog **2:**e39.
328. **Nekhai, S., and K. T. Jeang.** 2006. Transcriptional and post-transcriptional regulation of HIV-1 gene expression: role of cellular factors for Tat and Rev. Future Microbiol **1:**417-26.

329. **Nermut, M. V., C. Grief, S. Hashmi, and D. J. Hockley.** 1993. Further evidence of icosahedral symmetry in human and simian immunodeficiency virus. AIDS Res Hum Retroviruses **9:**929-38.
330. **Nermut, M. V., D. J. Hockley, P. Bron, D. Thomas, W. H. Zhang, and I. M. Jones.** 1998. Further evidence for hexagonal organization of HIV gag protein in prebudding assemblies and immature virus-like particles. J Struct Biol **123:**143-9.
331. **Nermut, M. V., D. J. Hockley, J. B. Jowett, I. M. Jones, M. Garreau, and D. Thomas.** 1994. Fullerene-like organization of HIV gag-protein shell in virus-like particles produced by recombinant baculovirus. Virology **198:**288-96.
332. **Newman, J. L., E. W. Butcher, D. T. Patel, Y. Mikhaylenko, and M. F. Summers.** 2004. Flexibility in the P2 domain of the HIV-1 Gag polyprotein. Protein Sci **13:**2101-7.
333. **Nguyen, D. H., and J. E. Hildreth.** 2000. Evidence for budding of human immunodeficiency virus type 1 selectively from glycolipid-enriched membrane lipid rafts. J Virol **74:**3264-72.
334. **Niedrig, M., H. R. Gelderblom, G. Pauli, J. Marz, H. Bickhard, H. Wolf, and S. Modrow.** 1994. Inhibition of infectious human immunodeficiency virus type 1 particle formation by Gag protein-derived peptides. J Gen Virol **75 (Pt 6):**1469-74.
335. **Norris, P. J., B. L. Pappalardo, B. Custer, G. Spotts, F. M. Hecht, and M. P. Busch.** 2006. Elevations in IL-10, TNF-alpha, and IFN-gamma from the earliest point of HIV Type 1 infection. AIDS Res Hum Retroviruses **22:**757-62.
336. **Nydegger, S., M. Foti, A. Derdowski, P. Spearman, and M. Thali.** 2003. HIV-1 egress is gated through late endosomal membranes. Traffic **4:**902-10.
337. **O'Brien, W. A., Y. Koyanagi, A. Namazie, J.-Q. Zhao, A. Diagne, K. ldler, J. A. Zack, and I. S. Y. Chen.** 1990. HIV-1 tropism for mononuclear phagocytes can be determined by regions of gp120 outside the CD4-binding domain. Nature **348:**69-73.
338. **Oancea, E., and T. Meyer.** 1998. Protein kinase C as a molecular machine for decoding calcium and diacylglycerol signals. Cell **95:**307-18.
339. **Oancea, E., M. N. Teruel, A. F. Quest, and T. Meyer.** 1998. Green fluorescent protein (GFP)-tagged cysteine-rich domains from protein kinase C as fluorescent indicators for diacylglycerol signaling in living cells. J Cell Biol **140:**485-98.
340. **Omer, C. A., R. Resnick, and A. J. Faras.** 1984. Evidence for involvement of an RNA primer in initiation of strong-stop plus DNA synthesis during reverse transcription in vitro. J Virol **50:**465-70.
341. **Omoto, S., M. Ito, Y. Tsutsumi, Y. Ichikawa, H. Okuyama, E. A. Brisibe, N. K. Saksena, and Y. R. Fujii.** 2004. HIV-1 nef suppression by virally encoded microRNA. Retrovirology **1:**44.
342. **Ono, A., S. D. Ablan, S. J. Lockett, K. Nagashima, and E. O. Freed.** 2004. Phosphatidylinositol (4,5) bisphosphate regulates HIV-1 Gag targeting to the plasma membrane. Proc Natl Acad Sci U S A **101:**14889-94.
343. **Ono, A., D. Demirov, and E. O. Freed.** 2000. Relationship between human immunodeficiency virus type 1 Gag multimerization and membrane binding. J Virol **74:**5142-50.
344. **Ono, A., and E. O. Freed.** 1999. Binding of human immunodeficiency virus type 1 Gag to membrane: role of the matrix amino terminus. J Virol **73:**4136-44.
345. **Ono, A., and E. O. Freed.** 2004. Cell-type-dependent targeting of human immunodeficiency virus type 1 assembly to the plasma membrane and the multivesicular body. J Virol **78:**1552-63.
346. **Ono, A., and E. O. Freed.** 2001. Plasma membrane rafts play a critical role in HIV-1 assembly and release. Proc Natl Acad Sci U S A **98:**13925-30.
347. **Ono, A., M. Huang, and E. O. Freed.** 1997. Characterization of human immunodeficiency virus type 1 matrix revertants: effects on virus assembly, Gag processing, and Env incorporation into virions. J Virol **71:**4409-18.
348. **Ono, A., J. M. Orenstein, and E. O. Freed.** 2000. Role of the Gag matrix domain in targeting human immunodeficiency virus type 1 assembly. J Virol **74:**2855-66.
349. **Owens, C. M., B. Song, M. J. Perron, P. C. Yang, M. Stremlau, and J. Sodroski.** 2004. Binding and susceptibility to postentry restriction factors in monkey cells are specified by distinct regions of the human immunodeficiency virus type 1 capsid. J Virol **78:**5423-37.
350. **Owens, C. M., P. C. Yang, H. Gottlinger, and J. Sodroski.** 2003. Human and simian immunodeficiency virus capsid proteins are major viral determinants of early, postentry replication blocks in simian cells. J Virol **77:**726-31.

351. **Page, K. A., N. R. Landau, and D. R. Littman.** 1990. Construction and use of a human immunodeficiency virus vector for analysis of virus infectivity. J Virol **64:**5270-6.
352. **Paillart, J. C., and H. G. Gottlinger.** 1999. Opposing effects of human immunodeficiency virus type 1 matrix mutations support a myristyl switch model of gag membrane targeting. J Virol **73:**2604-12.
353. **Pal, R., S. Mumbauer, G. M. Hoke, A. Takatsuki, and M. G. Sarngadharan.** 1991. Brefeldin A inhibits the processing and secretion of envelope glycoproteins of human immunodeficiency virus type 1. AIDS Res Hum Retroviruses **7:**707-12.
354. **Pal, R., M. S. Reitz, Jr., E. Tschachler, R. C. Gallo, M. G. Sarngadharan, and F. D. Veronese.** 1990. Myristoylation of gag proteins of HIV-1 plays an important role in virus assembly. AIDS Res Hum Retroviruses **6:**721-30.
355. **Panganiban, A. T., and H. M. Temin.** 1984. The retrovirus pol gene encodes a product required for DNA integration: identification of a retrovirus int locus. Proc Natl Acad Sci U S A **81:**7885-9.
356. **Panganiban, A. T., and H. M. Temin.** 1983. The terminal nucleotides of retrovirus DNA are required for integration but not virus production. Nature **306:**155-60.
357. **Park, J., and C. D. Morrow.** 1991. Overexpression of the gag-pol precursor from human immunodeficiency virus type 1 proviral genomes results in efficient proteolytic processing in the absence of virion production. J Virol **65:**5111-7.
358. **Partin, K., H. G. Krausslich, L. Ehrlich, E. Wimmer, and C. Carter.** 1990. Mutational analysis of a native substrate of the human immunodeficiency virus type 1 proteinase. J Virol **64:**3938-47.
359. **Paul, M., S. Mazumder, N. Raja, and M. A. Jabbar.** 1998. Mutational analysis of the human immunodeficiency virus type 1 Vpu transmembrane domain that promotes the enhanced release of virus-like particles from the plasma membrane of mammalian cells. J Virol **72:**1270-9.
360. **Paxton, W., R. I. Connor, and N. R. Landau.** 1993. Incorporation of Vpr into human immunodeficiency virus type 1 virions: requirement for the p6 region of gag and mutational analysis. J Virol **67:**7229-37.
361. **Pearl, L. H., and W. R. Taylor.** 1987. A structural model for the retroviral proteases. Nature **329:**351-4.
362. **Peliska, J. A., S. Balasubramanian, D. P. Giedroc, and S. J. Benkovic.** 1994. Recombinant HIV-1 nucleocapsid protein accelerates HIV-1 reverse transcriptase catalyzed DNA strand transfer reactions and modulates RNase H activity. Biochemistry **33:**13817-23.
363. **Peliska, J. A., and S. J. Benkovic.** 1992. Mechanism of DNA strand transfer reactions catalyzed by HIV-1 reverse transcriptase. Science **258:**1112-8.
364. **Peng, C., B. K. Ho, T. W. Chang, and N. T. Chang.** 1989. Role of human immunodeficiency virus type 1-specific protease in core protein maturation and viral infectivity. J Virol **63:**2550-6.
365. **Pepin, J., G. Morgan, D. Dunn, S. Gevao, M. Mendy, I. Gaye, N. Scollen, R. Tedder, and H. Whittle.** 1991. HIV-2-induced immunosuppression among asymptomatic West African prostitutes: evidence that HIV-2 is pathogenic, but less so than HIV-1. Aids **5:**1165-72.
366. **Pereira, L. A., K. Bentley, A. Peeters, M. J. Churchill, and N. J. Deacon.** 2000. A compilation of cellular transcription factor interactions with the HIV-1 LTR promoter. Nucleic Acids Res **28:**663-8.
367. **Perez-Caballero, D., T. Hatziioannou, J. Martin-Serrano, and P. D. Bieniasz.** 2004. Human immunodeficiency virus type 1 matrix inhibits and confers cooperativity on gag precursor-membrane interactions. J Virol **78:**9560-3.
368. **Perez-Caballero, D., T. Hatziioannou, A. Yang, S. Cowan, and P. D. Bieniasz.** 2005. Human tripartite motif 5alpha domains responsible for retrovirus restriction activity and specificity. J Virol **79:**8969-78.
369. **Perez-Caballero, D., T. Hatziioannou, F. Zhang, S. Cowan, and P. D. Bieniasz.** 2005. Restriction of human immunodeficiency virus type 1 by TRIM-CypA occurs with rapid kinetics and independently of cytoplasmic bodies, ubiquitin, and proteasome activity. J Virol **79:**15567-72.
370. **Perlman, M., and M. D. Resh.** 2006. Identification of an intracellular trafficking and assembly pathway for HIV-1 gag. Traffic **7:**731-45.
371. **Perron, M. J., M. Stremlau, B. Song, W. Ulm, R. C. Mulligan, and J. Sodroski.** 2004. TRIM5alpha mediates the postentry block to N-tropic murine leukemia viruses in human cells. Proc Natl Acad Sci U S A **101:**11827-32.

372. **Pettit, S. C., J. C. Clemente, J. A. Jeung, B. M. Dunn, and A. H. Kaplan.** 2005. Ordered processing of the human immunodeficiency virus type 1 GagPol precursor is influenced by the context of the embedded viral protease. J Virol **79:**10601-7.
373. **Pettit, S. C., L. E. Everitt, S. Choudhury, B. M. Dunn, and A. H. Kaplan.** 2004. Initial cleavage of the human immunodeficiency virus type 1 GagPol precursor by its activated protease occurs by an intramolecular mechanism. J Virol **78:**8477-85.
374. **Pettit, S. C., M. D. Moody, R. S. Wehbie, A. H. Kaplan, P. V. Nantermet, C. A. Klein, and R. Swanstrom.** 1994. The p2 domain of human immunodeficiency virus type 1 Gag regulates sequential proteolytic processing and is required to produce fully infectious virions. J Virol **68:**8017-27.
375. **Pfeffer, S., A. Sewer, M. Lagos-Quintana, R. Sheridan, C. Sander, F. A. Grasser, L. F. van Dyk, C. K. Ho, S. Shuman, M. Chien, J. J. Russo, J. Ju, G. Randall, B. D. Lindenbach, C. M. Rice, V. Simon, D. D. Ho, M. Zavolan, and T. Tuschl.** 2005. Identification of microRNAs of the herpesvirus family. Nat Methods **2:**269-76.
376. **Picker, L. J.** 2006. Immunopathogenesis of acute AIDS virus infection. Curr Opin Immunol **18:**399-405.
377. **Picker, L. J., and D. I. Watkins.** 2005. HIV pathogenesis: the first cut is the deepest. Nat Immunol **6:**430-2.
378. **Poljak, L., S. M. Batson, D. Ficheux, B. P. Roques, J. L. Darlix, and E. Kas.** 2003. Analysis of NCp7-dependent activation of HIV-1 cDNA integration and its conservation among retroviral nucleocapsid proteins. J Mol Biol **329:**411-21.
379. **Popov, S., M. Rexach, L. Ratner, G. Blobel, and M. Bukrinsky.** 1998. Viral protein R regulates docking of the HIV-1 preintegration complex to the nuclear pore complex. J Biol Chem **273:**13347-52.
380. **Powell, D. M., M. J. Zhang, D. A. Konings, P. T. Wingfield, S. J. Stahl, E. T. Dayton, and A. I. Dayton.** 1995. Sequence specificity in the higher-order interaction of the Rev protein of HIV-1 with its target sequence, the RRE. J Acquir Immune Defic Syndr Hum Retrovirol **10:**317-23.
381. **Prasad, V. R., and S. P. Goff.** 1990. Structure-function studies of HIV reverse transcriptase. Ann N Y Acad Sci **616:**11-21.
382. **Provitera, P., A. Goff, A. Harenberg, F. Bouamr, C. Carter, and S. Scarlata.** 2001. Role of the major homology region in assembly of HIV-1 Gag. Biochemistry **40:**5565-72.
383. **Reed, M., R. Mariani, L. Sheppard, K. Pekrun, N. R. Landau, and N. W. Soong.** 2002. Chimeric human immunodeficiency virus type 1 containing murine leukemia virus matrix assembles in murine cells. J Virol **76:**436-43.
384. **Reeves, J. D., and A. J. Piefer.** 2005. Emerging drug targets for antiretroviral therapy. Drugs **65:**1747-66.
385. **Reicin, A. S., S. Paik, R. D. Berkowitz, J. Luban, I. Lowy, and S. P. Goff.** 1995. Linker insertion mutations in the human immunodeficiency virus type 1 gag gene: effects on virion particle assembly, release, and infectivity. J Virol **69:**642-50.
386. **Reil, H., A. A. Bukovsky, H. R. Gelderblom, and H. G. Gottlinger.** 1998. Efficient HIV-1 replication can occur in the absence of the viral matrix protein. Embo J **17:**2699-708.
387. **Resh, M. D.** 2005. Intracellular trafficking of HIV-1 Gag: how Gag interacts with cell membranes and makes viral particles. AIDS Rev **7:**84-91.
388. **Resnick, R., C. A. Omer, and A. J. Faras.** 1984. Involvement of retrovirus reverse transcriptase-associated RNase H in the initiation of strong-stop (+) DNA synthesis and the generation of the long terminal repeat. J Virol **51:**813-21.
389. **Rey, M. A., B. Spire, D. Dormont, F. Barre-Sinoussi, L. Montagnier, and J. C. Chermann.** 1984. Characterization of the RNA dependent DNA polymerase of a new human T-lymphotropic retrovirus (lymphadenopathy associated virus). Biochem Biophys Res Commun **121:**126-33.
390. **Richman, D. D., S. J. Little, D. M. Smith, T. Wrin, C. Petropoulos, and J. K. Wong.** 2004. HIV Evolution and Escape. Trans Am Clin Climatol Assoc **115:**289-303.
391. **Richman, D. D., T. Wrin, S. J. Little, and C. J. Petropoulos.** 2003. Rapid evolution of the neutralizing antibody response to HIV type 1 infection. Proc Natl Acad Sci U S A **100:**4144-9.
392. **Robertson, D. L., J. P. Anderson, J. A. Bradac, J. K. Carr, B. Foley, R. K. Funkhouser, F. Gao, B. H. Hahn, M. L. Kalish, C. Kuiken, G. H. Learn, T. Leitner, F. McCutchan, S.**

Osmanov, M. Peeters, D. Pieniazek, M. Salminen, P. M. Sharp, S. Wolinsky, and B. Korber. 2000. HIV-1 nomenclature proposal. Science **288:**55-6.

393. **Rodgers, D. W., S. J. Gamblin, B. A. Harris, S. Ray, J. S. Culp, B. Hellmig, D. J. Woolf, C. Debouck, and S. C. Harrison.** 1995. The structure of unliganded reverse transcriptase from the human immunodeficiency virus type 1. Proc Natl Acad Sci U S A **92:**1222-6.
394. **Rose, K. M., M. Marin, S. L. Kozak, and D. Kabat.** 2004. The viral infectivity factor (Vif) of HIV-1 unveiled. Trends Mol Med **10:**291-7.
395. **Rosen, C. A., J. G. Sodroski, W. C. Goh, A. I. Dayton, J. Lippke, and W. A. Haseltine.** 1986. Post-transcriptional regulation accounts for the trans-activation of the human T-lymphotropic virus type III. Nature **319:**555-9.
396. **Rouzioux, C., D. Costagliola, M. Burgard, S. Blanche, M. J. Mayaux, C. Griscelli, and A. J. Valleron.** 1995. Estimated timing of mother-to-child human immunodeficiency virus type 1 (HIV-1) transmission by use of a Markov model. The HIV Infection in Newborns French Collaborative Study Group. Am J Epidemiol **142:**1330-7.
397. **Rouzioux, C., D. Costagliola, M. Burgard, S. Blanche, M. J. Mayaux, C. Griscelli, and A. J. Valleron.** 1993. Timing of mother-to-child HIV-1 transmission depends on maternal status. The HIV Infection in Newborns French Collaborative Study Group. Aids **7 Suppl 2:**S49-52.
398. **Royer, M., M. Cerutti, B. Gay, S. S. Hong, G. Devauchelle, and P. Boulanger.** 1991. Functional domains of HIV-1 gag-polyprotein expressed in baculovirus-infected cells. Virology **184:**417-22.
399. **Royer, M., S. S. Hong, B. Gay, M. Cerutti, and P. Boulanger.** 1992. Expression and extracellular release of human immunodeficiency virus type 1 Gag precursors by recombinant baculovirus-infected cells. J Virol **66:**3230-5.
400. **Saad, J. S., E. Loeliger, P. Luncsford, M. Liriano, J. Tai, A. Kim, J. Miller, A. Joshi, E. O. Freed, and M. F. Summers.** 2006. Point Mutations in the HIV-1 Matrix Protein Turn Off the Myristyl Switch. J Mol Biol.
401. **Saad, J. S., J. Miller, J. Tai, A. Kim, R. H. Ghanam, and M. F. Summers.** 2006. Structural basis for targeting HIV-1 Gag proteins to the plasma membrane for virus assembly. Proc Natl Acad Sci U S A **103:**11364-9.
402. **Safai, B., M. G. Sarngadharan, J. E. Groopman, K. Arnett, M. Popovic, A. Sliski, J. Schupbach, and R. C. Gallo.** 1984. Seroepidemiological studies of human T-lymphotropic retrovirus type III in acquired immunodeficiency syndrome. Lancet **1:**1438-40.
403. **Sakalian, M., C. P. McMurtrey, F. J. Deeg, C. W. Maloy, F. Li, C. T. Wild, and K. Salzwedel.** 2006. 3-O-(3',3'-dimethysuccinyl) betulinic acid inhibits maturation of the human immunodeficiency virus type 1 Gag precursor assembled in vitro. J Virol **80:**5716-22.
404. **Saksena, N. K., Y. C. Ge, B. Wang, S. H. Xiang, D. E. Dwyer, C. Randle, P. Palasanthiran, J. Ziegler, and A. L. Cunningham.** 1996. An HIV-1 infected long-term non-progressor (LTNP): molecular analysis of HIV-1 strains in the vpr and nef genes. Ann Acad Med Singapore **25:**848-54.
405. **Sakuma, R., A. A. Mael, and Y. Ikeda.** 2007. Alpha Interferon Enhances TRIM5{alpha}-Mediated Antiviral Activities in Human and Rhesus Monkey Cells. J Virol **81:**10201-6.
406. **Sakuma, R., J. A. Noser, S. Ohmine, and Y. Ikeda.** 2007. Rhesus monkey TRIM5alpha restricts HIV-1 production through rapid degradation of viral Gag polyproteins. Nat Med **13:**631-5.
407. **Sayah, D. M., E. Sokolskaja, L. Berthoux, and J. Luban.** 2004. Cyclophilin A retrotransposition into TRIM5 explains owl monkey resistance to HIV-1. Nature **430:**569-73.
408. **Schagger, H., and G. Von Jagow.** 1987. Tricine-dodecyl sulfate-polyacrylamide gel electrophoresis for the separation of proteins in the range from 1 to 100 kDa. Anal Biochem **166:**368-379.
409. **Schatz, O., J. Mous, and S. F. Le Grice.** 1990. HIV-1 RT-associated ribonuclease H displays both endonuclease and 3'----5' exonuclease activity. Embo J **9:**1171-6.
410. **Scholz, I., B. Arvidson, D. Huseby, and E. Barklis.** 2005. Virus particle core defects caused by mutations in the human immunodeficiency virus capsid N-terminal domain. J Virol **79:**1470-9.
411. **Schrofelbauer, B., D. Chen, and N. R. Landau.** 2004. A single amino acid of APOBEC3G controls its species-specific interaction with virion infectivity factor (Vif). Proc Natl Acad Sci U S A **101:**3927-32.

412. **Schrofelbauer, B., Q. Yu, and N. R. Landau.** 2004. New insights into the role of Vif in HIV-1 replication. AIDS Rev **6:**34-9.
413. **Schubert, U., S. Bour, A. V. Ferrer-Montiel, M. Montal, F. Maldarell, and K. Strebel.** 1996. The two biological activities of human immunodeficiency virus type 1 Vpu protein involve two separable structural domains. J Virol **70:**809-19.
414. **Sebastian, S., and J. Luban.** 2005. TRIM5alpha selectively binds a restriction-sensitive retroviral capsid. Retrovirology **2:**40.
415. **Sherman, M. P., C. M. de Noronha, L. A. Eckstein, J. Hataye, P. Mundt, S. A. Williams, J. A. Neidleman, M. A. Goldsmith, and W. C. Greene.** 2003. Nuclear export of Vpr is required for efficient replication of human immunodeficiency virus type 1 in tissue macrophages. J Virol **77:**7582-9.
416. **Sherman, M. P., C. M. de Noronha, M. I. Heusch, S. Greene, and W. C. Greene.** 2001. Nucleocytoplasmic shuttling by human immunodeficiency virus type 1 Vpr. J Virol **75:**1522-32.
417. **Shi, J., and C. Aiken.** 2006. Saturation of TRIM5 alpha-mediated restriction of HIV-1 infection depends on the stability of the incoming viral capsid. Virology **350:**493-500.
418. **Shioda, T., and H. Shibuta.** 1990. Production of human immunodeficiency virus (HIV)-like particles from cells infected with recombinant vaccinia viruses carrying the gag gene of HIV. Virology **175:**139-48.
419. **Sluis-Cremer, N., D. Arion, M. E. Abram, and M. A. Parniak.** 2004. Proteolytic processing of an HIV-1 pol polyprotein precursor: insights into the mechanism of reverse transcriptase p66/p51 heterodimer formation. Int J Biochem Cell Biol **36:**1836-47.
420. **Smith, P. F., A. Ogundele, A. Forrest, J. Wilton, K. Salzwedel, J. Doto, G. P. Allaway, and D. E. Martin.** 2007. Phase I and II Study of the Safety, Virologic Effect, and Pharmacokinetics/Pharmacodynamics of Single-Dose 3-O-(3',3'-Dimethylsuccinyl)Betulinic Acid (Bevirimat) against Human Immunodeficiency Virus Infection. Antimicrob Agents Chemother **51:**3574-81.
421. **Sodroski, J., W. C. Goh, C. Rosen, A. Dayton, E. Terwilliger, and W. Haseltine.** 1986. A second post-transcriptional trans-activator gene required for HTLV-III replication. Nature **321:**412-7.
422. **Sokolskaja, E., and J. Luban.** 2006. Cyclophilin, TRIM5, and innate immunity to HIV-1. Current Opinion in Microbiology **9:**404-408.
423. **Sokolskaja, E., D. M. Sayah, and J. Luban.** 2004. Target cell cyclophilin A modulates human immunodeficiency virus type 1 infectivity. J Virol **78:**12800-8.
424. **Sol-Foulon, N., M. Sourisseau, F. Porrot, M. I. Thoulouze, C. Trouillet, C. Nobile, F. Blanchet, V. di Bartolo, N. Noraz, N. Taylor, A. Alcover, C. Hivroz, and O. Schwartz.** 2007. ZAP-70 kinase regulates HIV cell-to-cell spread and virological synapse formation. Embo J **26:**516-26.
425. **Somasundaran, M., M. Sharkey, B. Brichacek, K. Luzuriaga, M. Emerman, J. L. Sullivan, and M. Stevenson.** 2002. Evidence for a cytopathogenicity determinant in HIV-1 Vpr. Proc Natl Acad Sci U S A **99:**9503-8.
426. **Song, B., H. Javanbakht, M. Perron, D. H. Park, M. Stremlau, and J. Sodroski.** 2005. Retrovirus restriction by TRIM5alpha variants from Old World and New World primates. J Virol **79:**3930-7.
427. **Sova, P., and D. J. Volsky.** 1993. Efficiency of viral DNA synthesis during infection of permissive and nonpermissive cells with vif-negative human immunodeficiency virus type 1. J Virol **67:**6322-6.
428. **Spearman, P., R. Horton, L. Ratner, and I. Kuli-Zade.** 1997. Membrane binding of human immunodeficiency virus type 1 matrix protein in vivo supports a conformational myristyl switch mechanism. J Virol **71:**6582-92.
429. **St Louis, M. E., M. Kamenga, C. Brown, A. M. Nelson, T. Manzila, V. Batter, F. Behets, U. Kabagabo, R. W. Ryder, M. Oxtoby, and et al.** 1993. Risk for perinatal HIV-1 transmission according to maternal immunologic, virologic, and placental factors. Jama **269:**2853-9.
430. **Stauffer, T. P., S. Ahn, and T. Meyer.** 1998. Receptor-induced transient reduction in plasma membrane PtdIns(4,5)P2 concentration monitored in living cells. Curr Biol **8:**343-6.

431. **Stein, B. S., and E. G. Engleman.** 1990. Intracellular processing of the gp160 HIV-1 envelope precursor. Endoproteolytic cleavage occurs in a cis or medial compartment of the Golgi complex. J Biol Chem **265:**2640-9.
432. **Stewart, S. A., B. Poon, J. B. Jowett, and I. S. Chen.** 1997. Human immunodeficiency virus type 1 Vpr induces apoptosis following cell cycle arrest. J Virol **71:**5579-92.
433. **Stewart, S. A., B. Poon, J. B. Jowett, Y. Xie, and I. S. Chen.** 1999. Lentiviral delivery of HIV-1 Vpr protein induces apoptosis in transformed cells. Proc Natl Acad Sci U S A **96:**12039-43.
434. **Sticht, J., M. Humbert, S. Findlow, J. Bodem, B. Muller, U. Dietrich, J. Werner, and H. G. Krausslich.** 2005. A peptide inhibitor of HIV-1 assembly in vitro. Nat Struct Mol Biol **12:**671-7.
435. **Strack, B., A. Calistri, S. Craig, E. Popova, and H. G. Gottlinger.** 2003. AIP1/ALIX is a binding partner for HIV-1 p6 and EIAV p9 functioning in virus budding. Cell **114:**689-99.
436. **Stremlau, M., C. M. Owens, M. J. Perron, M. Kiessling, P. Autissier, and J. Sodroski.** 2004. The cytoplasmic body component TRIM5alpha restricts HIV-1 infection in Old World monkeys. Nature **427:**848-53.
437. **Stremlau, M., M. Perron, M. Lee, Y. Li, B. Song, H. Javanbakht, F. Diaz-Griffero, D. J. Anderson, W. I. Sundquist, and J. Sodroski.** 2006. Specific recognition and accelerated uncoating of retroviral capsids by the TRIM5alpha restriction factor. Proc Natl Acad Sci U S A **103:**5514-9.
438. **Stremlau, M., M. Perron, S. Welikala, and J. Sodroski.** 2005. Species-specific variation in the B30.2(SPRY) domain of TRIM5alpha determines the potency of human immunodeficiency virus restriction. J Virol **79:**3139-45.
439. **Stuchell, M. D., J. E. Garrus, B. Muller, K. M. Stray, S. Ghaffarian, R. McKinnon, H. G. Krausslich, S. G. Morham, and W. I. Sundquist.** 2004. The human endosomal sorting complex required for transport (ESCRT-I) and its role in HIV-1 budding. J Biol Chem **279:**36059-71.
440. **Tachedjian, G., H. E. Aronson, M. de los Santos, J. Seehra, J. M. McCoy, and S. P. Goff.** 2003. Role of residues in the tryptophan repeat motif for HIV-1 reverse transcriptase dimerization. J Mol Biol **326:**381-96.
441. **Tan, W., M. Schalling, C. Zhao, M. Luukkonen, M. Nilsson, E. M. Fenyo, G. N. Pavlakis, and S. Schwartz.** 1996. Inhibitory activity of the equine infectious anemia virus major 5' splice site in the absence of Rev. J Virol **70:**3645-58.
442. **Tanaka, M., T. Ueno, T. Nakahara, K. Sasaki, A. Ishimoto, and H. Sakai.** 2003. Downregulation of CD4 is required for maintenance of viral infectivity of HIV-1. Virology **311:**316-25.
443. **Tang, C., E. Loeliger, I. Kinde, S. Kyere, K. Mayo, E. Barklis, Y. Sun, M. Huang, and M. F. Summers.** 2003. Antiviral inhibition of the HIV-1 capsid protein. J Mol Biol **327:**1013-20.
444. **Tang, C., E. Loeliger, P. Luncsford, I. Kinde, D. Beckett, and M. F. Summers.** 2004. Entropic switch regulates myristate exposure in the HIV-1 matrix protein. Proc Natl Acad Sci U S A **101:**517-22.
445. **Tang, C., Y. Ndassa, and M. F. Summers.** 2002. Structure of the N-terminal 283-residue fragment of the immature HIV-1 Gag polyprotein. Nat Struct Biol **9:**537-43.
446. **Tang, S., T. Murakami, B. E. Agresta, S. Campbell, E. O. Freed, and J. G. Levin.** 2001. Human immunodeficiency virus type 1 N-terminal capsid mutants that exhibit aberrant core morphology and are blocked in initiation of reverse transcription in infected cells. J Virol **75:**9357-66.
447. **Tang, S., T. Murakami, N. Cheng, A. C. Steven, E. O. Freed, and J. G. Levin.** 2003. Human immunodeficiency virus type 1 N-terminal capsid mutants containing cores with abnormally high levels of capsid protein and virtually no reverse transcriptase. J Virol **77:**12592-602.
448. **Tang, Y., U. Winkler, E. O. Freed, T. A. Torrey, W. Kim, H. Li, S. P. Goff, and H. C. Morse, 3rd.** 1999. Cellular motor protein KIF-4 associates with retroviral Gag. J Virol **73:**10508-13.
449. **Temin, H. M.** 1964. Homology between Rna from Rous Sarcoma Virous and DNA from Rous Sarcoma Virus-Infected Cells. Proc Natl Acad Sci U S A **52:**323-9.
450. **Temin, H. M.** 1964. The Participation of DNA in Rous Sarcoma Virus Production. Virology **23:**486-94.
451. **Temin, H. M., and S. Mizutani.** 1970. RNA-dependent DNA polymerase in virions of Rous sarcoma virus. Nature **226:**1211-3.

452. **Ternois, F., J. Sticht, S. Duquerroy, H. G. Krausslich, and F. A. Rey.** 2005. The HIV-1 capsid protein C-terminal domain in complex with a virus assembly inhibitor. Nat Struct Mol Biol **12:**678-82.
453. **Thali, M., A. Bukovsky, E. Kondo, B. Rosenwirth, C. T. Walsh, J. Sodroski, and H. G. Gottlinger.** 1994. Functional association of cyclophilin A with HIV-1 virions. Nature **372:**363-5.
454. **Tisdale, M., T. Schulze, B. A. Larder, and K. Moelling.** 1991. Mutations within the RNase H domain of human immunodeficiency virus type 1 reverse transcriptase abolish virus infectivity. J Gen Virol **72 (Pt 1):**59-66.
455. **Tomasselli, A. G., J. L. Sarcich, L. J. Barrett, I. M. Reardon, W. J. Howe, D. B. Evans, S. K. Sharma, and R. L. Heinrikson.** 1993. Human immunodeficiency virus type-1 reverse transcriptase and ribonuclease H as substrates of the viral protease. Protein Sci **2:**2167-76.
456. **Towers, G. J., T. Hatziioannou, S. Cowan, S. P. Goff, J. Luban, and P. D. Bieniasz.** 2003. Cyclophilin A modulates the sensitivity of HIV-1 to host restriction factors. Nat Med **9:**1138-43.
457. **Triboulet, R., B. Mari, Y. L. Lin, C. Chable-Bessia, Y. Bennasser, K. Lebrigand, B. Cardinaud, T. Maurin, P. Barbry, V. Baillat, J. Reynes, P. Corbeau, K. T. Jeang, and M. Benkirane.** 2007. Suppression of microRNA-silencing pathway by HIV-1 during virus replication. Science **315:**1579-82.
458. **Valentin, A., M. Rosati, D. J. Patenaude, A. Hatzakis, L. G. Kostrikis, M. Lazanas, K. M. Wyvill, R. Yarchoan, and G. N. Pavlakis.** 2002. Persistent HIV-1 infection of natural killer cells in patients receiving highly active antiretroviral therapy. Proc Natl Acad Sci U S A **99:**7015-20.
459. **van Gent, D. C., C. Vink, A. A. Groeneger, and R. H. Plasterk.** 1993. Complementation between HIV integrase proteins mutated in different domains. Embo J **12:**3261-7.
460. **Varthakavi, V., R. M. Smith, S. P. Bour, K. Strebel, and P. Spearman.** 2003. Viral protein U counteracts a human host cell restriction that inhibits HIV-1 particle production. Proc Natl Acad Sci U S A **100:**15154-9.
461. **Vink, C., R. A. Lutzke, and R. H. Plasterk.** 1994. Formation of a stable complex between the human immunodeficiency virus integrase protein and viral DNA. Nucleic Acids Res **22:**4103-10.
462. **Vink, C., A. M. Oude Groeneger, and R. H. Plasterk.** 1993. Identification of the catalytic and DNA-binding region of the human immunodeficiency virus type I integrase protein. Nucleic Acids Res **21:**1419-25.
463. **Voinnet, O.** 2005. Induction and suppression of RNA silencing: insights from viral infections. Nat Rev Genet **6:**206-20.
464. **von Schwedler, U., R. S. Kornbluth, and D. Trono.** 1994. The nuclear localization signal of the matrix protein of human immunodeficiency virus type 1 allows the establishment of infection in macrophages and quiescent T lymphocytes. Proc Natl Acad Sci U S A **91:**6992-6.
465. **von Schwedler, U., J. Song, C. Aiken, and D. Trono.** 1993. Vif is crucial for human immunodeficiency virus type 1 proviral DNA synthesis in infected cells. J Virol **67:**4945-55.
466. **von Schwedler, U. K., T. L. Stemmler, V. Y. Klishko, S. Li, K. H. Albertine, D. R. Davis, and W. I. Sundquist.** 1998. Proteolytic refolding of the HIV-1 capsid protein amino-terminus facilitates viral core assembly. Embo J **17:**1555-68.
467. **von Schwedler, U. K., K. M. Stray, J. E. Garrus, and W. I. Sundquist.** 2003. Functional surfaces of the human immunodeficiency virus type 1 capsid protein. J Virol **77:**5439-50.
468. **von Schwedler, U. K., M. Stuchell, B. Muller, D. M. Ward, H. Y. Chung, E. Morita, H. E. Wang, T. Davis, G. P. He, D. M. Cimbora, A. Scott, H. G. Krausslich, J. Kaplan, S. G. Morham, and W. I. Sundquist.** 2003. The protein network of HIV budding. Cell **114:**701-13.
469. **Wacharapornin, P., D. Lauhakirti, and P. Auewarakul.** 2007. The effect of capsid mutations on HIV-1 uncoating. Virology **358:**48-54.
470. **Wang, C. T., and E. Barklis.** 1993. Assembly, processing, and infectivity of human immunodeficiency virus type 1 gag mutants. J Virol **67:**4264-73.
471. **Wang, C. T., S. S. Chen, and C. C. Chiang.** 2000. Assembly and release of human immunodeficiency virus type 1 Gag proteins containing tandem repeats of the matrix protein coding sequences in the matrix domain. Virology **278:**289-98.
472. **Wang, C. T., J. Stegeman-Olsen, Y. Zhang, and E. Barklis.** 1994. Assembly of HIV GAG-B-galactosidase fusion proteins into virus particles. Virology **200:**524-34.
473. **Wang, C. T., Y. Zhang, J. McDermott, and E. Barklis.** 1993. Conditional infectivity of a human immunodeficiency virus matrix domain deletion mutant. J Virol **67:**7067-76.

474. **Wang, J., S. J. Smerdon, J. Jager, L. A. Kohlstaedt, P. A. Rice, J. M. Friedman, and T. A. Steitz.** 1994. Structural basis of asymmetry in the human immunodeficiency virus type 1 reverse transcriptase heterodimer. Proc Natl Acad Sci U S A **91:**7242-6.
475. **Wei, X., J. M. Decker, S. Wang, H. Hui, J. C. Kappes, X. Wu, J. F. Salazar-Gonzalez, M. G. Salazar, J. M. Kilby, M. S. Saag, N. L. Komarova, M. A. Nowak, B. H. Hahn, P. D. Kwong, and G. M. Shaw.** 2003. Antibody neutralization and escape by HIV-1. Nature **422:**307-12.
476. **Welker, R., M. Harris, B. Cardel, and H. G. Krausslich.** 1998. Virion incorporation of human immunodeficiency virus type 1 Nef is mediated by a bipartite membrane-targeting signal: analysis of its role in enhancement of viral infectivity. J Virol **72:**8833-40.
477. **Welker, R., H. Hohenberg, U. Tessmer, C. Huckhagel, and H. G. Krausslich.** 2000. Biochemical and structural analysis of isolated mature cores of human immunodeficiency virus type 1. J Virol **74:**1168-77.
478. **Welker, R., H. Kottler, H. R. Kalbitzer, and H. G. Krausslich.** 1996. Human immunodeficiency virus type 1 Nef protein is incorporated into virus particles and specifically cleaved by the viral proteinase. Virology **219:**228-36.
479. **Wiegers, K., G. Rutter, H. Kottler, U. Tessmer, H. Hohenberg, and H. G. Krausslich.** 1998. Sequential steps in human immunodeficiency virus particle maturation revealed by alterations of individual Gag polyprotein cleavage sites. J Virol **72:**2846-54.
480. **Wiegers, K., G. Rutter, U. Schubert, M. Grattinger, and H. G. Krausslich.** 1999. Cyclophilin A incorporation is not required for human immunodeficiency virus type 1 particle maturation and does not destabilize the mature capsid. Virology **257:**261-74.
481. **Wilk, T., I. Gross, B. E. Gowen, T. Rutten, F. de Haas, R. Welker, H. G. Krausslich, P. Boulanger, and S. D. Fuller.** 2001. Organization of immature human immunodeficiency virus type 1. J Virol **75:**759-71.
482. **Willey, R. L., F. Maldarelli, M. A. Martin, and K. Strebel.** 1992. Human immunodeficiency virus type 1 Vpu protein induces rapid degradation of CD4. J Virol **66:**7193-200.
483. **Wills, J. W., and R. C. Craven.** 1991. Form, function, and use of retroviral gag proteins. Aids **5:**639-54.
484. **Wohrl, B. M., and K. Moelling.** 1991. Coupling of reverse transcriptase and RNase H during HIV-1 replication. Behring Inst Mitt**:**100-7.
485. **Wong, J. K., M. Hezareh, H. F. Gunthard, D. V. Havlir, C. C. Ignacio, C. A. Spina, and D. D. Richman.** 1997. Recovery of replication-competent HIV despite prolonged suppression of plasma viremia. Science **278:**1291-5.
486. **Wong-Staal, F., L. Ratner, G. Shaw, B. Hahn, M. Harper, G. Franchini, and R. Gallo.** 1985. Molecular Biology of Human T-Lymphotropic Retroviruses. Cancer Res **45:**4539s-4544.
487. **Worthylake, D. K., H. Wang, S. Yoo, W. I. Sundquist, and C. P. Hill.** 1999. Structures of the HIV-1 capsid protein dimerization domain at 2.6 A resolution. Acta Crystallogr D Biol Crystallogr **55:**85-92.
488. **Wright, E. R., J. B. Schooler, H. J. Ding, C. Kieffer, C. Fillmore, W. I. Sundquist, and G. J. Jensen.** 2007. Electron cryotomography of immature HIV-1 virions reveals the structure of the CA and SP1 Gag shells. Embo J **26:**2218-26.
489. **Wu, X., J. L. Anderson, E. M. Campbell, A. M. Joseph, and T. J. Hope.** 2006. Proteasome inhibitors uncouple rhesus TRIM5alpha restriction of HIV-1 reverse transcription and infection. Proc Natl Acad Sci U S A **103:**7465-70.
490. **Wyma, D. J., A. Kotov, and C. Aiken.** 2000. Evidence for a stable interaction of gp41 with Pr55(Gag) in immature human immunodeficiency virus type 1 particles. J Virol **74:**9381-7.
491. **Yao, X. J., J. Friborg, F. Checroune, S. Gratton, F. Boisvert, R. P. Sekaly, and E. A. Cohen.** 1995. Degradation of CD4 induced by human immunodeficiency virus type 1 Vpu protein: a predicted alpha-helix structure in the proximal cytoplasmic region of CD4 contributes to Vpu sensitivity. Virology **209:**615-23.
492. **Yao, X. J., H. Gottlinger, W. A. Haseltine, and E. A. Cohen.** 1992. Envelope glycoprotein and CD4 independence of vpu-facilitated human immunodeficiency virus type 1 capsid export. J Virol **66:**5119-26.
493. **Yao, X. J., A. J. Mouland, R. A. Subbramanian, J. Forget, N. Rougeau, D. Bergeron, and E. A. Cohen.** 1998. Vpr stimulates viral expression and induces cell killing in human immunodeficiency virus type 1-infected dividing Jurkat T cells. J Virol **72:**4686-93.

494. **Yates, A., J. Stark, N. Klein, R. Antia, and R. Callard.** 2007. Understanding the Slow Depletion of Memory CD4+ T Cells in HIV Infection. PLoS Medicine **4:**e177.
495. **Yeung, M. L., Y. Bennasser, T. G. Myers, G. Jiang, M. Benkirane, and K. T. Jeang.** 2005. Changes in microRNA expression profiles in HIV-1-transfected human cells. Retrovirology **2:**81.
496. **Yu, Q., R. Konig, S. Pillai, K. Chiles, M. Kearney, S. Palmer, D. Richman, J. M. Coffin, and N. R. Landau.** 2004. Single-strand specificity of APOBEC3G accounts for minus-strand deamination of the HIV genome. Nat Struct Mol Biol **11:**435-42.
497. **Yu, X., X. Yuan, Z. Matsuda, T. H. Lee, and M. Essex.** 1992. The matrix protein of human immunodeficiency virus type 1 is required for incorporation of viral envelope protein into mature virions. J Virol **66:**4966-71.
498. **Zennou, V., D. Perez-Caballero, H. Gottlinger, and P. D. Bieniasz.** 2004. APOBEC3G incorporation into human immunodeficiency virus type 1 particles. J Virol **78:**12058-61.
499. **Zhang, Y., and E. Barklis.** 1997. Effects of nucleocapsid mutations on human immunodeficiency virus assembly and RNA encapsidation. J Virol **71:**6765-76.
500. **Zhang, Y., and E. Barklis.** 1995. Nucleocapsid protein effects on the specificity of retrovirus RNA encapsidation. J Virol **69:**5716-22.
501. **Zhang, Y., H. Qian, Z. Love, and E. Barklis.** 1998. Analysis of the assembly function of the human immunodeficiency virus type 1 gag protein nucleocapsid domain. J Virol **72:**1782-9.
502. **Zhou, J., and C. Aiken.** 2001. Nef enhances human immunodeficiency virus type 1 infectivity resulting from intervirion fusion: evidence supporting a role for Nef at the virion envelope. J Virol **75:**5851-9.
503. **Zhou, J., C. H. Chen, and C. Aiken.** 2006. Human immunodeficiency virus type 1 resistance to the small molecule maturation inhibitor 3-O-(3',3'-dimethylsuccinyl)-betulinic acid is conferred by a variety of single amino acid substitutions at the CA-SP1 cleavage site in Gag. J Virol **80:**12095-101.
504. **Zhou, J., C. H. Chen, and C. Aiken.** 2004. The sequence of the CA-SP1 junction accounts for the differential sensitivity of HIV-1 and SIV to the small molecule maturation inhibitor 3-O-{3',3'-dimethylsuccinyl}-betulinic acid. Retrovirology **1:**15.
505. **Zhou, J., L. Huang, D. L. Hachey, C. H. Chen, and C. Aiken.** 2005. Inhibition of HIV-1 maturation via drug association with the viral Gag protein in immature HIV-1 particles. J Biol Chem **280:**42149-55.
506. **Zhou, J., X. Yuan, D. Dismuke, B. M. Forshey, C. Lundquist, K. H. Lee, C. Aiken, and C. H. Chen.** 2004. Small-molecule inhibition of human immunodeficiency virus type 1 replication by specific targeting of the final step of virion maturation. J Virol **78:**922-9.
507. **Zhou, W., L. J. Parent, J. W. Wills, and M. D. Resh.** 1994. Identification of a membrane-binding domain within the amino-terminal region of human immunodeficiency virus type 1 Gag protein which interacts with acidic phospholipids. J Virol **68:**2556-69.
508. **Zhou, W., and M. D. Resh.** 1996. Differential membrane binding of the human immunodeficiency virus type 1 matrix protein. J Virol **70:**8540-8.
509. **Zlokarnik, G., P. A. Negulescu, T. E. Knapp, L. Mere, N. Burres, L. Feng, M. Whitney, K. Roemer, and R. Y. Tsien.** 1998. Quantitation of transcription and clonal selection of single living cells with beta-lactamase as reporter. Science **279:**84-8.
510. **Zuber, G., J. McDermott, S. Karanjia, W. Zhao, M. F. Schmid, and E. Barklis.** 2000. Assembly of retrovirus capsid-nucleocapsid proteins in the presence of membranes or RNA. J Virol **74:**7431-41.

Appendix 3

Sultam Thiourea Inhibition of West Nile Virus

Eric Barklis, Amelia Still, Mohammad I. Sabri, Alec J. Hirsch, Janko Nikolich-Zugich, James Brien, Tenzin Choesang Dhenub, Isabel Scholz, and Ayna Alfadhli

Statement of contribution

For this paper, I cultured BHK wt and BHK 26.5 cells, administered cell treatments, and performed immunofluorescence experiments (data not shown).

ANTIMICROBIAL AGENTS AND CHEMOTHERAPY, July 2007, p. 2642–2645 Vol. 51, No. 7
0066-4804/07/$08.00+0 doi:10.1128/AAC.00007-07

Sultam Thiourea Inhibition of West Nile Virus▽

Eric Barklis,[1]* Amelia Still,[1] Mohammad I. Sabri,[2] Alec J. Hirsch,[3,4] Janko Nikolich-Zugich,[3,4] James Brien,[3,4] Tenzin Choesang Dhenub,[1] Isabel Scholz,[1] and Ayna Alfadhli[1]

Vollum Institute and Department of Molecular Microbiology and Immunology, Oregon Health & Sciences University (OHSU), Portland, Oregon[1]; Center for Research on Occupational and Environmental Toxicology and Department of Neurology, OHSU, Portland, Oregon[2]; Department of Molecular Microbiology and Immunology and Vaccine and Gene Therapy Institute, OHSU, Portland, Oregon[3]; and Oregon National Primate Research Center, Beaverton, Oregon[4]

Received 3 January 2007/Returned for modification 26 February 2007/Accepted 11 April 2007

We have identified sultam thioureas as novel inhibitors of West Nile virus (WNV) replication. One such compound inhibited WNV, with a 50% effective concentration of 0.7 μM, and reduced reporter expression from cells that harbored a WNV-based replicon. Our results demonstrate that sultam thioureas can block a postentry, preassembly step of WNV replication.

West Nile virus (WNV) and *Japanese encephalitis virus* (JEV) are members of the *Flavivirus* genus of the *Flaviviridae* family of viruses (9, 13). These viruses are considered emerging human pathogens (11, 12, 19, 29, 32, 37). They are closely related to the yellow fever and dengue flaviviruses, and together, these four pathogens are responsible for a significant percentage of virally induced human encephalitis cases worldwide (10–12, 19, 29, 32, 37). One line of defense against flaviviruses is the formulation of vaccines, usually directed against the viral surface envelope (E) proteins (12, 37). Another possible option is the intravenous administration of antiviral antibodies (25, 35). A complementary approach has been the development of small-molecule flavivirus inhibitors (7, 9, 15, 17, 20, 26, 27, 29, 32, 36, 38, 39).

To assay for novel WNV inhibitors, we screened a diverse library of approximately 3,500 members for compounds that protected Vero cells from WNV-induced cytopathic effects (CPE). Cells were exposed continuously to a compound concentration of 10 μg/ml (10 to 50 μM) along with a 1% dimethyl sulfoxide (DMSO) carrier, infected with WNV (NY 1999) (19, 24) at a multiplicity of infection (MOI) of 0.2, and monitored for CPE at 3 to 5 days postinfection (p.i.). Of the candidate WNV inhibitors identified, the sultam thiourea TYT-1 (Fig. 1) appeared the most potent in replicate screens. TYT-1's anti-WNV effects were confirmed in virus yield reduction assays (19, 29). Mock-treated and TYT-1-treated Vero cells were infected for 24 h, after which virus-containing medium samples were titrated by limiting dilution on fresh cells in the absence of new compound. An example of our results is shown in Fig. 2. As illustrated and expected, medium from mock-treated, mock-infected ("no virus") cells yielded no deleterious effects on new cells. In contrast, dilutions of $\geq 10^5$ from mock-treated infected ("no TYT-1") cells generated virus sufficient to lyse new cell monolayers completely. However, treatment of cells with 2.3 or 23 μM TYT-1 reduced 24-h virus yields ≥100-fold (Fig. 2), substantiating the initial screen results.

Determination of the TYT-1 concentration needed to reduce WNV titers twofold (50% effective concentration [EC_{50}]) followed the virus yield reduction regimen described above. As illustrated in Fig. 3 (black bars), the EC_{50} of TYT-1 against WNV was approximately 0.7 μM. Since our original screening protocol scored for protection of cells from virus-induced CPE, it appeared that TYT-1 was not toxic to cells, at least at 23 μM. However, to test this directly, cells were treated with increasing concentrations of TYT-1 and assayed after 48 h for dehydrogenase levels in metabolically active cells, using MTS {3-[(4,5-dimethylthiazol-2-yl)-5-(3-carboxymethoxyphenyl)-2-(4-sulfophenyl)-2H-tetrazolium]} substrate (6). At the highest concentration tested (70 μM), TYT-1 did not reduce viability signals to the 50% level (Table 1). This result was confirmed microscopically by trypan blue (0.2%) exclusion (data not shown), indicating a 50% cytotoxic concentration (CC_{50}) for TYT-1 of >70 μM. Thus, the net therapeutic or selectivity index (CC_{50}/EC_{50}) for TYT-1 against WNV in Vero cells is >100.

Although TYT-1 showed antiviral effects against WNV, at 23 μM it did not inhibit adenovirus 5, the Prospect Hill (2) hantavirus, or a human immunodeficiency virus type 1 (HIV-1) expression vector (data not shown). However, in virus yield reduction tests with JEV (SA14-2-8) (30), TYT-1 again inhibited virus replication, albeit with an EC_{50} of 7 μM, which is 10-fold higher than its EC_{50} against WNV (Table 1). Because very few analogues of TYT-1 have been described (28), our ability to probe structure-activity relationships is currently limited. However, we have examined the cytotoxic and antiflavivirus effects of three available TYT-1 analogues, TYT-2, TYT-3, and TYT-4 (Fig. 1). As shown in Fig. 3 and Table 1, none of these showed impressive antiviral effects against WNV, with EC_{50} values of >20 μM. Moreover, TYT-2 and TYT-4 appeared to be cytotoxic at 50 to 100 μM (Table 1). However, TYT-3 was not cytotoxic at the highest concentration tested and gave some level of protection against JEV (Table 1).

To ascertain how TYT-1 might inhibit WNV, we initially

* Corresponding author. Mailing address: Vollum Institute and Department of Molecular Microbiology and Immunology, Oregon Health & Sciences University, Mail Code L220, 3181 SW Sam Jackson Park Road, Portland, OR 97201-3098. Phone: (503) 494-8098. Fax: (503) 494-6862. E-mail: barklis@ohsu.edu.

▽ Published ahead of print on 23 April 2007.

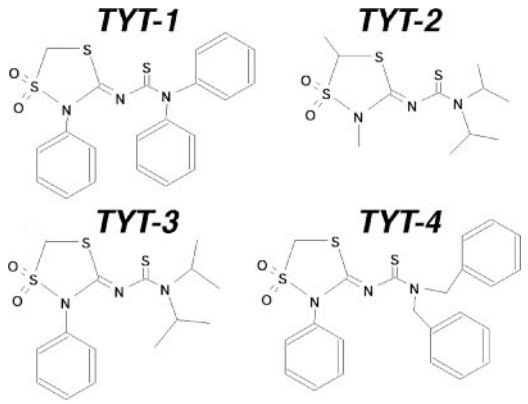

FIG. 1. Compound structures. The diagrams show the structures of the following sultams: TYT-1, *N′*-(1,1-dioxido-2-phenyl-1,4,2-dithiazolidin-3-ylidene)-*N*,*N*-diphenylthiourea (439.6 kDa); TYT-2, (2,5-dimethyl-1,1-dioxido-1,4,2-dithiazolidin-3-ylidene)bis(1-methylethyl)thiourea (323.5 kDa); TYT-3, [1,1-dioxido-2-(phenylmethyl)-1,4,2-dithiazolidin-3-ylidene]bis(1-methylethyl)-thiourea (385.6 kDa); and TYT-4, (1,1-dioxido-2-phenyl-1,4,2-dithiazolidin-3-ylidene)-bis(phenylmethyl)-thiourea (467.6 kDa).

probed viral protein levels in treated and untreated acutely infected cells. Vero cells that were mock treated or treated with TYT-1 were infected with WNV and processed for either immunofluorescence (4, 18) or immunoblot (18, 23) detection of the viral E protein. Importantly, regardless of the detection method employed, we found that TYT-1 treatment dramatically reduced E protein levels in infected cells (data not shown). We also addressed whether WNV RNA levels are reduced by TYT-1 treatment through quantitation of RNA levels by real-time PCR (8, 19). With mock-treated, mock-infected, negative control Vero cells, no WNV RNA signals were observed (data not shown). With mock-treated, infected, positive control cells, real-time PCR signals were halfway

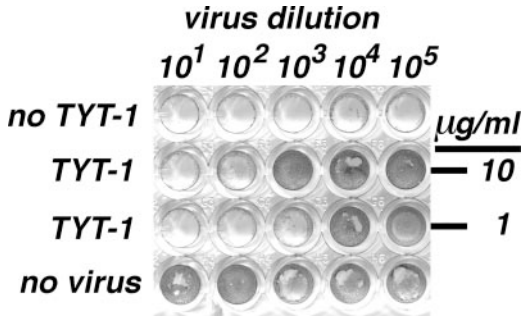

FIG. 2. WNV yield reduction. Vero cells in medium containing 100 U/ml penicillin and 0.1 mg/ml streptomycin were mock treated with DMSO (no TYT-1; no virus; final DMSO concentration, 1%) or treated with the indicated concentration of TYT-1 in DMSO and then mock infected (no virus) or infected with WNV at an MOI of 1.0. At 24 h p.i., virus-containing medium samples at the indicated dilutions were used to infect fresh cells. At 5 days p.i., surviving cells were stained with 0.0375% crystal violet. Infected, mock-treated wells were devoid of cells due to WNV-mediated cell killing, and wells were routinely scored as virus positive if cell staining levels were reduced three-fourths or more relative to uninfected cell staining levels. Note that 2.3 and 23 μM TYT-1 reduced WNV titers at least 100-fold and that these results are representative of more than 10 independent experiments.

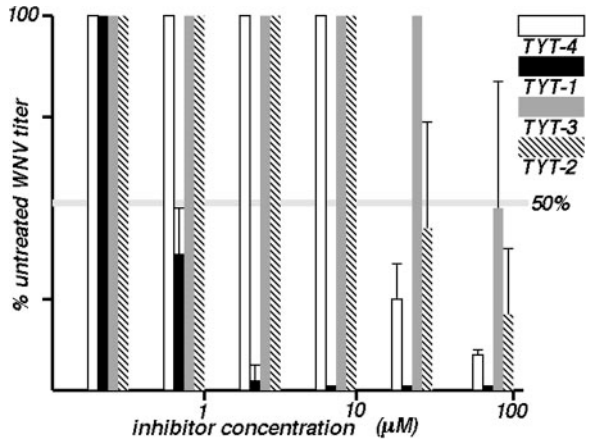

FIG. 3. Effective anti-WNV drug concentrations. Increasing concentrations of TYT-1 (black bars), TYT-2 (striped bars), TYT-3 (gray bars), and TYT-4 (white bars) were used to determine effective anti-WNV concentrations by virus yield reduction assays. Results are plotted as concentrations versus percentages of virus yields observed in mock-treated (1% DMSO [final concentration]) controls. Titers were determined by limiting dilution and scored as described in the legend to Fig. 2. Averages (means) were derived from three separate experiments for TYT-1 and at least two separate experiments for TYT-2 to -4, and standard deviations are shown.

through their exponential increase phase by cycle number 15 (Fig. 4), corresponding to 3,255 ± 325.8 WNV RNA copies per cell, as quantitated relative to an in vitro-transcribed NS3 RNA standard. Treatment of infected cells with TYT-1 clearly shifted the amplification signals to higher cycle numbers (Fig. 4), corresponding to 27.2 ± 1.6 WNV RNA copies per cell. Thus, TYT-1-mediated inhibition of WNV E expression was accompanied by a >100-fold reduction in WNV RNA levels.

The observed reductions of WNV protein and RNA levels imply that TYT-1 exerts its antiviral activity prior to the assembly stage of virus replication. However, these experiments did not discriminate whether inhibition occurs at viral entry or postentry steps. One way to distinguish between these possibilities is to screen for antiviral activity when an inhibitor is added after the onset of infection. When such time course experiments were undertaken, using a virus yield reduction readout, we found that TYT-1 application as late as 2 h p.i. gave similar levels of virus inhibition to those obtained when cells were pretreated with the drug (data not shown). Addi-

TABLE 1. Characteristics of sultam thiourea compounds

Compound	EC_{50}[a] (μM)		CC_{50}[b] (μM)
	WNV	JEV	
TYT-1	0.7	7	>70
TYT-2	30	30	90
TYT-3	80	8	>80
TYT-4	22	65	65

[a] Compound EC_{50} values for WNV were derived from the virus yield reduction results shown in Fig. 2, while EC_{50} values for JEV were obtained in a similar fashion from two to four independent experiments.

[b] The CC_{50} values were determined by MTS cytotoxicity assays performed in quadruplicate. Note that 50% cytotoxicity was defined as a 50% drop in background-subtracted MTS signals and that for TYT-1 and TYT-3, 50% cytotoxicity was not obtained with the highest drug concentrations employed.

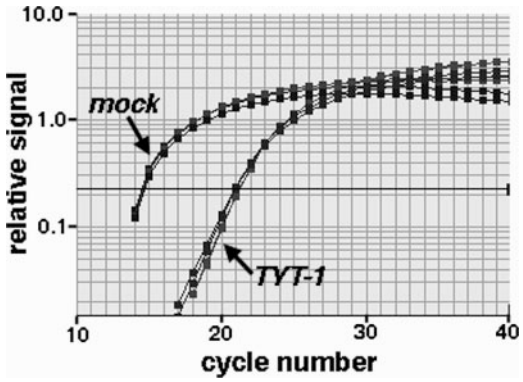

FIG. 4. WNV RNA levels in treated and untreated cells. Vero cells were mock treated with DMSO ("mock"; final concentration, 0.5% DMSO) or treated with 11 μM TYT-1 in DMSO ("TYT-1") and then mock infected (not shown) or infected with WNV at an MOI of 5. At 18 h p.i., RNAs were isolated, and equivalent input RNA amounts were reverse transcribed and subjected to real-time PCR quantitation of WNV RNA levels following previously described protocols (8, 19). The results, plotted as relative fluorescence signals versus PCR cycle numbers, indicate the following average ($n = 4$) WNV RNA copy numbers per cell, as quantitated relative to an in vitro-transcribed NS3 RNA standard: for uninfected cells, 0; for untreated cells, 3,255 ± 325.8; and for TYT-1-treated cells, 27.2 ± 1.6. Reverse transcription-PCR cycle parameters were 30 min at 48°C for the reverse transcription step, 10 min at 95°C for a denaturation step, and 40 cycles of 13 s at 95°C and 1 min at 60°C.

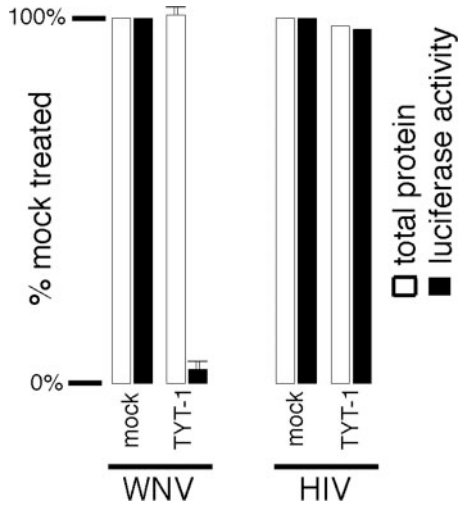

FIG. 5. WNV replicon inhibition. BHK cells expressing a WNV luciferase replicon (WNV) (33) or 293 cells transfected with an HIV-based luciferase expression vector (HIV) (34) were mock treated with DMSO (0.1% [final concentration]) or treated with 23 μM TYT-1 in DMSO. At 48 h posttreatment, cells were processed for detection of total protein levels (white bars) or luciferase activities (black bars). Protein levels and luciferase levels are expressed as percentages of the values obtained for mock-treated samples; background luciferase levels with parental BHK and untransfected 293 cells were <0.1% of the 100% values shown. Values obtained for WNV replicon samples were averaged from four separate experiments and are shown with standard deviations.

tionally, we tested TYT-1 effects on baby hamster kidney (BHK) 26.5 cells (33), which stably harbor a WNV replicon expressing a luciferase reporter gene. To do so, BHK or BHK 26.5 cells were mock treated for 48 h with DMSO (0.1% final concentration) or with 23 μM TYT-1 (final concentration) in DMSO and processed for determination of luciferase activities (34) and total protein levels (Bio-Rad). Significantly, TYT-1 treatment of these WNV replicon-expressing cells reduced luciferase reporter levels >20-fold but did not alter cellular total protein levels (Fig. 5, left panel). In contrast, TYT-1 did not reduce luciferase levels in control cells expressing the protein from an HIV-1-based (34) vector (Fig. 5, right panel).

The above results demonstrate that TYT-1 blocks a postentry, preassembly step of WNV replication. However, the precise mechanism by which TYT-1 exerts its antiviral effects is not known. Since the compound reduced virus levels in African green monkey Vero cells and viral replicon levels in BHK 26.5 cells, its effects are not specific to one cell type or species. Another observation which suggests that our sultam thioureas interfere with a virus-specific target is that TYT-1 and TYT-3 showed opposite differential effects on WNV versus JEV (Table 1); it is difficult to reconcile how these results might occur if the two compounds were to act on a common cellular factor. Thus, the accumulated data (Table 1; Fig. 2 to 5) suggest that TYT-1 targets a sensitive step somewhere in the middle of the virus replication cycle. Conceivably, inhibition could occur via a block to viral translation, polyprotein processing, or RNA replication, but further investigation will be needed to dissect the mechanism in greater detail and to determine whether the potency of TYT-1 will be sufficient for therapeutic purposes in vivo.

We could find no reports concerning the potential biological activities of sultam thioureas closely related to TYT1-4. However, numerous sulfonamides have been employed as inhibitors of a diverse set of proteases (1). Moreover, several sultams have been considered excellent antiarthritic drug candidates by virtue of their activities against matrix metalloproteinases (1, 14, 21, 22, 31). While these reports might point to the WNV protease as the TYT-1 target, sultams have been reported to block other enzyme activities. For instance, sultam derivatives have been shown to inhibit histone deacetylase (3), HIV reverse transcriptase (5), and HIV integrase (16) activities. Thus, available data on sultam activities do not help to implicate a particular TYT-1 target. Indeed, given the limited number of available TYT-1 analogues (Fig. 1), it is important to emphasize that even the requirement of a sultam ring for TYT-1 or TYT-3 antiflavivirus activity is uncertain. The results suggest that replacement of the TYT-1 thiourea nitrogen phenyl groups with isopropyl (TYT-3) or methylphenyl (TYT-4) substituents has a significant impact on antiviral activity (Table 1), but considerably more study will be needed to determine how and how well these inhibitors act as antivirals.

We are grateful to Peter Mason, who provided BHK and BHK 26.5 cells, along with advice concerning their use. We also appreciate the efforts of Kathy Shinall for secretarial support, of Travis Rogers for tissue culture support, and of Robin Lid Barklis for organizational support.

Our investigations were funded by a grant from the NIH (R21 AI56248) to E.B., by NIH contract support (1 50027) to J.N.-Z., and by NIH training grant support (5 T32 AI007472-12) to A.A and J.B.

OHSU and E.B. have filed a patent application on the use of the described compounds and derivatives as antivirals and thus have a commercial interest in these investigations.

REFERENCES

1. **Abbenante, G., and D. Fairlie.** 2005. Protease inhibitors in the clinic. Med. Chem. **1:**71–104.
2. **Alfadhli, A., Z. Love, B. Arvidson, J. Seeds, J. Willey, and E. Barklis.** 2001. Hantavirus nucleocapsid protein oligomerization. J. Virol. **75:**2019–2023.
3. **Anonymous.** 2003. Tricyclic lactam and sultam derivatives as histone deacetylase inhibitors. Expert Opin. Ther. Pat. **13:**387–391.
4. **Arvidson, B., J. Seeds, M. Webb, L. Finlay, and E. Barklis.** 2003. Analysis of the retrovirus capsid interdomain linker region. Virology **308:**166–177.
5. **Baker, D. C., and B. Jiang.** March 2002. Sultams: solid phase and other synthesis of anti-HIV compounds and compositions. U.S. patent 6,353,112 B1.
6. **Barltrop, J., T. Owen, A. Cory, and J. Cory.** 1991. 5-(3carboxymethoxyphenyl)-2-(4,5-dimethylthiazolyl)-3-(4-sulfophenyl)tetrazolium, inner salt (MTS) and related analogs of 3-(4,5-dimethylthiazolyl)-2,5-diphenyltetrazolium bromide (mTT) reducing to purple water-soluble formazans as cell-viability indicators. Bioorg. Med. Chem. Lett. **1:**611.
7. **Borowski, P., M. Lang, A. Haag, H. Schmitz, J. Choe, H.-M. Chen, and R. Hosmane.** 2002. Characterization of imidazo(4,5-*d*)pyridazine nucleosides as modulators of unwinding reaction mediated by West Nile virus nucleoside triphosphatase/helicase: evidence for activity on the level of substrate and/or enzyme. Antimicrob. Agents Chemother. **46:**1231–1239.
8. **Briese, T., W. Glass, and W. I. Lipkin.** 2000. Detection of West Nile virus sequences in cerebrospinal fluid. Lancet **355:**1614–1615.
9. **Brinton, M.** 2002. The molecular biology of West Nile virus. Annu. Rev. Microbiol. **56:**371–402.
10. **Centers for Disease Control and Prevention.** 1999. Outbreak of West Nile-like viral encephalitis—New York. Morb. Mortal. Wkly. Rep. **48:**25–28.
11. **Centers for Disease Control and Prevention.** 2002. Provisional surveillance summary of the West Nile virus epidemic—United States, January-November 2002. Morb. Mortal. Wkly. Rep. **51:**1129–1133.
12. **Centers for Disease Control and Prevention.** 2005. West Nile virus. Centers for Disease Control and Prevention, Atlanta, GA. http://www.cdc.gov/ncidod/dvbid/westnile/index.html.
13. **Chambers, T., C. Hahn, R. Galler, and C. Rice.** 1990. Flavivirus genome organization, expression, and replication. Annu. Rev. Microbiol. **44:**649–688.
14. **Cherney, R., R. Mo, D. Meyer, K. Hardman, R. Liu, M. Covington, M. Qian, Z. Wasserman, D. Christ, J. Trzaskos, R. Newton, and C. Decicco.** 2004. Sultam hydroxamates as novel matrix metalloproteinase inhibitors. J. Med. Chem. **47:**2981–2983.
15. **Courageot, M.-P., M.-P. Frenkiel, C. Duarte Dos Santos, V. Deubel, and P. Despres.** 2000. α-Glucosidase inhibitors reduce dengue virus production by affecting the initial steps of virion morphogenesis in the endoplasmic reticulum. J. Virol. **74:**564–572.
16. **Dayam, R., J. Deng, and N. Neamati.** 2006. HIV-1 integrase inhibitors: 2003–2004 update. Med. Res. Rev. **26:**271–309.
17. **Diamond, M., M. Zachariah, and E. Harris.** 2002. Mycophenolic acid inhibits dengue virus infection by preventing replication of viral RNA. Virology **304:**211–221.
18. **Hansen, M., L. Jelinek, S. Whiting, and E. Barklis.** 1990. Transport and assembly of Gag proteins into Moloney murine leukemia virus. J. Virol. **64:**5306–5316.
19. **Hirsch, A., G. Medigeshi, H. Meyers, V. DeFilippis, K. Fruh, T. Briese, W. I. Lipkin, and J. Nelson.** 2005. The Src family kinase c-Yes is required for maturation of West Nile virus particles. J. Virol. **79:**11943–11951.
20. **Hong, Z., and C. Cameron.** 2002. Pleiotropic mechanisms of ribavirin antiviral activities. Prog. Drug Res. **59:**41–69.
21. **Inagaki, M.** 2003. Studies on the new antiarthritic drug candidate S-2474. Yakugaku Zasshi **123:**323–330.
22. **Inagaki, M., T. Tsuri, H. Jyoyama, T. Ono, K. Yamada, M. Kobayashi, Y. Hori, A. Arimura, K. Yasui, K. Ohno, S. Kakudo, K. Koizumi, R. Suzuki, S. Kawai, M. Kato, and S. Matsumoto.** 2000. Novel antiarthritic agents with 1,2-isothiazolidine-1,1-dioxide (gamma-sultam) skeleton: cytokine suppressive dual inhibitors of cyclooxygenase-2 and 5-lipoxygenase. J. Med. Chem. **43:**2040–2048.
23. **Jones, T. A., G. Blaug, M. Hansen, and E. Barklis.** 1990. Assembly of Gag–β-galactosidase proteins into retrovirus particles. J. Virol. **64:**2265–2279.
24. **Jordan, I., T. Briese, N. Fischer, J. Lau, and W. I. Lipkin.** 2000. Ribavirin inhibits West Nile virus replication and cytopathic effect in neural cells. J. Infect. Dis. **182:**1214–1217.
25. **Kimura-Kuroda, J., and K. Yasui.** 1988. Protection of mice against Japanese encephalitis virus by passive administration with monoclonal antibodies. J. Immunol. **141:**3606–3610.
26. **Leung, D., K. Schroder, H. White, N.-X. Fang, M. Stoermer, G. Abbenante, J. Martin, P. Young, and D. Fairlie.** 2001. Activity of recombinant dengue 2 virus NS3 protease in the presence of a truncated NS2B cofactor, small peptide substrates, and inhibitors. J. Biol. Chem. **276:**45762–45771.
27. **Leyssen, P., J. Balzarini, E. De Clercq, and J. Neyts.** 2005. The predominant mechanism by which ribavirin exerts its antiviral activity in vitro against flaviviruses and paramyxoviruses is mediated by inhibition of IMP dehydrogenase. J. Virol. **79:**1943–1947.
28. **Linden, H., and J. Goerdeler.** 1977. Ring opening cycloadditions. 5. Reaction of iminodithiazoles with sulfenes in 5-membered sultams. Tetrahedron Lett. **20:**1729–1732.
29. **Morrey, J., D. Smee, R. Sidwell, and C. Tseng.** 2002. Identification of active antiviral compounds against a New York isolate of the West Nile virus. Antivir. Res. **55:**107–116.
30. **Ni, H., N. Burns, G. Chang, M. Zhang, M. Wills, D. Trent, P. Sanders, and A. Barrett.** 1994. Comparison of nucleotide and deduced amino acid sequence of the 5′ non-coding region and structural protein genes of the wild-type Japanese encephalitis virus strain SA14 and its attenuated vaccine derivatives. J. Gen. Virol. **75:**1505–1510.
31. **Page, M.** 2004. Beta-sultams—mechanism of reactions and use as inhibitors of serine proteases. Acc. Chem. Res. **37:**297–303.
32. **Puig-Basagoiti, F., M. Tilgner, B. Forshey, S. Philpott, N. Espina, D. Wentworth, S. Goebel, P. Masters, B. Falgout, P. Ren, D. Ferguson, and P.-Y. Shi.** 2006. Triaryl pyrazoline compound inhibits flavivirus RNA replication. Antimicrob. Agents Chemother. **50:**1320–1329.
33. **Rossi, S., Q. Zhao, V. O'Donnell, and P. Mason.** 2005. Adaptation of West Nile virus replicons to cells in culture and use of replicon-bearing cells to probe antiviral action. Virology **331:**457–470.
34. **Scholz, I., B. Arvidson, D. Huseby, and E. Barklis.** 2005. Virus particle core defects caused by mutations in the human immunodeficiency virus capsid N-terminal domain. J. Virol. **79:**1470–1479.
35. **Shimoni, Z., M. Niven, S. Pitlick, and S. Bulvik.** 2001. Treatment of West Nile virus encephalitis with intravenous immunoglobulin. Emerg. Infect. Dis. **7:**759.
36. **Whitby, K., T. Pierson, B. Geiss, K. Lane, M. Engel, Y. Zhou, R. Doms, and M. Diamond.** 2005. Castanospermine, a potent inhibitor of dengue virus infection in vitro and in vivo. J. Virol. **79:**8698–8706.
37. **World Health Organization.** 2002. Immunization vaccines and biologicals: Japanese encephalitis. World Health Organization, Geneva, Switzerland. http://www.who.int/vaccines-disease/diseases/je.shtml.
38. **Wu, S.-F., C.-J. Lee, C.-L. Liao, R. Dwek, N. Zitzmann, and Y.-L. Lin.** 2002. Antiviral effects of an iminosugar derivative on flavivirus infections. J. Virol. **76:**3596–3604.
39. **Zhang, N., H. Chen, V. Koch, H. Schmitz, M. Minczuk, P. Stepien, A. Fattom, R. Naso, K. Kalicharran, P. Borowski, and R. Hosmane.** 2003. Potent inhibition of NTPase/helicase of the West Nile virus by ring-expanded ("fat") nucleoside analogues. J. Med. Chem. **46:**4776–4789.

Appendix 4

HIV-1 Nef assembles a Src family kinase—ZAP-70/Syk—PI3K cascade to downregulate cell surface MHC-I

Chien-Hui Hung, Laurel Thomas, Carl E. Ruby, Katelyn M. Atkins, Nicholas P. Morris, Zachary A. Knight, Isabel Scholz, Eric Barklis, Andrew D. Weinberg, Kevan M. Shokat and Gary Thomas

Statement of contribution

For this paper, I cultured experimental T cells (H9 and CEM-SS), performed infections with HIV-1, and prepared cells for analysis.

Cell Host & Microbe
Article

HIV-1 Nef Assembles a Src Family Kinase-ZAP-70/Syk-PI3K Cascade to Downregulate Cell-Surface MHC-I

Chien-Hui Hung,[1,4,5] Laurel Thomas,[1,5] Carl E. Ruby,[2] Katelyn M. Atkins,[1] Nicholas P. Morris,[2] Zachary A. Knight,[3] Isabel Scholz,[1] Eric Barklis,[1] Andrew D. Weinberg,[2] Kevan M. Shokat,[3] and Gary Thomas[1,*]
[1] Vollum Institute, 3181 Southwest Sam Jackson Park Road, Portland, OR 97239, USA
[2] Providence Medical Center, Portland, OR 97213, USA
[3] Department of Cellular and Molecular Pharmacology, Howard Hughes Medical Institute, University of California, San Francisco, San Francisco, 94143, USA
[4] Department of Medicine, China Medical University, Taichung 40402, Taiwan
[5] These authors contributed equally to this work.
*Correspondence: thomasg@ohsu.edu
DOI 10.1016/j.chom.2007.03.004

SUMMARY

HIV-1 Nef, which is required for the efficient onset of AIDS, enhances viral replication and infectivity by exerting multiple effects on infected cells. Nef downregulates cell-surface MHC-I molecules by an uncharacterized PI3K pathway requiring the actions of two Nef motifs—$EEEE_{65}$ and $PXXP_{75}$. We report that the Nef $EEEE_{65}$ targeting motif enables Nef $PXXP_{75}$ to bind and activate a *trans*-Golgi network-localized Src family tyrosine kinase (SFK). The Nef/SFK complex then recruits and phosphorylates the tyrosine kinase ZAP-70, which binds class I PI3K to trigger MHC-I downregulation in primary $CD4^+$ T cells. In promonocytic cells, Nef/SFK recruits the ZAP-70 homolog Syk to downregulate MHC-I, implicating this PI3K pathway in multiple HIV-1 reservoirs. Isoform-specific PI3K inhibitors repress MHC-I downregulation, identifying them as potential therapeutic agents to combat HIV-1. The discovery of this Nef-SFK-ZAP-70/Syk-PI3K signaling pathway explains the hierarchal role of the Nef motifs in effecting immunoevasion.

INTRODUCTION

In infected people, HIV-1 establishes long-lived reservoirs in a number of cell types, including macrophages, dendritic cells, and resting $CD4^+$ T cells, which resist highly active antiretroviral therapy (HAART; Stevenson, 2003). To respond to the virus infection, the host activates an antiviral response, integrating adaptive immunity and apoptotic mechanisms to destroy the virus. Pathogenic viruses counter the host antiviral response by expressing specialized genes that prevent antigen presentation and apoptosis (Benedict et al., 2002; Peterlin and Trono, 2003). Unlike other pathogenic viruses, HIV-1 uses a limited set of gene products to coordinate the antiviral counterattack. One of these gene products, Nef, is a 27 kDa N-myristoylated protein that enhances viral replication and virion infectivity and is required for the onset of AIDS following HIV-1-infection (Das and Jameel, 2005; Peterlin and Trono, 2003). Nef affects cells in many ways, including altering T cell activation and maturation (Stevenson, 2003; Stove et al., 2003; Thoulouze et al., 2006), subverting the apoptotic machinery, and downregulating CD4 molecules and major histocompatibility complex class I (MHC-I) molecules encoded by the HLA-A and -B loci (Peterlin and Trono, 2003). The downregulation of MHC-I by SIV Nef in rhesus macaques limits $CD8^+$ T cell-mediated killing and contributes to the pathogenic effect of Nef, illustrating the importance of Nef-mediated immunoevasion to disease progression (Swigut et al., 2004).

Current HIV-1 therapeutics principally target the activities of virally encoded reverse transcriptase and protease. However, their effectiveness is compromised by the emergence of drug-resistant viral strains. A promising alternative approach is to develop therapeutics that interfere with the action of HIV-1 proteins on cellular factors (Greene, 2004). HIV-1 Nef represents a potential target for such an approach, as it binds to and stimulates the activity of several cellular kinases, including Src family tyrosine kinases (SFKs; Lee et al., 1995; Trible et al., 2006), which promotes HIV-1 disease in animal models (Hanna et al., 2001), and class I PI3K, which enables HIV-1 to increase virus production, block apoptosis, and downregulate cell-surface MHC-I (Blagoveshchenskaya et al., 2002; Linnemann et al., 2002; Peterlin and Trono, 2003). The profound ability of the Bcr-Abl and c-kit inhibitor Gleevec to cure specific cancers supports such an approach (Druker, 2004). Unfortunately, current PI3K inhibitors, including wortmannin and LY294002, are panselective, showing a similar IC_{50} against all PI3Ks (Ward et al., 2003). Moreover, the concentrations required for LY294002 to block PI3K are similar to the concentrations

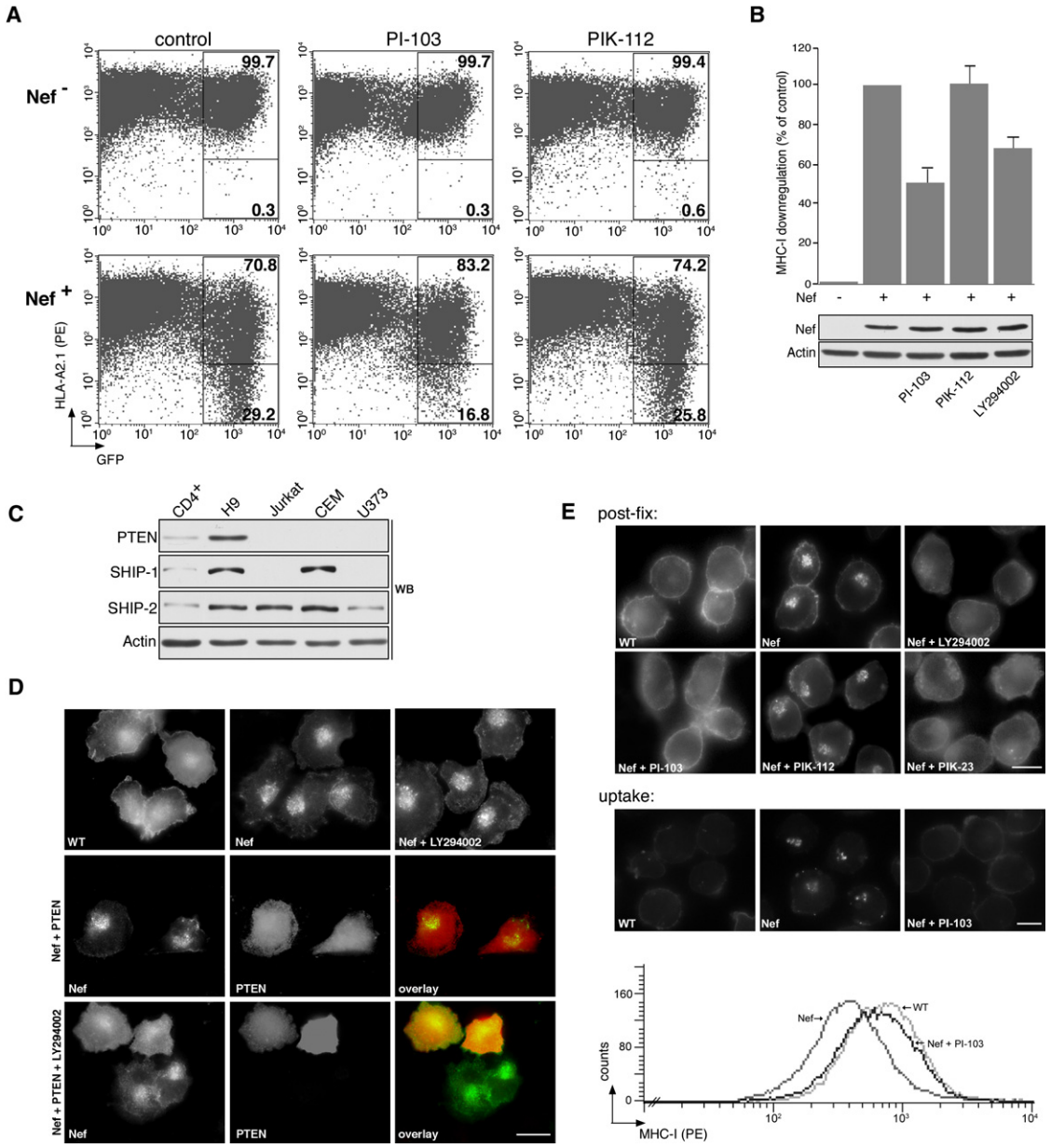

Figure 1. Nef-Triggered MHC-I Downregulation in Primary CD4+ T Cells Is Mediated by Class I PI3K

(A) Primary CD4+ T cells incubated with 2 ng/ml IL-7 for 4 days were infected with the Nef− or Nef+ pseudotyped viruses (moi = 5). At 40 hr postinfection cells were treated with 1 μM PI-103, 1 μM PIK-112, or 1% DMSO (control) for 3 hr. The cells were then incubated with mouse-anti-HLA-A2.1 followed by anti-mouse-PE-conjugated Ig and analyzed by flow cytometry. Viable cells were analyzed for eGFP and anti-HLA-A2.1. The frequency of eGFP^{high} cells displaying downregulated MHC-I is shown in the lower right gate. Similar results were obtained using PHA/IL-2-stimulated primary CD4+ T cells or using mAb W6/32 (data not shown). Western blot analysis showed that Nef expression was greater in eGFP^{high}/MHC-I^{low} cells than in eGFP^{high}/MHC-I^{high} cells, revealing an incomplete correlation between Nef and GFP expression in this vector (data not shown).

(B) Nef− or Nef+ pseudovirus-infected primary CD4+ T cells were treated with 1 μM PI-103, 1 μM PIK-112, 5 μM LY294002, or 1% DMSO for 3 hr and then analyzed by flow cytometry. The effect of each compound on MHC-I downregulation was then normalized to the extent of MHC-I downregulation in control cells infected with the Nef+ or Nef− pseudoviruses (set at 100 and 1, respectively). Bottom: Western blot showing the expression of Nef and the levels of actin (input). Error bars represent the mean ± SD of four independent experiments with cells isolated from three donors (n = 4).

(C) Primary CD4+ T cells or the indicated cell lines were harvested, and the expression of the indicated proteins was determined by western blot.

(D) U373 MG cells were transfected or not with pSG5-PTEN-HA for 48 hr and then infected with VV:WT or VV:Nef (moi =10, 4 hr). Where indicated, cells were treated with 5 μM LY294002 for 40 min prior to fixation. The cells were then fixed and stained with anti-MHC-I (mAb W6/32, green) and anti-HA (red). Scale bar, 20 μm.

(E) Top: H9 CD4+ T cells were infected with VV:WT or VV:Nef (moi = 10, 4 hr) and then treated or not with PI-103 (1 μM), PIK-112 (1 μM), or LY294002 (5 μM) for 1 hr. Cells were fixed and MHC-I molecules were stained with mAb W6/32. Scale bar, 10 μm. Middle: H9 CD4+ T cells infected with VV:WT

that cause cell death—precluding their use as therapeutics (Ward et al., 2003). Recently, a new group of small-molecule PI3K inhibitors were developed that are selective for the class I PI3K isoforms (Knight et al., 2006). One of these inhibitors, PI-103, which is a pyridinylfuranopyrimidine derivative, targets multiple class I p110 catalytic subunits, blocking PKB/Akt activation and arresting cells in G_0/G_1 without the toxicity associated with panselective PI3K inhibitors (Fan et al., 2006; Knight et al., 2006).

The development of isoform-specific PI3K inhibitors suggests a novel approach to combat HIV-1. However, the role of PI3K in Nef-mediated MHC-I downregulation is controversial. We reported that Nef diverts cell-surface MHC-I molecules to *trans*-Golgi network (TGN)-associated compartments in heterologous cells by a PI3K-stimulted, ARF6-dependent, endocytic pathway (Blagoveshchenskaya et al., 2002). This MHC-I downregulation requires the hierarchical action of three motifs (Das and Jameel, 2005; Peterlin and Trono, 2003): an acidic cluster ($EEEE_{65}$), required for binding to the cytosolic sorting protein PACS-1 (Piguet et al., 2000); an SH3 domain-binding motif ($PQVP_{75}$) that directs association of Nef with SFKs (Lee et al., 1995); and an N-proximal α-helical region containing a critical methionine (M_{20}), which promotes association of MHC-I with the heterotetrameric sorting adaptor AP-1 (Roeth et al., 2004). The conservation of these three motifs in the pandemic M group HIV-1, which accounts for over 90% of all AIDS cases worldwide, suggests that they control an essential pathway required for HIV-1 pathogenesis (Keele et al., 2006). But this model has been challenged by others who reported that in leukemic T cell lines or in U373 astrocytoma cell lines Nef acts solely on newly synthesized MHC-I molecules and not on cell-surface MHC-I, and that Nef acts independently of PI3K because the panselective PI3K inhibitors LY294002 or wortmannin failed to block MHC-I downregulation in these transformed cell lines (Kasper and Collins, 2003; Larsen et al., 2004).

We sought to determine the basis for the conflicting models of MHC-I downregulation, and in doing so, we discovered a PI3K activation pathway used by HIV-1 Nef to downregulate cell-surface MHC-I in HIV-1 target cells. We show that the Nef $EEEE_{65}$ targeting motif, which is required for efficient binding to PACS-1 (Piguet et al., 2000), enables the Nef $PXXP_{75}$ motif to bind and activate an SFK localized to TGN-associated reservoirs. The Nef/SFK complex then recruits and phosphorylates ZAP-70, which activates Nef-associated PI3K to trigger the PI-103-sensitive downregulation of MHC-I in primary $CD4^+$ T cells and model $CD4^+$ T cell lines. We also show that, in promonocytic cells and heterologous cell types, Nef/SFK recruits the ZAP-70 homolog Syk to stimulate the PI3K-dependent downregulation of cell-surface MHC-I. Our elucidation of this Nef-SFK-ZAP-70/Syk-PI3K signaling pathway explains the hierarchal role of the Nef motifs that control immunoevasion and identifies new targets for HIV-1 therapy with the potential to make use of newly developed isoform-specific PI3K inhibitors.

RESULTS

HIV-1 Nef Uses a PI3K-Dependent Pathway to Downregulate Cell-Surface MHC-I in $CD4^+$ T Cells

HIV-1 Nef utilizes PI3K to downregulate cell-surface MHC-I in heterologous cell types, but whether it uses this same pathway to downregulate MHC-I in HIV-1 target cells and the mechanism controlling this pathway are unknown. We thus tested the effect of PI3K inhibitors on Nef-induced MHC-I downregulation in primary $CD4^+$ T cells isolated from healthy donors. Cells were pretreated with PHA/IL-2 or IL-7 and then infected with VSV-G pseudotyped, GFP-expressing HIV-1 viruses derived from HIV-1 NL4-3 that either lack the Nef gene or express Nef (Husain et al., 2002). Whereas PHA/IL-2 robustly stimulates cellular PI3K activity and T cell activation, nonmitogenic levels of IL-7 used here do not (Figure S1 in the Supplemental Data available with this article online). We then determined the frequency of GFP-positive infected cells with downregulated cell-surface HLA-A2.1 by flow cytometry. Like the activity of other Nef alleles (Keppler et al., 2006), NL4-3 Nef downregulated cell-surface HLA-A2.1 by 40%–60% as determined by fluorescence intensity regardless of treatment with IL-7 or IL-2/PHA (Figures 1A and 1B and data not shown). Parallel cultures were treated with the class I PI3K inhibitor PI-103 or its inactive analog, PIK-112, for 3 hr prior to analysis, with no change in cell viability as determined by forward and side scattering. We found that PI-103 inhibited the Nef-induced MHC-I downregulation in primary $CD4^+$ T cells, whereas PIK-112 had no effect (Figure 1A), suggesting that Nef uses a PI3K-dependent pathway to efficiently downregulate cell-surface MHC-I in primary $CD4^+$ T cells. By contrast, PI-103 had no measurable effect on Nef-mediated CD4 downregulation (Figure S2). Moreover, the inhibition of MHC-I downregulation by PI-103 was similar to that observed with the commonly used, panselective PI3K inhibitor LY294002, which also inhibits MHC-I downregulation in heterologous cells (Figure 1B).

The ability of PI3K inhibitors to repress efficient downregulation of cell-surface MHC-I by HIV-1 Nef in primary $CD4^+$ T cells was in direct conflict with other reports. PI3K activity had no effect on Nef-mediated downregulation of MHC-I in the leukemic T cell lines Jurkat and CEM or in U373 cells (Kasper and Collins, 2003; Larsen et al., 2004). However, PIP_3, the product of the class I PI3Ks, is rapidly dephosphorylated by one of several D-3 (PTEN) or D-5 (SHIP-1 and -2) lipid phosphatases, attenuating PI3K-stimulated signaling pathways (Deane and Fruman, 2004). Interestingly, Jurkat, CEM, and U373 cell lines

or VV:Nef and treated or not with PI-103 as above were incubated with mAb W6/32 (3 μg/ml) for 30 min and then chased for an additional 30 min, fixed, and processed for immunofluorescence microscopy. Scale bar, 10 μm. Bottom: H9 $CD4^+$ T cells were infected with VV:WT or VV:Nef (moi = 10, 8 hr), then treated or not with PI-103 for 1 hr, and then analyzed by flow cytometry using mAb W6/32.

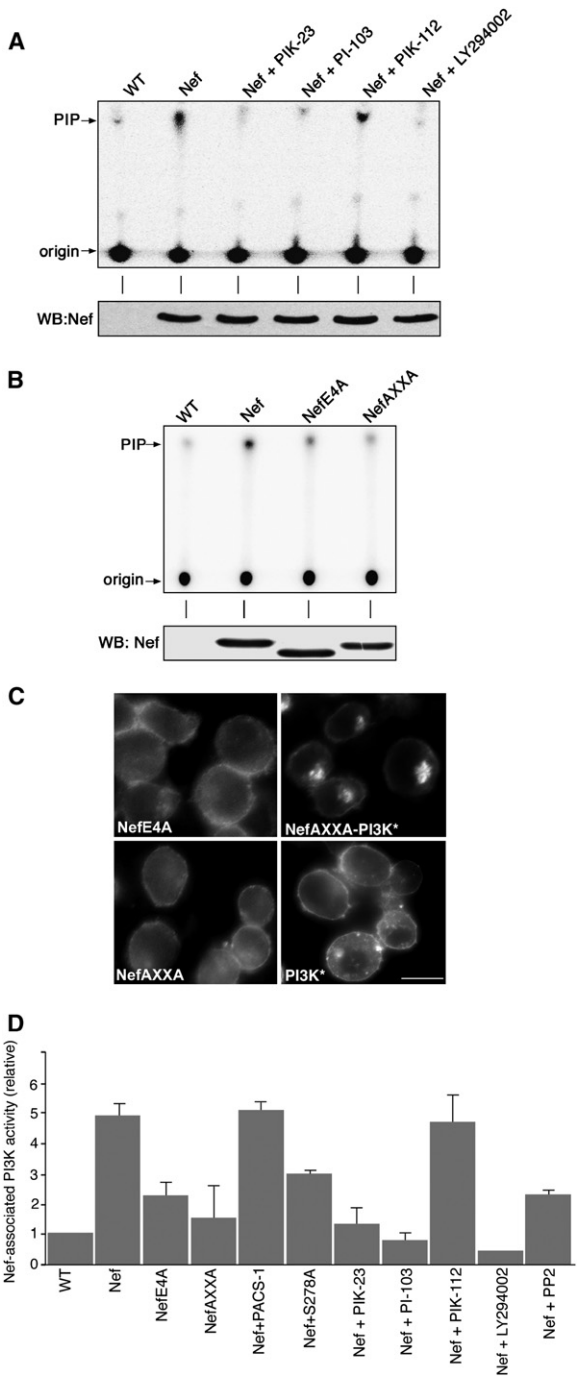

Figure 2. Nef-Stimulated PI3K Activity Requires Nef $EEEE_{65}$ and $PXXP_{75}$

(A) Primary $CD4^+$ T cells cultured in Il-7 were infected with VV:WT or VV:Nef/f (moi = 10, 12 hr). Following Nef/f immunoprecipitation (shown on western blot), the samples were treated or not with 0.1 μM PIK-23, PI-103, or PIK-112 or with 10 μM LY294002 or DMSO for 10 min, and Nef-associated PI3K activity was measured as described in the Experimental Procedures.

(B) H9 $CD4^+$ T cells infected with the indicated VV vectors (moi = 5, 8 hr) were lysed, and Nef-associated PI3K was measured as described in the Experimental Procedures. Bottom: Western blot showing the expression of Nef/f constructs.

(C) H9 $CD4^+$T cells expressing the indicated constructs were processed for immunofluorescence microscopy, and MHC-I molecules were detected with mAb W6/32 as described in the legend to Figure 1E. Scale bar, 10 μm.

(D) Replicate plates of H9 $CD4^+$ T cells infected with VV:WT or with VV recombinants expressing the indicated proteins (total moi = 5, 8 hr) were treated or not with 10 mM PP2 or, following immunoprecipitation with mAb M2, with the indicated PI3K inhibitors as described in (A) and then analyzed for PI3K activity. Error bars represent the mean ± SD of three independent experiments.

lack PTEN (Figure 1C). Consistent with the absence of PTEN, Jurkat cells contain inordinately high levels of PIP_3, an otherwise low-abundance and transiently produced phosphoinositide (Astoul et al., 2001). Therefore, we speculated that, in the absence of a PIP_3 phosphatase, transient inhibition of PI3K activity would marginally affect PIP_3 levels, thus negating the pharmacologic inhibition of PI3K-dependent HIV-1 Nef-mediated MHC-I downregulation. To test this possibility, we expressed HIV-1 Nef in U373 cells in the absence or presence of LY294002, and in agreement with others (Larsen et al., 2004), we found that the inhibitor had no effect on MHC-I downregulation (Figure 1D). We then asked whether rescue of PTEN expression in U373 cells would restore sensitivity of the Nef-mediated MHC-I downregulation pathway to LY294002. Accordingly, we found that LY294002 inhibited Nef-mediated MHC-I downregulation in PTEN-rescued U373 cells (Figure 1D).

Our determination that HIV-1 Nef requires a PI3K in U373 cells led us to ask whether PI3K activity is required for Nef to downregulate cell-surface MHC-I in H9 $CD4^+$ T cells, which like primary $CD4^+$ T cells are replete with expression of PTEN and other PIP_3 phosphatases (Figure 1C). Accordingly, the panselective inhibitor LY294002 and the class I PI3K inhibitor PI-103 hindered Nef-mediated downregulation of MHC-I in H9 cells (Figure 1E), but not in cells treated with PTEN siRNA (Figure S3). Because PI-103 inhibits mTOR and class I p110 catalytic subunits, we tested whether PIK-23, a quinazolinone purine derivative that selectively targets p110δ (Knight et al., 2006), could inhibit MHC-I downregulation. Like PI-103, PIK-23 repressed Nef-mediated MHC-I downregulation in H9 $CD4^+$ T cells at all concentrations tested (Figure 1E). The PI-103-sensitive, Nef-induced redistribution of MHC-I to the paranuclear region resulted primarily from the downregulation of cell-surface molecules as determined by antibody uptake and flow cytometry (Figure 1E), as well as by the inability of Nef to block delivery of newly synthesized MHC-I molecules to the cell surface (Figure S4). Control experiments showed that the amount of Nef expression per infected cell using either the vaccinia or pseudovirus vectors did not exceed the amount of Nef expressed in HIV-1-infected cells (Figure S5), supporting the physiologic relevance of these results. Furthermore, expression of mutant proteins that block the ARF6-dependent endocytic pathway—including $ARNOE_{156}K$, an inactive form of the PIP_3 binding ARF6 GEF, ARNO, and the ARF6 mutant, $ARF6Q_{67}L$—blocked Nef-mediated MHC-I downregulation in H9 cells

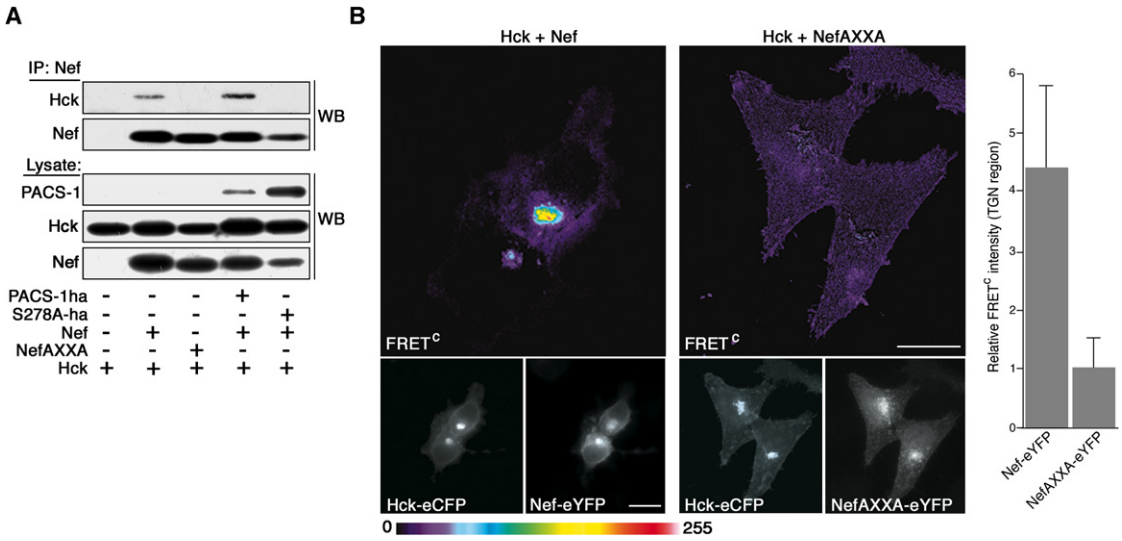

Figure 3. Nef $PXXP_{75}$ Recruits an SFK at the TGN

(A) A7 cells were infected with VV recombinants expressing the indicated proteins (total moi = 10, 16 hr) and were harvested, Nef constructs were immunoprecipitated from the membrane fractions with mAb M2, and coprecipitating Hck was detected by western blot. Bottom: Western blot showing expression of Hck, Nef, and the PACS-1 constructs.

(B) Left: Images of HeLa-$CD4^+$ cells coexpressing Hck-eCFP with Nef-eYFP or NefAxxA-eYFP were acquired using filters for CFP (lower left), YFP (lower right), and FRET (data not shown). $FRET^C$ (top) was calculated as described in the Experimental Procedures and is presented as a quantitative pseudocolor image with the corresponding pseudocolor scale (bottom). Scale bar, 20 μm. Right: Difference in $FRET^C$ between samples expressing Nef-YFP or NefAXXA-YFP. Error bars represent the mean ± SD of two independent experiments (n = 20).

(Figure S6). Thus, HIV-1 Nef requires a PI3K-stimulated, ARF6-controlled endocytic pathway to efficiently downregulate cell-surface MHC-I in $CD4^+$ T cells lines, and a functional PTEN is required to observe this effect.

Nef $EEEE_{65}$ and $PXXP_{75}$ Motifs Act Sequentially to Stimulate Nef-Associated PI3K Activity

The ability of Nef to bind the p85 regulatory subunit of PI3K (Linnemann et al., 2002), together with the requirement for Nef $EEEE_{65}$ and $PXXP_{75}$ to promote MHC-I downregulation by triggering the PIP_3-dependent activation of an ARF6-dependent endocytic pathway (Blagoveshchenskaya et al., 2002), raised the possibility that these two Nef motifs combine to stimulate a Nef-associated PI3K activity necessary to downregulate cell-surface MHC-I in $CD4^+$ T cells. To test this possibility, we first determined if Nef recruited PI3K in primary $CD4^+$ T cells. We expressed epitope (FLAG)-tagged Nef in IL-7-treated cells, then measured the amount of coprecipitating PI3K activity using an in vitro kinase assay (Figure 2A). In agreement with the immunofluorescence data (Figure 1E), the coprecipitating PI3K activity was blocked by LY294002, PIK-23, and PI-103, but not by PIK-112, demonstrating that Nef recruited a class I PI3K in vivo (Figure 2A). We extended these studies to H9 $CD4^+$ T cells and found that Nef mutants containing an $EEEE_{65} \rightarrow AAAA_{65}$ mutation (NefE4A), which disrupts binding of Nef to PACS-1, or a $PXXP_{75} \rightarrow AXXA_{75}$ mutation (NefAXXA), which blocks binding of Nef to SH3 domain-containing proteins, including SFKs, inhibited PI3K stimulation and MHC-I downregulation (Figures 2B and 2C). In agreement with the requirement for Nef $EEEE_{65}$ binding to PACS-1 to efficiently downregulate cell-surface MHC-I (Piguet et al., 2000), we found that the interfering mutant PACS-$1S_{278}A$, which inhibits binding of PACS-1 to Nef (Scott et al., 2003), reduced the amount of Nef-associated PI3K activity and inhibited MHC-I downregulation in H9 $CD4^+$ T cells (Figure 2D). However, as PI3K binds to the C-terminal region of Nef and not to the Nef $PXXP_{75}$ SH3 domain-binding motif (Linnemann et al., 2002), our results did not explain why NefAXXA failed to stimulate PI3K. Nef $PXXP_{75}$, but not $AXXA_{75}$, binds to SFKs, so we tested whether Nef-stimulated PI3K activity required an active SFK. Accordingly, we found that the SFK inhibitor PP2 blocked the stimulation of Nef-associated PI3K activity (Figure 2D; see also Figure 4A).

Nef $EEEE_{65}$-Mediated Targeting Enables $PXXP_{75}$ to Bind Src Family Kinases

Our results suggested that the Nef $EEEE_{65}$ and $PXXP_{75}$ motifs cooperate with a PP2-sensitive SFK to stimulate PI3K activity. Thus, Nef $EEEE_{65}$ may enable Nef $PXXP_{75}$ to bind an SFK, many of which localize to the TGN (Bard et al., 2002; Carreno et al., 2000). To test this possibility, we asked whether $EEEE_{65}$ regulates association of Nef with Hck (Figure 3A). We chose to examine Hck because Nef binding activates Hck (Lerner and Smithgall, 2002), and Hck is also required for rapid onset of HIV pathogenesis in transgenic mouse models (Hanna et al., 2001), while interfering fragments of Hck containing the SH3 domain block MHC-I downregulation (Chang et al., 2001). First, we coexpressed Hck with Nef or NefAXXA in cells

and, in agreement with an essential role for $PXXP_{75}$ to bind SFKs, we found that Nef, but not NefAXXA, coimmunoprecipitated Hck. Second, we coexpressed Nef and Hck with PACS-$1S_{278}$A or PACS-1, finding that PACS-$1S_{278}$A blocked the association of Nef with Hck on cell membranes, while PACS-1 had no effect (Figure 3A).

To determine whether HIV-1 Nef binds to SFKs at the TGN, we conducted an intermolecular FRET assay. We coexpressed Hck-CFP in HeLa-$CD4^+$ cells with Nef-YFP or NefAXXA-YFP, which localize to the TGN and emit a fluorescent signal with similar intensity (Figure 3B). To detect the intermolecular FRET signal, we exposed the cells to 436 nm light to excite Hck-CFP and measured fluorescence of Nef-YFP or NefAXXA-YFP at 535 nm. Only cells coexpressing Hck-CFP and Nef-YFP, but not NefAXXA-YFP, revealed a positive paranuclear FRET signal, indicating that the Nef-YFP binds to Hck-CFP at the TGN. Together, these results suggest that targeting to the TGN enables Nef to then bind an SFK, which subsequently stimulates PI3K activity required for Nef to downregulate cell-surface MHC-I.

Nef Binding to SFK Increases Association with PI3K

Our determination that PP2 inhibits Nef-associated PI3K activity and that Nef $PXXP_{75}$ binds to TGN-localized SFKs (Figures 2 and 3) suggested that bound SFKs enhance the recruitment of PI3K to Nef. In agreement with this possibility, we found that coexpression of Hck with Nef, but not NefAXXA, increased the amount of class I PI3K regulatory subunit p85 that coprecipitated with Nef and correspondingly increased the amount of Nef-associated PI3K activity (Figure 4A). Because Nef $PXXP_{75}$ binds and activates Hck (Lerner and Smithgall, 2002; and Figure S7), we asked whether the increased association of Nef with PI3K required SFK activity. We determined that, indeed, treatment of the cells with PP2 or coexpression of Nef with a catalytically inactive Hck mutant (Hck-KE; Lerner and Smithgall, 2002) blocked Hck activation (Figure S7) and the increase in coprecipitating PI3K activity, suggesting that an active SFK bound to $PXXP_{75}$ is required for Nef to stimulate recruitment of PI3K. The ability of Hck-KE to block Nef-mediated PI3K stimulation agrees with the report that a fragment of Hck containing the SH3 domain can block MHC-I downregulation in $CD4^+$ T cells (Chang et al., 2001). Next, we asked whether the association of PI3K with Hck was dependent upon Nef expression. We immunoprecipitated endogenous PI3K from cells that coexpressed Hck with Nef or NefAXXA and detected coimmunoprecipitating Hck by western blot (Figure 4B), finding that p85 coimmunoprecipitated Hck in the presence of Nef, but not NefAXXA. In addition to activating Hck, Nef also directly activates Src and Lyn (Trible et al., 2006). As Hck is most abundantly expressed in myeloid cells, we asked whether Src, which is broadly expressed, can similarly promote recruitment of PI3K to Nef. Accordingly, we found Src stimulated the amount of PI3K associated with Nef, but not NefAXXA. It also stimulated Nef-associated PI3K activity (Figure S8). Together, these findings suggest Nef serves as a scaffold to link activated SFKs to PI3K.

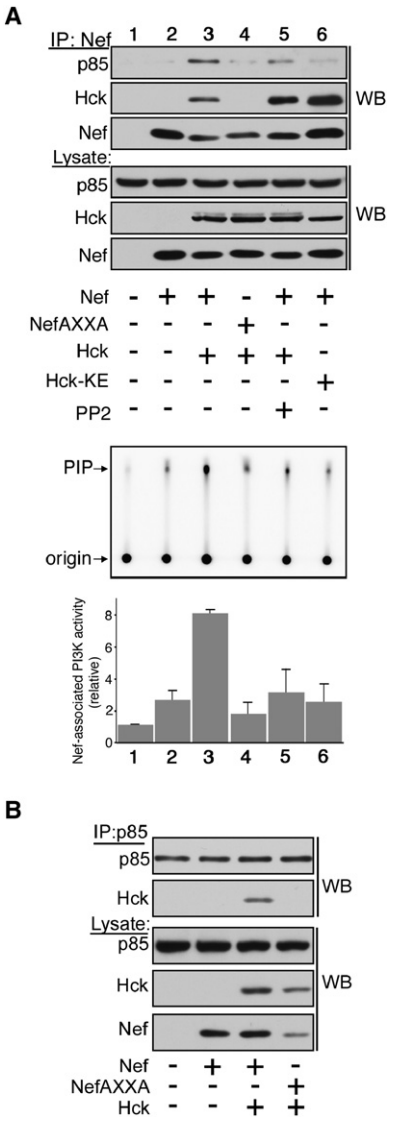

Figure 4. PI3K Recruitment by Nef Requires an Activated SFK Bound to Nef $PXXP_{75}$

(A) H9 $CD4^+$T cells infected with VV:WT or recombinant VV expressing the indicated proteins (moi = 6, 8 hr) were harvested, Nef proteins were immunoprecipitated, and coimmunoprecipitated Hck and p85 were detected by western blot. Coimmunoprecipitated PI3K activity was quantified as described in the legend to Figure 2. PP2 (10 μM) was added 2 hr prior to cell harvesting where indicated.

(B) H9 $CD4^+$ T cells infected with VV recombinants expressing the indicated proteins (moi = 6 total, 8 hr) were harvested, and p85 was immunoprecipitated from the extracts. Coimmunoprecipitated Hck and Nef were detected by western blot.

Bottom (A and B): Western blot showing expression of Nef and Hck and the amount of cellular p85.

Nef-SFK Recruits ZAP-70 to Stimulate PI3K

The requirement for an active SFK bound to Nef $PXXP_{75}$ to stimulate PI3K activity suggested that a Nef-bound SFK

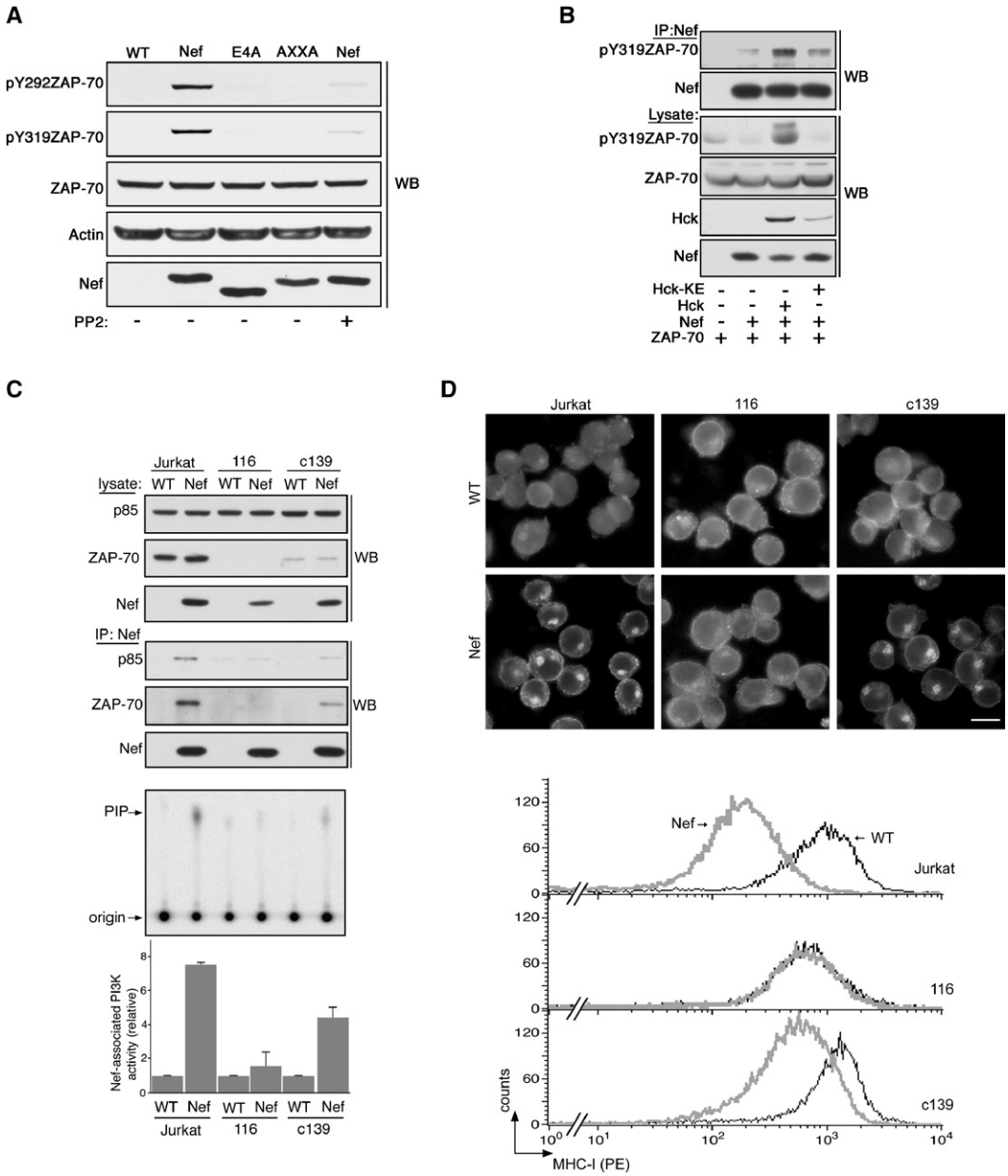

Figure 5. Nef/SFK Recruits and Activates ZAP-70 to Stimulate MHC-I Downregulation

(A) Jurkat CD4$^+$T cells infected with VV:WT or recombinant VV expressing the indicated proteins (moi = 10, 8 hr) in the absence or presence of PP2 (10 μM) were harvested, and pY_{292}ZAP-70 pY_{319}ZAP-70 were detected by western blot. Bottom: Western blot showing expression of the Nef constructs and the amount of cellular ZAP-70 and actin.

(B) 293T cells expressing ZAP-70 were infected with VV recombinants expressing the indicated proteins and were harvested, Nef proteins were immunoprecipitated, and coimmunoprecipitated phospho-ZAP-70 was detected by western blot. Bottom: Western blot showing expression of the Nef, Hck, and cellular ZAP-70.

(C) Replicate plates of Jurkat, JurkatP116, or JurkatP116.c139 cells were infected with VV:WT or VV:Nef/f (moi = 10, 8 hr). Nef was immunoprecipitated, and coimmunoprecipitating ZAP-70 and p85 were detected by western blot. The amount of coimmunoprecipitated PI3K activity was quantified as described in the legend to Figure 2. Top: Western blot showing the expression of Nef constructs and cellular ZAP-70 and p85.

(D) Jurkat, JurkatP116, or JurkatP116.c139 cells were infected with VV:WT or VV:Nef (moi = 10, 4 hr). The cells were fixed and stained with anti-MHC-I mAb W6/32 (scale bar, 10 μm). Bottom: Replicate cell cultures were stained with mAb W6/32 and processed for flow cytometry as described in the Experimental Procedures.

may directly phosphorylate PI3K. Yet we failed to detect phosphotyrosine on the p85 regulatory subunit that coimmunoprecipitates with Nef, suggesting that an activated SFK bound to Nef is necessary but not sufficient to stimulate PI3K. We thus sought to identify a substrate of the bound SFK that would stimulate PI3K. Recent studies

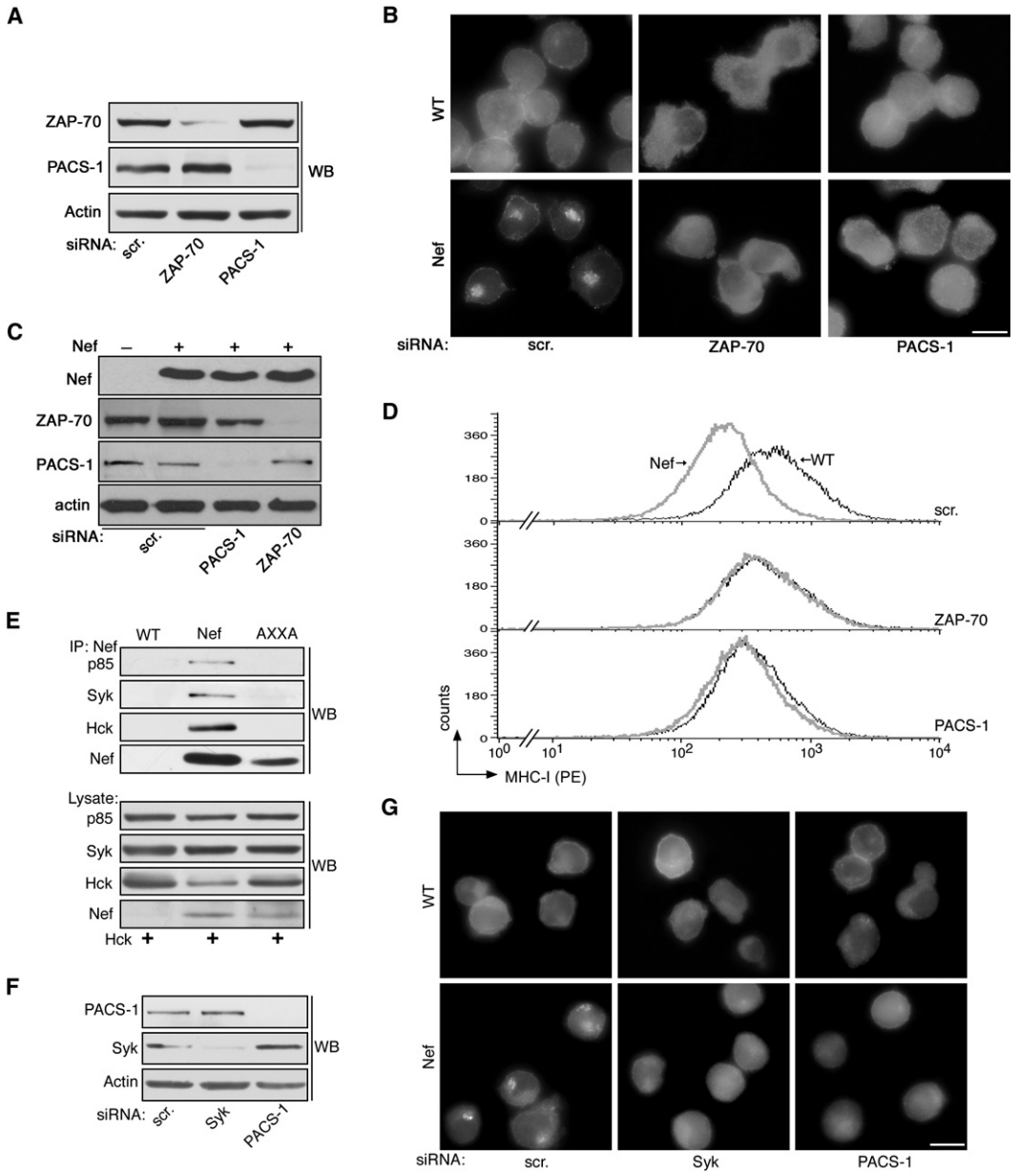

Figure 6. siRNA Depletion of PACS-1 and ZAP-70/Syk Block MHC-I Downregulation in H9 and Primary CD4$^+$ T Cells and in Promonocytic TF-1 Cells

(A) H9 CD4$^+$ T cells were nucleofected with pmaxGFP and either a control siRNA (scr) or siRNAs specific for ZAP-70 or PACS-1. After 60 hr, cells expressing GFP were collected by FACS, and the amounts of PACS-1, ZAP-70, and actin were determined by western blot.

(B) H9 CD4$^+$ T cells from (A) were infected with VV:WT or VV:Nef (moi = 10, 5 hr) and fixed, and MHC-I molecules were stained with mAb W6/32. Scale bar, 10 μm.

(C) Primary CD4$^+$ T cells isolated from a healthy donor were cultured in IL-7 and then nucleofected with a control siRNA (scr) or with siRNAs specific for ZAP-70 or PACS-1. After 60 hr, the cells were infected with VV:WT or VV:Nef (moi = 10, 16 hr) and analyzed by western blot.

(D) Primary CD4$^+$ T cells from (D) were analyzed by flow cytometry using mAb W6/32. Similar results were obtained using Nef$^+$ and Nef$^-$ pseudotyped viruses (data not shown).

(E) TF-1 cells infected with VV recombinants coexpressing Hck with Nef or NefAXXA (moi = 10 total, 8 hr) were harvested, and Flag-tagged Nef or NefAXXA were immunoprecipitated from the extracts. Coimmunoprecipitated Hck, Syk, and p85 were then detected by western blot. Bottom: Western blot showing expression of Nef, NefAXXA, and Hck constructs and the levels of cellular Syk and p85.

(F) TF-1 cells were nucleofected with pmaxGFP and either a control siRNA (scr) or siRNAs specific for Syk or PACS-1. After 48 hr, cells expressing GFP were collected by FACS and harvested, and the amounts of PACS-1, Syk, and actin were determined by western blot.

(G) TF-1 cells from (F) were infected with VV:WT or VV:Nef (moi = 10, 5 hr) and fixed, and MHC-I molecules were stained with mAb W6/32. Scale bar, 10 μm.

show that SFK phosphorylation of Syk or ZAP-70 forms a tyrosine motif that binds the C-terminal SH2 domain of p85 to stimulate PI3K- and ARF6-dependent phagocytosis (Moon et al., 2005; Zhang et al., 1998). We tested whether Nef/SFK usurped ZAP-70 to stimulate PI3K and found that Nef stimulated the tyrosine phosphorylation of ZAP-70 at Tyr_{292}, which is necessary for binding p85 (Figure 5A and Moon et al., 2005). By contrast, NefE4A, NefAXXA, or treatment of Nef-expressing cells with PP2 failed to activate ZAP-70, suggesting that $EEEE_{65}$ and binding of an active SFK to Nef $PXXP_{75}$ are essential for ZAP-70 activation. We also asked whether Hck could increase the association of Nef with ZAP-70, finding that Hck, but not inactive Hck-KE, increased the association of Nef with phosphorylated ZAP-70 (Figure 5B).

We then asked if ZAP-70 is required for Nef-mediated stimulation of PI3K activity and for Nef to downregulate cell-surface MHC-I. We expressed Nef in genetically paired Jurkat-derived cell lines that either lack Syk/ZAP-70 (P116 cells) or are rescued for ZAP-70 expression (P116.c39 cells, Figure 5C, top), immunoprecipitated the Nef molecules, and then quantified the amount of Nef-associated PI3K activity (Figure 5C). In agreement with our studies in H9 $CD4^+$ T cells, we found that Nef associated with PI3K in Jurkat cells. However, Nef failed to associate with PI3K in ZAP-70-deficient 116 cells. By contrast, Nef coimmunoprecipitated PI3K in the ZAP-70-rescued 139 cells. We used the ZAP-70-deficient and -rescued cell lines to determine whether ZAP-70 is required for Nef to downregulate cell-surface MHC-I and found that Nef failed to downregulate MHC-I in the ZAP-70-deficient 116 cells (Figure 5D). However, Nef downregulated cell-surface MHC-I in the ZAP-70-rescued 139 cells. As these experiments did not rely on PI3K inhibitors, results from these Jurkat cells were not confounded by the lack of PTEN.

siRNA Depletion of PACS-1 or ZAP-70 Inhibits Nef-Mediated MHC-I Downregulation in Primary $CD4^+$ T Cells

To establish that our results demonstrating the importance of ZAP-70 for the Nef-mediated downregulation of cell-surface MHC-I were not restricted to the Jurkat-derived cell clones, we asked whether siRNA depletion of ZAP-70 from H9 $CD4^+$ T cells would similarly block MHC-I downregulation. We treated H9 $CD4^+$ T cells with a control siRNA or with siRNAs that specifically depleted ZAP-70 or PACS-1 (Figure 6A), then expressed Nef in the siRNA-treated cells and measured MHC-I downregulation (Figure 6B). Depletion of ZAP-70 or PACS-1 repressed MHC-I downregulation, whereas the control siRNA had no effect. Next, to test whether Nef requires PACS-1 and ZAP-70 to downregulate MHC-I in primary $CD4^+$ T cells, we treated primary $CD4^+$ T cells with a control siRNA or with siRNAs that deplete PACS-1 or ZAP-70 (Figure 6C), then infected the cells with VV:WT or VV:Nef and measured downregulation of cell-surface MHC-I by flow cytometry (Figure 6D). Depletion of either PACS-1 or ZAP-70 inhibited Nef from efficiently downregulating MHC-I in primary $CD4^+$ T cells.

Finally, whereas ZAP-70 is expressed principally in T cells, its homolog Syk is broadly expressed in diverse cell types, including macrophages, which, like resting $CD4^+$ T cells, constitute a long-lived HIV-1 reservoir (Stevenson, 2003). Therefore, we asked whether Nef can use Syk in addition to ZAP-70 to stimulate PI3K. We determined that Nef, but not NefAXXA, associated with Hck, Syk, and PI3K in TF-1 promonocytic cells (Figure 6E). Accordingly, we treated TF-1 cells with siRNAs that depleted Syk or PACS-1 (Figure 6F). We then expressed Nef in the cells and found that siRNA depletion of Syk or PACS-1 blocked Nef-mediated downregulation of MHC-I (Figure 6G). Similar results were obtained using heterologous HeLa-$CD4^+$ cells, which also express Syk (Figure S9). Together, our results identify a novel Nef-SFK-ZAP-70/Syk-PI3K pathway that downregulates cell-surface MHC-I molecules in diverse HIV-1 target cells.

DISCUSSION

We identify a Nef-SFK-ZAP-70/Syk-PI3K signaling/trafficking pathway that HIV-1 Nef employs to downregulate cell-surface MHC-I. This pathway appears to be ubiquitous, since interference with SFKs, Syk/ZAP-70, or PI3K disrupts Nef-mediated MHC-I downregulation in all cell types examined that express a functional PIP_3 phosphatase, including primary $CD4^+$ T cells (Figures 1, 5, and 6 and Figures S3 and S9). Whereas SFK activation is usually triggered by C-terminal dephosphorylation, which relieves interdomain interactions that mask the active site, HIV-1 Nef overrides these inhibitory interactions by direct binding of its $PXXP_{75}$ motif to the SH3 domain on Hck, thereby unmasking the catalytic domain independent of dephosphorylation (Lerner and Smithgall, 2002). Recent studies show that this mode of Nef-mediated SFK activation also includes activation of Lyn and Src (Trible et al., 2006), supporting a role for Nef to directly activate SFKs expressed in multiple cell types. Interestingly, although Hck and Src have prominent roles at the plasma membrane, pools of these SFKs are present in other cellular compartments, including the Golgi/TGN (Bard et al., 2002; Carreno et al., 2000). Thus, Nef $EEEE_{65}$, which directs binding to PACS-1, enables Nef $PXXP_{75}$ to bind and directly activate SFKs sequestered in TGN-associated reservoirs. Our determination that PACS-$1S_{278}$A, PP2, and Hck-KE block the Nef-mediated stimulation of PI3K in multiple cell types, whereas expression of Hck or Src promotes recruitment of PI3K to Nef, supports this model (Figures 2, 4, and 5 and Figure S8).

Following activation, the Nef-associated SFK promotes recruitment and activation of ZAP-70, which is required to stimulate the PI3K-dependent downregulation of cell-surface MHC-I (Figures 5 and 6). In response to T cell receptor (TCR) ligation, ZAP-70 is recruited to phosphorylated immunoreceptor tyrosine-based activation motifs (ITAMs) present on the CD3ζ cytosolic domain, activating this Syk family kinase to phosphorylate

adaptor molecules that activate T cells (Deane and Fruman, 2004). We do not know if Nef directly binds ZAP-70. Nef lacks an ITAM motif, suggesting that ZAP-70 does not bind by this method. Interestingly, however, a mutant SIV Nef containing an ArgGln→TyrGlu substitution creates an ITAM motif that binds to and activates ZAP-70, mimicking the TCR and costimulatory signals that permit the aberrant and robust replication of the virus in unstimulated $CD4^+$ T cells, followed by rapid death of the host (Luo and Peterlin, 1997). The recent demonstration that SFK phosphorylation of ZAP-70 at the non-YXXM motif pY_{292} promotes binding of ZAP-70 to PI3K to increase receptor endocytosis suggests that HIV-1 usurps components of this cellular PI3K signaling pathway to stimulate MHC-I downregulation (Moon et al., 2005). Moreover, the ability of tyrosine phosphorylated Syk to also bind p85 (Moon et al., 2005) supports our determination that Nef can use Syk in place of ZAP-70 to stimulate PI3K and downregulate cell-surface MHC-I in cell types ranging from TF-1 promonocytic cells to HeLa-$CD4^+$ cells, which also express Syk (Figure 6 and Figure S9).

Our experiments identify the hierarchical role of the Nef $EEEE_{65}$ and $PXXP_{75}$ motifs in controlling MHC-I downregulation. Nef $EEEE_{65}$ and $PXXP_{75}$ combine to assemble a Nef-SFK-ZAP-70-PI3K complex that stimulates the ARF6-controlled endocytosis of cell-surface MHC-I, whereas Nef M_{20} promotes delivery of the endocytosed MHC-I to paranuclear compartments. The inability of Nef to block delivery of newly synthesized MHC-I to the surface of H9 $CD4^+$ T cells (Figure S4) supports our model that Nef triggers the downregulation of cell-surface MHC-I. The recent determination that Nef M_{20} is required for recruiting intracellular MHC-I to AP-1, which is necessary for endosome-to-TGN trafficking, is also consistent with our model (Roeth et al., 2004). However, our results differ from those of others (Kasper and Collins, 2003; Larsen et al., 2004), who reported that Nef-mediated MHC-I downregulation was controlled by a PI3K-independent mechanism and that Nef blocks delivery of newly synthesized MHC-I to the cell surface. Several factors may have contributed to these differing results. First, these authors relied on PTEN-deficient cells to ascertain the role of PI3K in Nef-mediated downregulation of MHC-I, which possess inordinately high levels of PIP_3 and thus respond poorly to PI3K inhibitors (Deane and Fruman, 2004). The ability of PTEN to rescue sensitivity of Nef-expressing U373 cells to LY294002 confirms the shortcoming of these cell lines to study Nef's role in HIV-1 immunoevasion (Figure 1) and underscores the large number of conflicting studies in T cell biology attributed to the use of PTEN-deficient cell lines (Astoul et al., 2001). Second, that cell-surface MHC-I is endocytosed by an ARF6-dependent pathway and is not blocked by dynamin/AP-2 mutants (Blagoveshchenskaya et al., 2002; Le Gall et al., 2000) may also have confounded elucidation of this MHC-I downregulation pathway (Swann et al., 2001). Third, in contrast to others (Williams et al., 2005), we found that the inability of NefE4A and NefAXXA mutants to downregulate MHC-I was due, at least in part, to specific defects in the PI3K signaling pathway. The various studies of Nef expression may also define two physiologically relevant modes of MHC-I downregulation—a signaling-dependent mode identified here, which triggers downregulation of cell-surface MHC-I, and a stoichiometric mode, which blocks transport of newly synthesized MHC-I molecules to the cell surface (Kasper and Collins, 2003; Roeth et al., 2004). Whether the two modes of MHC-I downregulation reflect reservoir- or host cell-activation-state-dependent activities of Nef warrants further investigation.

The recent identification of isoform-specific PI3K inhibitors provides new strategies to combat disease. For example, PI-103 constrains the growth of gliomas in vivo (Fan et al., 2006). Thus, the ability of PI-103 to suppress Nef-mediated downregulation of MHC-I in $CD4^+$ T cells (Figure 1) suggests that HIV-1 may be an additional target for this novel inhibitor. Importantly, Nef induces macrophages to release chemokines, luring nonactivated T cells and causing them to become permissive to the virus, thereby creating a very long-lived HIV-1 reservoir unlikely to be eradicated by HAART (Stevenson, 2003). Thus, the ability of PI-103 to inhibit Nef-mediated MHC-I downregulation in naive IL-7-treated primary $CD4^+$ T cells suggests a novel strategy to combat the virus (Figure 1). Interestingly, whereas PI-103 is a multitargeted PI3K inhibitor, quinazolinone purines, including PIK-23, are exquisitely selective for p110δ, which is largely restricted to leukocytes. As mice lacking an active p110δ are viable (Okkenhaug et al., 2002), specifically targeting this PI3K isoform may provide a novel approach to disrupt HIV-1 in leukocyte reservoirs without affecting PI3K activity in other tissues.

The Nef-SFK-ZAP-70/Syk-PI3K axis that we report here may have implications beyond solely controlling MHC-I downregulation. The same Nef motifs controlling MHC-I downregulation are also involved in PAK2 activation, in the blocking of T cell maturation, and perhaps in MHC II-mediated antigen presentation. The Nef $EEEE_{65}$ and $PXXP_{75}$ SH3 motifs and PI3K are all required to activate PAK2, which further arms the HIV-1 antiviral counterattack (Das and Jameel, 2005 and our unpublished data). Similarly, Nef requires the Nef $EEEE_{65}$ and $PXXP_{75}$ motifs to disrupt maturation of $CD34^+$ thymocytes (Stove et al., 2003), and PI3K inhibitors block the Nef-induced increase in cell-surface levels of immature MHC-II and FasL, raising the possibility that Nef turns the host's own apoptotic arsenal against itself, such that infected cells kill the very same $CD8^+$ CTLs that target them by Fas-FasL binding (Das and Jameel, 2005; Peterlin and Trono, 2003; Zauli et al., 1999). Together, our results explain the role of the Nef $EEEE_{65}$ and $PXXP_{75}$ motifs for mediating HIV-1 immunoevasion and potentially additional facets of HIV-1 disease by directing the formation of a Nef-SFK-ZAP-70/Syk-PI3K multikinase signaling complex in diverse cell types, and in doing so, we suggest new strategies to block this pathway in the treatment of AIDS.

EXPERIMENTAL PROCEDURES

Cells and Recombinant Virus

293T, HeLa-CD4$^+$, A7 melanoma, U373 astrocytoma, and Jurkat CD4$^+$ leukemic T cells were cultured as described (Blagoveshchenskaya et al., 2002; Crump et al., 2003). Jurkat-derived P116 and P116.c139 cells (provided by A. Weiss) and H9 CD4$^+$ T cells were cultured in RPMI-1640 supplemented with 10% FBS. TF-1 promonocytic cells were cultured in RPMI-1640 supplemented with 10% FBS and 2 ng/ml GM-CSF (Sigma).

Naive CD4$^+$ T cells were isolated from freshly drawn blood or from leukapheresed cells donated by four healthy volunteers using a MACS CD4$^+$ T cell isolation kit (Miltenyi Biotec). The purity of the CD4$^+$ T cell population was verified by FACS using PE-conjugated anti-CD4 (mAb Leu-3a, BD). Isolated cells were cultured in RPMI 1640 containing 10% FBS and supplemented with 2 ng/ml IL-7 for 4 days or treated with IL-2 (1 U/ml for siRNA studies or 5 U/ml for PI3K studies; Sigma) and 1 μg/ml PHA (Sigma) prior to infection.

HIV-1 NL4-3 was grown and titered as described (Scholz et al., 2005). Vaccinia virus (VV) expressing flag-tagged Nef, NefE4A, NefAXXA, and NefAXXA-PI3K*, as well as PI3K*, ARF6, ARF6Q$_{67}$L, ARNO, ARNOE$_{156}$K, Src, PACS-1, and PACS-1S$_{278}$A were generated and titered on BSC-40 cells as described (Blagoveshchenskaya et al., 2002; Ely et al., 1994; Scott et al., 2003). VV expressing Hck or Hck-KE cDNAs (provided by T. Smithgall) or ZAP-70 cDNA (provided by A. Weiss) were prepared as described (Blagoveshchenskaya et al., 2002). To produce the HIV pseudotyped viruses NL4-3ΔG/P-EGFP and NL4-3ΔG/P-EGFP/Δ Nef, 293T cells were cotransfected with the packaging vector pCMVΔR8.2, pMD.G, which expresses VSV-G and either pNL4-3ΔG/P-EGFP or pNL4-3:ΔG/P-eGFP/ΔNef (provided by P. Klotman). At 48 hr postinfection, viruses were collected and titered on 293T cells based on GFP expression. Cells were infected with NL4-3ΔG/P-EGFP or NL4-3:ΔG/P-eGFP/ΔNef (moi = 5) in the presence of 6 μg/ml polybrene (Sigma).

PI3K Inhibitors and siRNA

PI-103, PIK-23, and PIK-112 (Knight et al., 2006), and LY294002 (Calbiochem), were used as indicated. For cell experiments, inhibitors were added at 21–48 hr postinfection; cells were processed for flow cytometry at 24–60 hr postinfection, depending upon the donor. Control (scr) siRNA and siRNAs specific for PACS-1, ZAP-70, Syk, and PTEN (Dharmacon) were nucleofected into cells according to the vendor's instructions (Amaxa). In some experiments, cells were conucleofected with pmaxGFP to enrich transfected cell populations by FACS.

FACS and Flow Cytometric Analysis

Where indicated, GFP$^+$ cells were selected using a FACS Vantage flow cytometer cell sorter. For flow cytometry, cells were washed and resuspended in FACS buffer (PBS [pH 7.2] containing 0.5% BSA and 0.1% NaN_3). Cells were incubated with mAb W6/32 (1:4000) or mAb BB7.1 (anti-HLA-A2.1, 1:400; BD) at 4°C for 1 hr. An isotype-matched antibody was used as a negative control. Cells were then washed and incubated with PE-conjugated donkey anti-mouse IgG (1:400; Jackson IR) at 4°C for 30 min. Cells were washed and analyzed by listmode acquisition on a FACSCalibur (BD) using CellQuest acquisition/analysis software (BD).

FRET Analysis

Nef-YFP and NefAXXA-YFP were constructed by subcloning the Nef and NefAXXA cDNAs into peYPF-N1 (Clontech); Hck-eCFP was constructed by subcloning the Hck cDNA into peCFP-N1 (Clontech). HeLa-CD4$^+$ cells were cotransfected with pHck-eCFP and either pNef-eYFP or pNefAXXA-eYFP (Fugene, Roche). After 24 hr, images were captured using a 63× oil immersion objective lens and a cooled CCD camera and recorded using MetaMorph software (Molecular Dynamics). To measure FRET, three images were acquired in the beginning with a CFP filter set (λ_{ex} 436/10 nm, λ_{em} 470/30 nm), followed by a YFP filter set (λ_{ex} 500/20 nm, λ_{em} 535/30 nm) and then a FRET filter set (λ_{ex} 436/10, λ_{em} 535/30 nm). Images were background subtracted, and the corrected FRET (FRET^C) was obtained from the raw FRET images by subtracting the bleedthrough signals emitted through the CFP and YFP channels from cells expressing Hck-CFP, Nef-YFP, or NefAXXA-YFP alone on a pixel-by-pixel basis. The percentage of bleedthrough from the eCFP and eYFP fluorescent signals (typically 45% CFP and 25% YFP) was determined by dividing the average intensity of the image obtained using the FRET filter configuration by the average intensity of the image obtained using the CFP or YFP filter configuration, respectively. The difference in FRET^C between cells expressing Nef-YFP or NefAXXA-YFP was quantified by the following formula: $[(\text{mean pixel intensity})_T \bullet \text{area}] - [(\text{mean pixel intensity})_B \bullet \text{area}]/[(\text{mean pixel intensity})_C \bullet \text{area}] - [(\text{mean pixel intensity})_B \bullet \text{area}]$, where T = TGN, C = cytosol, and B = background in the extracellular space.

Coimmunoprecipitation, Western Blot, and Antibody Uptake

Cells infected with the indicated VV recombinants were harvested in PBS containing 1% NP40, protease inhibitors (0.5 mM PMSF and 0.1 μM each of aprotinin, E-64, and leupeptin) and phosphatase inhibitors (1 mM Na_3VO_4 and 20 mM NaF). Where indicated, cells were treated with 10 μM PP2 (Calbiochem) or 5 μM LY294002 prior to harvesting. In some experiments, cells were harvested in PBS and inhibitor cocktails without detergent, and then 100,000 × g membrane pellets were collected and resuspended in PBS containing 1% TX-100 plus inhibitors. FLAG-tagged Nef constructs were immunoprecipitated with mAb M2-agarose (Sigma), and coimmunoprecipitating proteins were detected by western blot. The following antibodies were obtained as indicated: mAb HA.11 (Covance); anti-Hck, anti-Syk, and anti-SHIP-1 (Santa Cruz); anti-Src, anti-p85, anti-ZAP-70, and anti-SHIP-2 (Upstate); anti-pY$_{418}$ (Biosource); anti-phospho$_{292}$ZAP-70 (BD); anti-phospho$_{319}$ZAP-70 and anti-PTEN (Cell Signaling); anti-actin (Chemicon); anti-Nef (AIDS Research and Reference Reagent Program, NIH); and anti-PACS-1(703) (Scott et al., 2006). Antibody uptake using mAb W6/32 was performed as described (Blagoveshchenskaya et al., 2002). Residual cell-surface-bound antibody was removed by a brief acid strip (1% acetic acid, 0.5 M NaCl [pH 3.0]; 30 s) prior to fixation.

PI3 Kinase Assay

Immunoprecipitates from H9 cells expressing the designated Nef constructs were resuspended in assay buffer (20 mM HEPES [pH 7.4], 30 mM $MgCl_2$, and 20 μM ATP) and then incubated with 0.2 mg/ml PI (Sigma) and 10 μCi [γ-^{32}P]ATP for 15 min at RT. Phospholipids were extracted with an HCl, chloroform/methanol (1:1) solution, spotted on TLC plates (Fisher), and separated in a solvent mixture composed of chloroform/methanol/water/NH_4OH (45:35:8.5:1.5). ^{32}P-PIP was visualized by autoradiography and quantified by phosphorimage analysis.

Immunofluorescence Microscopy

Cells were infected with the designated VV recombinants and either fixed or pelleted (suspension cell lines) onto poly-L-lysine-treated coverslips and then fixed with 4% paraformaldehyde and processed for immunofluorescence. Images were captured using a 63× oil immersion objective on a Leica DM-RB microscope and Hamamatsu C4742-95 digital camera and processed with Scion Image 1.62.

Supplemental Data

The Supplemental Data include nine supplemental figures and can be found with this article online at http://www.cellhostandmicrobe.com/cgi/content/full/1/2/121/DC1/.

ACKNOWLEDGMENTS

We thank S. Kaech Petrie (CROET Imaging Center) and A. Boyd (OHSU Cancer Center Flow Cytometry Core) for instruction and S. Feliciangeli and J. Yang for experimental assistance. We thank P. Klotman, W. Sellers, T. Smithgall, P. Stork, and A. Weiss for reagents

and T. Dillon, M. Forte, J. Scott, G. Thomas, and V. Piguet for discussions. This work was supported by NIH grants AI49793 and DK37274 (G.T.). E.B. and I.S. are supported by NIH grant GM060170.

Received: October 10, 2006
Revised: January 25, 2007
Accepted: March 20, 2007
Published: April 18, 2007

REFERENCES

Astoul, E., Edmunds, C., Cantrell, D.A., and Ward, S.G. (2001). PI 3-K and T-cell activation: Limitations of T-leukemic cell lines as signaling models. Trends Immunol. *22*, 490–496.

Bard, F., Patel, U., Levy, J.B., Jurdic, P., Horne, W.C., and Baron, R. (2002). Molecular complexes that contain both c-Cbl and c-Src associate with Golgi membranes. Eur. J. Cell Biol. *81*, 26–35.

Benedict, C.A., Norris, P.S., and Ware, C.F. (2002). To kill or be killed: Viral evasion of apoptosis. Nat. Immunol. *3*, 1013–1018.

Blagoveshchenskaya, A.D., Thomas, L., Feliciangeli, S.F., Hung, C.H., and Thomas, G. (2002). HIV-1 Nef downregulates MHC-I by a PACS-1- and PI3K-regulated ARF6 endocytic pathway. Cell *111*, 853–866.

Carreno, S., Gouze, M.E., Schaak, S., Emorine, L.J., and Maridonneau-Parini, I. (2000). Lack of palmitoylation redirects p59Hck from the plasma membrane to p61Hck-positive lysosomes. J. Biol. Chem. *275*, 36223–36229.

Chang, A.H., O'Shaughnessy, M.V., and Jirik, F.R. (2001). Hck SH3 domain-dependent abrogation of Nef-induced class 1 MHC downregulation. Eur. J. Immunol. *31*, 2382–2387.

Crump, C.M., Hung, C.H., Thomas, L., Wan, L., and Thomas, G. (2003). Role of PACS-1 in trafficking of human cytomegalovirus glycoprotein B and virus production. J. Virol. *77*, 11105–11113.

Das, S.R., and Jameel, S. (2005). Biology of the HIV Nef protein. Indian J. Med. Res. *121*, 315–332.

Deane, J.A., and Fruman, D.A. (2004). Phosphoinositide 3-kinase: Diverse roles in immune cell activation. Annu. Rev. Immunol. *22*, 563–598.

Druker, B.J. (2004). Molecularly targeted therapy: Have the floodgates opened? Oncologist *9*, 357–360.

Ely, C.M., Tomiak, W.M., Allen, C.M., Thomas, L., Thomas, G., and Parsons, S.J. (1994). pp60c-src enhances the acetylcholine receptor-dependent catecholamine release in vaccinia virus-infected bovine adrenal chromaffin cells. J. Neurochem. *62*, 923–933.

Fan, Q.W., Knight, Z.A., Goldenberg, D.D., Yu, W., Mostov, K.E., Stokoe, D., Shokat, K.M., and Weiss, W.A. (2006). A dual PI3 kinase/mTOR inhibitor reveals emergent efficacy in glioma. Cancer Cell *9*, 341–349.

Greene, W.C. (2004). The brightening future of HIV therapeutics. Nat. Immunol. *5*, 867–871.

Hanna, Z., Weng, X., Kay, D.G., Poudrier, J., Lowell, C., and Jolicoeur, P. (2001). The pathogenicity of human immunodeficiency virus (HIV) type 1 Nef in CD4C/HIV transgenic mice is abolished by mutation of its SH3-binding domain, and disease development is delayed in the absence of Hck. J. Virol. *75*, 9378–9392.

Husain, M., Gusella, G.L., Klotman, M.E., Gelman, I.H., Ross, M.D., Schwartz, E.J., Cara, A., and Klotman, P.E. (2002). HIV-1 Nef induces proliferation and anchorage-independent growth in podocytes. J. Am. Soc. Nephrol. *13*, 1806–1815.

Kasper, M.R., and Collins, K.L. (2003). Nef-mediated disruption of HLA-A2 transport to the cell surface in T cells. J. Virol. *77*, 3041–3049.

Keele, B.F., Van Heuverswyn, F., Li, Y., Bailes, E., Takehisa, J., Santiago, M.L., Bibollet-Ruche, F., Chen, Y., Wain, L.V., Liegeois, F., et al. (2006). Chimpanzee reservoirs of pandemic and nonpandemic HIV-1. Science *313*, 523–526.

Keppler, O.T., Tibroni, N., Venzke, S., Rauch, S., and Fackler, O.T. (2006). Modulation of specific surface receptors and activation sensitization in primary resting CD4+ T lymphocytes by the Nef protein of HIV-1. J. Leukoc. Biol. *79*, 616–627.

Knight, Z.A., Gonzalez, B., Feldman, M.E., Zunder, E.R., Goldenberg, D.D., Williams, O., Loewith, R., Stokoe, D., Balla, A., Toth, B., et al. (2006). A pharmacological map of the PI3-K family defines a role for p110alpha in insulin signaling. Cell *125*, 733–747.

Larsen, J.E., Massol, R.H., Nieland, T.J., and Kirchhausen, T. (2004). HIV Nef-mediated major histocompatibility complex class I down-modulation is independent of Arf6 activity. Mol. Biol. Cell *15*, 323–331.

Le Gall, S., Buseyne, F., Trocha, A., Walker, B.D., Heard, J.M., and Schwartz, O. (2000). Distinct trafficking pathways mediate Nef-induced and clathrin-dependent major histocompatibility complex class I down-regulation. J. Virol. *74*, 9256–9266.

Lee, C.H., Leung, B., Lemmon, M.A., Zheng, J., Cowburn, D., Kuriyan, J., and Saksela, K. (1995). A single amino acid in the SH3 domain of Hck determines its high affinity and specificity in binding to HIV-1 Nef protein. EMBO J. *14*, 5006–5015.

Lerner, E.C., and Smithgall, T.E. (2002). SH3-dependent stimulation of Src-family kinase autophosphorylation without tail release from the SH2 domain in vivo. Nat. Struct. Biol. *9*, 365–369.

Linnemann, T., Zheng, Y.H., Mandic, R., and Peterlin, B.M. (2002). Interaction between Nef and phosphatidylinositol-3-kinase leads to activation of p21-activated kinase and increased production of HIV. Virology *294*, 246–255.

Luo, W., and Peterlin, B.M. (1997). Activation of the T-cell receptor signaling pathway by Nef from an aggressive strain of simian immunodeficiency virus. J. Virol. *71*, 9531–9537.

Moon, K.D., Post, C.B., Durden, D.L., Zhou, Q., De, P., Harrison, M.L., and Geahlen, R.L. (2005). Molecular basis for a direct interaction between the Syk protein-tyrosine kinase and phosphoinositide 3-kinase. J. Biol. Chem. *280*, 1543–1551.

Okkenhaug, K., Bilancio, A., Farjot, G., Priddle, H., Sancho, S., Peskett, E., Pearce, W., Meek, S.E., Salpekar, A., Waterfield, M.D., et al. (2002). Impaired B and T cell antigen receptor signaling in p110delta PI 3-kinase mutant mice. Science *297*, 1031–1034.

Peterlin, B.M., and Trono, D. (2003). Hide, shield and strike back: How HIV-infected cells avoid immune eradication. Nat. Rev. Immunol. *3*, 97–107.

Piguet, V., Wan, L., Borel, C., Mangasarian, A., Demaurex, N., Thomas, G., and Trono, D. (2000). HIV-1 Nef protein binds to the cellular protein PACS-1 to downregulate class I major histocompatibility complexes. Nat. Cell Biol. *2*, 163–167.

Roeth, J.F., Williams, M., Kasper, M.R., Filzen, T.M., and Collins, K.L. (2004). HIV-1 Nef disrupts MHC-I trafficking by recruiting AP-1 to the MHC-I cytoplasmic tail. J. Cell Biol. *167*, 903–913.

Scholz, I., Arvidson, B., Huseby, D., and Barklis, E. (2005). Virus particle core defects caused by mutations in the human immunodeficiency virus capsid N-terminal domain. J. Virol. *79*, 1470–1479.

Scott, G.K., Gu, F., Crump, C.M., Thomas, L., Wan, L., Xiang, Y., and Thomas, G. (2003). The phosphorylation state of an autoregulatory domain controls PACS-1-directed protein traffic. EMBO J. *22*, 6234–6244.

Scott, G.K., Fei, H., Thomas, L., Medigeshi, G.R., and Thomas, G. (2006). A PACS-1, GGA3 and CK2 complex regulates CI-MPR trafficking. EMBO J *25*, 4423–4435.

Stevenson, M. (2003). HIV-1 pathogenesis. Nat. Med. *9*, 853–860.

Stove, V., Naessens, E., Stove, C., Swigut, T., Plum, J., and Verhasselt, B. (2003). Signaling but not trafficking function of HIV-1 protein Nef is essential for Nef-induced defects in human intrathymic T-cell development. Blood *102*, 2925–2932.

Swann, S.A., Williams, M., Story, C.M., Bobbitt, K.R., Fleis, R., and Collins, K.L. (2001). HIV-1 Nef blocks transport of MHC class I

molecules to the cell surface via a PI 3-kinase-dependent pathway. Virology *282*, 267–277.

Swigut, T., Alexander, L., Morgan, J., Lifson, J., Mansfield, K.G., Lang, S., Johnson, R.P., Skowronski, J., and Desrosiers, R. (2004). Impact of Nef-mediated downregulation of major histocompatibility complex class I on immune response to simian immunodeficiency virus. J. Virol. *78*, 13335–13344.

Thoulouze, M.I., Sol-Foulon, N., Blanchet, F., Dautry-Varsat, A., Schwartz, O., and Alcover, A. (2006). Human immunodeficiency virus type-1 infection impairs the formation of the immunological synapse. Immunity *24*, 547–561.

Trible, R.P., Emert-Sedlak, L., and Smithgall, T.E. (2006). HIV-1 Nef selectively activates SRC family kinases HCK, LYN, and c-SRC through direct SH3 domain interaction. J. Biol. Chem. *281*, 27029–27038.

Ward, S., Sotsios, Y., Dowden, J., Bruce, I., and Finan, P. (2003). Therapeutic potential of phosphoinositide 3-kinase inhibitors. Chem. Biol. *10*, 207–213.

Williams, M., Roeth, J.F., Kasper, M.R., Filzen, T.M., and Collins, K.L. (2005). Human immunodeficiency virus type 1 Nef domains required for disruption of major histocompatibility complex class I trafficking are also necessary for coprecipitation of Nef with HLA-A2. J. Virol. *79*, 632–636.

Zauli, G., Gibellini, D., Secchiero, P., Dutartre, H., Olive, D., Capitani, S., and Collette, Y. (1999). Human immunodeficiency virus type 1 Nef protein sensitizes CD4(+) T lymphoid cells to apoptosis via functional upregulation of the CD95/CD95 ligand pathway. Blood *93*, 1000–1010.

Zhang, Q., Cox, D., Tseng, C.C., Donaldson, J.G., and Greenberg, S. (1998). A requirement for ARF6 in Fcgamma receptor-mediated phagocytosis in macrophages. J. Biol. Chem. *273*, 19977–19981.

Cell Host & Microbe, Volume *1*

Supplemental Data

HIV-1 Nef Assembles a Src Family Kinase-ZAP-70/Syk-PI3K Cascade to Downregulate Cell-Surface MHC-I

Chien-Hui Hung, Laurel Thomas, Carl E. Ruby, Katelyn M. Atkins, Nicholas P. Morris, Zachary A. Knight, Isabel Scholz, Eric Barklis, Andrew D. Weinberg, Kevan M. Shokat, and Gary Thomas

Figure S1. Induction of PI3K activity in primary $CD4^+$ T-cells.

Replicate samples of freshly isolated $CD4^+$ T-cells were harvested immediately or cultured in the presence of IL-2 (5U/ml)/PHA (1 μg/ml) or IL-7 at either 5 ng/ml or 20 ng/ml. At the indicated time points, cells were harvested, p85 immunoprecipitated, and co-immunoprecipitated PI3K activity was measured as described in Experimental Procedures.

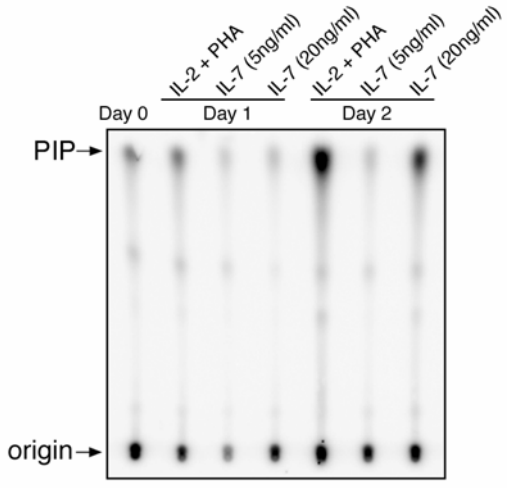

Figure S2. Nef-mediated CD4 downregulation does not require PI3K activity.

Primary $CD4^+$ T-cells infected with the Nef^- or Nef^+ pseudotyped viruses were monitored for cell surface CD4 by flow cytometry using APC-conjugated anti-CD4 (BD) as described in Experimental Procedures.

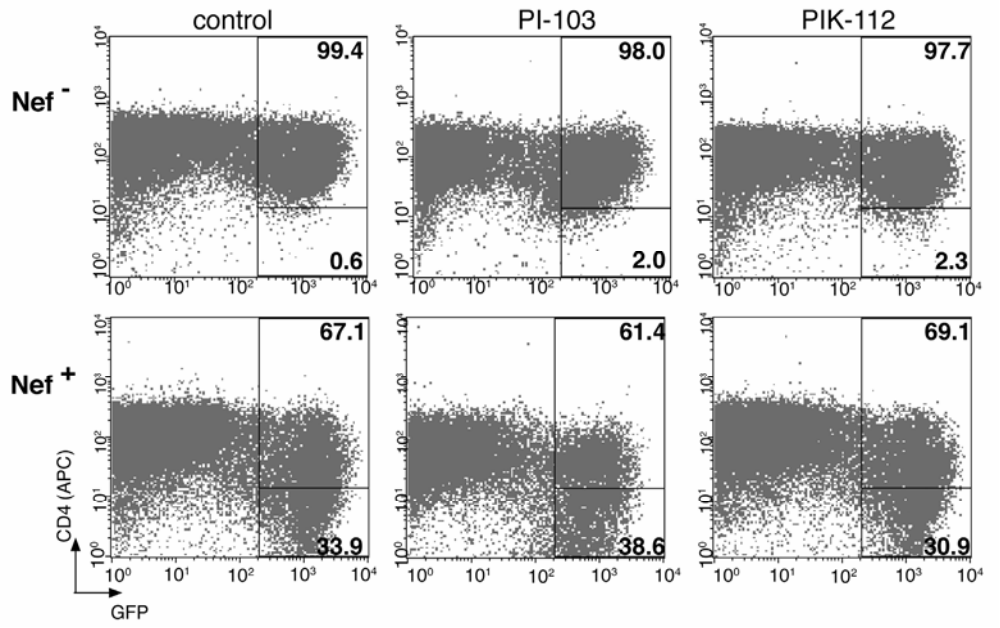

Figure S3. PTEN siRNA disrupts the ability of PI-103 to inhibit Nef-mediated MHC-I downregulation in H9 CD4$^+$ T-cells.

H9 CD4$^+$ T-cells were nucleofected with pmaxGFP and a control siRNA (scr.) or PTEN siRNA. After 60 hr, the cells were infected with VV:Nef (m.o.i. = 10, 4 hr) and then treated or not with 1 μM PI-103 for 1 hr. Cells were then processed for immunofluorescence microscopy using mAb W6/32 as described in Experimental Procedures. Scale bar, 10 μm.

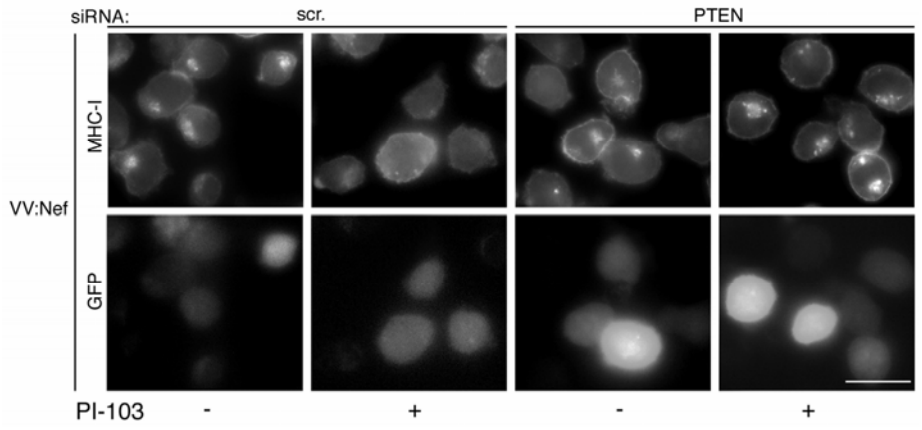

Figure S4. Effect of HIV-1 Nef on cell surface delivery of newly synthesized MHC-I in H9 CD4$^+$ T-cells.

Replicate wells of H9 CD4$^+$ T-cells were infected with VV:WT or VV:Nef for 8 hr and then pulse-labeled with [^{35}S]Met/Cys for 10 min and chased in the presence of extracellular biotin for the indicated times. MHC-I molecules were immunoprecipitated and the biotinylated forms were captured with strepavidin agarose and analyzed by SDS-PAGE followed by fluorography. An aliquot of each cell lysate was also analyzed by western blot to detect expression of Nef and cellular levels of MHC-I (bottom). Quantitation of the [^{35}S]Met/Cys-labeled, biotinylated bands revealed Nef reduced the efficiency of cell surface delivery of newly synthesized MHC-I by 7%.

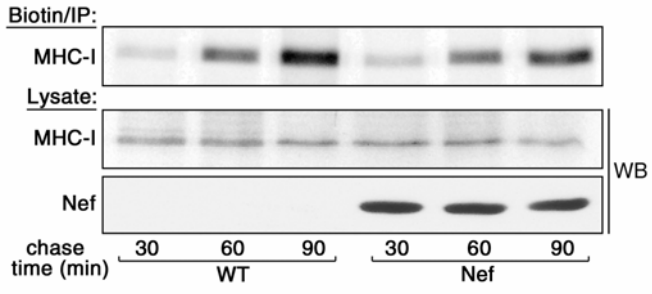

Figure S5. Nef expression in different vector backgrounds.

Replicate plates of H9 $CD4^+$ T-cells were infected with HIV-1 NL4-3, NL4-3G/P-EGFP (pseudotyped Nef^+ virus) or VV:Nef/f and the percent of each cell population infected with each virus was determined. HIV-1 NL4-3 persistently infected 10% of the cells as determined by immunofluorescence microscopy using anti-Gag mAb Hy183, NL4-3G/P-EGFP infected 35% of the cells after 60 hr infection as determined by flow cytometry ($eGFP^+$ cells), and VV:Nef/f infected 100% of the cells as determined by immunofluorescence microscopy using anti-FLAG mAb M2. Based on these values, a proportionate number of total cells in each culture corresponding to an equal number of infected cells were harvested and analyzed by western blot using anti-Nef. Nef/f migrates slower due to the presence of the FLAG tag.

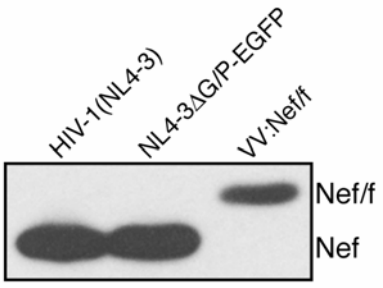

Figure S6. HIV-1 Nef-mediated downregulation of cell surface MHC-I requires a functional ARF6 pathway in H9 $CD4^+$ T-cells.

H9 $CD4^+$ T-cells expressing Nef alone or co-expressing Nef with either $ARF6Q_{67}L$ or $ARNOE_{156}K$ were processed for immunofluorescence microscopy and MHC-I molecules were detected with mAb W6/32. Scale bar, 10 μm.

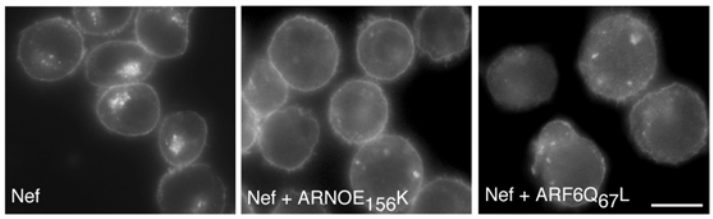

Figure S7. HIV-1 Nef activates Hck in vivo.

Replicate wells of A7 cells infected with VV recombinants expressing the indicated proteins (m.o.i. = 10 total, 8 hr) were harvested and Hck was immunoprecipitated from the extracts. Co-immunoprecipitated phospho(activated)Hck was then detected by western blot using anti-pY_{418}Src. The expression levels of Nef and Hck were monitored by western blot (bottom).

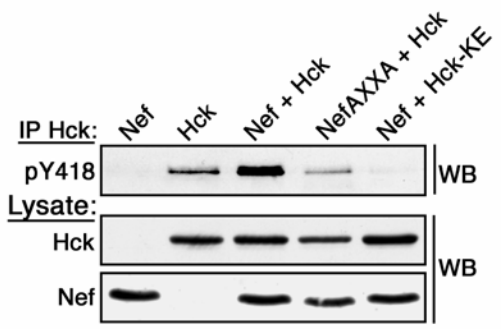

Figure S8. HIV-1 Nef combines with Src to stimulate PI3K.

Replicate wells of TF-1 cells co-infected with VV:Src and either VV:WT, VV:Nef/f or VV:NefAXXA/f (m.o.i. = 10 total, 16 hr) were harvested and Nef proteins were immunoprecipitated with mAb M2. Co-immunoprecipitated p85, Syk and Src were detected by western blot and co-immunoprecipitated PI3K activity was detected as described in the legend to Fig. 2. The levels of cellular p85 and Syk as well as the levels of expressed Nef and Src were monitored by western blot as shown.

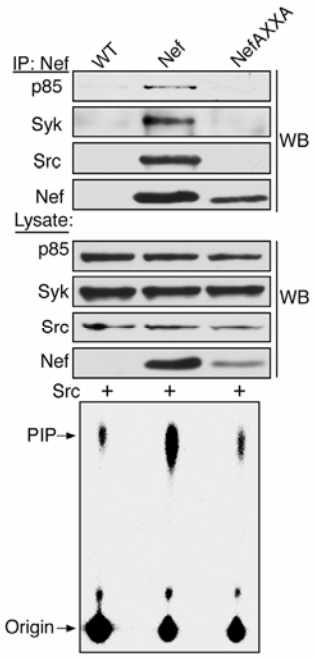

Figure S9. HIV-1 Nef uses the SFK-ZAP70/Syk-PI3K axis to downregulate cell surface MHC-I in heterologous cells.

HeLa-CD4^{+} cells were nucleofected (Amaxa) with pmaxGFP and either a control siRNA (scr.) or siRNAs specific for Syk or PACS-1. After 48 hr, cells were infected with VV:WT or VV:Nef (m.o.i. = 10, 3 hr). The cells were then fixed and permeabilized, and MHC-I molecules were stained with mAb W6/32 followed by an Alexa546-conjugated secondary antibody. Cells transfected with siRNAs specific for Syk or PACS-1 were detected by GFP fluorescence. Scale bar, 20 μm.